REPORT NO.
UCB/EERC-87/12
SEPTEMBER 1987

EARTHQUAKE ENGINEERING RESEARCH CENTER

INELASTIC SEISMIC RESPONSE OF STRUCTURES WITH MASS OR STIFFNESS ECCENTRICITIES IN PLAN

by

MICHEL BRUNEAU
STEPHEN A. MAHIN

Report to the National Science Foundation

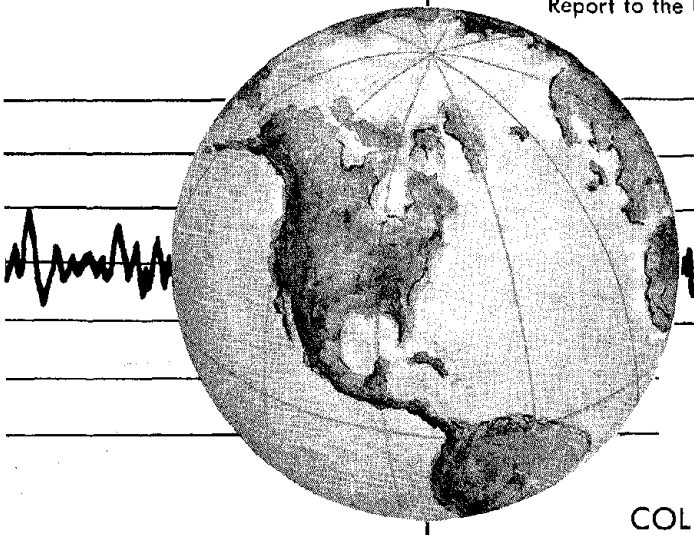

COLLEGE OF ENGINEERING

UNIVERSITY OF CALIFORNIA AT BERKELEY

For sale by the National Technical Information Service, U.S. Department of Commerce, Springfield, Virginia 22161

See back of report for up to date listing of EERC reports.

50272-101

REPORT DOCUMENTATION PAGE	1. REPORT NO. NSF/ENG-87046	2.	PB90-262650

4. Title and Subtitle
" Inelastic Seismic Response of Structures with Mass or Stiffness Eccentricities in Plan"

5. Report Date
September 1987

6.

7. Author(s)
N. Bruneau and S.A. Mahin

8. Performing Organization Rept. No.
UCB/EERC-87/12

9. Performing Organization Name and Address
Earthquake Engineering Research Center
University of California
1301 South 46th Street
Richmond CA 94804

10. Project/Task/Work Unit No.

11. Contract(C) or Grant(G) No.
(C)
(G)CEE-8316662

12. Sponsoring Organization Name and Address
National Science Foundation
1800 G. Street
Washington D.C. 20550

13. Type of Report & Period Covered

14.

15. Supplementary Notes

16. Abstract (Limit: 200 words) Systems with only two lateral load resisting elements are shown to be appropriate for the study. A tentative classification scheme for various types of inelastic torsionally coupled systems is proposed. The concept of equivalent non-linear systems is obtained from the expansion of the incremental equations of motion and the requirements for geometry-independence are enunciated.

For mass and stiffness symmetric systems having elements with different yield capacities, torsional coupling is created by the desynchronizing inelastic element responses, despite the existence of symmetry in the elastic domain. An extensive parametric study demonstrates that the element ductility levels remain within reasonable bounds provided the ratio of uncoupled frequencies Ω is not excessively large and the yield level of the weaker element is accurately estimated.

A similar extensive parametric study is conducted for initially eccentric systems. A procedure to insure a fair comparison between the coupled system and an equivalent single degree of freedom is formulating; it provides a capability for predicting element ductilities in the coupled system from readily available design tools. Using this new procedure, the resulting ductility demand of the weaker element in the two-element torsionally coupled systems becomes almost equal to that in the equivalent single degree of freedom, independently of the traditional parameters Ω, e/r and T_x. The case of Ω=1 produces even more reliable preductions of weak element response. Preliminary results indicate that the findings in relation to both initially symmetric and eccentric systems may be also applied to equivalent multi-element single-

17. Document Analysis a. Descriptors tory systems, systems with various sypes of element models and multi-story systems.

b. Identifiers/Open-Ended Terms

c. COSATI Field/Group

18. Availability Statement	19. Security Class (This Report)	21. No. of Pages 316
	20. Security Class (This Page)	22. Price

(See ANSI-Z39.18) *See Instructions on Reverse* OPTIONAL FORM 272 (4-77) (Formerly NTIS-35) Department of Commerce

INELASTIC SEISMIC RESPONSE OF STRUCTURES WITH MASS AND STIFFNESS ECCENTRICITIES IN PLAN

by

Michel Bruneau

and

Stephen A. Mahin

A Report to the
National Science Foundation

Report No. UCB/EERC-87/12
Earthquake Engineering Research Center
University of California
Berkeley, California

September 1987

ABSTRACT

This report investigates the inelastic behavior of structural systems having plan eccentricities created by non-coincidence of centers of mass and stiffness and subjected to seismic excitation. The basic concepts inherent to the response of torsionally coupled systems are reviewed and the pertinent equations of motion are derived. A literature review emphasizes the lack of agreement between different researchers on how variations in the fundamental parameters influence the response.

The selection of systems with only two lateral load resisting elements for the following studies is demonstrated to be appropriate. A tentative classification scheme for various types of inelastic torsionally coupled systems is proposed. The concept of equivalent non-linear systems is obtained from the expansion of the incremental equations of motion and the requirements for geometry-independence are enunciated.

For mass and stiffness symmetric systems having elements with different yield capacities, torsional coupling is created by the desynchronizing inelastic element responses, despite the existence of symmetry in the elastic domain. An extensive parametric study demonstrates that the element ductility levels remain within reasonable bounds provided the

ratio of uncoupled frequencies Ω is not excessively large and the yield level of the weaker element is accurately estimated.

A similar extensive parametric study is conducted for initially eccentric systems. A procedure to insure a fair comparison between the coupled system and an equivalent single degree of freedom is formulated. This procedure simultaneously provides a capability for predicting element ductilities in the coupled system from readily available design tools. Using this new procedure, the resulting ductility demand of the weaker element in the two-element torsionally coupled systems becomes almost equal to that in the equivalent single degree of freedom, independently of the traditional parameters Ω, e/r and T_x. The special case of Ω=1 produces even more reliable predictions of weak element response and this phenomenon is clearly explained.

Finally, preliminary results are shown to indicate that the findings in relation to both initially symmetric and eccentric systems may be also applied to equivalent multi-element single-story systems, systems with various types of element models and multi-story systems. Additional research is recommended to assess this possibility in greater detail.

ACKNOWLEDGEMENT

This research program was supported by National Science Foundation. This support is sincerely appreciated. The findings and recommendations in this report, however, are those of the author and not necessarily those of the sponsor.

UNITS

Due to the highly non-dimensional nature of this work, most values are generally expressed in "units". In some rare instances where units were specified, the imperial values have been used. Equivalent S.I. (metric) values can be obtained through the following relationships:

1	inch	=	25.4	millimetre
1	foot	=	0.3048	metre
1	square inch	=	645.16	square millimetre
1	square foot	=	0.0929	square metre
1	kilogram	=	2.2046	pound
1	pound	=	4.448	newton
1	ksi	=	6.895	Mpa

AVAILABLE DATA ON FLOPPY DISK

In Chapters 4 and 5 of this report, it is mentioned that the complete results of this study (more than actually presented here) are available from two 5-1/4" floppy disks. These are not included in the present EERC Report as they do not constitute an essential part of this work and their absence does not impair the integrity of this work (they simply provide a more complete set of results for those wanting additional information). If desired, the two floppy disks can be obtained (for a nominal charge) by writing to :

National Information Service for Earthquake Engineering
Computer Applications
Earthquake Engineering Research Center
404A Davis Hall
University of California, Berkeley
Berkeley, CA 94720
Tel.: (415) 642-5113

TABLE OF CONTENTS

1. INTRODUCTION

1.1 Introductory Remarks

When buildings are forced to respond inelastically, as it is the case during rare and unusually intense earthquakes, their true three dimensional response may differ significantly from that predicted using conventional elastic analysis methods. This difference can be particularly acute when the distribution of the lateral load resisting elements, or of the centers of mass (or both), is such that eccentricities in plan induce an unequal demand on different resisting elements. When inelastic response develops, the behavior of the system can be greatly modified thus inducing larger than expected demand on some resisting elements. This can lead to excessive local damage to these elements or to even collapse of the entire structure. Observations of this behavior are made after each major earthquake, including the recent Mexican earthquake of September 1985 (Bruneau (1986) [9], Meli (1986) [37], Mitchell et. al. (1986) [38]) for which "plan eccentricity" was reported to be one of the three major factors responsible for the severe damage or collapse of structures (Meli (1986) [37]).

Consequently, it is desirable to develop a better understanding of the three dimensional behavior of buildings under earthquake excitation. A large portion of this very

broad problem consists of improving current knowledge about the inelastic behavior of structures with stiffness and/or mass eccentricities in plan. Such structures are also often referred to as being torsionally coupled.

1.2 Objectives and Organization

The objectives of this report are to investigate the inelastic behavior of some simple structural systems to improve our understanding of the sensitivity of seismic response to plan eccentricities created by non-coincidence of centers of mass and stiffness and to devise guidelines appropriate for preliminary design. This study will by no means solve completely this complicated problem, but it is expected that it will result in a greater understanding of the factors affecting the inelastic behavior of such structures.

In Chapter 2, a brief review of the basic concepts involved in the estimation of the response of torsionally coupled systems is presented. The elastic dynamic equations of motion are revieved in Section 2.1. Research on inelastic torsional coupling is summarized in Section 2.2. This section also examines qualitatively the origins of inelastic response in torsionally coupled systems and the necessity of

considering this inelastic behavior in seismic resistant design.

The structural idealizations used in these studies are developed in Chapter 3. To simplify those preliminary studies, all systems are modeled as monosymmetric, have rigid diaphragm floor slabs, and are subjected to unidirectional earthquake excitation. The selection of systems with only two lateral load resisting elements for the following studies is demonstrated to be appropriate in Section 3.1. The incremental inelastic equations of motion are expanded for torsionally coupled systems in order to illustrate what parameters influence the inelastic response of these types of structures. These parameters are examined in order to formulate parametric studies to be performed in the following chapters.

The inelastic response of mass and stiffness symmetric two element systems with different yield strengths is investigated in Chapter 4. This parametric study presents a special case of systems where the torsionally coupled state is transient.

The inelastic response of initially eccentric two element systems having same yield strengths is investigated in Chapter 5. The parameters affecting global response are clearly identified, and elastic and inelastic responses are

compared. Simplified analysis and design methods are identified.

In Chapter 6, cases studies are performed to investigate the effect of inelastic torsional coupling on structures with multi-element systems, systems with degrading restoring force characteristics (braced frames), and multistory structures. Performance of these systems is assessed.

Conclusions and design recommendations are presented in Chapter 7. Recommendations for further research are also offered.

2. REVIEW OF PREVIOUS RESEARCH AND BASIC CONCEPTS IN DESIGN OF TORSIONALLY COUPLED SYSTEMS

2.1 Elastic Response of Torsionally Coupled Systems

2.1.1 Some Historical Notes

The knowledge that structures with stiffness and/or mass eccentricities will have significantly different behavior than symmetric systems is not new. In 1938, R.S. Ayre [4] (inspired by the preliminary work of L.S. Jacobsen) was already using small scale models to investigate the dynamic response of irregular building forms. Basic concepts related to this type of structure were enunciated. For example, the fundamental definition of torsional coupling was developed: "(...) in general, the center of rigidity (...) does not coincide with the center of mass, and we may therefore expect translation in horizontal directions to be accompanied by torsion whether of not there is rotation in the ground motion". Ayre studied the general free vibration elastic response of a three degree of freedom structure (a one-story building with a rigid floor diaphragm) with arbitrarily oriented resisting elements. He clearly illustrated the difference between the coupled and uncoupled frequencies as a function of eccentricity, and demonstrated the striking

difference between the traces of motion (at the center of mass) when torsional coupling is present or absent.

Ayre pursued his ideas further in a second paper in 1943 [5] which investigated the response of a one story building to an idealized sinusoidal ground motion. He observed that the larger rotations induced occurred at resonance of a "translational" mode rather than at resonance of a "rotational" mode. This is in agreement with current behavior observations of eccentric structures under uniaxial earthquake excitation where the largest displacements are often produced by the "predominantly translational" modes. It is important to understand that torsional coupling means that torsion is present in all modes, and not, as sometimes believed, that the predominantly torsional modes become dominant. However, only one model was tested by Ayre under forced excitation, and no direct conclusions could be drawn then as to how other parameters influence the response.

The first conclusions of practical significance were produced fifteen years later when G.W.Housner and H.Outinen (1958) [28] demonstrated clearly that in the case of a system with walls of different stiffnesses in the direction parallel to the earthquake excitation, the forces in each wall obtained considering eccentricity by static analysis are different from those calculated by dynamic analysis. The stiffer wall will get a smaller stress than predicted

statically, and the more flexible wall will get a larger one, the effect being more dramatic when the walls are farther away from the center of mass.

From that moment in time, the potentially damaging effects of eccentricity gained wider recognition. Building codes introduced provisions for a magnified calculated static eccentricity, and some minimum eccentricity. But adoption of these code requirements were also in answer to observation and analysis of buildings damaged by torsional oscillations during severe earthquakes (among those, the 1957 Mexico City earthquake).

Attempting a complete chronological history of the evolution of knowledge about torsionally coupled system is beyond the scope of this study, and would be very extensive. Helped by the modern formulations of matrix theory and increased computer power, a great number of authors added their contribution to the study of elastic response of single or multiple story systems with eccentricities. Valuable research has been conducted by Bustamante and Rosenbluth (1960) [10], Shiga (1965) [53], Skinner, Skilton and Laws (1965) [54], Medearis (1966) [36], Shepherd and Donald (1967) [52], Newmark (1969) [41], Gibson, Moody and Ayre (1972) [22 & 23], Anagnostopoulos and Roesset (1973) [1], Douglas (1973) [16], Hart (1975) [26], Kan and Chopra (1976) [30], Rutenberg, Tso and Heidebrecht (1977) [49], Foutch (1978)

[18], Rutenberg, Hsu and Tso (1978) [48], Rutenberg (1979) [47], Gluck, Reinhorn and Rutenberg (1979) [25], Wittrick and Horsington (1979) [71], Tso and Dempsey (1980) [61], Spanos (1981) [55], Tsicnias and Hutchinson (1981) [58], Dempsey and Tso (1982) [14], Tso and Meng (1982) [63], Balendra (1983) [6], Heidebrecht and Tso (1983) [27], Tso, Heidebrecht and Cherry (1983) [65], Humar and Awad (1983) [29], Rutenberg and Pekau (1983) [50], Tso (1983) [64], Béjar and Gergeley (1984) [7 and 21], Kung and Pecknold (1984) [32], Scholz (1984) [51].

Since it is the inelastic response of torsionally coupled structures which is of interest in this study, only the fundamentals of the elastic theory will be summarized in the following sections.

2.1.2 Choosing a Reference Center

Two different approaches have been generally followed in the derivation of the equations of motion for torsionally coupled systems. Dynamic equilibrium is computed around the center of stiffness or around the center of mass, with the advantage of producing diagonal stiffness or mass matrix, respectively. There is no consensus as to which approach is the more convenient. An argument can be made that the

derivation around the center of mass is more practical because:

(1) the center of mass will not move during inelastic response as might the center of stiffness, and

(2) the center of mass is easier to define for multistory structures, whereas the definition of the center of stiffness for multistory buildings is still the subject of active research (in particular, the contributions of Riddell and Vásquez (1984) [46] and Cheung and Tso (1986) [12] should be noted).

The argument may seem weak since, in order to be able to calculate the eccentricity e, both centers will need to be known. Nevertheless, to assemble the global stiffness matrix for use in dynamic analysis, a reference point is required at each floor, and the center of mass seems a practical choice.

Still, derivation around the center of stiffness has been favored by some researchers, probably because it provides a more continuous parametric variation (i.e. all combinations of the various parameters are possible) as will be seen in the following Section.

The chosen reference for this study will be the center of mass. In order to allow comparison of results with studies by other authors, transformation factors will be presented in Section 2.1.4.

2.1.3 Equations of Motion Around the Center of Mass

The equations will be derived here for a single story system. The multistory system derivation follows similar ideas, but requires added complications related to the definition of the centers of rigidity. Also, only structural elements oriented parallel or orthogonal to each other are considered, although more general systems can also be treated by determining first the directions of the principal axes of stiffness (Ayre (1938) [4]).

If we call $K_{i\,x}$ and $K_{i\,y}$ the translational stiffnesses of the i-th resisting element along the principal axes x and y, and x_i and y_i the distances of the i-th resisting element from the center of mass, then we have:

$$K_x = \sum_i K_{i\,x} \qquad \text{and} \qquad K_y = \sum_i K_{i\,y}$$

as the translational stiffnesses, and:

$$K_\theta = \sum_i K_{i\,x}\, y_i^2 + \sum_i K_{i\,y}\, x_i^2$$

as the torsional stiffness of the structure (torsional stiffnesses of individual resisting elements are not included as they are generally negligible).

The center of rigidity (where a static lateral load could be applied without creating any rotation in the system) in this case would be located at the distances (static eccentricities) e_x and e_y:

$$e_x = \frac{1}{K_y} \sum_i x_i K_{i\,y} \qquad \text{and} \qquad e_y = \frac{1}{K_x} \sum_i y_i K_{i\,x}$$

measured from the center of mass along the principal directions x and y.

Assembling the equations of motions, we obtain:

$$M\,\ddot{v} + K\,v = -M\,\ddot{v}_g$$

$$\begin{bmatrix} m & 0 & 0 \\ 0 & mr^2 & 0 \\ 0 & 0 & m \end{bmatrix} \begin{bmatrix} \ddot{v}_x \\ \ddot{v}_\theta \\ \ddot{v}_y \end{bmatrix} + \begin{bmatrix} K_x & -K_x e_y & 0 \\ -K_x e_y & K_\theta & K_y e_x \\ 0 & K_y e_x & K_y \end{bmatrix} \begin{bmatrix} v_x \\ v_\theta \\ v_y \end{bmatrix} = - \begin{bmatrix} m\ddot{v}_{g\,x} \\ 0 \\ m\ddot{v}_{g\,y} \end{bmatrix}$$

where r is the radius of gyration about the center of mass, m is the mass of the floor, v and $\ddot{v}$ are displacement and acceleration of the reference point in the appropriate degree of freedom, and $\ddot{v}_g$ is the ground acceleration. Viscous damping could be introduced in the equations without complications (typically Rayleigh damping is used), but there is no loss in generality in neglecting it for the moment. Similarly, only translational components of ground motion will be considered.

We can express the equations in a dimensionless form by transforming them to obtain the following result:

$$\begin{bmatrix} \ddot{v}_x \\ r\ddot{v}_\theta \\ \ddot{v}_y \end{bmatrix} + \begin{bmatrix} \omega_x^2 & -\omega_x^2 (e_y/r) & 0 \\ -\omega_x^2 (e_y/r) & \omega_\theta^2 & \omega_y^2 (e_x/r) \\ 0 & \omega_y^2 (e_x/r) & \omega_y^2 \end{bmatrix} \begin{bmatrix} v_x \\ rv_\theta \\ v_y \end{bmatrix} = - \begin{bmatrix} \ddot{v}_{g\,x} \\ 0 \\ \ddot{v}_{g\,y} \end{bmatrix}$$

where ω_x , ω_y and ω_θ are known as the uncoupled frequencies of the system (they are the natural frequencies of the system if there is no eccentricity between the center of mass and center of stiffness) defined as:

$$\omega_x^2 = K_x/m \qquad \omega_y^2 = K_y/m \qquad \text{and} \quad \omega_\theta^2 = K_\theta/mr^2 .$$

The notation can also be simplified by introducing other parameters that will be call the ratios of uncoupled frequencies Ω_y and Ω_x. These are defined by the ratio of uncoupled torsional frequency divided by the uncoupled translational frequency in a given direction, such that:

$$\Omega_x = \omega_\theta/\omega_x = T_x/T_\theta \qquad \Omega_y = \omega_\theta/\omega_y = T_y/T_\theta$$

For a monosymmetric system (where there is an eccentricity only along one of the principal directions) under unidirectional earthquake excitation, we usually drop the subscript for Ω since we are talking about a two degree of freedom system (with one translational and one rotational degree of freedom) and there is no possible confusion.

The equations for a monosymmetric structure then reduce to:

$$\begin{bmatrix} \ddot{v}_x \\ r\ddot{v}_\theta \end{bmatrix} + \omega_x^2 \begin{bmatrix} 1 & -e/r \\ -e/r & \Omega^2 \end{bmatrix} \begin{bmatrix} v_x \\ rv_\theta \end{bmatrix} = \begin{bmatrix} -\ddot{v}_g \\ 0 \end{bmatrix}$$

Therefore, the elastic response parameters v_x and rv_θ are uniquely defined for all torsionally coupled systems with similar uncoupled frequencies ω_x^2 and ω_θ^2 (and ω_y^2 if not monosymmetric) and ratio e/r (e_x/r and e_y/r generally) for a given damping and earthquake excitation. Note that it is not the rotation angle that is uniquely defined, but the radius of gyration times the angle.

We could also calculate the true frequencies of the monosymmetric system as:

$$\omega_{1,2}^2 = \omega_x^2 \left[\frac{(\Omega^2+1) \pm (\Omega^4-2\Omega^2+1+4(e/r)^2)^{0.5}}{2} \right]$$

and: $\Omega_N^2 = \omega_N^2/\omega_x^2 \quad N=1,2$

with the equivalent mode shapes:

$$\Phi_N = \begin{bmatrix} \Phi_{x\,N} \\ \Phi_{\theta\,N} \end{bmatrix} = \begin{bmatrix} 1 \\ (\Omega_N^2-1)/(e/r) \end{bmatrix}$$

The resulting values of Ω_N^2 as a function of the ratio of uncoupled frequencies (Ω) are presented in Figure 2.1. The ratios of the terms in each true mode shape (in

absolute value) $|\Phi_{x\,n}/\Phi_{z\,n}|$ as a function of the ratio of uncoupled frequencies (Ω) are presented in Figure 2.2. Curves for different values of normalized eccentricities are presented, the solid lines being for the first mode and the dashed lines being for the second mode. It is interesting to note that for some combination of eccentricities and ratios of uncoupled frequencies (measured around the center of mass), no physical systems can be represented as the true Ω_n's are negative (no real square root, i.e. no real frequencies). This is the discontinuous parameter variation consequent with the choice of the center of mass as the reference point (as mentioned in the preceding section). Clearly, the ratio of uncoupled frequencies obtained when the equations are derived around the center of mass (Ω^m) will differ from the ratio obtained when the center of stiffness is the reference point (Ω^s or Ω^e). The relation between the two is presented in Figure 2.3. It is also obvious from that figure, that the ratio of uncoupled frequencies around the center of stiffness is continuous while around the center of mass is not. The equations used in the development of Figure 2.3 are derived in the next section.

It is interesting to note from Figure 2.1 that for large values of Ω, the true first frequency is closer to the uncoupled lateral frequency ω_x, while for small values of Ω, the true second frequency is closer to the uncoupled lateral frequency ω_x. The two real frequencies are close only for

small eccentricities and when Ω is close to unity. From Figure 2.2, it can be observed that for small Ω, the first mode is subjected to large torsional participation where for large Ω the translational participation becomes dominant. The opposite occurs for the second mode.

2.1.4 Transformation Function for Ratio of Uncoupled Frequencies as Derived from Different Centers

If the equations of motion are derived about the center of rigidity instead, similar equations are obtained (for a complete derivation in that case, the reader is referred to Tso and Dempsey (1980) [61], or Tsicnias and Hutchinson (1981) [58], a few among many who used the center of rigidity as their reference point). The radius of gyration is now denoted ρ, taken around the center of stiffness, and therefore, $\omega_\theta^2 = K_\theta / m\rho^2$. By doing this, the resulting value of Ω is different from the Ω obtained by derivation around the center of mass. The "uncoupled torsional frequency" is not the same for the two cases (still defining Ω as the ratio of uncoupled frequencies).

Since we know the simple relationship, $\rho^2 = r^2 + e^2$, we can establish a relationship between Ω found from the two different derivations.

Let's define for the system derived around the center of rigidity:

$$\Omega_R^2 = K_\theta^R / K_X^R \rho^2 = \frac{\sum_i K_{iX} (y_i - e)^2}{(\sum_i K_{iX}) (r^2 + e^2)}$$

and around the center of mass:

$$\Omega_M^2 = K_\theta^M / K_X^M r^2 = \frac{\sum_i K_{iX} y_i^2}{(\sum_i K_{iX}) r^2}$$

where y_i is the distance measured from the center of mass to element i.

We can now derive a transformation factor such that:

$$\Omega_R^2 = F \Omega_M^2$$

By simply expending the expressions above, we get:

$$F = \frac{\Omega_R^2}{\Omega_M^2} = \frac{K_\theta^R / K_X^R \rho^2}{K_\theta^M / K_X^M r^2} = \left[\frac{\sum_i^n K_{iX} (y_i^2 - 2y_i e + e^2)}{\sum_i^n K_{iX} y_i^2 [1 + (e/r)^2]} \right]$$

Noting that $\Sigma K_{i,M} y_i = e$, and distributing the summation on the numerator, we obtain:

$$F = \left[\frac{\Omega_R}{\Omega_M}\right]^2 = \left[\frac{r^2}{r^2 + e^2}\left[1 - (e^2 K_i / K_{e,M})\right]\right]$$

where $K_{e,M} = \Sigma y_i^2 K_{i,i}$

Since the relation is not linear, it is actually preferable to express the relationship directly without making use of a factor F at all.

Therefore:

$$\left[\frac{\Omega_R}{\Omega_M}\right]^2 = \left[\frac{1}{1 + (e/r)^2}\left[1 - (e/r)^2 * (1/\Omega_M)^2\right]\right]$$

Finally:

$$\Omega_R = \left[\frac{1}{1 + (e/r)^2}\left[\Omega_M^2 - (e/r)^2\right]\right]^{0.5}$$

$$\Omega_M = \left[\Omega_R^2 \left[1 + (e/r)^2\right] + (e/r)^2\right]^{0.5}$$

which are the relations plotted in Figure 2.3.

For the case of a two element stiffness eccentric system, which will be a very important case studied herein, this expression can be further developed.

If the stiffnesses of the two elements are related such that:

$$K_1 = \alpha K_2 = \alpha K$$

and the geometry is fixed such that $y_1 = -y_2$, then:

$$e = \frac{(\alpha-1)}{(1+\alpha)} y_1$$

2.2 Review of Literature on the Inelastic Response of Torsionally Coupled System

Many authors have studied the problems of three dimensional structures subjected to multi-directional ground motions in the inelastic range (Pecknold and Sozen (1973) [43], Fujiwara and Kitahara (1982 & 1984) [19 & 20], Takizawa (1984) [57], to list just a few), and others have studied the three dimensional non-linear behavior of columns, beams and various other structural elements (Wen and Farhoomand (1970) [69], Chen and Atsuta (1973) [11], Mondkar and Powell (1975) [40], Uzgider (1980) [67], Zeris (1986) [73] and many more).

Although these are topics directly related to the subject at hand, the general field of three-dimensional response of structures will not be reviewed herein. This summary will be limited to the subject of torsionally coupled structures in the inelastic range.

2.2.1 Conventional Design Approaches

From structural damage investigations performed after many major earthquakes, it has been observed that plan eccentricity between a structure's center of mass and its center of stiffness could lead to very dramatic inelastic response. These investigations also indicate that it is very difficult to predict this damage by elastic analyses. Some results of relevant studies are summarized below.

Anagnostopoulos, Roesset and Biggs (1972) [1] were apparently the first to present analytical evidence to support that observation by performing some non-linear analyses for buildings with large plan eccentricities. Unfortunately, the scope of their results with respect to torsional coupling was rather limited.

A more extensive study of the problem was undertaken by Kan and Chopra (1979) [31]. At the heart of their approach was the definition of an interaction surface in the shear-

torsion space, thereby replacing the whole structure by a single-element model with an equivalent interaction surface. No particular relation between the inelastic response and the system parameter Ω (defined as before) was noted. The effects of torsional coupling were observed to depend on this and other parameters in a complicated manner with no apparent systematic trend, except for Ω larger than 2. In this latter case, the effect of torsional coupling on deformations increased with increasing e/r and a/b (The a/b ratio affects the location of the edge columns in a rectangular building of plan dimensions a and b). Their research also underlined the fact that column deformations can be considerably amplified because of torsional coupling for systems with Ω=1. This last statement has been re-examined by many other researchers, as will be noted in following chapters.

Kan and Chopra explained that because most buildings are strong in torsion, yielding of the system is controlled primarily by the translational yield strength. Thus, looking at the center of mass response, it was stated: "torsional coupling generally affects the maximum deformations in inelastic systems to a lesser degree compared to corresponding elastic system", and "except for that one difference, inelastic and elastic systems are affected similarly by torsional coupling".

Tso and Sadek (1984) [62] studied the effect of bi-directional ground motions for unisymmetric eccentric buildings with uncoupled periods of 0.5 seconds in each direction as well as torsionally (i.e., Ω=1 in each direction). An idealized bi-directional yield relationship was used. According to their research, buildings with small eccentricities have column ductility demands similar to the ones predicted for the symmetrical case. However, buildings with large eccentricities have ductility demands that can be as much as twice as large as those for unidirectional excited symmetrical systems.

Finally, Tso and Bozorgnia (1986) [8] studied the behavior of monosymmetric structures under different earthquake excitations (unidirectionally applied). Using a bilinear model with identical yield deformation for all elements, they compared the response of symmetric and eccentric three-element systems. All structures were designed such that, for the uncoupled translational direction:

$$F_o = K_v v_o = ma^*/R$$

where v_o and F_o are the yield deformation and yield strength of the symmetric system, K_v is the elastic lateral stiffness of the system, m is the mass of the floor, and R is a modification factor (independent of the uncoupled lateral

period T_y) relating the yield strength of the structure to the intensity of the ground excitation. The characteristic acceleration a^* is a measure of the strength of the ground acceleration. It was taken as a smooth elastic pseudo-acceleration from a design spectrum such that a^* is assumed constant for $T_y \leq 0.5$ second and varies inversely proportional to the period for $T_y > 0.5$ second. Parametric studies were performed using step-by-step non-linear analysis procedures and real earthquake records, and the responses computed for the symmetric and eccentric systems were compared. The difference between the ductility demand on the structural elements of the symmetric and eccentric systems was noted to be larger in the short period range. The difference decreased steadily toward the long period range (the eccentric system having a larger ductility demand most of the time). The increase in ductility demand created by the effect of eccentricity was also observed to be more important for weaker systems (designed for larger R values). It is interesting to note that Ω did not influence ductility levels significantly. However, to get different Ω values, different system geometries were used by the authors. This change in geometry may account for the lack of influence of Ω on the response. To compensate for this geometry dependency, an arbitrarily defined edge displacement was introduced. This was shown to be somehow more sensitive to Ω, with lower Ω usually creating larger response.

The Tso and Bozorgnia study is of great interest, but it is likely that some of the conclusions reached may be a consequence of comparing eccentric systems with symmetric systems proportioned using a reduced-smooth elastic pseudo-acceleration design spectrum. This design method produces a decreasing ductility demand with increasing period even for the inelastic response of symmetric structures. Consequently, it is not known how the observed parametric sensitivity of eccentric systems would change should the symmetric systems be instead designed to have a similar ductility demand for any period.

2.2.2 A Special Type of Approach to Some Particular Cases

A special type of inelastic torsional coupling was first reported by Tso & Amis (1971) [60]. They observed this behavior when the equations of motion are numerically integrated for the response of a single mass symmetric structure containing special type of non-linear resisting elements and excited by actual ground acceleration records. The two types of element models used by the authors were, (1) hysteretic slip-type with the Ramberg-Osgood function serving as the backbone curve, and (2) elastic with a small softening non-linearity below yield level with plastic deformations at the yield level. Torsional coupling was also noted to occur only for certain values of Ω near 1. By using the Mathieu-

Hill equation (Tso (1975) [59]), variational methods (Antonelli, Meyer and Oppenheim (1981) [2]), and the Kryloff-Bogoliuboff method (Pekau, Syamal (1981 & 1984) [44 and 45], several researchers attempted to provide an analytical explanation for this coupling mechanism. The element model chosen in all of these studies was elastic with weakly cubic non-linear softening and a sinusoidal excitation was typically used.

This kind of inelastic torsional coupling derives from the expansion of the element load-displacement mathematical model into a truncated Taylor series. Once substituted into the dynamic equations of motion, this non-linear restoring force relationship produces torsional coupling of even symmetric systems.

Various parametric studies were performed using this analytical approach. One must realize the limiting assumptions in these studies (i.e. the type of element model used and sinusoidal excitations). The major conclusion of these studies has been that the likelihood of exciting torsional motion is stronger when the uncoupled translational frequencies were nearly equal to the sinusoidal excitation frequency, but can only occur if the uncoupled torsional frequencies of the system is higher than the exciting translational frequency. (The reader interested in further

reading on this topic is referred to Pekau and Syamal (1984) [45] for the most complete treatment).

A very recent study (Pekau and Syamal (1985) [56]) extended these analytical techniques to obtain approximate solutions for the inelastic response of eccentric single-story structures with bilinear hysteretic behavior subjected to sinusoidal ground excitations. Despite the limitations produced by the sinusoidal loading, this study is of interest as it presents analytical results obtained for the response of two-element systems with stiffness eccentricities and bilinear hysteretic relationship for the elements.

The model used had equal strength and stiffness ratios, that is:

$$k_{e\,x}/k_{i\,x} = R_{y\,e}/R_{y\,i}$$

Thus yielding occurred for each element at the same yield displacement, δ_y. The slope of the strain hardening portion of the model was denoted α, with $\alpha=1$ being a perfectly elastic system, and $\alpha=0$ being a elastic-perfectly plastic model.

A different notation was adopted for this paper. The response parameters Ω^* was defined as the ratio of the sinusoidal exciting frequency divided by the uncoupled translational frequency, and Ω_θ^* was defined as the uncoupled

torsional frequency divided by the uncoupled translational frequency (with uncoupled torsional frequency measured around the center of mass). One must be careful about this change in notation.

For α=1, elastic resonance occurred (as expected) at each of the true frequencies, which for the cases studied were close to the value of Ω^*=1. For very low values of α (α=0 and α=0.05), the peaks of maximum amplification of the response occurred for lower values of Ω^*. Response was not as significant at Ω^*=1. The peak maximum inelastic amplification for low values of α (in terms of peak ductility demand response amplitude) was large for the weak element, and rather small for the strong element (and in both cases less than the peak maximum elastic amplification). This maximum inelastic amplification of the weak element response also rapidly increased with increasing normalized eccentricity (e/r). For large values of (e/r) (above 0.15), there was a very rapid increase in the maximum inelastic amplification of the weak element with decreasing values of Ω_θ^*. For smaller values of (e/r), this same maximum inelastic element amplification was very slowly decreasing along with decreasing values of Ω_θ^*. In all cases, large amplifications occur only for low values of Ω^*, usually with peak amplification between Ω^*=0.25 and Ω^*=0.5 (in which range the inelastic amplifications always exceeded the elastic ones).

Finally, it is observed that a structure with small eccentricity does not experience pronounced torsional coupling when the uncoupled torsional and translational frequencies are close, in contrast to the much emphasized observation for linear elastic structures.

2.3 Concluding Remarks

Results from past studies were summarized above in hope of giving a more complete picture of what are currently believed to be the parameters governing the inelastic response of structures with mass and/or stiffness eccentricities. Since many researchers started with different assumptions, it is not surprising that conclusions may appear contradictory at times. Obviously, it can be said that much remains to be learned about this important phenomenon at the heart of many structural failures during major earthquakes. Consequently, more basic work on simple systems is desirable to better understand how torsionally coupled systems are affected by different parameters.

3. INELASTIC RESPONSE OF ECCENTRIC SYSTEMS

In this chapter, a simplified model is introduced in which basic behavioral modes for mass, stiffness and strength eccentricities can be investigated. After describing the mechanical and dynamic characteristics of this system, examples are presented to illustrate sensitivity to various parameters. More extensive parametric studies using this model are presented in the subsequent chapters. More complex structural models are considered in Chapter 6.

3.1 Selection of Basic Structural Model

For simplicity in understanding the coupled torsional response of structures, a simple one story structure with two lateral resisting elements is considered. The structure is monosymmetric with uniaxial loading applied in the direction of the resisting elements. Reasons for choosing this structural model are examined below.

3.1.1 Existence of Structures with Only Two Lateral Resisting Elements

Since architectural functionality of single-story (or low-rise) commercial buildings is often dominant over

structural concerns, dissimilar structural syatems are frequently used jointly in a given principal direction. In fact, many difficult architectural problems can require special structural solutions with large eccentricities and only two lateral resisting elements in the principal directions (for example, large open atriums at the entrance level of tall building). These problems are often unavoidable as even many small and medium size municipalities nov include special architectural requirements in their zoning regulations to favor complex plan and complex elevation (Arnold and Reitherman (1982) [3]). Engineering innovations also contribute to lower structural redundancy (for example, the use of 100 MPa (14.5 ksi) concrete can significantly reduce the number of shear walls needed in each direction). Obviously modern structures have a lower redundancy in their number of lateral resisting elements.

3.1.2 Issues Related to Two-Element Systems

Most current codes allow the use of an equivalent static lateral force design method for regular eccentric structures. The problem of eccentricity is then considered as originating from two sources: accidental eccentricity and true eccentricity. The true eccentricity occurs when the calculated "true" positions of the center of mass and center of rigidity do not coincide. It must be recognized that

these centers can hardly be accurately defined, especially in the case of non-rigid diaphragms or multi-story systems. The accidental eccentricity is usually set by different codes to a small percentage (usually 5 or 10%) of the maximum plan dimension. In an apparently symmetric building, it provides a minimum design eccentricity which is thought to account for uncertainties in mechanical properties, mass distribution, and ground motion.

Should only two lateral load resisting elements be present in each principal directions (see Figure 3.1), 5% accidental eccentricity will increase the design forces in each element by 10%. The translational and torsional stiffnesses will also increase by 10%. If we now consider four equally spaced elements with equal stiffnesses (with a rigid diaphragm assumption), then the design forces will be increased by 18% for the edge elements and by 6% for the inside elements. The net translational stiffness is thereby increased 12% and the net torsional stiffness is increased 17%. This example makes the two element system appear to be the more economic design solution. This appears discordant with earthquake engineering's traditional wisdom that redundancy improves the behavior of structures. Therefore, because they constitute a non-negligeable portion of structural systems used for construction in seismic regions, and also because codes do not discourage their use, it is

appropriate to study further the behavior of two-element systems.

3.2 Systematic Approach to Eccentricity Cases

Even if all variations of system properties cannot be accurately determined, no generality is lost in studying only "truly" eccentric systems. Once the behavior of systems with "true" eccentricities is better understood, allowance for the uncertainly in determining this eccentricity can be included in the design method. Hence, except for a special case of initially symmetric systems with elements of unequal strengths, all structures considered can be classified as initially eccentric systems.

3.2.1 Detailed Description of the Cases Considered

We observe that the two-element system is statically determinate, and consequently the lateral shear force must be distributed to the elements by the laws of equilibrium. A static lateral force applied at the center of mass will be distributed to the resisting elements by geometric relations, and independently of their respective stiffness. In a design process, this will force the resisting elements to be proportioned in such a way that the center of resistance will

coincide with the center of mass (unless the center of mass is not contained between the resisting elements as would be the case for a building with an eccentric core). This will be always possible to achieve if the engineer has total control on the structural layout and dimensioning. If three (or more) resisting elements are provided for the lateral resistance system, many different combinations of stiffness distribution among the resisting elements can be achieved. If the engineer has unrestrained freedom in the structural design, the centers of mass and stiffnesses may be superimposed. However, it must be emphasized that many other eccentric solutions can be found still satisfying the static equilibrium requirement.

In order to clarify the different situations possible for the two element model, a flowchart has been prepared and is presented in Figure 3.2. If the two elements are exactly of equal stiffness and the center of mass is located at mid-distance between them, the system will be considered symmetric provided both resisting elements yield simultaneously.

Nevertheless, a special situation exists when the system is considered to be perfectly symmetric initially, but where the different resisting elements do not yield simultaneously. A transient state of torsional coupling will therefore be excited during the inelastic part of the response; that is,

torsion will be excited when one of the element is yielded and the other one remains elastic, creating an instantaneous eccentricity. When the system response diminishes and returns to the elastic range, torsional movements will be eventually damped out provided the resisting elements are represented by ideal elasto-plastic models. Thus, eccentricity here exists primarily in the non-linear phase of the response, and only coupled torsional/translational inelastic analyses can provide an estimate of the maximum deviation from the otherwise predicted purely translational movement.

In the case where both elements are of equal stiffness, if the center of mass is not at mid-distance between the two elements, we will have a mass eccentric system. This is possible for irregularly shaped floor plans, nonuniform mass distributions, or when the center of mass is not contained between the two resisting elements.

Frequently, architectural requirements impose resisting elements of unequal stiffnesses. As an illustration, we might consider a simple situation in which columns on one side of an otherwise symmetric structure are held captive over a portion of their height by "rigid" non-structural partitions. The effect of the partitions is to truncate the effective length of the column, thereby increasing the stiffness of the columns. Moreover, as the captive columns

are present only on one side of the structure, a strong difference in the stiffness of the lateral load resisting elements is now created. To provide symmetry, the center of mass would have to coincide with the center of stiffness which has now moved toward the stiffer element. Obviously, the engineer cannot move the center of mass easily.

Since the force in each resisting element is independent of the stiffness of each resisting element in a two-element system, the engineer may simply design each element to be at least able to resist the design force (with the stiffer element simply having more than needed capacity). Although the displacements are dramatically different than for the symmetric case, the design still appears safe since the edge displacement of each element is equal or less than for the symmetric case. This is illustrated in Figure 3.3. The truth is quite different as may be demonstrated by an example.

It is reasonable to assume that this system (Figure 3.3) would undergo large inelastic deformations during a real earthquake having intensity equivalent to the design earthquake, and it is not unrealistic to expect it to reach a ductility of four or so in some cases. So to reveal the inelastic behavior of this system, the N-S component of the 1940 El Centro earthquake record was scaled such that the symmetric two-element system would reach a ductility of

exactly four from an inelastic step-by-step dynamic analysis. Then, the stiffness and strength of one of the elements was increased successively by 50% and 100% resulting in the structure shown on the right-hand-side of Figure 3.3. Elements were modeled as bi-linear hysteretic with 0.5% strain hardening. The results are presented in Table 3.1 and Figure 3.4. Also presented are the results for the elastic analysis with the same earthquake scaling.

Clearly, these results demonstrate the large edge displacement amplification produced by the inelastic torsional coupling of the structure. The ductilities so obtained are substantially different from anything that could be predicted from the static analysis. Also, the elastic dynamic step-by-step analysis could not predict the significantly increased demand on the weak element. This is of large consequence: i.e., even if the engineer had invested more effort and performed an elastic step-by-step dynamic analysis, the large ductility demand on the weaker element could not have been identified (not even inaccurately).

3.2.2 The Type of Eccentric Systems Considered

Two major types of eccentric systems were identified in the preceding section: the initially symmetric and initially eccentric systems.

The initially symmetric system occurred when the designer could control exactly the structural design and superpose both centers of mass and stiffness. As soon as there is a discrepancy in the yielding stress of one of the elements, inelastic torsional coupling will result from the instantaneous eccentricity created by the inelastic behavior of the structure.

The initially eccentric systems will be further subdivided into the mass eccentric and stiffness eccentric systems. Of course, a combination of both cases is possible, but keeping the simpler classification is adequate for now. These are the two type of systems adopted for this study.

A major problem then is to be able to understand how significantly inelastic behavior will deviate from elastically predicted behavior. More specifically, if a designer uses the elastic dynamic analysis method in hope of setting the overstress to some predetermined value in all resisting elements of a given structure, is this sufficient to assure that the structure will not reach intolerable ductilities during a severe earthquake? Another major concern is to understand how the inelastic eccentric system behavior will differ from an "equivalent" inelastic symmetric system.

3.3 Models Used for Initial Parametric Studies

For inelastic analyses to predict the true behavior of torsionally coupled structures supposes that the resisting elements are properly modelled. Since very little is known about inelastic response of torsionally coupled systems, it would be premature to introduce too many modeling refinements at this stage.

The traditional bi-linear elasto-plastic hysteretic model (with strain hardening) seems appropriate for these preliminary studies. When the influence of different parameters (Ω, e/r, etc.) on the inelastic response of torsionally coupled systems is better understood, other models will be considered, as done in Chapter 6.

Finally, for the bi-linear elasto-plastic hysteretic model, it must be decided how the different elements relate to each other. Here again, an extensive coverage of all possibilities is beyond the reach of this study, and some simplifying assumptions are required. The element models adopted for this study (presented in Figure 3.5) are described by their restoring force-displacement relationships. Therefore, any structural layout conforming to this model representation will produce similar results. For simplicity's sake, bi-linear hysteretic springs were

chosen for computer modelling since they are sufficient to provide insight into the real behavior. Therefore, the restoring force equation in the elastic range can be expressed by:

$$R = K\,\delta = (AE/L)\,\delta = A\,\sigma$$

where E (modulus of elasticity) and L (spring length) are preselected, and only the spring area A needs changing to provide the various stiffnesses required. Moreover, for a given structural stiffness, the yield strength becomes directly related to the yield stress (and yield displacement) by:

$$R_y = K\,\delta_y = (AE/L)\,\delta_y = A\,\sigma_y = A\,F_y \quad \text{(Notation } \sigma_y = F_y\text{)}$$

and either term can be used to express the variation in yield level. Also, as shown in Figure 3.5, the center of mass of the floor is assumed equidistant to each element. Reasons for studying the stiffness eccentric system first will be presented below.

The models used for initially eccentric systems have equal yield displacement. This situation is representative of moment resisting frames if the section used as columns in both frames are of the same nominal depth and of the same length, or also of braced frames where the compression brace

does not buckle but yields in compression (very stocky braces). Initially eccentric models where the yield displacements do not coincide for each element could have also been considered, but it was thought that the present model is sufficiently realistic, and also limits the parametric studies to reasonable bounds. This model is also similar to ones used in previous studies, which will allow some comparison of results with this earlier research. Nevertheless, in order to illustrate the effect of different yield levels for the stronger element, some dynamic analyses will be presented Section 3.10.

The model used for initially symmetric system is representative of a case where the designer succeeded in calibrating the stiffnesses such that they are equal, but yielding does not occur simultaneously. As explained previously, this model is realistic if dissimilar systems are used on each side, although it could also represent statistical variations in yield capacities of similar systems.

An additional advantage of the bi-linear type of element model is the ability to easily compute an instantaneous eccentricity corresponding to all possible steps during the progression of yielding. There is a relatively small number of possible values of instantaneous eccentricities for this well behaved model. This will allow subsequent establishment

of some equivalence between the inelastic behavior of different systems. This is by opposition to stiffness degrading element models where there is an infinite number of instantaneous values for the inelastic eccentricity.

Furthermore, for the bi-linear hysteretic elements in this study, the ductility factor is simply defined as the maximum element displacement (in absolute value) divided by its yield displacement, that is:

$$\mu = | \delta_{max} | / \delta_y$$

This maximum displacement ductility factor definition is an adequate indicator of the severity of the inelastic element response for this investigation. If we wish to quantify the severity of an elastic response instead, an overstress factor is defined similarly where δ_{max} is now the maximum elastic response (δ_y being still the yield displacement from the equivalent inelastic model).

Finally, Rayleigh type damping is specified at 2% of the critical damping at each mode of the two-degree of freedom systems studied.

3.4 Requirements for Geometry-Independence in the Inelastic Response of Two-Element Systems

It is demonstrated in Appendix A that two systems have the same dynamic inelastic response $v_1(t)$ and $rv_\theta(t)$ [$v_1(t)$ and $v_\theta(t)$ being the translational and rotational degrees of freedom at the center of mass], if they have the same uncoupled torsional and translational frequencies (ω_x and ω_θ), have the same normalized eccentricity (e/r), are modelled with the same Rayleigh-type damping, are submitted to the same earthquake excitation and change to the same tangent properties simultaneously all the time (this last requirement implies same element models and same inter-element model relations are used for the whole system). This seems to be very restrictive, but in fact it still allows some freedom in geometry for the two-element model.

Figure 3.6 illustrates how two-element systems with the same ratio $d/r=D$ can be of different geometry and still have the same element response (recall that d is the distance from the center of mass to the elements in a stiffness eccentric system). This ratio $d/r=D$ fixes the proportional geometric configuration of a system as scaled by its radius of gyration. It is more restrictive than simply fixing the e/r ratio. It means that similar element time histories and ductility demands can be obtained from a wider structure with a larger radius of gyration as long as the d/r is ratio is

preserved. However, the maximum angular response will be lower (recall from derivations in Section 2.1.3 that $rv_e(t)$ is preserved, not $v_e(t)$).

In mass eccentric systems, we will have different values of $d_i/r=D_i$ (i being index for i-th element). Whereas it is possible to have a mass eccentric system and stiffness eccentric system sharing the same e/r values, their D_i's will be different. It is therefore predicted that their inelastic response will not be the same. Of course, the (e'/r) values wouldn't be the same either in that situation and the inelastic response could have been predicted to be different without considering the d_i/r ratios. Since the D values are calculated from initial properties only, it is preferable (and easier) to keep track of the D_i's than evaluating all possible instantaneous eccentricities e'.

3.5 Additional Remarks for Multi-Element Systems

For multi-element systems, the same geometric non-dimensional form derived for the two-element system in the above section is applicable. Again, all constants ($d_i/r = D_i$) must be the same between the two systems for the response to be similar.

Therefore, all systems with the same D_i's, ω_x, ω_θ and (e/r) (and of course same damping, earthquake excitations, element models and model inter-relation between different elements) will have the same element inelastic response.

For a given value of ω_x, ω_θ and e/r, only one geometric pattern is possible for a stiffness eccentric two-element system with equidistant elements, and thus only one set of D_i's. A unique geometry is defined by also specifying r. For a multi-element system, even if the elements are equidistant to the center of mass in pairs, there are still many possible values of D_i's for given ω_x, ω_θ, e/r and r. This is easily illustrated for the case of initially symmetric systems with four elements. We notice (Figures 3.7a and 3.7b) that some systems with very stiff near elements and very weak far elements can be elastically equivalent to more balanced systems. Since all these systems have same ω_x, ω_θ, and e/r, their elastic response will be the same, and since they also have the same radius of gyration (r), their angular response will be similar. This leads to the prediction of early yielding (and likely relatively larger ductility demands) of the edge elements. If we release the constraint of equidistant elements for stiffness eccentric systems (or similarly the constraint of symmetric stiffness distribution for mass eccentric systems), we now have a situation of arbitrarily eccentric systems, and therefore, many geometries (sharing equal parameters ω_x, ω_θ,

e/r and r) can be possible even for the two-element systems, as illustrated in Figures 3.7a and 3.7c. The center of mass is always outside of both resisting elements for these figures. This is an additional advantage of considering the analysis of mass or stiffness eccentric systems rather than arbitrarily eccentric systems.

3.6 Effect of Strain Hardening

A relatively simple (although incomplete) way to illustrate the effect of strain hardening on bi-linear hysteretic model is by the application of a monotonically increasing load at the center of mass. In a static loading situation, when there is no strain hardening, any two element system becomes unstable as soon as only one of the elements yield, and the maximum angle of rotation is infinite.

For initially symmetric systems, if we still consider a monotonically increasing static load but now with a finite value of strain hardening, the maximum rotation developed during the phase where only one element is yielding can be calculated. When both elements are yielded, the displacement returns to a purely translational state if the strain hardening stiffnesses are equal (the new instantaneous center of stiffness again coincides with the center of mass). This type of analysis reveals a very important consideration for

initially symmetric systems with different yield values: torsional coupling is only excited when one of the two resisting elements is yielded. Increases in strain hardening will obviously reduce the maximum calculated static angle of rotation.

Dynamic analysis of initially symmetric system reveals similar observations as torsion can be observed to behave in a "damped free vibration" manner after being abruptly excited during inelastic excursions. Increases in strain hardening also tended to reduce the maximum angle reached during the response. This is illustrated by the time history results from an inelastic dynamic analysis as shown on Figure 3.8.

Initially eccentric systems exhibit constantly varying rotations (even when loaded statically), but this rotation is again significantly amplified while the system has only one element yielded. Monotonically increasing loading produces trends similar to the ones mentioned for the initially symmetric systems. Unfortunately, the torsional contribution to dynamic response does not necessarily decrease with increasing strain hardening. Figures 3.9a and 3.9b illustrate two cases: an increase in strain hardening reduces the maximum response (translational as well as rotational) in one case, but increases it in another. Nevertheless, the final displacement offset is reduced for larger strain hardening values in both cases. It is obvious that very

minor differences in the early response of comparable systems with different strain hardening have major effects on the overall behavior, especially under large ductility demands. It is understood that after an initial yield excursion, the bi-linear model will make the element with the largest strain hardening yield at a lower stress during load reversal; this may account for the striking differences in behavior.

The above observations illustrate the strong element model dependency of the torsionally coupled problem in the inelastic range which will be the subject of further studies in the following chapters.

3.7 Effect of the Rotational Inertia

Although the radius of gyration r (around the center of mass) is not a non-dimensional parameter, something fundamental about torsional response can be detected by simply varying this parameter. Practically speaking, varying r alone is synonymous to varying the floor plan, which is not possible usually in practice. Nonetheless, the study of the effects of variation in radius of gyration on response is of interest.

A reduction in the radius of gyration r will increase the value the normalized eccentricity (e/r), but will not

change the true eccentricity. More importantly, it will reduce the mass moment of inertia mr^2 (therefore increasing $\Omega=[K_\theta/(r^2K_x)]$). If the mass moment of inertia is very small, it is easy to produce a rotational movement as there is little inertial resistance to the induction of angular motion. In the opposite fashion, if the mass moment of inertia is very large, considerable inertial resistance to angular motion exists and very little of it may develop.

Figures 3.10a and 3.10b demonstrate this phenomenon for an initially symmetric system of uncoupled frequency $T_x=0.1$ seconds, bi-linear elements with 0.5% strain hardening (one of them yielding at 80% F_y, the other one at F_y), 2% damping and values of Ω of 0.4, 1.0 and 1.6, under the N-S component of the 1940 El Centro earthquake record scaled to a level such that a single degree of freedom system of 0.1 second period would reach a ductility of 4. Obviously from these figures, the systems with lower radii of gyration (higher Ω) produce a larger angular motion.

3.8 Effect of Different Earthquake Intensities

It has been noted in previous research (Kan and Chopra (1979) [31]), while comparing the inelastic and elastic response of torsionally coupled single story systems subjected to a given earthquake, that the translation at the

center of mass is usually larger for the elastic response. Without undertaking a complete parametric study, it is interesting to briefly investigate the effect of increased earthquake intensity on some typical structures for the two types of inelastic systems discussed previously.

3.8.1 Initially Symmetric System

For this study, a two-element system with period of 0.4 seconds, 2% viscous damping, d/r=1.6, r=31.25, Ω=1.6 and with bi-linear element models with 0.5% strain hardening, was subjected to the N-S component of the 1940 El Centro earthquake record. Inelastic torsional coupling was produced by the unequal yield stress of the two elements: one element would yield at 0.8 Fy, the other at Fy. For these examples, an earthquake level of unity is defined as producing a maximum displacement equal to the yield displacement for the elastic symmetric system (yielding at Fy). Any other level is simply a direct scaling of the earthquake by that value (for example, for a yield displacement of δ_y=0.12 inch, a earthquake level of 5 will produce an elastic symmetric system response of 0.6 inch).

The results for this initially symmetric system under earthquake levels from 1 to 12 are presented in Figures 3.11 through 3.13. Response of symmetric elastic and inelastic

systems without torsional coupling are represented by solid lines, whereas the element response of the two-element system with unequal yield stress are shown by dotted lines. Despite the fact that the center of mass is equidistant from each element in the model, the maximum displacement at the center of mass is not necessarily equal to the mean value of the maximum response of both elements (although this is often a good approximation). From Figure 3.11, it can be said that the mean value of the maximum response of each element (in the system with unequal yielding) is approximately equal to the maximum response of the uncoupled inelastic systems. However, at some times the coupled systems have a slightly larger response. For all levels, the uncoupled inelastic response curve is between the ones for the coupled system; the element with smaller yield stress having the largest ductility demand at all times. The cyclic ductility, defined as the sum of the absolute values of the maximum displacement in each direction divided by the yield displacement, has also been calculated and results are presented in Figure 3.12. Conclusions are similar to those for the standard ductility definition case, with the exception that the ductility demands are larger.

It is of great interest to see how the earthquake level affects the maximum rotations recorded during the response. As expected, the maximum attained angles increase somewhat

proportionally with the earthquake level in a well behaved manner as indicated in Figure 3.13.

Finally, some sample time histories are presented in Figures 3.14a and 3.14b in order to emphasize the high degree of similitude between the responses of both types of system. However, general behavioral characteristics cannot be concluded from just a few examples. The following chapters will provide more in-depth studies.

3.8.2 Initially Eccentric System

For this study, a two-element stiffness eccentric system with uncoupled period T_x of 0.1 seconds, 2% damping, $(e/r)=0.3$, $r=33.3$, $\Omega=1.5$ and bi-linear element model with 0.5% strain hardening, was subjected to the N-S component of the 1940 El Centro earthquake record. Similarly to the previous examples, an earthquake is said to be of level one when it makes the first element yield. Ductilities and other earthquake levels are defined as in the preceding section.

The results for this initially eccentric system under earthquake levels from 1 to 12 are presented in Figures 3.15 and 3.16. The weak and strong element responses are plotted with dotted lines, the weaker element always having the larger ductility demand. Although, the true coupled system

has periods of 0.1036 and 0.0657 seconds, it is interesting to compare its response with the similar response obtained from a symmetric system of period 0.1 second (some 0.1036 sec. symmetric systems were also analyzed and they compared well with the 0.1 sec. case; the 0.1036 sec. system developing 15% less demand at low earthquake levels, and 4% more demand at high levels). This symmetric response, along with the coupled elastic response of the weak element (in which case overstress is plotted instead of ductility) are the solid lines on the same figure. Note that the ductility demand is very severe for both the uncoupled and coupled systems, and that actual structures are not expected to be excited to the extreme ductility values indicated on these plots.

Again, it can be said that the average between the strong and weak element maximum response in the inelastic torsionally coupled system is approximately equal to the uncoupled inelastic system response, except for large earthquake levels where the symmetric system seems more demanding (although both systems have unreasonable ductility demands at that point).

The maximum rotations recorded during the responses again increase proportionally with the earthquake level (Figure 3.16). In this case the rotations become huge, and

some care must be taken in interpreting the results. Some representative time histories are presented in Figure 3.17.

3.9 Mass Eccentricity vs Stiffness Eccentricity

In the elastic domain, it is not necessary to distinguish between mass eccentricity and stiffness eccentricity. As demonstrated in Chapter 2, all systems sharing the same response parameters ω_x, ω_θ and (e/r) will have similar response ($v_1(t)$ and $rv_2(t)$) around their center of mass. Nevertheless, it is understood that an individual element response is not only affected by its distance from the center of mass, but also by the global distribution of the resisting elements.

In the inelastic domain, the response at the center of mass is not guaranteed to be the same anymore unless the global distribution of the resisting elements is also the same. Sections 3.2 and 3.3 have already described the differences between mass eccentric and stiffness eccentric systems and addressed the necessary conditions to insure similar response between two inelastic systems. This section briefly studies mass and stiffness eccentric systems which would be equivalent in the elastic domain. Observations regarding differences in their response are made.

Two sets of "elastically equivalent" mass and stiffness systems are investigated here, corresponding to cases of large and small actual eccentricity. Both sets have an uncoupled translational period of 0.1 seconds, 2% damping, 5% strain hardening (higher than the 0.5% value used in most previous sections), and were subjected to the same N-S component 1940 El Centro earthquake record arbitrarily scaled to produce reasonable overstress (measured elastically) in all elements.

The first set had a ratio of uncoupled frequencies Ω=1.5 and a normalized eccentricity (e/r)=0.3. For elements a distance of 100 inches apart, this translates into a true eccentricity of 10.2 inches for the mass eccentric system and 10 inches for the stiffness eccentric system. The true periods were calculated to be 0.1036 and 0.0657 seconds. The second set has a ratio of uncoupled frequencies Ω=0.5 and a normalized eccentricity (e/r)=0.3. For elements 100 inches apart, this translates into true eccentricities of 37.5 inches and 30 inches for the mass and stiffness eccentric systems, respectively. The true periods were calculated to be 0.2628 and 0.0951 seconds.

Results from elastic and inelastic step-by-step analyses are presented in Figures 3.18 and 3.19 (all plotted at the same scale to provide a better perspective). As predicted, the elastic response at the center of mass is similar in each

set, but the element responses are different, affected by their relative position with respect to the global system. Furthermore, the inelastic systems responded differently, even at their centers of mass. The set with the larger eccentricities presented more significant differences. The actual time histories are presented in Figure 3.19 to better illustrate the differences in behavior.

It appears that the more severe element ductility demand was produced in the weak element for the stiffness eccentric system. That is logical, as the distance from the weak element to the center of mass is greater in the case of stiffness eccentric system. The stiffness eccentricity is, therefore, believed to be more conservative (for the same earthquake intensity). If this is the case, conclusions obtained from stiffness eccentric systems may be conservatively used for mass eccentric systems.

Also, if it is desired to set the elastic response of the front element to be similar for the mass and stiffness eccentric systems, it would be necessary to scale each system to different earthquake levels. In such a case, the mass eccentric system may need to be subjected to a much larger earthquake, and consequently, the inelastic response of the mass eccentric system may largely exceed that of the stiffness eccentric system.

3.10 Plastic Centroid --- Inter-Element Model Relations

As mentioned earlier, the inelastic response of systems with plan eccentricities strongly depends on the element model chosen. Furthermore, for a given model, the relative yielding levels between different elements will also affect the global behavior. For a bi-linear strain-hardening two-element model (and a given set of Ω, (e/r) and T_x, of course), the respective yield displacements (and thus yield stresses for the spring model) between the two elements will completely define this inter-element model relation.

By analogy with reinforced concrete theory, a plastic centroid can be defined: this is the point where a static lateral load must be applied in order to produce a purely translational displacement when all elasto-perfectly plastic elements are yielded. The plastic centroid distance from the center of mass can be used yet as another indicator of the severity of the system inelastic eccentric behavior. A plastic centroid distance of zero would produce simultaneous yielding of both elements under a monotonically increasing static loading, although under dynamic excitation it is not necessarily the case (as two modes are actually excited here).

In order to gain some insight into the effect of the plastic centroid distance on the global system response, the two stiffness eccentric systems used previously (Ω=0.5 & 1.5 for e/r=0.3 and T_x=0.1) were reanalyzed using various yield stress levels for the stronger element (thus changing the plastic centroid distance). Figure 3.20 summarizes the cases studied and the maximum displacements obtained are listed in Table 3.2. As the yield strengths and stresses are uniquely related for the spring model used, it is more expedient to present the results in terms of stresses, the lower values in Table 3.2 corresponding to R_1 in Figure 3.20. Figure 3.21 displays the complete displacement and rotation time histories. These should be compared with the ones obtained for the case of equal element yield stresses presented in a preceding section (Figure 3.19).

Interestingly, changes in plastic centroid distance have a serious effect on the element whose yielding stress is varied, and relatively little effect on the "weak" element whose yield stress is kept constant throughout the parametric study. From Table 3.2, the maximum response variation of the weak element is not more than 16% whereas the strong element response variation exceeds 500% when comparing the results from the smallest and largest plastic centroid distance analyzed. Actually, if the maximum response of the weak element is of concern, it appears adequate to adopt a model with equal yield stresses (and yield displacements), as has

been done for most of this chapter. If the strong element's response is also of interest, its high sensitivity to the plastic centroid distance makes the inter-element model relation a more important issue (despite the fact that for this example, the maximum measured rotations were not as considerably affected by the plastic centroid distance as the maximum measured displacement). Nevertheless, only two examples (e/r, T_x, Ω=constant) are studied here, and too many generalizations should be avoided.

3.11 Additional Observations on Symmetric vs Eccentric Systems

It is interesting to observe how the inelastic eccentric response compares with the inelastic symmetric response of similar true period (i.e. the symmetric system translational period equal to the true first period of the eccentric system). For this purpose, a 0.263 seconds period system was scaled such that its elastic response would be the same as the weak edge element elastic response for the stiffness eccentric system with parameters T_x=0.1, Ω=0.5 and e/r=0.3 and equal element yield stresses (which also has a first true period of 0.263). This symmetric system was then analyzed inelastically and compared with the eccentric system inelastic behavior: results are presented in Figure 3.22. It is shown that the symmetric system response tends to follow

rather closely the weak edge element response. No general conclusions should however be drawn from this observation at this stage.

3.12 Concluding Remarks

Structural systems with two lateral load resisting elements in each principal direction constitute a significant portion of construction in seismically active regions (Section 3.1.1). When concerned with inelastic torsional coupling, it is useful to consider the existence of initially symmetric systems and initially eccentric systems, this last category further divided into mass eccentric and stiffness eccentric systems.

Results presented clearly indicate that the inelastic response of torsionally coupled systems may not be accurately predicted by equivalent static or dynamic elastic analyses. Thus, the ability to predict and control the severity of the resulting inelastic deformations is a major concern. To achieve this goal, a simple bi-linear hysteretic model is selected for study along with an appropriate inter-element relationship. An initially eccentric system model with resisting elements having identical yield displacements is adequate when concerned with the "weak" element response.

The requirements for geometry-independence in the inelastic response of two element systems is far more restrictive than in the elastic case, but the establishment of an equivalent geometric pattern is made possible by the introduction of proportional geometric configuration ratios D_i's.

Increases in strain hardening tend to reduce the maximum angle reached during the response of initially symmetric systems. In the case of initially eccentric systems, the effect of strain hardening seems inconsistent from case to case, although the final displacement offset decreased with increased strain hardening in all cases studied. These observations outline the high sensitivity of the response to the hysteretic model characteristics.

The mass moment of inertia influences the torsional response by offering an inertial resistance to the introduction of angular motion. This parameter was demonstrated to directly affect the response of initially symmetric systems where torsional response is a "transient" state. For initially eccentric systems, variations of the mass moment of inertia alter the fundamental parameters to a larger extent and a more complete treatment is presented in Chapter 5.

Stiffness eccentric systems have more severe element ductility demand than their corresponding mass eccentric systems. It is believed that study of these systems will provide conservative conclusions.

The effect of the traditional torsionally coupled response parameters (namely Ω, (e/r) and T') on the inelastic response of initially symmetric and eccentric systems remains to be determined. This more comprehensive investigation will be accomplished in the following chapters.

4. INITIALLY SYMMETRIC SYSTEMS: PARAMETRIC STUDY

The concepts underlying the study of initially symmetric systems have been discussed extensively in the previous chapters. Once it is realized that the initial coincidence of the centers of mass and rigidity will not insure a torsion-free response, it becomes imperative to investigate in more detail the influence of the system's other basic parameters. This is the intent of this chapter. The effect of period, ratio of uncoupled frequencies, and ductility levels will be studied on two element systems with different combinations of yield levels; the results will be compared with those for equivalent single-degree-of-freedom systems. Furthermore, it will be assessed how these observations will impact the design of structures.

4.1 Choice of Parameters

The bi-linear hysteretic element with strain-hardening was again chosen for this study. Its simplicity is warranted here in order to discover the trends in response. Strain-hardening was chosen as 0.5% (i.e. E_{s_H} = 0.005 E), making the element model nearly elasto-perfectly plastic.

Since a time history approach (step-by-step analyses) is adopted in this study, it is essential to use many earthquake records; this is to insure that the observed trends will not

be affected by special characteristics of a particular earthquake. On the other hand, as there is already a substantial quantity of parameter combinations to be considered, using a large number of earthquake records could very quickly require unreasonable amounts of computer time. As a compromise, five earthquake records were used: El-Centro 1940, Olympia 1949, Taft 1952, Parkfield 1966 and Pacoima Dam 1971 (more detailed descriptions of the components used are presented in Table 4.1). These earthquakes represent a wide variety of earthquake types and magnitudes as well as site conditions. All these earthquakes were truncated after 15 seconds; this facilitates the parametric study and is deemed acceptable in light of the apparent duration of the accelerograms. The earthquakes records used are shown in Figure 4.1.

The main system parameters that were varied during this investigation were: the uncoupled period T_x, the ratio of uncoupled frequencies Ω, the ductility levels and the element yield level combinations. Ten values of uncoupled periods were used (0.1, 0.2, 0.3, 0.4, 0.6, 0.8, 1.0, 1.2, 1.6 and 2.0 seconds), as were six ratios of uncoupled frequencies (0.4, 0.8, 1.0, 1.2, 1.6, 2.0), two ductility levels (4 and 8) and four element yield combinations (0.8 Fy and Fy, Fy and 1.2 Fy, Fy and 1.5 Fy, Fy and 2 Fy).

The ten uncoupled period values are believed to be representative of most structures potentially affected by torsional response. It should be noted that the 1.6 and 2.0 seconds cases will undergo very few cycles of structural response when only 15 seconds of earthquake excitation is considered, and therefore, some caution must be taken here in interpreting these results. However, these are also probably tall structures, wherein extensive redundancy tends to induce an apparent strain hardening.

The six ratios of uncoupled frequencies were chosen to allow a good distribution of values around the case with $\Omega=1$ (traditionally quoted as the unfavorable situation). The case $\Omega=2$ was added to extend further the possibility of studying the effect of the radius of gyration (and mass moment of inertia) as explained in the previous chapters.

The four chosen yield level differences are thought to bracket most of the possible situations. It should be noted that further increasing the difference between the strong and weak elements could lead to permanent elastic response of the strong element, and past that threshold, all greater yield differences would produce no change in element response. The difference in yield levels is not intended to represent a statistical variation on the yield level of a given material (although it can be part of it), but rather the difference in yield levels as a direct result from the difficulty

(impossibility in some cases) in achieving similar stiffnesses and yield levels. This is especially true when the structural systems used to resist the lateral excitation in a given direction differ among themselves. This difference also implicitly considers the difficulty in accurately predicting the yield level of some structural systems. The cases of "0.8 FY and Fy", and "Fy and 1.2 Fy" are representative of a small mismatch in yield level, where the error alternatively consists of an understrength and an overstrength. The cases "Fy and 1.5 Fy" and "Fy and 2 Fy" represent larger differences (the possibility of crossing the threshold where the stronger element would remain elastic was not explicitly considered). All of these cases will be compared to the response of the equivalent symmetric case with yields levels "Fy and Fy". The intent is not to compare systems of similar strengths, but rather to assess how significant would be an over or under-estimation of the yield level of one element.

The systems studied in this section consisted of two elements equidistant to the center of mass. Therefore, for a unique set of parameters T_x, Ω and e/r, a unique d/r ratio is produced which allows non-dimensionality of the structure. Nevertheless, in this modeling, d was arbitrarily chosen as 50 units. Therefore, for the systems under study, there is a direct relation between r, d and Ω which simplifies to:

$\Omega = d/r = 50/r$ (specific case) or $r = 50/\Omega$

In order to better illustrate the effect of torsional coupling, it was decided that the response of these systems should be compared with that of their equivalent symmetric (SDOF) single degree of freedom systems. Also, to insure a fair comparison at different period values, it was decided to help isolate the influence of the period response by using uniform ductility levels. Not having any variations in the ductility levels of the different SDOF systems would insure that any changes in the response of the torsionally coupled systems with the period could not be attributed to an underlying modification in the equivalent SDOF system's inelastic response. This disassociation of the period from the SDOF's response allows observation of how the period as a parameter in itself affects inelastic torsional response. Ductility levels of 4 and 8 were chosen. The ductility level of four represents the traditional ductility value that has long been used by the profession. The ductility of eight represents an upper bound that might be considered for some types of structural systems. Also using a ductility of eight for this study will allow one to see how the torsionally coupled response of initially symmetric systems is affected by varying levels of excitation.

Since the systems are initially symmetric (e/r = 0), the relation between the uncoupled frequencies and the true frequencies is rather simple. By simplifying the expression

in Chapter 2, the true frequencies are found to be equal to the uncoupled translational frequency and Ω times the uncoupled translational frequency, or in term of periods:

$$T_1 = T_x / \Omega$$
$$T_2 = T_x \qquad \text{when } \Omega < 1.0$$

$$T_1 = T_x$$
$$T_2 = T_x / \Omega \qquad \text{when } \Omega > 1.0$$

$$T_1 = T_2 = T_x \qquad \text{when } \Omega = 1.0$$

with T_x the uncoupled translational period.

In all cases, the only period of system excited before initialization of yielding is T_x, which is also the period chosen for the equivalent SDOF systems.

The damping was chosen to be of the Rayleigh type, arbitrarily set to 2% of the critical damping at each of the true frequencies of any given system analyzed. That is, the mass proportional and stiffness proportional coefficients were recalculated for each set of parameters.

The inelastic step-by-step time history analyses were performed using the program ANSR (Powell and Mondkar (1975) [39] & [40]). ANSR was chosen mainly for its ease of

incorporating three dimensional models, which will be useful in the later stages of this study. The time step used in each time history analysis was chosen to be smaller than T/40, where T is the smallest of the two true periods (the only exception being for T_x=0.1 seconds when Ω=1.6 and 2.0 where T/30 and T/25 were used, respectively).

4.2 Procedure Followed

In order to be able to compare the results from the parametric study described above, the following procedure was adopted:

1) The single-degree-of-freedom systems with the equivalent periods T_x and yielding at the stress Fy were analyzed inelastically. The task was to find the proper strength factors for which the attained target ductilities would be 4 and 8. The program NOSPEC (Khatib & Mahin [34] and Mahin & Lin (1983) [33]) was used, and for every combination of parameters, the strength factor,

$$\eta = R_y \; / \; m \; a_{MAX},$$

was estimated (where a_{MAX} is the maximum acceleration for a given earthquake record). Since in the two element system the element dimensions are unique for a

given set of uncoupled translational and rotational frequencies (and e/r, but here it is always zero), either the yield stress or the earthquake maximum acceleration could have been changed to get the proper strength factor in any given case. For simplicity, it was decided to scale the earthquake as necessary for each parametric case.

2) Once, the strength factors were determined (and the earthquake levels calibrated as predicted by NOSPEC), the SDOF systems were analyzed using ANSR to obtain an accurate estimate of the ductility demand. All final ductilities for the SDOF systems analyzed were between 3.8 and 4.2 when the target ductility was 4, and between 7.7 and 8.3 when the target ductility was 8. This represents a deviation of 5% or less from the targeted ductilities.

3) The same systems were analyzed (using the "fine tuned" earthquake levels), but now the unequal element yield strengths were taken into account. For each individual analysis, the maximum element displacements and the maximum angular response attained during the whole time history were calculated.

4) For each analysis with unequal yield levels, the new ductility demands were calculated. One must recall

Figure 3.5 and realize that the elements were modeled such that the yield displacement δ_y would always be directly proportional to the yield stress (more precisely, the model was such that for a given geometry, modulus of elasticity and yield stress, the yield displacement would always be the same). Although the yield displacement differs for unequal element yield stresses, it is still easy to obtain them back from the ductilities as they are proportional to the yield stress F_y. For example, in the case "F_y and 2 F_y", the strong element would be said to have a ductility of 1.0 when its displacement would reach $2x\delta_y$, since δ_y is the same for all elements having a yield stress of F_y. As this study is more concerned with damage issues, the ductilities will be the basis of comparison, but one must not forget the serious implications of larger displacement on other issues like non-structural damage, stability (for P-delta effects), or other parameters more sensitive to the relative displacements.

5) The ductilities calculated for each individual case analyzed above are then divided by their respective target ductility obtained in the equal yield stress cases. If all the SDOF ductilities would have been exactly calculated as 4 and 8, there wouldn't really be a need for this stage of data manipulation, but as the targeted ductilities were imperfectly matched, this

additional "scaling" will insure a proper perspective while interpreting the data. For example, a SDOF system could have reached a ductility factor of 3.8, and the weak element could have only increased to a ductility of 3.95 in the case of unequal yield stresses. The ratio of ductility factors would then be 1.04. Although the variation might not be significant, it would clearly indicate an increase in demand. It could have been otherwise believed that the "unequal yield case" response was less than the equivalent "equal yield case". Therefore, the results are plotted in terms of ductility ratios, meaning the "unequal yielding case" element ductility factor divided by the "equal yielding case" element ductility factor.

6) Finally, the mean and mean-plus-one-standard-deviation are calculated for all response values over the five earthquakes to provide results less sensitive to the particular characteristics of single earthquakes.

To provide an example of how to interpret the results, let's assume that for a given period and Ω value, and for the "F_y and 2 F_y" case, the ductility ratio is calculated as 2.5 for the weak element and 0.75 for the strong element (the strong element being defined as the one with the higher yield stress) when the target ductility was 8. Interpretation of these results must be done as follow: The target ductility

being 8, the ductility in the case with unequal yielding must then be 2.5 x 8 = 20 for the weak element, and 0.75 x 8 = 6 for the strong element. Since the yield displacement is δ_y for the weak element and $2\delta_y$ for the strong element, the weak element absolute displacement is 20 δ_y, and the strong element absolute displacement is 12 δ_y.

Another indicator of the occurrence of torsional motion would be the maximum angular response. This response parameter (calculated in radians) not only indicates the existence of angular motion, but also illustrates its severity for a given case. Traditionally, the radius of gyration times the maximum angular motion has been used to quantify the sensitivity of the systems (as it is the response value used in the derivation of the nondimensionalized elastic equations). Although it is an indicator of how serious the torsional motion is with respect with the center of mass, it does not directly reflect the magnitude of torsional effects on the elements. Furthermore, as Ω increases, the radius of gyration times the maximum angular motion will reduce along with r, making its significance more difficult to perceive. In the present case of a system with both elements having equal stiffnesses and located at a distance d from the center of mass, the maximum possible contribution of the angular response to the displacement at the element level can be estimated as the

ratio of d times the maximum angular response divided by the yield displacement:

$$d\ \Theta_{MAX}\ /\delta_y\ =\ \Omega\ r\ \Theta_{MAX}/\delta_y$$

For the particular model used in these examples, d is equal to 50 units and δ_y is equal to 0.12 units. If this calculated value is large, it can be assumed that the angular motion is large, although it is not necessarily in-phase with the maximum translational motion. There is no attempt made at this stage to estimate the phase between the angular motion and the translational motion. It should also be obvious from Figure 3.10b (in the previous chapter) that for initially symmetric systems, the torsional motion is a secondary effect triggered by first yielding and further excited by each yield excursions of the system. The inelastic deformations are <u>not a consequence</u> of large angular motion in the case of initially symmetric systems. Accordingly, large angular motion here merely reflects the large inelastic deformations of the system, which the measured element ductility ratios does equally well, if not better. It should also be emphasized that the maximum angular response, may not necessarily coincide with the maximum element response, and in that respect must not be misinterpreted or given disproportionate importance. It is merely an indicator of the severity of the angular motion and nothing else. Better indicators can be developed to gauge

the proportions of predominantly torsional and predominantly rotational motions, but as these become more complicated, their estimation is not appropriate in this stage of research.

It is believed that the ductility ratios of the demands on each element of the two-element systems provide the best quantitative measure of the damage sensitivity of the systems. Some results of maximum angular response, and radius of gyration times the maximum angular response, will be presented, but the emphasis should remain on the ductility ratio calculations.

4.3 Presentation of the results

Since the influence of many parameters on the element response are being studied, a three dimensional presentation of the results is thought to transmit a better conceptual understanding along with a stronger visual impact. This is especially true when a large number of curves are to be plotted simultaneously.

The advantage of a two-dimensional plot mainly lies in the ability to better read a value off the graph. On the other hand, a three-dimensional presentation of the results allows simplicity in labelling, and ease in visualizing the fluctuations in response along with parametric variations.

The major disadvantage lies in the difficulty in reading accurate values off the graph. Figures 4.2 and 4.3 illustrate the above discussion. Figure 4.2 consists of a two-dimensional plot of part of Figure 4.3, with the equivalent three-dimensional plot as an insert.

Since the trends in the response are of primary interest for this part of the study, the best combination will be to use three-dimensional graphics in parallel with access to the exact values of the data. Therefore, the values plotted on all three-dimensional graph in this report are available on floppy disk (5.25" double density PC/MS-DOS format) for consultation. Table 4.2 links the data files to the proper graphs along with short descriptions of how the results are presented, file formats, and detailed column descriptions. Finally, the results of the statistical compilations will be printed here as they are the most important values for this study.

Figures 4.3 to 4.7 present weak element ductility ratios when the target SDOF system ductility is 4, and for each of the five earthquake used in this study of initially symmetric systems. Figures 4.8 and 4.9 illustrate some of the strong element responses for the same cases described above. Similarly, Figures 4.10 to 4.14 present weak element ductility ratios when the target ductility is 8. Note that all graphs in the figure set 4.3 to 4.14 are plotted to the

same scale with the exception of the following cases: "0.8 Fy and Fy" for Parkfield and Taft earthquakes (in the case of target ductility of 4 only). It was not judged necessary to reduce the magnification of all the other graphs just to insure an uniform scale. The inadequacy of the present scale for only two isolated cases is more acceptable than the overall loss of readability/accuracy that could result from a scale change.

The previous results could also be rearranged in a different format in order to include more information on a single graph. A direct comparison is better achieved by grouping the results by their type of unequal yield case, or by their type of ratios of uncoupled frequencies. Figures 4.15 to 4.27 will present such "global graphs". To allow the reader to develop familiarity with the new perspective, results previously presented in Figure 4.10 and 4.13 are rearranged into Figures 4.15 and 4.16.

Finally, statistical calculations are performed on all the system response indicators over the five earthquakes used. Mean and mean-plus-one-standard-deviation results are presented in Figures 4.17 to 4.24. These graphs are all to the same scale.

Some effect of angular motion (for the El Centro earthquake) can be seen from graphs in Figures 4.25 to 4.27.

The maximum angular response (for target ductility of 4) is presented in Figure 4.25, and the radius of gyration times the maximum angular response is presented in Figures 2.26 and 2.27 (for target ductility level of 4 and 8, respectively).

Numerical values resulting of the statistical analysis are presented in Table 4.3. These tabulated values are important for this part of the study, and having prompt access to those will compensate for the slight difficulty in reading them from the three dimensional graphics.

4.4 Discussion

Since systems of different ultimate strengths were compared, the case "0.8 Fy and Fy" (being weaker than the reference system) was expected to have the more severe weak element ductility ratios of all the yield combinations analyzed. Nevertheless, it remains impressive to observe the rather large magnification of weak element ductilities obtained (e.g., Figure 4.3), in some instances almost reaching a value of six (Figure 4.6). This translates into a weak element ductility of almost 24 for the target ductility of 4. This is hardly a reasonable design ductility. It is also more than what might intuitively be expected for a 20% underestimation in the yield level of one structural element. But one must nevertheless realize that the equivalent SDOF

system with yield level of 0.8 Fy (but using the same earthquakes scaling as determined for the Fy yield level) would also produce large ductilities, sometimes up to near 17 (in the case of target ductilities of 4) or 25 (in the case of target ductilities of 8). See Table 4.4.

In the cases where the strength was superior to the equivalent SDOF system, the ductility ratios were nowhere as severe as for the under-strength cases (e.g., Figure 4.3). Still some large amplifications occurred, often up to 2.5 (e.g., Figures 4.4 and 4.11), meaning a weak element ductility of 10 or 20 for the respective target ductilities of 4 and 8.

Also, in the cases with over-strength elements, when $\Omega \geq 1.0$, the weak element ductility ratios were increasing with increasing differences in unequal yield levels, despite the increased ultimate strength of the systems (e.g., Figure 4.4 or Table 4.3 A). This is surprising as it implies that the added torsional behavior induced by the increase in yield level differential more than overcomes the benefit one might associate with the increase in strength (or balances it in the best case). Thus, there is no guarantee that increased strength in a symmetric system decreases ductility. It should be noted that at some point further increase in yield level differential would produce no additional change in

response for either elements. This would occur when the strong element reaches permanently elastic behavior.

A special consideration must be given for the element yielding at Fy (i.e. the strong one in the case "0.8 Fy and Fy", and the weak one in the other cases). This element will always have the same inelastic response as the SDOF system yielding at Fy when Ω=1.0, and therefore the element ductility ratios will always be 1.0 (e.g., Figure 4.14). This rather interesting phenomenon is explained in Chapter 5 in great detail by specializing the equations derived in Appendix "A" (from the incremental analysis of one step). For the moment, it will be just mentioned that this fact can be accurately predicted by theory.

The results clearly illustrate that larger Ω values produce larger ductility demands on the weak element (e.g., Figure 4.3) (and accordingly an also lower ductility demand on the strong element (e.g., Figure 4.8)). This can be explained by the lower resistance to angular motion provided by systems with larger Ω values, as discussed previously in Section 3.7. Obviously, this increase in weak element ductility ratios with Ω is not observed for all periods when looking at the response under a given earthquake excitation. Because of the particular characteristics of any single earthquake, the response may have odd localized behavior. For example, when only looking at the results from the El

Centro earthquake (Figure 4.3), the trend broke 3 times (out of 50 possible break points) between Ω=1.6 & 2.0, and once between Ω=1.2 & 1.6 for the "0.8 & 1.0 Fy" case. For other yield combinations (but the same earthquake), 31 reductions in response were noticed with increases in Ω (as compared with 119 increases in response), but most of those reductions mentioned above create non-significant changes in ductility. The general increase in response is also not as important for these yield combinations as for the "0.8 & 1.0 Fy" case.

Many more breaks in the trend can be observed taking all the other responses for individual earthquakes one by one. Nevertheless, one should be more concerned about the general trend as revealed by the mean responses for the five earthquakes used in this study. Tables 4.3 A-F can be referred to for the following discussion. Note that because of the relatively small number of earthquake records used, the mean values should be considered the most significant of the results provided by this study (the mean plus one standard deviation being mainly provided as an indicator of the scatter and for completeness; also note that the standard deviation is highly irregular for different Ω values, being always zero for the element yielding at Fy when Ω=1).

Now, there is obviously more consistency in the trend as a clear increase in the weak element ductility ratios follows the increases in Ω (Tables 4.3 A and 4.3 E or Figures 4.17

and 4.21). There are a few decreases from point to point, but most of them are negligible (less than 0.05 for the means, and 0.10 for the mean plus one standard deviations). Only eight changes on Table 4.3A are of higher magnitude (maximum differences of 0.20 and all occurring when going from Ω=0.4 to 0.8 or from Ω= 0.8 to 1.0, for cases "1.0 & 1.5 Fy" and "1.0 & 2.0 Fy"), and no such cases occur in Table 4.3E. As expected, more "exceptions" are found in the cases of mean-plus-one-standard-deviations (Tables 4.3 B and 4.3 F or Figures 4.17 and 4.21), but the trend is in no way jeopardized.

The strong element ductility ratios basically follow the reverse trend. That is element response decreases with increasing Ω (Tables 4.3 C and 4.3 G or Figures 4.18 and 4.22).

In order to evaluate the effect of torsional response on the initially symmetric systems with unequal yield levels, one must first define what is a significant change. In that respect, an element ductility ratio of 1.25 or less will be neglected in view of the general uncertainty and assumptions associated with these analyses. Moreover, the effect on design of such a change in ductility (i.e. from 4 to 5 or 8 to 10) is not believed meaningful in a practical sense. There is then a "grey zone" where the importance of a change in ductility can be debated to be significant or not. For

the purpose of this study, changes of 25% to 50% are considered of moderate importance, and changes of more than 50% are judged to be of major importance. The reader is in no way limited by this interpretation as the tabulated results are readily available.

With the emphasis placed on the means of the five earthquakes (differences with the mean plus one standard deviation case will also be briefly described), one can observe the following:

A) The weak element ductility ratios for the case "0.8 & 1.0 Fy" are always at least of moderate importance, and often of major importance (Tables 4.3 A and 4.3 E or Figures 4.17 and 21). Special attention should be given to cases with small periods or large Ω values, and most significantly a combination of both, where ductility values can be 2 to 4 times their target values (Table 4.3 A or Figure 4.17). (The same is true for the case of mean plus one standard deviation with the difference that the worst measured ductility values were up to 5 times their target ductility (Table 4.3 B or Figure 4.17)).

B) When the yield level of one element is superior to that estimated, the weak element ductility ratios are mostly non-affected until Ω becomes 1.6 or more (1.2 or more in

the case of mean plus one standard deviation). In that case, there is also a slight increase in response occurring along with the yield stresses differentials. Increases of 100% are to be expected for large Ω and large yield level differences (Tables 4.3 A and 4.3 E or Figures 4.17 and 4.21).

C) The strong element ductility ratios are all less than 1.0, except in the 0.8 & 1.0 Fy case where the systems ultimate strengths are less than that of the equivalent SDOF systems, thus making larger inelastic deformations also possible in the stronger element (Tables 4.3 C and 4.3 G or Figures 4.18 and 4.22).

Note that the decrease in strong element ductility ratios occurring with the increase in the ultimate strength of the system is partly a consequence of the increase of the yield level of the strong element. As explained before, the increase in yield level corresponds to an equivalent increase in the yield displacement, and thus for an equal displacement, a reduction in the ductility. A value below 1.0 on the graph simply reflects that situation; it does not mean that the strong element remains elastic, but simply that it yields less than does the corresponding SDOF system which yields at Fy (which is really no surprise).

Despite all of this, the displacements recorded were sometimes large enough to produce increases in ductility (e.g., Table 4.3 C). Amplification of the ductility demand of moderate importance can be noticed in the case of low periods ($T \leq 0.2$) and low Ω values ($\Omega \leq 0.8$). For the case of mean plus one standard deviation, the increases are of moderate importance when $T \leq 0.6$ and $\Omega \leq 0.8$, and of major importance when $T \leq 0.2$ and $\Omega \leq 0.4$ (e.g., Table 4.3 D).

For the other yield cases, the strong element ductility ratios reduce in proportion to the increase in yield differential. There appears still to be a tendency toward reduction of ratios when Ω is increasing, but all changes are of minimal significance (e.g., Table 4.3 C).

D) The effect of different target ductility levels is of practically no effect. Although the large element ductility ratios are mostly higher for the case of the target ductility of 4, the difference is often not significant. The ratios for the target ductility of 8 are seen to exceed those for the target ductility of 4 mainly for moderate levels of ductility increases (Tables 4.3 A and 4.3 E).

E) Tables 4.3 I-L and Figures 4.26 and 4.27 present the statistical results (on five earthquakes) of the traditional response parameter: radius of gyration times maximum angular response. Because of the reduction in the radius of gyration with the increase in Ω, this response parameter can be very misleading. As explained previously, multiplying these values by Ω would give a better indicator of the severity of the torsional response. This can be performed visually from the results in Tables 4.3 I-L. The trends noticed would then be practically similar as the ones described in the case of element ductility ratios. (The increase in angular response along with Ω can also be noticed in Figure 4.25, although this plot relates only to a single earthquake record).

Weak element ductility ratios are also generally higher for systems with small periods in the case of "0.8 and 1 Fy" (e.g., Figure 4.17). This is expected as the ductilities of the equivalent SDOF systems have been set uniform when yielding occurs at Fy. The case "0.8 and 1.0 Fy" being weaker that the equivalent SDOF system, the natural tendency of short period systems to have larger response than more flexible systems (for earthquakes typical of the West Coast of the United States) resurfaces. For comparison, presented in Table 4.4 are the ductilities of the SDOF systems yielding

at 0.8 Fy but subjected to the same scaled earthquakes used to calibrate the ductilities of SDOF systems yielding at Fy. It can be seen how a 20% reduction in yield level can bring back the apparent period dependency, despite the fact it had been removed for the SDOF systems yielding at Fy. This alone is sufficient to explain the large effect of period noticed in the case of systems with weaker than estimated yield levels. Finally, the period has no significant influence on the response of systems with yield levels larger than their equivalent SDOFs.

4.5 Conclusions on the Study of Initially Symmetric Systems

The unequal yield levels of initially symmetric systems will create torsional coupling as a secondary response initiated by the occurrence of inelastic behavior.

The ductilities predicted by equivalent single degree of freedom systems can be dangerously exceeded if the equivalent SDOF system's yield level match the yield level of the stronger of the element in the two-element system. Large amplifications can also be expected when the SDOF system's yield level matches the yield level of the weaker element in the two-element system and if the ratio of uncoupled frequencies (Ω) is large (typically $\Omega \geq 1.2$).

In the case of Ω=1.0, the equivalent SDOF system response will perfectly match the response of the element (in the two element system) with the same yield level as that SDOF system.

The observed behavior has not been found to be dependant on the level of earthquake excitation (target ductilities). Also, the period of the systems does not affect significantly the magnitude of the torsional response, except when the equivalent SDOF system's yield level matches the larger yield level of the two element system.

The following design recommendation could be formulated based on the results of this chapter:

For structural systems with elasto-perfectly plastic hysteretic behavior (other type of systems will be studied in Chapter 6) where only two structural elements are used in each lateral resisting direction, and where the exact yield levels cannot be accurately predicted or matched, the ductility of the element yielding sooner is expected to exceed by approximately 50% the one predicted for a SDOF with yield level equal to the lower yield level of the two element system, if the ratio of the uncoupled frequencies (Ω) is larger than 1.2. The designer expecting to limit the ductility demand on structural members in those cases should reduce its target ductility demand by 30% (1/1.5 = 0.67).

5. INITIALLY ECCENTRIC SYSTEMS

Although torsional movements are thought to be responsible for the failure of many structures during major earthquakes, a simple method to estimate the inelastic response of torsionally coupled systems does not yet exist. A major reason for this void is the lack of fundamental understanding of how inelastic response of initially eccentric systems is affected by various parameters.

Other researchers have speculated that the uncoupled period, the normalized eccentricities and the ratio of uncoupled frequencies (Ω) strongly affect response (refer to Section 2.2 for details), but it seems that these observations may be strongly dependant on the way the analyses were performed in each study. The major difficulty related to the study of initially eccentric systems seems to lie partly in the difficulty in finding a reliable comparative "benchmark" (that is an equivalent torsion-free system whose response would not be sensitive to any of the parameters thought to influence the inelastic torsional response), and on the difficulty of setting a meaningful liaison between the true system and its "benchmark" (as the liaison itself may be responsible in generating parameter dependency, independently of the sensitivity of the system to potential torsional motion).

It is highly desirable for design purposes to find an appropriate "benchmark" and liaison procedure such that the prediction of the inelastic response of initially eccentric systems could be safely achieved from elastic dynamic analysis and other readily available analysis tools, without explicitly performing any inelastic analysis.

In this chapter, efforts will be made to develop an improved understanding of the fundamental inelastic behavior of torsionally coupled systems. Then, it will be attempted to solve these design difficulties by providing a new benchmark system and liaison procedure. The validity of these will be assessed by performing studies on simple two-element initially eccentric systems.

5.1 Exact Prediction of Response by Equivalent SDOF for Ω=1

Before going into the details of how the parametric study will be conducted, it is important to demonstrate how the inelastic response of the weak element can be exactly predicted by an equivalent SDOF system when the ratio of uncoupled frequencies equals unity (Ω=1.0).

The whole proof derives mainly from a specialization of the equations derived in Appendix A.

We recall that the fundamental step-by-step incremental equation,

$$K^*(t) * \Delta v(t) = \Delta p^*(t)$$

when specialized for torsionally coupled systems as follows,

$$K^*(t) = \begin{bmatrix} K_x' + C_3 & K_x'e' + B_3 \\ K_x'e' + B_3 & K_\theta' + C_4 \end{bmatrix}$$

and,

$$\Delta p^*(t) = \begin{bmatrix} \Delta p_1(t) \\ \Delta p_2(t) \end{bmatrix} + \begin{bmatrix} m\ C_8(t) \\ mr^2 C_9(t) \end{bmatrix} + \begin{bmatrix} K_x C_{10}(t) \\ K_\theta C_{11}(t) \end{bmatrix}$$

where,

$$C_1 = \frac{1}{\beta(\Delta t)^2} \quad \text{and} \quad C_2 = \gamma / (\beta \Delta t)$$

(constants dependant on the Newmark method used)

and where,

$$C_3 = (C_1 + a\,C_2)\,m + b\,C_2\,K_x$$
$$C_4 = (C_1 + a\,C_2)\,m + b\,C_2\,K_\theta$$
$$B_3 = b\,C_2\,K_x\,e$$

$$B_4 = 1 / \beta\Delta t \qquad B_6 = \gamma a / \beta \qquad B_8 = \Delta t[(\gamma/2\beta)-1)a$$
$$B_5 = 1 / 2\beta \qquad B_7 = \gamma b / \beta \qquad B_9 = \Delta t[(\gamma/2\beta)-1)b$$

$$C_8(t) = (B_4+B_6)\dot{v}_1(t) + (B_5+B_7)\ddot{v}_1(t)$$
$$C_9(t) = (B_4+B_6)\dot{v}_2(t) + (B_5+B_7)\ddot{v}_2(t)$$
$$C_{10}(t) = B_8[\dot{v}_1(t)+e\dot{v}_2(t)] + B_9[\ddot{v}_1(t)+e\ddot{v}_2(t)]$$
$$C_{11}(t) = B_8[(K_x e/K_\theta)e\dot{v}_1(t)+\dot{v}_2(t)] + B_9[(K_x e/K_\theta)\ddot{v}_1(t)+\ddot{v}_2(t)]$$

produced the following result:

$$r\Delta v_\theta(t) = \left[\frac{\begin{array}{l} [\omega_x^{2\prime} + C_1]\,[B_4 r\ddot{v}_2(t) + B_5 r\ddot{v}_2(t)] \\ \qquad -\omega_x^{2\prime}(e'/r)\,[\Delta\ddot{v}_g(t) + B_4\ddot{v}_1(t) + B_5\ddot{v}_1(t)] \end{array}}{\omega_x^{2\prime}\omega_\theta^{2\prime} + C_1[\omega_x^{2\prime}+\omega_\theta^{2\prime}] + C_1^2 - \omega_x^4(e'/r)^2} \right]$$

when damping is neglected (without loss of generality).

For completeness, the Δv_1 response can also be calculated, and is:

$$\Delta v_1 = \left[\frac{\begin{array}{l} [\omega_\theta^{2\prime} + C_1][\Delta\ddot{v}g(t) + B_4\ddot{v}_1(t) + B_5\ddot{v}_1(t)] \\ \qquad - [\omega_x^{2\prime}(e'/r)\,[B_4 r\ddot{v}_2(t) + B_5 r\ddot{v}_2(t)]\,] \end{array}}{[\omega_x^{2\prime}\omega_\theta^{2\prime} + C_1(\omega_x^{2\prime}+\omega_\theta^{2\prime}) + C_1^2 - \omega_x^{4\prime}(e'/r)\,]} \right]$$

Now, when setting the ratio of uncoupled frequencies to unity (Ω=1.0), one implies:

$$\omega_x^2 = \omega_\theta^2$$

Furthermore, in the stiffness eccentric situation of interest here, $K_\theta = K_x d^2$, and $K_\theta' = K_x' d^2$, which directly results in:

$$\omega_x^{2\prime} = \omega_\theta^{2\prime}$$

Therefore, replacing all $\omega_e{}^{2\prime}$ by $\omega_x{}^{2\prime}$ in the equations above, one is left with:

$$\Delta v_1(t) = \frac{[\omega_x{}^{2\prime} + C_1]\,[\Delta\ddot{v}g(t) + B_4(t)\dot{v}_1(t) + B_5(t)\ddot{v}_1(t)] - \omega_x{}^{2\prime}(e'/r)\,[B_4 r\dot{v}_2(t) + B_5 r\ddot{v}2(t)]}{[\omega_x{}^{2\prime} + C_1]^2 - \omega_x{}^{4\prime}(e'/r)^2}$$

$$r\Delta v_2(t) = \frac{[\omega_x{}^{2\prime} + C_1]\,[B_4 r\dot{v}_2(t) + B_5 r\ddot{v}2(t)] - \omega_x{}^{2\prime}(e'/r)\,[\Delta\ddot{v}g(t) + B_4(t)\dot{v}_1(t) + B_5(t)\ddot{v}_1(t)]}{[\omega_x{}^{2\prime} + C_1]^2 - \omega_x{}^{4\prime}(e'/r)^2}$$

Now, in the case where $e < 0$, the weak element response can be calculated by:

$$\Delta v_{\text{weak}}(t) = \Delta v_1(t) + r\Delta v_2(t) \qquad \text{as } d=r \text{ when } \Omega=1$$

(Note that the following derivation could be done equally well for $e > 0$ without any difficulty and would lead to the same conclusions with respect to the weak element then located on the other side of the structure. Here, since $e < 0$ will be used, e is implicitly negative unless forced positive by the use of absolute values.)

Expanding each terms, one obtains after some simplifications:

$$\Delta v_{rel}(t) = \frac{[\ \Delta\ddot{v}g(t) + B_4\,\dot{v}_{rel}(t) + B_3\,\ddot{v}_{rel}(t)\ ]}{\omega_x^2\ '\ [\ 1 + (e'/r)\ ] + C_1}$$

where the real sign of e' must be used.

Furthermore, the equation presented in Chapter 2 to calculate the two true frequencies of monosymmetric systems, which was:

$$\omega_{1,2}^2 = \omega_x^2 \left[\frac{(\Omega^2+1) \pm (\Omega^4 - 2\Omega^2 + 1 + 4(e/r)^2)^{0.5}}{2} \right]$$

can be greatly simplified for the case $\Omega=1$; and becomes:

$$\omega_1^2 = \omega_x^2\ [\ 1 - (\ |e|/r\ )\ ]$$

$$\omega_2^2 = \omega_x^2\ [\ 1 + (\ |e|/r\ )\ ]$$

(Note that |e| is used only to insure that the first mode is properly identified, independently of the reference axis system chosen)

Now looking at these equations, it appears a good idea to define an equivalent SDOF system such that:

$$\omega_{equiv}^2 = \omega_1^2 = \omega_x^2\ [\ 1 - (\ |e|/r\ )\ ]$$

That is further justified when looking at the equation for $\Delta v_i(t)$ for a SDOF system (i.e. e/r = 0), which is:

$$\Delta v_i(t)_{sdof} = \frac{[\Delta \ddot{v}g(t) + B_4 \dot{v}_i(t)_{sdof} + B_5 \ddot{v}_i(t)_{sdof}]}{[\omega_{sdof}^{2\prime} + C_i]}$$

Obviously, when Ω=1, an equivalent SDOF system elastic response would be similar to the weak element response provided that the SDOF system frequency would be defined as above.

When the weak element is tuned to yield simultaneously with the equivalent SDOF system, the inelastic response can also be matched (assuming both systems share the damping ratio and same element model, i.e. same strain hardening and yield displacements in the case of the bi-linear element model).

Formally, in order to insure the match one must prove:

$$\omega_{sdof}^{2\prime} = \omega_x^{2\prime} [\, 1 + (e'/r) \,]$$

(Recall the prime (') implies instantaneous properties.)

To perform the complete proof, one must check the four situations possible for a two-element system:

1) Both element remains elastic.

2) The strong element alone yields, the weak element remaining elastic.

3) The weak element alone yields, the strong element remaining elastic.

4) Both elements yield.

Note that the equivalent SDOF system's yield state is in phase with the one for the weak element at all times.

Case 1 is directly proven by the above derivation, as this is how the equivalent SDOF system concept has been defined.

Case 2 can be easily proven as follow:

$$\omega_x^{2\prime}\,[\,1 + (\,e'/r\,)\,] = \frac{\in Ks + Kw}{m}\left[\,1 + \frac{(Kw - \in Ks)\,d}{(Kw + \in Ks)\,r}\right]$$

$$= \frac{Kw + \in Ks + Kw - \in Ks}{m}$$

$$= \frac{2\,Kw}{m} = \frac{Kw + Kw + Ks - Ks}{m}$$

$$= \frac{(Kw + Ks)}{m}\,\frac{[(Kw + Ks) + (Kw - Ks)]}{(Kw + Ks)}$$

$$= \omega_x^2\,[\,1 + e/r\,]$$

$$= \omega_{sdof}^2 = \omega_{sdof}^{2\prime}$$

(that is both weak element and equivalent SDOF system remain elastic, as expected)

where Kw is the stiffness of the weak element
Ks is the stiffness of the strong element
ϵ is the strain hardening ratio
e' is taken here as positive, so Kw > Ks
(e' negative would also give the same results)

Case 3 can be proven in a similar manner:

$$\omega_x^{2\prime} \left[1 + (e'/r) \right] = \frac{\epsilon Kw + Ks}{m} \left[1 + \frac{(\epsilon Kw - Ks)\, d}{(\epsilon Kw + Ks)\, r} \right]$$

$$= \frac{\epsilon Kw + Ks + \epsilon Kw - Ks}{m}$$

$$= \frac{2 \epsilon Kw}{m} = \epsilon \frac{Kw + Kw + Ks - Ks}{m}$$

and directly from above $= \epsilon \omega_x^2 \left[1 + e/r \right]$

$$= \epsilon \omega_{SDOF}^2 = \omega_{SDOF}^{2\prime}$$

Case 4 is straight forward too:

$$\omega_x^{2\prime} \left[1 + (e'/r) \right] = \frac{\epsilon (Kw + Ks)}{m} \left[1 + \frac{\epsilon (Kw - Ks)\, d}{\epsilon (Kw + Ks)\, r} \right]$$

$$= \epsilon \omega_x^2 \left[1 + e/r \right]$$

$$= \epsilon \omega_{SDOF}^2 = \omega_{SDOF}^{2\prime}$$

As said previously, all of the above is true provided that the equivalent single degree of freedom system yields simultaneously with the weak element, which is easily achieved here as the SDOF system is related to the weak element by:

$$\omega_{SDOF}^2 = Kw / (m/2)$$

The SDOF system can be directly defined by keeping the same stiffness, tributary mass and yield displacement as for the weak element. Model similarity will then be easily assured.

Therefore, when Ω = 1.0, the weak element displacement in the torsionally coupled system is EXACTLY EQUAL to the displacement of a single degree of freedom system with a period equal to the first period of the torsionally coupled system, as long as they share the same element model in the inelastic range.

The whole approach, despite not being tremendously elegant, will prove very useful in helping define what should be considered an equivalent SDOF system for the study of inelastic response of torsionally coupled systems.

5.2 Procedure for Determining the Equivalent SDOF System

The difficulty in investigating the effect of various parameters on torsional coupled systems has already been mentioned. What would be a reliable benchmark for comparison purposes? In particular, is there an equivalent torsion-free system whose response would not be sensitive to any of the

parameters thought to influence the inelastic torsional response?

It is judged appropriate to compare torsionally coupled systems with equivalent SDOF systems having a period equal to the predominantly translational period of the torsionally coupled system. Therefore, an equivalent SDOF system's period will be set equal to the first period of the torsionally coupled systems for $\Omega \geq 1.0$, and equal to the second period otherwise.

The work of Section 5.1 presented some evidence to support that decision, although it alone is not sufficient to justify the approach for all Ω values.

Additional support for this decision is provided by some observations on how modal analysis takes into account the participation of each mode in an elastic torsionally coupled system.

We recall that the modal displacement is calculated as:

$$v_{N,max} = (\Xi_N \, L_N \, / \, M_N) \, Sd(\xi_N, T_N)$$

where $(\Xi_N \, L_N \, / \, M_N)$ is the participation factor for mode N,

and where $\Xi_N = \begin{bmatrix} \Xi_{1,N} \\ \Xi_{2,N} \end{bmatrix}$, N = 1,2 (i.e. mode 1 and mode 2).

One must not forget that the corresponding degree of freedoms for torsionally coupled systems are (as specified in Chapter 2): $\begin{bmatrix} v_x \\ r v_\theta \end{bmatrix}$

By expanding, one obtains an expression for the participation factors:

$$(\Xi_1 \; L_1 \; / \; M_1) = \begin{bmatrix} 1 \; / \; [\; 1 + (\Xi_{2,1}/\Xi_{1,1})^2 \;] \\ 1 \; / \; [\; (\Xi_{1,1}/\Xi_{2,1}) + (\Xi_{2,1}/\Xi_{1,1}) \;] \end{bmatrix}$$

$$(\Xi_2 \; L_2 \; / \; M_2) = \begin{bmatrix} 1 \; / \; [\; 1 + (\Xi_{2,2}/\Xi_{1,2})^2 \;] \\ 1 \; / \; [\; (\Xi_{1,2}/\Xi_{2,2}) + (\Xi_{2,2}/\Xi_{1,2}) \;] \end{bmatrix}$$

Finally, the edge displacement modal participation factor at a distance r from the center of mass can be calculated (for mode N) by:

$$(\text{Edge at } r)_N = (\Xi_N \; L_N \; / \; M_N)_1 + (\Xi_N \; L_N \; / \; M_N)_2$$

and, similarly, the edge displacement modal participation factor at a distance d from the center of mass can be calculated (for mode N) by:

$$(\text{Edge at } d)_N = (\Xi_N \; L_N \; / \; M_N)_1 + (d/r)(\Xi_N \; L_N \; / \; M_N)_2$$

Using the mode shape quantities expressed as a function of Ω and e/r (as developed in Chapter 2), all the above quantities can be easily calculated. The effect of Ω on these modal participation factors is presented in Figures 5.1 to 5.4. Figure 5.1 illustrates the modal participation factor's first component only (this is the one corresponding to v_x) with respect to Ω. The second component's effect (corresponding to rv_θ) is plotted in Figure 5.2. The edge displacement modal participation factor (as defined above) is plotted in Figure 5.3 (at distance r) and Figure 5.4 (at distance d).

Obviously, the final response will be largely affected by the respective values of the pseudo-displacements Sd appropriate for each mode. Nevertheless, it is apparent from the four graphs presented above, that for small and moderate normalized eccentricities (say, e/r from 0 to 0.5), unless Sd for one mode is significantly larger than for the other mode, the response will be primarily affected by a single vibration mode, except in the close neighborhood of Ω=1.0. Further, the dominant mode always seems to be the primarily translational one; that is, the first mode when $\Omega > 1.0$ and the second one when $\Omega < 1.0$.

All these observations lead to the decision to set the equivalent SDOF system's period equal to the first mode of

the torsionally coupled system when $\Omega > 1.0$, and to the second mode when $\Omega < 1.0$. The case $\Omega = 1.0$ has already been examined in the preceding section, and it has been demonstrated, in that case, that the equivalent SDOF system's period must be set to the first mode of the torsionally coupled system.

Finally, in order to assess the validity of this decision, many time history analyses were performed and fully plotted for various combinations of periods, Ω values and normalized eccentricities (these numerous plots are not presented here for brevity). In those analyses, the torsionally coupled displacement histories were compared with the histories for the equivalent SDOF system in accordance with a scaling method to be described in the following sections. It was found that this decision on the choice of period for the equivalent SDOF system was appropriate, most of the time providing a response history response curve for the equivalent SDOF system which would closely resemble the one for the elements in the torsionally coupled system.

5.3 Choice of Parameters

For reasons explained in previous chapters, the bi-linear element with strain-hardening was chosen for this study. Again, strain-hardening was set to 0.5% (E_{s_H} = 0.005

E), making the element model practically elasto-perfectly plastic. The inter-element relationship is illustrated in Figure 3.5. The reasons for this selection are explained in Chapter 3.

Five earthquakes (again truncated in duration to 15 seconds) were used to insure that final observations will not be peculiar to a single ground motion. The acceleration records used are listed in Table 4.1 (i.e., the same ones as used in Chapter 4).

The main system parameters varied during this investigation were: the uncoupled period T_x, the ratio of uncoupled frequencies Ω, the target ductility levels and the normalized eccentricities e/r. The same values of uncoupled period, uncoupled frequencies and ductility levels as in the case of initially symmetric systems were used; T_x was taken equal to 0.1, 0.2, 0.3, 0.4, 0.6, 0.8, 1.0, 1.2, 1.6, and 2.0; Ω was equal to 0.4, 0.8, 1.0, 1.2, 1.6 and 2.0; and ductility levels of 4 and 8 were employed. The justifications for choosing these values are presented in Section 4.1 and will not be repeated here.

The normalized eccentricities e/r were chosen as 0.1 and 0.3, as these values were judged representative of real-life structures; they are also of the same magnitude as those commonly used in previous studies, allowing some level of

comparison with the other studies. Because stiffness eccentric two-element systems are studied (i.e. center of mass at distance d from each element), a better physical interpretation of the normalized eccentricities e/r is provided by calculation of the equivalent e/d values for each system analyzed; results are presented in Table 5.1. It can be seen that a wide range of physical eccentricities is actually covered by the study. Interestingly, the true eccentricity becomes the largest for the combined case of large e/r and low Ω. In fact, for the two elements stiffness eccentric systems analyzed, $e/d = (e/r)/\Omega$.

As before, the damping was chosen to be of the Rayleigh type, arbitrarily set to be 2% of critical damping at each of the true frequencies of any given system analyzed. The mass proportional and stiffness proportional coefficients were thus recalculated for each individual analysis.

The relation between the uncoupled frequencies and the true frequencies (derived in Section 2.1.3 and graphically demonstrated in Figure 2.1) is used here to calculate the actual period corresponding to each mode of the initially eccentric two-degree-of-freedom systems under consideration.

The time step used in the time history analyses (using ANSR again) was chosen to be at least less than T/30 of the

smallest of the two true periods of each system, but never smaller than 0.002 seconds or larger than 0.02 seconds.

5.4 Procedure Followed in this Analytical Study

The intent of this parametric study is to establish the relationship between the equivalent SDOF system ductility and the torsionally coupled element ductilities, more specifically to investigate the effect of various parameters on the torsionally coupled element response when the equivalent SDOF system are calibrated to target ductilities. The way the liaison between the true systems and the benchmark systems was accomplished is described below.

1) The single-degree-of-freedom systems was defined to have a period equal to the first period of the torsionally coupled system when $\Omega \geq 1.0$, and equal to the second period of the torsionally coupled system when $\Omega < 1.0$. Furthermore, the SDOF system was designed to yield at the same yield displacement δy as the elements of the torsionally coupled systems.

   Then, in a manner similar to the one described in Section 4.2, the proper strength factors were calculated for each SDOF system in order to attain target ductilities of 4 and 8 (using the program NOSPEC), and

again, for simplicity, the earthquake levels were scaled as necessary for each parametric case. These steps insured that the SDOF systems were insensitive to variations in ground motion intensity, as explained earlier.

2) Once the strength factors were determined, the SDOF systems were analyzed using ANSR to obtain a more accurate estimate of the ductility demand. Strength corrections were made if needed to improve the ductility demands. All final ductilities for the SDOF systems analyzed were between 3.6 and 4.4 when the target ductility was 4, and between 7.2 and 8.8 when the target ductility was 8. This represents a deviation of 10% or less from the targeted ductilities, a more liberal tolerance than the one adopted in the case of initially symmetric systems. It was made necessary to facilitate consideration of the much larger number of SDOF systems analyzed in the case of initially eccentric systems.

3) The same equivalent SDOF systems were then re-analyzed elastically, using the earthquake levels needed to obtain the target ductilities in the previous part of the work.

4) The torsionally coupled systems were also analyzed <u>elastically</u>. Then, for each individual parametric case,

a new earthquake scaling to be applied to the torsionally coupled systems was calculated such that the torsionally coupled system's weak (flexible) element elastic response would match the equivalent SDOF system elastic response.

5) Using the new earthquake scalings found in the previous step, the inelastic response of the torsionally coupled systems were calculated.

6) For each analysis of torsionally coupled systems, the new ductility demands were calculated. Recall that the model chosen had equal yield displacement for both elements. Therefore, for this study, similar ductilities implied similar absolute displacements, both for the weak and strong element (the strong element being defined as the stiffer element).

7) The ductilities factors calculated for each individual case analyzed above were then divided by the ductility factors obtained from their respective equivalent SDOF system. Calculation of the ratio of these ductility factors (the ductility ratio) was intended to remove the variations dues to the inaccuracies in calculating the target ductilities of the equivalent SDOF systems. Therefore, all element results will be presented in terms of those "ductility ratios".

8) The mean and mean-plus-one-standard-deviation were calculated for all response values over the five earthquakes to provide results mostly independent of the particular characteristics of single earthquakes.

This procedure is basically the reverse of a design logistic; it is nevertheless adequate as the intent is to reveal the parametric trends inherent with these systems. This procedure will further allow one to verify whether the equivalent SDOF system method accurately predicts the ductility demand on the torsionally coupled system.

Finally, the maximum angular responses were also calculated, along with the "maximum possible contribution of angular response to the displacement at the element level" as expressed by the ratio of d times the maximum angular response divided by the yield displacement:

$$d\ \Theta_{MAX}\ /\delta_Y\ =\ \Omega\ r\ \Theta_{MAX}/\delta_Y$$

for stiffness eccentric systems with resisting elements equidistant to the center of mass. For the specific model analyzed, δy is equal to 0.12 units and d equals 50 units.

Nevertheless, it is still believed that the ductility ratios for each element of the two-element systems provide

the best quantitative measure of the damage sensitivity of the systems. Therefore, the detailed results of the maximum angular response and the "maximum possible contribution of angular response to element displacement" will be only included on the floppy disk containing the results files (see Table 5.6), but will not be explicitly presented in this report. Furthermore, only the results from the statistical analysis from five earthquakes will be tabulated herein for reference.

5.5 Presentation of the Results

Again, three dimensional graphics are used, and the files used to produce the graphics are available for consultation on floppy disk. Table 5.6 relates the data files to the proper graphs along with short descriptions of how the results are presented. Also, the mean and mean-plus-one-standard-deviation results are readily available in Tables 5.2 to 5.5.

Figures 5.5 to 5.9 present the weak (flexible) and strong (stiff) element ductility ratios for equivalent SDOF system with a target ductility of 4, and for each of the five earthquakes used in this study of initially eccentric systems. Similarly, Figures 5.10 to 5.14 present the same response indicators when the target ductility is 8.

The statistical analysis results are presented in Figures 5.15 to 5.18. All graphs are formatted to share the same scale. When individual values are larger than the maximum scale of the graph, a numerical value is provided to indicate up to where the given peak should reach. This was thought to be more appropriate in this case, as the few extremely high peaks noticed would have severely distorted the graphs should the scale have been adjusted to include them.

5.6 Discussion of the Results

By observation of the ductility ratio results, one may directly notice that for the Ω=1.0 case, the numerically obtained values corroborate the predicted theoretical values, as all weak element ductility ratios are generally equal to 1.0 (i.e. weak element ductility demands are equal to the equivalent SDOF system ductility demands (e.g., Table 5.2)).

Nevertheless, one can observe some inaccuracies at times, as not all weak element ductility ratios are perfectly equal to unity when Ω=1. The reason for these imperfect results has been found to be a consequence of small inaccuracies in the prediction of the equivalent SDOF system response: the use of a time step of T/30 in the calculation

of the SDOF time histories was found to produce errors of up to 3% when compared with histories performed with smaller time steps. A maximum possible error of 3% was thought to be insignificant (especially when dealing with ductilities), but because of the way this study progressed, it also meant a maximum increase of 3% in the earthquake level used in the time history analyses of the torsionally coupled systems. In a few critical cases, it was found that a 3% increase in the earthquake level used could increase the element response by up to 16% (effects on the mean response being much less as seen in Figures 5.2 and 5.4). Because this response sensitivity was not encountered often, and because a 16% variation of ductility is still thought to be relatively insignificant from the perspective of this study, it was not judged worthwhile to repeat the analysis with smaller time steps. Therefore, the results are left unaltered.

In order to evaluate qualitatively the importance of the ductility ratios, the same convention as in the previous chapter will be maintained to indicate what is a significant ductility ratio: an element ductility ratio of 1.25 or less will be simply neglected in view of the general uncertainty in the structure and the excitation; ductility ratios from 1.25 to 1.5 are considered increases of moderate importance; ratios above 1.5 are judged to be of major importance.

Because response based on individual earthquake records tends to be highly varying as the system parameters change, it is more appropriate to rely mainly on the mean response from all earthquake records used when looking for trends in the behavior of the torsionally coupled systems. It is apparent from Tables 5.2 and 5.4, and Figures 5.15 and 5.17, that the element ductility ratios are independent of the uncoupled periods (T_x), normalized eccentricities (e/r), target ductility, and ratios of uncoupled frequencies (Ω). This is very interesting as it means that the method provided here is rather unsensitive to variations in these parameters, contrary to what other researchers have indicated. The method is mainly stable in providing a reliable estimate of the torsionally coupled system's element ductilities based on the concept of an equivalent SDOF system.

It should be noted briefly that the maximum angular response (and maximum angular response possible contribution to element displacement) statistical results from five earthquakes are also in agreement with this parameter independence. These results are not presented here as they are deemed less meaningful than the element ductility ratios.

The ductility ratios calculated for individual earthquake records are of course a lot more variable than the one measured for the mean response for five earthquakes. The ductility ratios can become very large for individual

combinations of parameters (e.g. Figures 5.7 and 5.12). The sensitive combinations also change for different earthquakes, and no trends have been thus far identified in the occurrence of those sensitive combinations. This illustrates that any design based on the mean response to five earthquakes may still encounter a much larger ductility demand than planned for when excited by a particular earthquake; this is in no way different than problems related to the earthquake resistant design of symmetric structures in general. Nevertheless, the mean response from five earthquake excitations should be taken as the meaningful response entity, as it provides a more uniform indicator of the severity of the structural response.

The ductility ratios, as measured by the mean of response for five earthquakes, remain mainly close to unity, only exceeding a value of 2.0 for the weak element when T_x = 0.4, Ω=0.8 and (e/r)=0.3 (Tables 5.2 and 5.4 or Figures 5.15 and 5.17). This is a direct consequence of the unique extreme ductility ratio that occurred for the Pacoima Dam earthquake for this same set of parameters (Figures 5.7 and 5.12). Should the Pacoima Dam contribution at this particular point be removed, the mean for the weak element response would drop to 1.39 for target ductility of 4, and 1.05 for target ductility of 8. Other than this particular point of unusually high sensitivity, the mean weak element response exceeds 1.5 only in five occasions (the maximum

value being 1.7). This is extremely satisfying as it shows the predicted increase in ductility from this method to be mostly of moderate importance. A conservative strategy would be to plan for a weak element ductility ratio of 1.5, and a strong element ductility ratio of 1.0 (although when Ω=1, a weak element ductility of 1 can be used, of course).

At times, the method can also be seen to be rather conservative. If one defines ductility ratios of 0.75 and less to be moderately conservative, then one can notice that these points occur for the weak element for (e/r)=0.3 when Ω=0.4 and $T_x \leq 0.3$, and when Ω=0.8 and T_x=0.1, for both target ductilities (Tables 5.2 and 5.4), as well as for the strong element on a regular basis (Figures 5.16 and 5.18) (except maybe for long periods and low e/r values). This conservatism in weak element response, besides being infrequent, is by no means excessive, and surely does not invalidate the equivalent SDOF system method. In fact, for comparison purposes in those particular cases, if the initially eccentric system had been excited to the same earthquake level needed to produce a ductility of 4 for the equivalent SDOF system (instead of scaling the earthquake to match the inelastic response as explained before), the resulting responses would have been excessively unconservative. For example, for the N-S component of the 1940 El Centro record, the case T_x=0.1, Ω=0.4 and e/r=0.3 which resulted in a conservative ductility of 2 for target

ductility of 4, would reach a ductility of 13.5, if the motion was not scaled to match the elastic response. Some ductility ratios obtained with and without the proposed scaling methods are briefly compared in Table 5.7 to illustrate the advantage in performing the appropriate matching of the elastic response.

Although no particular trend can be observed for the strong element, it is notable that some ductility ratios are extremely conservative, especially for systems with short periods and high e/r ratio (Figures 5.16 and 5.18). Nevertheless, the main concern here being the weak element's behavior, conservatism in the strong element response is not regarded negatively.

Mean-plus-one-standard-deviation results have been provided mainly for the purpose of completeness, and to illustrate the often large dispersion of the results (Tables 5.3 and 5.5 or Figures 5.15 to 5.18 Bottom). A conservative strategy based on the mean-plus-one-standard-deviation would indicate to be more appropriate a weak element ductility ratio of 2.0 (except for the special case of Ω=1 where a ratio of 1 is acceptable), and a strong element ductility ratio of 1.0 when $\Omega \geq 1.0$, and 1.5 otherwise. Nevertheless, one should be careful in using the results for mean-plus-one-standard-deviation values obtained from only five earthquake records.

5.7 Suggested Method to Use the Equivalent SDOF System Concept

Obviously, the concept of an equivalent SDOF system can be potentially very useful in design. Although there apparently is no easy way to obtain an EXACT match of the weak element displacement with a meaningful equivalent SDOF system for all values of Ω, it has been shown in the preceding section that the proposed method can provide a relatively accurate prediction of the initially eccentric system's element ductility factor.

It will now be illustrated how the equivalent SDOF system procedure can be used, in a design approach, to predict the inelastic response of torsionally coupled system

A design engineer using dynamic elastic analysis tools (like elastic response spectrum method or time history analysis) may easily calculate the elastically predicted response for the weak element. It is supposed for simplicity (for the time being) that the calculation is performed for a single ground motion; let this calculated elastic response be called R_w.

The elastic response of the equivalent SDOF system can be read from an SDOF elastic response spectrum (readily available for most earthquake records); let this SDOF response be called R_{SDOF}.

In order to match the elastic response of the weak element and of the equivalent SDOF system, the earthquake applied to the equivalent SDOF system should be scaled by R_w/R_{SDOF}.

It is now possible to obtain a prediction of the ductility demand on the equivalent SDOF system subjected to this corrected earthquake level by consulting inelastic response spectra. Some of these spectra are presented by Mahin & Lin [33]. It is relatively straight forward to calculate such spectra for particular records using standard numerical analysis procedures. Moreover, where conditions permit, simplified methods for deriving smoothed inelastic design response spectra may be appropriate (Newmark-Hall [42]). It is understood that like elastic response spectra, inelastic response spectra need only be constructed once for each combination of earthquake, damping and element model. Single earthquake or multiple earthquake spectra can also be constructed.

Of course, the element model for the single degree of freedom must match the one for the weak element of the

torsionally coupled system (which would herein imply a bi-linear model with same yield displacement and strain hardening). One must not forget that so far, the findings are limited to the type of inter-element relationship studied herein.

It is then straight forward to calculate the strength ratio, defined as:

$\eta = R_y / m\, a_{max}$ where a_{max} is the maximum earthquake ground acceleration,

and read the ductility demand for this equivalent SDOF system off the inelastic response spectrum. If Ω=1, this equivalent SDOF system's ductility demand can be assumed equal to both the weak and strong element ductilities of the torsionally coupled system; otherwise, a conservative weak element ductility should be estimated as being possibly 50% larger.

To provide a concrete illustration of the above procedure, an initially eccentric two-element structure is analyzed having the set of response parameters T_x=0.2, Ω=1 and e/r=0.1. For this system, the two true periods are T_1=0.211 and T_2=0.191. The element model is bi-linear with 0.5% strain hardening, and damping is 2% of critical. The yield displacement of this system is δy=0.12 inch. The 1940 El Centro earthquake (N-S component) was scaled to a peak

acceleration of 0.4g and an elastic dynamic time-history analysis was performed; the resulting edge displacement for the weak element was 0.43 inches.

Then using an elastic response spectrum for this earthquake component (Figure 5.19) with an actual peak acceleration of 0.348g, the pseudo-displacement for the equivalent SDOF system (with period T_{SDOF}=0.211) was found to be Sd=0.35 inch (of course, that much accuracy cannot be read from the spectrum itself, but is easily obtained by interpolation from the tabulated values of the pseudo-displacement, which is equally accessible).

In order to match the weak element elastic displacement with the equivalent SDOF system, the earthquake used in the equivalent SDOF concept must be scaled as:

$$\frac{\text{Weak element displacement}}{\text{Sd from equivalent SDOF}} = \frac{0.43}{0.35} = 1.23$$

Therefore, the peak acceleration for this equivalent SDOF becomes: 1.23 x 0.348g = 0.428g = 165 in/s²

Then, using the same yield displacement of 0.12 inch for the equivalent SDOF system, the strength level can be estimated by:

$$\eta = \frac{Ry}{m\, a_{MAX}} = \frac{K\ \delta y}{m\, a_{MAX}} = \omega_{SDOF}^2\ \frac{\delta y}{a_{MAX}} = \frac{886\ (0.12)}{165} = 0.63$$

Finally, reading from the constant ductility response spectra of Figure 5.20 (which has been derived for two ductility levels, 2% damping and bi-linear model with 0.5% strain hardening), one can see that for a period of 0.211 and a strength ratio of 0.63, the ductility demand on the equivalent SDOF system is approximately 4. Since Ω=1, it can be assumed that the eccentric system's weak element inelastic response will also be 4, and the strong element's response shouldn't exceed 4 either. This is correct, as the true calculated inelastic weak element response is 3.9, and strong element response is 3.7.

Especially in the case where $\Omega \neq 1$, it would not be adequate to use only a single earthquake record for design purposes. Nevertheless, for expediency here, only the El Centro earthquake record will be considered. Following the same steps as above (element modeling, damping ratio, yield displacement are also the same), the inelastic element response can be predicted for the system with parameters T_x=0.2, Ω=2 and e/r=0.1 (true periods T_t=0.20 and T_θ=0.10), where the 1940 N-S El Centro peak acceleration is now arbitrarily scaled to 0.46g. The weak element elastic dynamic response is calculated as 0.50 inch. The pseudo-displacement from Figure 5.19 is Sd=0.36. The earthquake scaling for the equivalent SDOF system becomes 186 inch/sec.^{2}. The strength ratio is now 0.64, and the

predicted ductility (from Figure 5.20) is again 4. Nevertheless, since Ω is not equal to unity anymore, it has been shown to be conservative to increase by 50% the predicted weak element value. The estimated weak element ductility is then 6, and the estimated strong element ductility remains 4. This is adequate, as the calculated strong and weak element ductilities for the initially eccentric system are respectively 5.2 and 3.0.

In order to illustrate the methodology, only one earthquake excitation has been used. In a true design procedure, it is essential that many earthquake records be included.

For design purposes, the steps in the above process can be interchanged to produce the required strength for a desired ductility level. Thus, the earthquake scaling factor would be determined as before. Nonlinear response spectrum would be used to determine η for a target weak element ductility. For conservatism a value 1/1.5 to 1/2 times smaller than the desired ductility should be used. With the scaled earthquake peak acceleration and η value, the required yield displacement can be obtained directly.

5.8 Conclusions of the Study of Initially Eccentric Systems

In order to investigate the effect of different parameters on the torsional response of initially eccentric systems, many cases of initially eccentric systems were analyzed and compared with equivalent SDOF systems. The equivalent SDOF systems were defined in a way that was thought to be useful in the perspective of elastic dynamic analysis. A methodology has been proposed to perform a meaningful liaison between the equivalent SDOF system and corresponding initially eccentric system.

For elasto-perfectly plastic hysteretic element models, it was found that the equivalent SDOF system provided a reliable way to predict the inelastic response of structural elements in a two-element system. Contrary to what has been found by other researchers who studied this problem from other approaches, the proposed method is not affected by the level of excitation (target ductility level), ratio of uncoupled frequencies Ω, uncoupled period T_x, and normalized eccentricities (e/r).

In the case of Ω=1.0, the equivalent SDOF response will perfectly match the weak element response of the initially eccentric system (provided the yield displacements are similar). A formal proof has been developed.

For other values of Ω, it was shown that the ductility ratios obtained by the proposed equivalent SDOF method (methodology explained in Section 5.4) are often close to unity in the case of mean response from five earthquake excitations, with a conservative design value to be taken as 1.5. It is understood that response under a single earthquake excitation may strongly differ from the one predicted using the mean response from five earthquake, the same way this can also be expected in the case of symmetric structures.

A proposed design procedure, relying mainly on elastic analysis and readily available simple design tools, has been proposed.

6. EXTENSION OF INVESTIGATION TO MORE ELABORATE CASE STUDIES

Using relatively simple structural and element models, several basic conclusions were developed in Chapters 4 and 5. In this chapter some more complex structures will be investigated. In particular, results will be obtained to verify whether those previous findings remain valid. Rather than performing a comprehensive investigation of all the possible variables (number of stories, number of elements, element model, structural configuration, etc.), it was decided to approach the problem in a case-study manner by studying those variations individually using a common reference case as a benchmark.

6.1 Single Story Multi-Element Systems

In all of the prior analyses only two lateral load resisting elements were considered. The reasons for this were discussed in Chapter 3 as were some of the problems with generalizing results obtained with multi-element models. In this section, selected analyses of the types performed previously will be run now considering systems with up to eight lateral load resisting elements. For all of the multi-element cases considered here, the hysteretic bi-linear model with 0.5% strain hardening was adopted and the slab was constrained to be rigid in-plane to insure two dynamic

degrees-of-freedom. Damping was again of the Rayleigh type set at 2% of critical for each systems's two vibration periods.

6.1.1 Initially Symmetric Systems

The reference cases used for the initially symmetric multi-element systems had uncoupled translational periods of T_x=0.4 (no eccentricity of course), and were subjected to the N-S component of the 1940 El Centro earthquake scaled to produce a target ductility of 4 on the equivalent SDOF system.

The initially symmetric two element systems revealed a trend for the weak element response to increase along with the ratio of uncoupled frequencies Ω. So, the chosen reference system was the "1.0 Fy and 1.5 Fy" case with Ω values of 0.4, 0.8, 1.0, 1.2, 1.6 and 2.0. For these cases, the weak element ductility ratios were 0.84, 0.90, 1.0, 1.25, 1.80 and 1.94, respectively. These results are compared with those for multi-element systems having various juxtapositions of element yielding at these two levels.

The combinations investigated are shown in Table 6.1 and consist mainly of a single transition from a group of "strong" elements to a group of adjacent "weak" elements.

The primary variables were the total number of elements and number of elements in each group. Combinations with increased number of transitions from strong to weak elements were not studied. Despite the fact that some of the examples explored were improbable, the chosen set covers a wide spectrum of multi-element initially symmetric systems.

All multi-element initially symmetric systems studied were symmetric with respect to the center of mass, meaning that each element on one side of the center of mass had a equidistant counterpart of same stiffness on the other side of this center. Within this limitation, systems with equally spaced elements of equal stiffness were studied, as well as more general systems with unequally spaced elements of unequal stiffness.

The weak element ductility ratios for the multi-element system with equally spaced elements with equal stiffness are presented in Table 6.1. The weak element considered here of course is the edge weak element. The results for the equivalent two-element systems are inserted in the upper right corner of the Table for comparison purposes. The strong edge element ductility ratios are similarly presented in Table 6.2.

As expected, the weak element ductility ratio is not unity anymore when $\Omega=1$; even though the multi-element

system's response would be the same elastically. Following the first yield excursion, the inelastically initiated rotational motion will force the various elements along different hysteresis loops, thereby violating the conditions for the responses to be identical.

It can be observed from Table 6.1 that the weak element ductility ratios obtained for two-element systems are very similar to the ones for multi-element systems with equally spaced elements of equal stiffnesses. For low Ω values, the results are very similar, and for high Ω values, the two-element systems's results are conservative in many instances. For most multi-element combinations, the differences between ductility ratios for multi-element and two-element systems are not significant. The response variations from equivalent multi-element systems (4, 6 and 8 elements) were even less noticeable than when going from a two-element system to a four-element system. For all combinations, the trend of increasing weak element ductility ratios with increases in Ω remained visible.

Investigation of multi-element systems with non-equally spaced elements and/or dissimilar stiffnesses was performed on four-element systems only (in light of the mostly invariable response from equivalent multi-element systems with different number of elements). The element distribution (location and stiffness) was constrained to be symmetric

around the center of mass, and all elements yielded at 1.0 Fy on one side of that center (weak side), and at 1.5 Fy on the other side (strong side). Therefore, an outside stiffness K_1 and distance D_1 as well as an inside stiffness K_2 and distance D_2 could be defined. A unique combination of K_1/K_2 and D_1/D_2 (along with T_x and Ω of course) corresponds to a unique system (geometrically non-dimensionalized as explained in Chapter 3).

For all six values of Ω, three different spacing were investigated along with seven different stiffness ratios. The resulting weak element ductility ratios are tabulated in Table 6.3 (outside (i.e. edge) weak element) and Table 6.4 (inside weak element). The resulting strong element ductility ratios are not presented here. It must be realized that $D_1/D_2=3$ is an equally spaced element system, and $K_1/K_2=1$ is an equal stiffness distribution system. Systems with $D_1/D_2=4$ have the two inside elements closer near the center, while $D_1/D_2=2$ systems have their inside elements more toward the edges. Large K_1/K_2 values represent systems with stiffer element on the edges, where small K_1/K_2 values produce just the opposite.

From Tables 6.3 and 6.4, it is clear that systems with stiffer elements on the edge are rather insensitive to the D_1/D_2 and K_1/K_2 ratios, with the outside weak element's results being practically similar to what was obtained in the

case of equally spaced elements of equal stiffnesses. On the other hand, systems with more flexible elements on the edge are greatly affected by the stiffness ratio K_1/K_2; very low ratios of 1/16 produce the largest increase in outside and inside weak element ductility ratios, especially for large Ω values (although the inside weak element seems practically unaffected by K_1/K_2 for Ω less than unity). The D_1/D_2 ratio mainly affects the inside weak element's response when Ω is large, although the maximum effect is less than 40% in the worst situation. The D_1/D_2 ratio is seen to produce even less significant response variations on the outside weak element, at most slightly affecting the zone of combined "low Ω and high K_1/K_2" and of "high Ω and low K_1/K_2".

When compared with the two-element system ductility ratios, the inside weak element results are mainly conservative, where as the outside weak element results grow from conservative (for high K_1/K_2) to slightly unconservative (for low K_1/K_2). Magnifications of more than 25% from the two-element reference cases start to occur from $K_1/K_2 = 1/8$ and reaches up to 60% in some instances. Since the ductility ratios were already high for large Ω, additional amplifications in those ratios could eventually become seriously detrimental to the behavior of those edge elements, and in that respect, <u>excessively small K_1/K_2 ratios should be avoided</u>.

6.1.2 Initially Eccentric Systems

The reference cases selected to investigate initially eccentric systems had an uncoupled translational period of T_x=0.4 and a normalized eccentricity of 0.3. These were subjected to the N-S component of the 1940 El Centro earthquake scaled to produce a target ductility of 4 on the equivalent SDOF systems. Again, for consistency, six Ω values (0.4, 0.8, 1.0, 1.2, 1.6 and 2.0) were used for every system studied.

A wide variety of stiffness distributions were considered (Tables 6.5 and 6.6). A linear stiffness variation is first studied with three different regular geometric configurations for four-element systems, and one configuration for six-element systems. All of these have equally spaced elements. Then, single-step and double-step stiffness variations were studied on four element systems; a single-step variation implies that all elements on a given side of the center of mass have the same stiffness (the value differs from side to side), whereas a double-step change means that one outside element has a high stiffness value, the other one has a low stiffness value, and both inside elements have the same median value. Finally, a single four-element case of totally irregular stiffness and geometric distribution was analyzed; the configuration chosen is

illustrated in Table 6.6 (it represents an odd structure where the mass and stiffness variations along the length would be opposed, creating a rather severe case of eccentricity). All multi-element initially eccentric systems studied were geometrically symmetric with respect to the center of mass, such that each element on one side of the center of mass had an equidistant counterpart (of different stiffness) on the other side of this center (except for the totally irregular case, of course). These multiple analyses were expected to cover a wide range of conceivable structures.

The method described in Chapter 5 was used (i.e. matching of the maximum elastic displacement of both the equivalent SDOF system and the eccentric system's edge weak element in order to provide appropriate SDOF strength ratios) and the resulting edge element ductility ratios were computed. The equivalent SDOF element model was intended to match the one of the edge weak element.

Element ductility ratios thus obtained are summarized in Tables 6.5 and 6.6. Variations from one type of stiffness distribution to the other do not produce significant changes in the ductility ratios (one must remember that it is not implied that all those systems have the same edge response, but only that, when compared to an equivalent SDOF system based on the previously explained method, the ductility

predictions seem to have a consistent level of accuracy). Further, when compared to the reference two-element systems, it is observed that the number of elements does not significantly affect the magnitude of the ductility ratios. An increase of ductility ratio of approximately 25% is the highest amplification observed for regularly spaced elements. For the totally irregular four-element system, the discrepancy with the reference system is somewhat larger, but is by no means exceptional in itself.

Therefore, it appears that the conclusions of Chapter 5 may be equally applicable to single story multiple-element systems.

6.2 Various Element Models for Single Story Systems

Up to this point, all analyses conducted have relied on a bi-linear hysteretic model (with 0.5% deformation hardening). It is therefore appropriate to investigate the effect of different element model on torsional coupling. To do this, two different brace models were chosen: 1) A simple brace model that allows yielding in tension and elastic buckling in compression (See Figure 6.1 and Mondkar & Powell [39]); 2) A more complex physical brace model that is capable of better representation of the true behavior of braces (See Figure 6.2 and Ikeda & Mahin [35]). All structural elements

considered consisted of pairs of opposing models representing X-braced frames (with braces not connected in their mid-point).

The reference set for the case study is again Tx=0.4 (e/r=0.3 for initially eccentric case), 2% damping, a target ductility of 4 for the equivalent SDOF systems, and the N-S component of the 1940 El Centro earthquake. The usual six values of Ω are considered in each situation.

6.2.1 Initially Symmetric Systems

6.2.1.1 Elastic Buckling Brace Element

For the "elastic buckling" type of braced frame, the X-braced frame model's hysteretic relation becomes more complex. Typical hysteretic loops are presented in Wakabayashi (1986) [68]. The yield displacement was taken as the value at the onset of first yielding of the brace in tension under a monotonically increasing loading. Frames were considered of equivalent strength, if the sum of the strengths of their compression and tension braces were equal, with the implication that thus defined equivalent frames would not necessarily have the same yield and buckling displacements. Consequently, torsional coupling could be introduced in an initially symmetric system with two frames

of equivalent strength. Nevertheless, it was decided to combine elements to produce systems having one frame 50% stronger than the other in order to allow some level of comparison with the two-element "1.0 Fy and 1.5 Fy" case.

Three weak element combinations, representing different levels of slenderness, were investigated: 1) Yield and buckling at Fy; 2) Yield at 1.25 Fy and buckling at 0.75 Fy; 3) Yield at 1.50 Fy and buckling at 0.5 Fy (the yield stresses are useful as strength indicators here since the geometry and areas are the same for all braces studied). To each of these "weak element" combinations were matched three different "strong element" combinations whose yield and buckling levels are presented in Table 6.7.

Ductility ratios are calculated by comparing the "weak" and "strong" element ductility demands with the respective equivalent braced frame SDOF ductility demand. Note that the earthquake levels found in the case of the bi-linear hysteretic element were not applicable (these produced ductilities exceeding the target ductility by factors of up to 3 or more. Scaling to the proper target ductility of 4 had to be redone for this new type of element. It must also be well understood that each ductility ratio involved a comparison between an initially symmetric two element braced frame of the type described above and an equivalent SDOF

braced frame with yielding and buckling levels identical to the weak element in the initially symmetric system.

From the results in Table 6.7, it is difficult to perceive a clear trend, although larger Ω values produce larger ductility ratios in general. There is apparently a very slight tendency of the weak element to have a larger response when the strong brace is more slender (i.e. yields in tension at higher stress along with earlier buckling). However, because of the way the equivalent braced frames were defined, one should refrain from any attempt to identify which sets produce the most sensitive combinations. Rather, the emphasis here is placed in demonstrating the relatively minor sensitivity of the initially symmetric systems to various strong element constructions.

In line with the terminology defined in Chapter 4, the ductility ratios can be said to be of moderate importance, except for an occasional value here and there (always when Ω is above unity). Notably, the weak element ductility ratios are all unity when Ω=1, as already demonstrated for two-element systems sharing similar element models with their equivalent SDOF system (which is the case here).

6.2.1.2 Physical Brace Element

In the case of the physical brace model, the element model relation for the X-Braced frame is again very complex and largely dependent on the slenderness ratio of the braces. There is a great number of differences between the physical brace model and the more simplistic model presented before. It is beyond the scope of this study to provide detailed explanations regarding the X-braced behavior. For more information, the reader unfamiliar with this material should consult Wakabayashi (1986) [68] or Mahin & Ikeda (1984) [35].

It should be noted that even under monotonically increasing loads, the capacity of the compression brace deteriorates so that it carries much less load than its buckling load when yielding occurs in the tension brace. Therefore, the concept of frames with equivalent strength used in the preceding section is not applicable here. It was therefore decided to simply investigate one simple case of a two-element system with dissimilar braces. Structures having dissimilar braces are often created when the design engineer uses a single strong X-braced frame at one end of a building and two smaller X-braced frames at the other end. Although it is possible using elastic analysis methods to calibrate the brace stiffnesses such that the structure is symmetric, the inelastic action starting to occur with brace buckling will induce torsional motion in this structure.

Here, the weak element is defined as yielding at 1.25 Fy and buckling at 0.75 Fy, whereas the strong element was set as yielding at 1.5 Fy and buckling at 0.5 Fy. The post-buckling loss in compression capacity being found to be rather rapid, the frame with braces yielding at 1.25 Fy was indeed found to have a lower ultimate strength for a given displacement. Nevertheless, this example points to the difficulty in defining the weak element in some instances, and to some of the problems associated with torsion in strength deteriorating systems.

To use the physical brace model, the slenderness ratios were calculated to produce the desired buckling stresses (KL/r of 103 for the weak element, 128 for the strong element), and other brace properties were determined to model buckling along the weak axis of a typical wide-flange section.

The level of earthquake excitation is adjusted such that an equivalent X-braced frame SDOF system (made of physical brace element yielding at 1.25 Fy and buckling at 0.75 Fy) reaches a target ductility of 4. Thereafter, the initially symmetric system described above is subjected to the same earthquake excitation. The resulting ductility ratios are presented in Table 6.8. It must be emphasized again that the level of excitation needed to reach the target ductility of 4

is much lower for the physical brace element than for the bi-linear hysteretic element.

As observed in Table 6.8, the sensitivity of the ductility ratios for this type of element model is very similar to that noted in Chapter 4. However, in this particular case no trend with Ω can be noticed. Of course, generalization should not be made from this single set of analysis.

Here again, the peak weak element ductility ratios are mostly representative of magnifications of moderate importance. Therefore, the element model seems to have no major influence in the predicted ductility demand of initially symmetric systems as long as the comparison is performed with the proper equivalent SDOF element model.

6.2.2 Initially Eccentric Systems

As for all other initially eccentric systems, the torsionally coupled results are compared with an equivalent SDOF system with an identical element model. This is important as braced frames can often be more sensitive than bi-linear hysteretic systems (in some cases, the physical brace element reached ductilities more than 10 times the ones attained for the bi-linear hysteretic model under the same

level of earthquake excitation). Clearly, the intent here is to compare a torsionally coupled system with it's equivalent SDOF system such that the true contribution of the coupling can be extracted. Recall that an initially eccentric system's equivalent SDOF system has a period equal to the predominantly translational period of the torsionally coupled system, a force-displacement relationship identical to the one for the weak element in the coupled system, and is subjected to a different earthquake level such that its elastic displacement will match the one for the weak element in the coupled system.

Inelastic response spectra for X-braced frames (as well as for other complex models) are not commonly available. They are also sensitive to modeling uncertainties. Therefore, use of the proposed method in a preliminary design stage will require considerably more effort and judgement on the part of the engineer.

6.2.2.1 Elastic Buckling Brace Element

In the case of initially eccentric systems with elastic buckling brace element models (corresponding to X-braced frames) the same three yield combinations described in Section 6.2.1 were used with the exception that now both weak

and strong elements yield and buckle at similar levels (again interpreted in terms of stresses).

From Table 6.9, it is apparent that the scaling method applied to the new element model preserves the parametric insensitivity first observed in Chapter 5. Results even tend to be more clustered around the ductility ratio of 1 than for the reference two-element hysteretic system, although one single set of parametric variation is insufficient to generalize this observation.

The conclusions of Chapter 5 seems equally applicable to the case of two-element systems with X-braces modeled with elastic buckling members.

6.2.2.2 Physical Brace Element

For initially eccentric systems with physical brace models used for the X-braced frames, only two yield combinations were investigated: intermediate (KL/r = 103) and large (KL/r = 128) slenderness. Of course, here, both elements share the same slenderness in any given case. These respectively correspond to the "Yield = 1.25 Fy, Buckling = 0.75 Fy case", and "Yield = 1.5 Fy, Buckling = 0.5 Fy case", as previously explained.

Results are presented in Table 6.9, and again, when ductilities of comparable eccentric and SDOF systems are related, the conclusions of Chapter 5 seem equally valid.

6.3 Multi-Story Systems

One of the major problems associated with multi-story systems is the definition and determination of the centers of rigidity. A good treatment of this topic can be found in Cheung and Tso (1986) [12]. Nevertheless, for the purpose of this study, the centers of rigidity were not essential to perform the ensuing examples and thus were not identified.

For the following case studies, all elements were modelled as being bi-linear hysteretic with 0.5% strain hardening. Rayleigh damping of 2% was chosen at the first and last period of the multi-story system, which implies than the intermediate periods had a somewhat lower damping.

Exceptionally here, no target ductility was fixed for the equivalent SDOF systems. Because of the various ductility definitions that will be used thereafter, it was judged more appropriate to simply apply the N-S component of the 1940 El Centro earthquake (with peak acceleration scaled to 0.5g) to the multi-story systems of interest. In any event, the ductility ratios of torsionally coupled systems

were demonstrated in previous chapters to be independent of the target level of excitation.

The response of multi-story torsionally coupled systems and equivalent SDOF systems will be compared in hope of extending the validity of the concepts derived for the single-story systems. The main concern evidently lies in the proper identification of the equivalent SDOF system. Therefore, in parallel with the definition of Chapter 5, the equivalent SDOF system's period was defined as that of the first dominantly translational mode of the multi-story system. Unfortunately, for many multi-story systems, it may be particularly difficult to visually recognize this mode. The following equations allow a formal determination of the mode shape identification factor (percentage of torsional or rotational) in each direction (some programs, like SAP80 [70], provide this information automatically when performing modal analysis):

For a system with normalized mode shapes such that:

$$\Phi_N^T \; m \; \Phi_N = M_N = I$$

where m is the mass matrix, I is the identity matrix, Φ_N is N^{TH} mode shape, and M_N is the generalized mass of the N^{TH} normal mode, the expression for the "effective modal participation factors" can be expanded into:

$$\Phi_N \; L_N \; / \; M_N \; = \; \Phi_N \; L_N \; = \; \Phi_N \; \Phi_N^T \; m \; r^*$$

where L_N is the modal earthquake-excitation factor and r^* is the pseudostatic influence-coefficient vector. Using the equations derived around the center of mass (m_I being the terms of the diagonal mass matrix), the mode shape identification factors can be obtained by summing the diagonal elements of the ($\Phi_N \; \Phi_N^T \; m$) matrix, such that:

$$\sum_{I=1}^{N} \Phi_{I\,N}^2 \; m_I \; = \; \Phi_{1\,N}^2 m_1 \; + \; \Phi_{2\,N}^2 m_2 \; + \; \ldots \; + \; \Phi_{I\,N}^2 m_I$$
$$\Phi_{J\,N}^2 (mr^2)_J \; + \; \ldots \; + \; \Phi_{N\,N}^2 (mr^2)_N$$

where the translational masses terms are grouped separately from the mass moment of inertia terms. The highest period for which the grouped translational terms equals or exceeds 50% of the sum is defined as the equivalent period (an exact 50% split is typical of systems with Ω=1).

An additional problem comes from the impossibility of finding a SDOF model which would perfectly match at all times the behavior of the weak side of an initially eccentric multi-story system. Even if δ_y is set to each level interstory's yield displacement, these are not necessarily reached simultaneously during dynamic response of this system. Nevertheless, it was decided to model the SDOF system as a bi-linear system with yield displacement equal to the sum of the multi-story system's interstory yield

displacements. In light of the general goals pursued in this chapter, that simplification was thought to be acceptable.

Three types of two-story systems were used in this part of the study. Each will be described in the following sections.

6.3.1 Initially Eccentric Systems - Regular Configuration

Systems with regular configuration are simply defined here as systems for which the floor plan remains the same at each story (equal mass and mass moment of inertia) and where the reduction in stiffness from story to story remains proportional for each structural element resisting lateral forces.

Since the location of the center of stiffness has not been identified, it is equally logical not to attempt to define a ratio of uncoupled frequencies Ω for multi-story systems. Nevertheless, it was decided to conserve the same strong-to-weak element stiffness ratio as for the cases of two-element systems studied. For $e/r=0.3$ and $\Omega=0.4$, 0.8, 1.0, 1.2, 1.6 and 2.0, the stiffness ratios were 7.0, 2.2, 1.86, 1.67, 1.46 and 1.35, respectively. Of course, these ratios were kept constant from story to story.

Two different stiffness variations from the first to the second story were investigated. In one case, the ratio of second story over first story stiffnesses was 2/3, and in the other case 1/3. The corresponding two uncoupled translational periods were 0.28 and 0.12 seconds for the first case, and 0.34 and 0.14 seconds for the second case.

Because there was a need to equate elastic displacements in order to perform the proper ductility comparison, it was judged consistent with the equivalent SDOF model approach to match the maximum elastic displacement with the maximum roof displacement on the weak side of the multi-story system.

Maximum interstory drifts and their corresponding interstory displacement ductilities were also calculated for each element. The roof displacement ductilities as well as each interstory displacement ductilities have been divided by the ductility of the equivalent SDOF system, providing three different ductility ratio indicators. These are tabulated in Table 6.10 for the weak and strong elements. Note that in a manner similar to that done for the equivalent SDOF systems, the roof yield displacement has simply been taken as the sum of each story's element yield displacement.

It can be observed from Table 6.10 that the roof ductility ratios, although different to what has generally been obtained for two-element systems, are not necessarily

better or worse (i.e. most results are conservative or slightly above unity with a few occasionally larger values). This is remarkable considering the approximations in the equivalent SDOF model used as well as the slight non-uniformity of damping in all modes.

Unfortunately, the interstory ductility ratios do not fare as well. For the case when the ratio of second story over first story stiffnesses is 2/3, the lower story's interstory ductility ratios tend to be rather large whereas the upper story's ones are all conservative. For the case where the second to first story ratio of stiffnesses is 1/3, the situation is reversed as it is now the top story ductility ratios that are considerably high.

Clearly, the equivalent SDOF method as presently formulated is not suitable in predicting interstory ductilities, although it may still reasonably predict roof displacement ductilities. As noted in the above examples, the equivalent SDOF system analogy is somewhat impaired when inelastic action tends to concentrate in a given story. This same phenomenon also occurs when comparing inelastic response of planar multi-story frames (without torsional coupling) with inelastic SDOF systems. More research on this topic should help circumvent this difficulty.

6.3.2 Initially Symmetric Systems - Regular Configuration

In this section, the definition of regular configuration is the same as in the preceding section. Here, only cases were considered where the top story over bottom story stiffness ratio was 2/3. Both elements on a given story had the same stiffness, and elements on one side were yielding at a strength 50% larger than on the other side (thus defining a weak and a strong side). As before, the uncoupled translational periods were 0.28 and 0.12 seconds, and the radius of gyration used (still the same at each story) were identical to those of two-element systems having the same edge distance d (recall Ω was equal to d/r).

In this section, each initially symmetric system is compared to a similar two-story system where elements on a given story always yield simultaneously (that is an equivalent uncoupled two-degree-of-freedom system and not an equivalent SDOF). Here, the force-displacement relationship of the regular two-story two-degrees-of-freedom system is identical to the one of the weak side of the initially symmetric system (weak side being the one with elements of lower yield strength element). This approach is in agreement with the one followed for all other initially symmetric systems studied up to this point.

The roof displacement ductilities as well as each of the interstory displacement ductilities have been calculated for both systems (i.e. the one with unequal story yield strengths, and the equal story yield strength one), and the corresponding ratios for each element were directly obtained. The results are tabulated in Table 6.11. Again, the roof yield displacement has simply been taken as the sum of each story's element yield displacement.

As expected, all weak element ductility ratios are unity when (d/r)=1, since the weak side model is identical to the uncoupled two-story reference system's one. Otherwise, the weak elements ductility ratios tend to become generally larger with a decrease in radius of gyration (as originally noted in the two-element systems). The largest ductility ratio measured was 1.36, which is relatively low.

Therefore, the conclusions of Chapter 4 may be equally applicable for multi-story systems with regular configuration, as long as the initially symmetric systems are compared with their equivalent uncoupled multi-story systems.

6.3.3 Multi-Story Systems with Irregular Configuration

In order to obtain a severely irregular configuration, a single two-story structure with a set-back was analyzed. The

top slab had half the floor area (and mass) of the lower slab, and consequently, the mass moment of inertia was 5 times less (r^2 being 2.5 times less). Both floors were assumed infinitely rigid in their plan.

Severe stiffness variations were chosen to accentuate the coupling. The structure, still monosymmetric, is schematically illustrated above Table 6.12. The lateral resisting elements are located on three equally spaced design lines on the lower floor, and two on the top floor. The stiffness on the first design line (the common edge to both story) was set to be the largest and uniform along height. If the interstory stiffness along the first design line is referred as K, then the stiffness along the second design line is taken to be K/2 on the lower story, and K/6 on the top story, and again K/6 on the third design line. Still, all elements have similar yield displacement (and thus yield stresses of Fy) in accordance with the model previously defined for the initially eccentric systems in this study.

The first two periods (0.6 and 0.4 sec.) are dominantly rotational, and the last two (0.18 and 0.082 sec.) are dominantly translational. The equivalent SDOF systems period is thus taken as 0.18 seconds.

The real problem with such an irregular system is to determine which maximum elastic displacement should be made

to match the maximum elastic displacement of the SDOF system. Here, a weaker side can fortunately be identified, but for other structural configurations, this may not be possible. Generally, some judgement is needed, especially since it may be possible to encounter some unusual set-back structures where the largest elastic edge displacement could occur on the lower story. In this current example, it was judged appropriate to use the roof weak side maximum displacement for the comparison. Other steps were executed as before, and the results are presented in Table 6.12.

Of course, since only one case is analyzed, there is no intent to draw general conclusions. Still, it is interesting to notice in this case that although the roof displacement ductility ratios were conservative to good, the interstory ductility ratios were definitely worse. Nevertheless, considering the severe irregularity of this sample structure, the resulting ductility ratios remain reasonably well behaved, the maximum value being 1.76.

6.4 Concluding Remarks

These examples do not entirely demonstrate that the equivalent SDOF system concept can lead to adequate ductility predictions in the case of severely irregular structures or ones having complex lateral load behavior. They do however indicate that the method is promising for the cases studied

and that it deserves additional consideration in future research.

7. SUMMARY AND CONCLUSIONS

7.1 Summary

The basic concepts inherent in the response of torsionally coupled systems have been reviewed in Chapter 2. The equations of motion around the center of mass have been derived as well as expressions for the fundamental parameters globally describing the elastic response. Additional relationships have been presented for the special case of monosymmetric systems. A literature review with respect to the inelastic response of torsionally coupled systems has also been presented in that chapter. The lack of agreement between different researchers on how variations in the fundamental parameters influence the response was emphasized.

Some preliminary observations related to the response of torsionally coupled systems were identified in Chapter 3. A tentative classification scheme for various types of inelastic torsionally coupled systems was proposed. A series of relatively isolated analyses supported the decision to focus the attention on: two-element single-story stiffness eccentric systems; bi-linear hysteretic element models; and equal yield displacement for both elements in any given case.

The concept of equivalent non-linear systems was obtained from the expansion of the incremental equations of

motion in Appendix A. The requirements for geometry-independence were enunciated in Chapter 3.

A parametric study of initially symmetric systems was performed in Chapter 4. The effects of the ratio of uncoupled frequency Ω, the uncoupled period T_x, ductility levels and various yield combinations were investigated. This parametric study was repeated for five different earthquake records and the mean responses were calculated. The seismic performance of every initially symmetric system was compared with the performance of its equivalent SDOF system: ratios of ductility factors were thus obtained and judged the best indicator of the severity of the torsional response induced by the unequal yield strengths. The effect of the various parameters on the system's behavior were assessed.

A similar parametric study was conducted for the initially eccentric systems. The corresponding findings are presented in Chapter 5. The effect of Ω, T_x, ductility levels, and normalized eccentricities (e/r) were again investigated under five earthquake excitations, and mean responses were again calculated. The procedure for determining an equivalent SDOF system was formulated. The special case of Ω=1 produced a more predictable weak element response and this phenomenon was clearly explained by specializing the equations of Appendix A. A method was

formulated to provide a fair comparison between the coupled system and an equivalent SDOF system, simultaneously providing a capability to predict element ductilities in the coupled system from readily available design tools. Consequently, some examples of preliminary design were presented making use of the knowledge acquired in that chapter.

Finally, Chapter 6 investigated to what extent the findings of the two previous chapters (obtained on two-element single-story systems) could be extended safely to other situations, namely: multi-element single-story systems; other types of element models; regular multi-story systems; and systems with totally irregular configurations. Individual case studies were performed in all of those situations, the intent being not to provide a comprehensive study of all possibilities, but rather investigate whether the previously obtained results might be extended to other less restrictive situations.

7.2 Suggested Future Research

Although different element models, multi-element systems and multi-story systems were analyzed, this part of the investigation was far from being comprehensive. Future research should clearly attempt to provide additional insight

on those topics especially in the case of multi-story systems. The equivalent SDOF system concept could probably be extended or modified to account for higher order effects and the occurrence of soft stories. The case of irregular systems should be given particular attention.

Despite the fact that the element model was found to be a non-influential factor on the ductility predictions obtained through the equivalent SDOF concept, there is still a possibility of identifying other types of stiffness degrading systems which could lead to unacceptably unstable response under coupled behavior. The importance of parameters controlling the basic sensitivity of torsional response to various models should be explored too.

Realistic three dimensional models should also be investigated in order to acquire an understanding of how the elements along lines perpendicular to the earthquake excitation contribute to the resistance. In that case, it would appear desirable to concurrently study bi-directional seismic input.

The study of actual structures that have sustained serious damage as a consequence of inelastic torsional coupling, as well as shaking table analysis of prototype structures, would also be greatly beneficial.

Finally, some additional guidance should be provided on how to integrate into current seismic codes the new knowledge about the inelastic response of systems with mass and/or stiffness eccentricities.

7.3 Conclusions

Preliminary work indicates that both static and dynamic elastic analysis methods may be unable to predict how torsionally coupled systems will respond when excited by rare and unusually intense earthquakes. The damage concentration that may occur in the weaker element of such systems is revealed by inelastic analysis methods.

In the case of initially symmetric systems, the torsional response is created by the desynchronizing inelastic element response, despite the existence of symmetry in the elastic domain. It has been demonstrated that the element ductility levels will remain within reasonable bounds (when compared to the ductility levels obtained with an identical system free of torsional coupling, that is, having synchronized element yielding) as long as:

1) The ratio of uncoupled frequencies Ω is not excessively large (preferably 1.2 and lower); large Ω produces larger element ductilities since the reduced mass moment

of inertia provides a lower resistance to angular motion.

2) The yield level of the weaker element in the initially symmetric system is not less than the yield level of the system with synchronized yielding; furthermore, as long as this condition is satisfied, the system's period does not affect this conclusion.

Finally, the ratios of element ductility factors for the torsionally coupled system to those of equivalent SDOF systems are insensitive to the levels of earthquake excitation.

In the case of initially eccentric systems, an equivalent SDOF system was defined and related to the torsionally coupled system in a manner such that the weak element response is now unaffected by the traditional parameters Ω, e/r T_x and level of earthquake excitation; a conservative approach would suggest that the weak element's ductility in the coupled situation is generally 50% higher than for its equivalent SDOF system.

For all types of <u>two-element</u> systems studied, the weak element ductilities are always equal to their equivalent SDOF ductilities when Ω=1.0.

It appears that the findings in relation to both initially symmetric and eccentric systems may be equally applied to equivalent multi-element single-story systems and systems with various types of element models. However, initially symmetric systems with excessively small K_t/K_e should be generally avoided. The extension of those same results to the case of simple multi-story systems seems adequate in terms of roof displacement ductility, but often fails to provide a good interstory ductility prediction. General multi-story systems with severe configuration and stiffness distribution irregularities are less appropriately treated by this equivalent SDOF concept.

8. REFERENCES

1. Anagnostopoulos, S.A., Roesset, J.M., Biggs, J.M., "Non-linear Dynamic Analysis of Buildings with torsional effects", 5th World Conference on Earthquake Engineering, Vol. 2, Rome, Italy, 1973, pp.1822-1825.

2. Antonelli, R.G., Meyer, K.J., Oppenheim, I.J., "Torsional Instability in Structures", International Journal of Earthquake Engineering and Soil Dynamics, Vol. 9, 1981, pp.221-237.

3. Arnold, C., Reitherman, R., Building Configuration and Seismic Design, John Wiley & Sons Inc, 1982.

4. Ayre, R.S., "Interconnection ot Translational and Torsional Vibrations in Buildings", Bulletin of the Seismological Society of America, Vol. 28, No. 2, April 1938, pp. 89-130.

5. Ayre, R.S., "Experimental Response of an Asymmetric, One-Story Building Model to an Idealized Transient Ground Motion", Bulletin of the Seismological Society of America, Vol. 33, No. 2, April 1943, pp. 91-119.

6. Balendra, T., "A Simplified Model for Lateral Load Analysis of Asymmetrical Buildings", Engineering Structures, Vol. 5, 1983, pp.154-162.

7. Béjar, L.A., Gergeley, P., "Linear Response of Torsionally Coupled Buildings for Multicomponent Earthquake Excitations", 8th World Conference on Earthquake Engineering, San-Francisco, United-States, 1984, pp.219-226.

8. Bozorgnia, Y., Tso, W.K., "Inelastic Earthquake Response of Asymmetric structures", Journal of Structural Engineering, ASCE, Vol. 112, No.2, February 1986, pp.383-400.

9. Bruneau, M., Personal Observations During a Damage Investigation of Mexico City, January 1986.

10. Bustamante, J.I., Rosenbluth, E., "Building Code Provisions on Torsional Oscillations", Proceedings of the Second World Conference on Earthquake Engineering, Vol. 2, Tokyo, Japan, 1960, pp.879-894

11. Chen, W.F., Atsuta, T., "Inelastic Response of Column Segments Under Biaxial Loads", Journal of the Engineering Mechanics Division, ASCE, Vol. 99, No. EM4, August 1973, pp.685-701.

12. Cheung, V.W.-T., Tso, W.K., "Eccentricity in irregular multistory buildings", Canadian Journal of Civil Engineering, Vol. 13, No. 1, February 1986, pp.46-52.

13. Clough R.W., Penzien J.P., Dynamics of Structures, McGraw-Hill Inc. ,1975

14. Dempsey, K.M., Tso, W.K., "An Alternative Path to Seismic Torsional Provisions", Soil Dynamics and Earthquake Engineering, Vol. 1, No. 1, 1982, pp.3-10.

15. Dewell, H.D., "Earthquake-Resistant Construction II-Principles of Design", Engineering News Record, Vol. 100, No. 18, May 3, 1928, pp.699-702.

16. Douglas, B.M., Trabert, T.E., "Coupled Torsional Dynamic Analysis of a Multistory Building", Bulletin of the Seismological Society of America, Vol. 63, No.3, 1973, pp.1025-1039.

17. Engle, H.M., "The Earthquake Resistance of Buildings from the Underwriters' point of view", Bulletin of the Seismological Society of America, Vol. 19, No. 2, June 1929, pp.86-95.

18. Foutch, D.A., "The Vibrational Characteristics of a Twelve-Storey Steel Frame Building", International Journal of Earthquake Engineering and Soil Dynamics, Vol. 6, 1978, pp.265-294.

19. Fujiwara, T., Kitahara, A., "Dynamic Failure Tests of Space Structures Subjected to Bi-Directional Horizontal Ground Motion", Proceedings of the 6th Japan Earthquake Engineering Symposium, 1982.

20. Fujiwara, T., Kitahara, A., "On the Aseismic Safety of Space Structures under Bi-Directional Ground Motion", 8th World Conference on Earthquake Engineering, 1984, San-Francisco, United-States.

21. Gergeley, P., Béjar, L.A., "Non-Linear Response of Torsionally Coupled Buildings for Multicomponent Earthquake Excitations", 8th World Conference on Earthquake Engineering, San-Francisco, United-States, 1984, pp.227-234.

22. Gibson, R.E., Moody, M.L., Arye, R.S., "Free Vibration of an Unsymmetrical Multistoried Building Modeled as a Shear-Flexible Cantilever Beam", Bulletin of the Seismological Society of America, Vol. 62, No. 1, 1972, pp.195-213.

23. Gibson, R.E., Moody, M.L., Arye, R.S., "Response Spectrum solution for Earthquake Analysis of Unsymmetrical Multistoried Buildings", Bulletin of the Seismological Society of America, Vol. 62, No. 1, 1972, pp.215-229.

24. Gillies, A.G., Shepherd, R., "Post-Elastic Dynamics of Three- Dimensional Frames", Journal of the Structural Division, ASCE, Vol. 107, No. ST8, 1981, pp.1485-1501.

25. Gluck, J., Reinhorn, A., Rutenberg, A., "Dynamic Torsional Coupling in Tall Building Structures", Proceedings of the Institution of Civil Engineers, Vol. 67, Part 2, 1979, pp.411-424.

26. Hart, G.C., DiJulio, R.M.Jr, Lew, M., "Torsional Response of High-Rise Buildings", Journal of the Structural Division, ASCE, Vol. 101, No. ST2, February 1975, pp.397-415.

27. Heidebrecht, A.C., Tso, W.K., "Proposed Seismic Loading Provision National Building Code of Canada 1985", 4th Canadian Conference on Earthquake Engineering, Vancouver 1983, pp.K19-K33.

28. Housner, G.W., Outinen, H., "The Effect of Torsional Oscillations on Earthquake stresses", Bulletin of the Seismological Society of America, Vol.48, No.2, July 1958, pp.221-229.

29. Humar, J.L., Awad, A.M., "Design for Seismic Torsional Forces", 4th Canadian Conference on Earthquake Engineering, Vancouver 1983, pp.251-260.

30. Kan, C.L., Chopra, A.K., "Coupled Lateral Torsional Response of Buildings to Ground Shaking", Report No. EERC 76-13, Earthquake Engineering Research Center, University of California, Berkeley, Calif., May 1976.
(Also summarized in 2 consecutive papers in the Journal of the Structural Division, ASCE, Vol. 103, No. ST4, pp.805-838.)

31. Kan, C.L., Chopra, A.K., "Linear and Non-Linear Earthquake Responses of Simple Torsionally Coupled Systems", Report No. EERC 79-03, Earthquake Engineering Research Center, University of California, Berkeley, Calif., February 1979.
(Also summarized in 2 papers: Journal of the Engineering Mechanics Division, ASCE, Vol. 107, No. EM5, 1980, pp.935-951, and Journal of the Structural Division, ASCE, Vol. 107, No. ST8, 1981, pp.1569-1587.)

32. Kung, S.Y., Pecknold, D.A., "Seismic Response of Torsionally Coupled Single-Storey Structures", 8th World Conference on Earthquake Engineering, San-Francisco, United States, 1984, pp.235-242.

33. Mahin, S.A., Lin, J., "Construction of Inelastic Response Spectra for Single-Degree-of-Freedom Systems", EERC Report No. 83-17, University of California, Berkeley, June 1983.

34. Mahin, S.A., Khatib, I.F., "NOSPEC Users Guide", To be published.

35. Mahin, S.A., Ikeda, K., "A Refined Physical Theory Model for Predicting the Seismic Behavior of Braced Steel Frames", EERC Report No. 84-12, University of California, Berkeley, July 1984.

36. Medearis, K., "Coupled Bending and Torsional Oscillations of a Modern Skyscraper", Bulletin of the Seismological Society of America, Vol. 56, No. 4, August 1966, pp437-946.

37. Meli, R., "Evaluation of Performance of Concrete Buildings Damaged by the September 19, 1985 Mexico Earthquake", The Mexico Earthquakes 1985 - Proceedings of the International COnference (ASCE), Mexico City, 1986, pp. 308-327.

38. Mitchell, D., Adams, J., DeVall, R.H., Lo, R.C., Weichert, D., "Lessons from the 1985 Mexican Earthquake", Canadian Journal of Civil Engineering, Vol. 13, No. 5, October 1986, pp. 535-557.

39. Mondkar, D.P., Powell, G.H., "Ansr 1 - General Purpose program for analysis of nonlinear structural response", EERC Report No. 75-37, University of California, Berkeley, December 1975.

40. Mondkar, D.P., Powell, G.H., "Ansr 1 - Static and dynamic analysis of nonlinear structures", EERC Report No. 75-10, University of California, Berkeley, March 1975.

41. Newmark, N.M., "Torsion in Symmetrical Buildings", 4th World Conference on Earthquake Engineering, Vol. 2, Santiago, Chile, 1969, pp.A3-19 to A3-32.

42. Newmark, N.M., Hall, W.J., Earthquake Spectra and Design, Earthquake Engineering Research Institute Monograph.

43. Pecknold, D.A.W., Sozen, M.A., "Calculated Inelastic Structural Response to Uniaxial and Biaxial Earthquake Motions", 5th World Conference on Earthquake Engineering, Vol. 2, Rome, Italy, 1973, pp.1792-1795.

44. Pekau, O.A., Syamal, P.K., "Coupling in the Dynamic Response of Nonlinear Unsymmetric Structures", Computer and Structures, Vol.13, 1981, pp.197-204.

45. Pekau, O.A., Syamal, P.K., "Non-Linear Torsional Coupling in Symmetric Structures", Journal of Sound and Vibrations, Vol. 94, No. 1, 1984, pp.1-18.

46. Riddell, R., Vasquez, J., "Existence of Centers of Resistence and Torsional Uncoupling of Earthquake Response of Buildings", 8th World Conference on Earthquake Engineering, San-Francisco, United-States, 1984, pp.187-194.

47. Rutenberg, A., "A Consideration of the Torsional Response of Building Frames", Bulletin of the New-Zealand National Society of Earthquake Engineering, Vol. 12, No. 1, Mars 1979, pp.11-21.

48. Rutenberg, A., Hsu, T.I., Tso, W.K., "Response Spectrum techniques for Asymmetric Buildings", International Journal of Earthquake Engineering and Soil Dynamics, Vol. 6, 1978, pp.427-435.

49. Rutenberg, A., Tso, W.K., Heidebrecht, A.C., "Dynamic Properties of Asymmetric Wall-Frame Structures", International Journal of Earthquake Engineering and Soil Dynamics, Vol. 5, 1977, pp.41-51.

50. Rutenberg, A., Pekau, O.A., "Earthquake Response of Asymmetric Buildings: A Parametric Study", 4th Canadian Conference on Earthquake Engineering, Vancouver 1983, pp.271-281.

51. Scholz, H., "Interaction Analysis of Asymmetric Sway Subassemblages", Journal of Structural Engineering, ASCE, Vol. 110, No. 10, October 1984, pp.2412-2423.

52. Shepherd, R. and Donald, R.A.H., "Seismic Response of Torsionally Unbalanced Buildings", Journal of Sound and Vibrations, Vol. 6, No. 1, 1967, pp.20-37.

53. Shiga, T., "Torsional Vibration of Multi-storied Buildings", 3rd World Conference on Earthquake Engineering, Vol.2, Auckland and Wellington, New-Zealand, 1965, pp.569-585.

54. Skinner, R.I., Skilton, D.W.C., Laws D.A., "Unbalanced Buildings, and Buildings with Light Towers, Under Earthquake Forces", 3rd World Conference on Earthquake Engineering, Vol. 2, Auckland and Wellington, New Zealand, 1965, pp.586-603.

55. Spanos, P.T.D., "Monte-Carlo Simulations of Responses of Non-Symmetric Dynamic System to Random Excitations", Computer and Structures, Vol. 13, 1981, pp.371-376.

56. Syamal, P.K., Pekau, O.A., "Dynamic Response of Bilinear Asymmetric Structures", International Journal of Earthquake Engineering and Soil Dynamics, Vol. 13, 1985, pp.527-541.

57. Takisawa, H., "Coupled Lateral and Torsional Failure of Buildings under Two-Dimensional Earthquake Shakings", 8th World Conference on Earthquake Engineering, San-Francisco, United-States, 1984, pp.195-202.

58. Tsicnias, T.G., Hutchinson, G.L., "Evaluation of Code Requirements for the Earthquake Resistant Design of Torsionally Coupled Buildings", Proceedings of the Institution of Civil Engineers, Vol. 71, Part 2, 1981, pp.821-843.

59. Tso, W.K., "Induced Torsional Oscillations in Symmetrical Structures", International Journal of Earthquake Engineering and Soil Dynamics, Vol. 3, 1975, pp.337-346.

60. Tso, W.K., Asmis, K.G., "Torsional Vibration of Symmetrical Structures", Proceedings of the First Canadian Conference on Earthquake Engineering, Vancouver, 1971, pp.178-186.

61. Tso, W.K., Dempsey, K.M., "Seismic Torsional Provisions for Dynamic Eccentricity", International Journal of Earthquake Engineering and Soil Dynamics, Vol. 8, 1980, pp.275-289.

62. Tso, W.K., Sadek, A.W., "Inelastic Response of Eccentric Buildings Subjected to Bi-Directional Ground Motions", 8th World Conference on Earthquake Engineering, San-Francisco, United-States, 1984, pp.203-210.

63. Tso, W.K., Meng, V., "Torsional Provisions in Building Codes", Canadian Journal of Civil Engineering, Vol. 9, No. 1, March 1982, pp.38-46.

64. Tso, W.K., "A Proposal to Improve the Static Torsional Provisions for the National Building Code of Canada", Canadian Journal of Civil Engineering, Vol. 10, No. 4, December 1983, pp.561-565.

65. Tso, W.K., Heidebrecht, A.C., Cherry, S., "Canadian Seismic Code Provision Beyond 1985", 4th Canadian Conference on Earthquake Engineering, Vancouver 1983, pp.K34-K45.

66. Tso, W.K., Sadek, A.W., "Inelastic Response of Eccentric Structures", 4th Canadian Conference on Earthquake Engineering, Vancouver 1983, pp.261-270.

67. Uzgider, E.A., "Inelastic Response of Space Frames to Dynamic Loads", Computer and Structures, Vol.11, 1980, pp.97-112.

68. Wakabayashi, M., Design of Earthquake Resistant Buildings, McGraw Hill Inc., 1986.

69. Wen, R.K., Farhoomand, F., "Dynamic Analysis of Inelastic Space Frames", Journal of the Engineering Mechanics Division, ASCE, Vol.96, No.EM5, October 1970, pp.667-686.

70. Wilson, E.L., Habibullah, A., SAP80 Structural Analysis Programs, Computers & Structures Inc., 1984.

71. Wittrick, W.H., Horsington, R.W., "On the Coupled Torsional and Sway Vibrations of a Class of Shear Buildings", International Journal of Earthquake Engineering and Soil Dynamics, Vol. 7, 1979, pp.477-490.

72. Yamazaki, Y., "Inelastic Torsional Response of Structures Subjected to Earthquake Ground Motions", Report No. EERC 80-07, Earthquake Engineering Research Center, University of California, Berkeley, Calif., April 1980.

73. Zeris, C., "Three Dimensional Response of Reinforced Concrete Buildings", Thesis Submitted in Partial Satisfaction for the Requirements for the Degree of Doctor of Philophy in Engineering, University of California, Berkeley, December 1986.

(Weak edge stiff. = k)		Maximum displacement (inch) Weak	Center	Strong
Inelastic Analysis Strong edge stiff. =	k	0.486	0.486	0.486
	1.5k	0.748	0.423	0.118
	2.0k	0.681	0.368	0.073
Elastic Analysis Strong edge stiff. =	k	0.265	0.265	0.265
	1.5k	0.205	0.181	0.157
Yield displacement = 0.12 (inch) (for stiff. = k)				

Table 3.1 Displacement for a Two Resisting Element Structure with Various Strong Element Stiffnesses as Calculated by Elastic and Inelastic Step-by-step Dynamic Analysis (N-S Component of 1940 El-Centro Earthquake Record Scaled to Obtain a Ductility of 4 in the Symmetric Inelastic Case, 2% Damping, T_x=0.1 sec., Ω=1.6, Bi-linear Hysteretic Model Elements Yielding at 36 ksi, and Strain Hardening Equal to 0.005 E).

Yield Stress (ksi)	Plastic Centroid Distance (inch)	Max. Displacement Positive Weak edge (inch)	Negative Strong edge (inch)	Max. Angle Positive (rad.)	Negative (rad.)
24	0.0	1.062 0.555	-1.997 -1.352	0.0053	-0.0071
30	-5.5	1.110 0.287	-2.054 -0.754	0.0093	-0.0135
36	-10.	1.153 0.212	-2.150 -0.294	0.0102	-0.0192
42	-13.6	1.199 0.216	-2.215 -0.153	0.0108	-0.0216
48	-16.7	1.232 0.204	-2.218 -0.149	0.0116	-0.0217

Above Table for Stiffness Eccentric Systems with Ω=1.5, (e/r)=0.3, T_x=0.1 sec., d=50 inches.

Yield Stress (ksi)	Plastic Centroid Distance (inch)	Max. Displacement Positive Weak edge (inch)	Negative Strong edge (inch)	Max. Angle Positive (rad.)	Negative (rad.)
9	0.0	2.394 2.085	-2.569 -2.941	0.0206	-0.0287
22.5	-21.4	2.571 1.133	-2.863 -1.705	0.0213	-0.0333
36	-30.	2.541 0.978	-2.608 -0.512	0.0251	-0.0341
49.5	-34.6	2.566 0.651	-2.898 -0.132	0.0261	-0.0322
63	-37.5	2.577 0.371	-2.953 -0.175	0.0264	-0.0306

Above Table for Stiffness Eccentric Systems with Ω=0.5, (e/r)=0.3, T_x=0.1 sec., d=50 inches.

Table 3.2: Effect of Various Plastic Centroid Distances on Response of Stiffness Eccentric Systems (Ω=1.5 & 0.5, (e/r)=0.3, T_x=0.1, d=50 inches, 2% Damping, 5% Strain Hardening, N-S Component of 1940 El Centro Earthquake Record Arbitrarily Scaled (see Section 3.9).

El Centro, May 18 1940, Comp. S00E El Centro Site Imperial Valley Irrigation District Max. Acceleration: 0.348 g at 2.12 sec.
Olympia, April 13 1949, Comp. N04W Washington Hwy Test Lab Max. Acceleration: 0.165 g at 10.94 sec.
Taft, July 21 1952, Comp. N21E (Kern County) Taft Lincoln School Tunnel Max. Acceleration: 0.156 g at 9.1 sec.
Parkfield, June 27 1966, Comp. N65E Cholame, Shandon, California Array No. 2 Max. Acceleration: 0.489 g at 3.74 sec.
Pacoima Dam, February 9 1971, Comp. S16E (San Fernando Earthquake) Pacoima Dam, Cal. Max. Acceleration: 1.17 g at 7.74 sec.

Table 4.1 : Expanded description of the five earthquake records used in this study (From Caltech Strong Motion Database Volume II).

Table 4.2:

1) Initially Symmetric Systems Results Diskettes:

File Name	Location	Description	Format
	A:		
ductrat.ec	\ratios\.	Ductility of 4	1
ductrat.ol		Ratios of	
ductrat.pd		ductilities for	
ductrat.pk		both elements.	
ductrat.tf			
ductrat.ec8	\ratios\.	Same as above but	1
ductrat.ol8		Ductility of 8	
ductrat.pd8			
ductrat.pk8			
ductrat.tf8			
weak-ec.dat	\omega\.	Bloc Comparisons	2
weak-ol.dat		of Omega values	
weak-pd.dat		For weak elements	
weak-pk.dat		Ductility of 4	
weak-tf.dat			
weak-ec8.dat	\omega\.	Bloc Comparisons	2
weak-ol8.dat		of Omega values	
weak-pd8.dat		For weak elements	
weak-pk8.dat		Ductility of 8	
weak-tf8.dat			
strg-ec.dat	\omega\.	Bloc Comparisons	2
strg-ol.dat		of Omega values	
strg-pd.dat		For Strong elements	
strg-pk.dat		Ductility of 4	
strg-tf.dat			
strg-ec8.dat	\omega\.	Bloc Comparisons	2
strg-ol8.dat		of Omega values	
strg-pd8.dat		For Strong elements	
strg-pk8.dat		Ductility of 8	
strg-tf8.dat			
omyk-ec.dat	\yield\.	Bloc Comparisons	3
omyk-ol.dat		of Yield levels	
omyk-pd.dat		For Weak elements	
omyk-pk.dat		Ductility of 4	
omyk-tf.dat			
omyk-ec8.dat	\yield\.	Bloc Comparisons	3
omyk-ol8.dat		of Yield levels	
omyk-pd8.dat		For Weak elements	
omyk-pk8.dat		Ductility of 8	
omyk-tf8.dat			

Table 4.2 (continued):

File Name	Location	Description	Format
	A:		
omsg-ec.dat	\yield\.	Bloc Comparisons	3
omsg-ol.dat		of Yield levels	
omsg-pd.dat		For Strong elements	
omsg-pk.dat		Ductility of 4	
omsg-tf.dat			
omsg-ec8.dat	\yield\.	Bloc Comparisons	3
omsg-ol8.dat		of Yield levels	
omsg-pd8.dat		For Strong elements	
omsg-pk8.dat		Ductility of 8	
omsg-tf8.dat			
allangle.ec4	\angle\.	Angles and angles	4
allangle.ol4		time radius of	
allangle.pd4		gyration (r)	
allangle.pd4		Ductility of 4	
allangle.tf4			
allangle.ec8	\angle\.	Angles and angles	4
allangle.ol8		time radius of	
allangle.pd8		gyration (r)	
allangle.pd8		Ductility of 8	
allangle.tf8			

Where the labels ec, ol, pd, pk and tf relate the each individual earthquake records used to generate those results, that is:

ec : El Centro 1940
ol : Olympia 1949
pd : Pacoima Dam 1971
pk : Parkfield 1966
tf : Taft 1952

Table 4.2 (continued):

Furthermore, the files calculating the mean for the five earthquake used (as well as the mean plus one standard deviation) are labeled as follow:

For the means (all located in a:\stats):

File Name	Mean of	Ductility of	Format
meandurt.4	ductrat files	4	1
meandurt.8	ductrat files	8	1
meanang .4	allangle files	4	4
meanang .8	allangle files	8	4
weakmnd4.dat	weak....files	4	2
weakmnd8.dat	weak... files	8	2
strgmnd4.dat	strg... files	4	2
strgmnd8.dat	strg... files	8	2
omwkmnd4.dat	omwk... files	4	3
omwkmnd8.dat	omwk... files	8	3
omsgmnd4.dat	omsg... files	4	3
omsgmnd8.dat	omsg... files	8	3

For the means-plus-one-standard-deviations (all located in a:\stats):

File Name	Mean + 1 SDV	Ductility of	Format
mp1sdvdr.4	ductrat files	4	1
mp1sdvdr.8	ductrat files	8	1
mp1sang .4	allangle files	4	4
mp1sang .8	allangle files	8	4
weakmp14.dat	weak....files	4	2
weakmp18.dat	weak... files	8	2
strgmp14.dat	strg... files	4	2
strgmp18.dat	strg... files	8	2
omwkmp14.dat	omwk... files	4	3
omwkmp18.dat	omwk... files	8	3
omsgmp14.dat	omsg... files	4	3
omsgmp18.dat	omsg... files	8	3

*warning: Some titles were mixed up in the files relating to element ductility ratios only in the cases of mean-plus-one-standard-deviation for target ductility of 4 and mean for target ductility of 8. This table is verified to be correct and overrides any minor mistakes in identification as herein described.

Table 4.2 (continued) - List of Formats:

To Read any file:

All files presented above are wide files (more than 80 columns wide; refer to format list for details). Therefore, the usual DOS utilities are not adequate to allow easy reading of the results. To compensate for this problem, a public domain utility (list.com) has been provided to view the files. It is self explanatory (type ? for help). To view results from a file, just type "list filename". The program also accepts wild-card character (*). All files in format type 2 and 4 can be read by spreadsheet programs that can read ASCII files longer than 256 characters. The proper amount of quotes is provided to allow proper column positioning.

Format 1 & 4:

The files under format 1 & 4 are 132 columns wide. They can therefore be printed on wide-carriage printers (or printer that can emulate wide-printing) without undesirable line folding. The columns are organized as follow (after some brief comment lines):

Columns 1 and 2 respectively contain the period and omega (Ω) values for that given set of analyses. The following 8 columns are related (two-by-two) to the 4 yield cases studied: "0.8 & 1.0 Fy", "1.0 & 1.2 Fy", "1.0 & 1.5 Fy" and "1.0 & 2.0 Fy".

For format 1, the columns 3, 5, 7, and 9 always contains the ductility ratios results for the elements yielding at Fy, and columns 4, 6, 8 and 10 will hold the results for the elements with different yields levels. Thus, the proper heading could read: Period, Omega, Strong & Weak Case 1, Weak & Strong Case 2, Weak & Strong Case 3, Weak & Strong Case 4 (note the reversal between strong & weak).

For format 4, the maximum angular value (in radians) in the first column of each group (columns 3, 5, 7 and 9) where the radius of gyration times the maximum angular value is in the second column of each group (columns 4, 6, 8 and 10).

Table 4.2 (continued) - List of Formats:

Format 2 & 3:

These files are more than 256 characters long. These files are formatted with current standards for ASCII file-reading by spreadsheet programs like LOTUS 1-2-3 version 2.1 (although a few spreadsheet programs may not be able to read ASCII files of more than 256 characters wide, like earlier versions of LOTUS). Actually only the second line of each file is very wide. Using an editor to kill that line would allow a spreadsheet without wide-ascii-lines capabilities to read these files too. After a few heading lines, the first column is always blank, and the second contains the periods.

The format 2 columns are grouped as follow: For each of the 4 yield combinations studied, the columns represent the omega values increasing from 0.4 to 2.0. A column of zeros separates the four 10x6 "blocs".

The format 3 columns are grouped as follow: Each omega value studied, the different yield combinations are places next to each other starting with "1 & 2 Fy" to "0.8 & 1 Fy". This is to allow easy comparison between the yield levels for a given omega value. There is therefore 6 "blocs" of 10x4, delimited by columns of zeros.

Weak Element Ductility Ratios						
Omega	0.4	0.8	1.0	1.2	1.6	2.0
Period	Case: 0.8 Fy and 1.0 Fy			Mean - 5 Earthquakes		
0.1	2.130	2.550	2.765	3.201	3.390	3.829
0.2	1.976	2.203	2.643	2.701	3.200	3.245
0.3	1.583	1.580	1.638	1.757	2.098	2.500
0.4	1.439	1.498	1.695	1.834	2.047	2.367
0.6	1.367	1.435	1.473	1.595	1.901	2.026
0.8	1.300	1.362	1.426	1.434	1.495	1.688
1.0	1.362	1.467	1.585	1.568	1.656	1.814
1.2	1.315	1.365	1.393	1.425	1.536	1.753
1.6	1.269	1.319	1.400	1.465	1.582	1.652
2.0	1.274	1.235	1.237	1.274	1.345	1.428
	Case: 1.0 Fy and 1.2 Fy			Mean - 5 Earthquakes		
0.1	0.884	1.010	1.000	1.100	1.243	1.452
0.2	0.839	0.886	0.999	1.026	1.148	1.202
0.3	0.892	0.978	1.000	1.086	1.220	1.561
0.4	0.905	0.917	1.000	0.999	1.349	1.408
0.6	0.905	0.940	0.998	1.055	1.293	1.346
0.8	0.981	1.019	1.001	1.033	1.148	1.279
1.0	0.929	0.953	1.000	0.999	1.038	1.246
1.2	0.938	0.980	1.000	1.033	1.077	1.179
1.6	0.957	0.968	1.000	1.000	1.124	1.294
2.0	0.980	0.975	1.000	1.053	1.080	1.107
	Case: 1.0 Fy and 1.5 Fy			Mean - 5 Earthquakes		
0.1	0.834	0.984	1.000	1.112	1.412	1.481
0.2	0.832	0.815	0.999	1.067	1.283	1.473
0.3	0.974	0.956	1.000	1.150	1.381	1.846
0.4	0.934	0.891	1.000	1.100	1.515	1.927
0.6	0.900	0.891	0.998	1.069	1.405	1.590
0.8	1.102	1.061	1.001	1.076	1.267	1.531
1.0	0.934	0.946	1.000	0.998	1.218	1.449
1.2	0.860	0.977	1.000	1.073	1.141	1.296
1.6	0.973	0.935	1.000	1.040	1.340	1.496
2.0	0.956	0.923	1.000	1.074	1.157	1.298
	Case: 1.0 Fy and 2.0 Fy			Mean - 5 Earthquakes		
0.1	0.834	0.995	1.000	1.128	1.437	1.468
0.2	0.763	0.904	0.999	1.130	1.370	1.595
0.3	1.094	0.896	1.000	1.156	1.397	1.911
0.4	1.049	0.933	1.000	1.261	1.480	2.225
0.6	0.980	0.857	0.998	1.068	1.448	1.693
0.8	1.210	1.197	1.001	1.096	1.317	1.558
1.0	0.967	0.942	1.000	1.030	1.438	1.462
1.2	0.812	0.976	1.000	1.132	1.374	1.397
1.6	1.102	0.992	1.000	1.090	1.529	1.511
2.0	0.975	0.901	1.000	1.119	1.247	1.480

Table 4.3 A: Mean of Weak Element Ductility Ratios
Target Ductility of 4

Weak Element Ductility Ratios						
Omega	0.4	0.8	1.0	1.2	1.6	2.0
Period	Case: 0.8 Fy and 1.0 Fy			Mean + 1 Stand. Dev.		
0.1	2.607	3.683	3.830	4.411	4.508	5.133
0.2	2.787	3.040	3.683	3.956	4.688	4.624
0.3	1.900	1.860	2.027	2.173	2.595	3.024
0.4	1.626	1.785	2.099	2.242	2.535	2.715
0.6	1.451	1.673	1.743	1.993	2.252	2.346
0.8	1.400	1.487	1.555	1.604	1.848	2.164
1.0	1.429	1.601	1.732	1.664	1.841	2.097
1.2	1.435	1.524	1.596	1.706	1.808	2.007
1.6	1.322	1.379	1.528	1.644	1.810	1.997
2.0	1.381	1.394	1.391	1.418	1.487	1.808
	Case: 1.0 Fy and 1.2 Fy			Mean + 1 Stand. Dev.		
0.1	1.013	1.136	1.001	1.219	1.316	1.615
0.2	1.091	1.014	1.001	1.098	1.304	1.461
0.3	1.038	1.062	1.001	1.195	1.433	1.767
0.4	0.956	0.969	1.000	1.114	1.527	1.697
0.6	1.034	1.038	1.002	1.235	1.518	1.640
0.8	1.035	1.108	1.002	1.083	1.326	1.485
1.0	1.013	1.012	1.000	1.032	1.174	1.439
1.2	0.963	1.014	1.000	1.072	1.129	1.298
1.6	1.011	1.007	1.000	1.055	1.263	1.474
2.0	1.031	1.014	1.000	1.097	1.126	1.333
	Case: 1.0 Fy and 1.5 Fy			Mean + 1 Stand. Dev.		
0.1	1.059	1.107	1.001	1.245	1.630	1.616
0.2	1.211	0.991	1.001	1.184	1.585	1.843
0.3	1.265	1.150	1.001	1.253	1.635	2.320
0.4	1.087	1.040	1.000	1.239	1.813	2.322
0.6	1.117	0.994	1.002	1.373	1.648	2.015
0.8	1.235	1.235	1.002	1.187	1.526	1.979
1.0	1.152	1.020	1.000	1.071	1.358	1.590
1.2	0.906	1.021	1.000	1.187	1.201	1.500
1.6	1.055	1.024	1.000	1.074	1.645	1.692
2.0	1.033	1.003	1.000	1.166	1.264	1.521
	Case: 1.0 Fy and 2.0 Fy			Mean + 1 Stand. Dev.		
0.1	1.082	1.107	1.001	1.282	1.692	1.589
0.2	1.071	1.153	1.001	1.271	1.724	2.036
0.3	1.505	1.173	1.001	1.304	1.773	2.453
0.4	1.281	1.208	1.000	1.491	1.864	2.888
0.6	1.228	0.970	1.002	1.377	1.583	2.133
0.8	1.481	1.412	1.002	1.275	1.584	2.253
1.0	1.272	1.044	1.000	1.144	1.495	1.699
1.2	0.918	1.063	1.000	1.367	1.679	1.727
1.6	1.352	1.234	1.000	1.126	1.970	1.633
2.0	1.009	0.984	1.000	1.218	1.458	1.725

Table 4.3 B: Mean plus one Standard Deviation of Weak Element Ductility Ratios, Target Ductility of 4

Strong Element Ductility Ratios						
Omega	0.4	0.8	1.0	1.2	1.6	2.0
Period	Case: 0.8 Fy and 1.0 Fy			Mean - 5 Earthquakes		
0.1	1.439	1.192	1.000	0.936	0.819	0.700
0.2	1.492	1.374	0.999	0.900	0.873	0.831
0.3	1.147	1.096	1.000	0.902	0.756	0.758
0.4	1.210	1.140	1.000	1.016	0.829	0.770
0.6	1.093	1.100	0.998	0.971	0.729	0.611
0.8	1.093	1.072	1.001	1.036	1.054	0.783
1.0	1.127	1.053	1.000	0.975	0.973	0.828
1.2	1.061	1.033	1.000	0.958	0.908	0.815
1.6	1.045	1.017	1.000	0.977	0.997	0.883
2.0	1.002	1.017	1.000	0.953	0.864	0.854
	Case: 1.0 Fy and 1.2 Fy			Mean - 5 Earthquakes		
0.1	0.634	0.593	0.611	0.518	0.488	0.434
0.2	0.621	0.624	0.532	0.601	0.485	0.495
0.3	0.747	0.718	0.713	0.631	0.606	0.571
0.4	0.752	0.759	0.724	0.772	0.659	0.575
0.6	0.794	0.753	0.736	0.734	0.624	0.520
0.8	0.832	0.837	0.867	0.856	0.809	0.589
1.0	0.769	0.742	0.738	0.741	0.734	0.652
1.2	0.790	0.773	0.762	0.725	0.709	0.658
1.6	0.834	0.810	0.786	0.786	0.853	0.733
2.0	0.812	0.810	0.795	0.758	0.727	0.725
	Case: 1.0 Fy and 1.5 Fy			Mean - 5 Earthquakes		
0.1	0.401	0.378	0.400	0.336	0.275	0.266
0.2	0.530	0.487	0.494	0.437	0.344	0.311
0.3	0.575	0.563	0.565	0.419	0.376	0.373
0.4	0.525	0.607	0.559	0.570	0.473	0.350
0.6	0.583	0.561	0.565	0.509	0.436	0.324
0.8	0.664	0.684	0.742	0.603	0.553	0.402
1.0	0.605	0.671	0.667	0.654	0.523	0.469
1.2	0.619	0.613	0.596	0.529	0.474	0.440
1.6	0.625	0.650	0.663	0.611	0.690	0.536
2.0	0.663	0.676	0.634	0.589	0.526	0.546
	Case: 1.0 Fy and 2.0 Fy			Mean - 5 Earthquakes		
0.1	0.265	0.258	0.279	0.225	0.199	0.193
0.2	0.398	0.394	0.361	0.278	0.234	0.222
0.3	0.408	0.428	0.393	0.276	0.234	0.234
0.4	0.430	0.448	0.459	0.437	0.310	0.261
0.6	0.414	0.427	0.403	0.358	0.297	0.221
0.8	0.477	0.487	0.485	0.411	0.380	0.293
1.0	0.487	0.526	0.519	0.522	0.357	0.336
1.2	0.426	0.452	0.475	0.444	0.352	0.296
1.6	0.488	0.600	0.568	0.531	0.560	0.360
2.0	0.491	0.515	0.488	0.441	0.399	0.408

Table 4.3 C: Mean of Strong Element Ductility Ratios
Target Ductility of 4

Strong Element Ductility Ratios						
Omega	0.4	0.8	1.0	1.2	1.6	2.0
Period	Case: 0.8 Fy and 1.0 Fy			Mean + 1 Stand. Dev.		
0.1	1.847	1.389	1.001	1.075	1.136	0.927
0.2	1.717	1.596	1.001	1.120	1.190	0.945
0.3	1.337	1.231	1.001	1.049	0.992	1.055
0.4	1.346	1.241	1.000	1.166	1.089	1.169
0.6	1.275	1.267	1.002	0.993	0.815	0.753
0.8	1.134	1.142	1.002	1.138	1.303	1.014
1.0	1.185	1.101	1.000	1.008	1.054	1.041
1.2	1.130	1.069	1.000	0.996	0.986	0.909
1.6	1.170	1.086	1.000	1.004	1.115	1.027
2.0	1.060	1.045	1.000	0.989	0.967	0.965
	Case: 1.0 Fy and 1.2 Fy			Mean + 1 Stand. Dev.		
0.1	0.708	0.769	0.784	0.673	0.637	0.578
0.2	0.820	0.807	0.690	0.843	0.587	0.600
0.3	0.906	0.849	0.878	0.791	0.816	0.679
0.4	0.816	0.851	0.786	0.880	0.790	0.706
0.6	0.838	0.892	0.841	0.897	0.698	0.598
0.8	0.880	0.910	0.920	0.957	0.930	0.698
1.0	0.797	0.797	0.811	0.842	0.843	0.755
1.2	0.845	0.849	0.840	0.820	0.796	0.754
1.6	0.894	0.887	0.857	0.862	0.984	0.832
2.0	0.872	0.886	0.877	0.862	0.826	0.862
	Case: 1.0 Fy and 1.5 Fy			Mean + 1 Stand. Dev.		
0.1	0.486	0.503	0.550	0.468	0.325	0.320
0.2	0.751	0.667	0.771	0.651	0.417	0.351
0.3	0.761	0.689	0.746	0.531	0.536	0.446
0.4	0.584	0.689	0.675	0.701	0.733	0.425
0.6	0.624	0.702	0.690	0.596	0.493	0.385
0.8	0.744	0.762	0.817	0.713	0.795	0.509
1.0	0.666	0.770	0.801	0.815	0.667	0.620
1.2	0.708	0.693	0.692	0.661	0.572	0.581
1.6	0.682	0.738	0.772	0.733	0.935	0.735
2.0	0.723	0.755	0.703	0.658	0.609	0.672
	Case: 1.0 Fy and 2.0 Fy			Mean + 1 Stand. Dev.		
0.1	0.327	0.329	0.367	0.279	0.226	0.224
0.2	0.651	0.560	0.517	0.382	0.262	0.243
0.3	0.505	0.558	0.527	0.330	0.288	0.254
0.4	0.494	0.503	0.561	0.569	0.431	0.311
0.6	0.472	0.500	0.495	0.422	0.334	0.240
0.8	0.574	0.552	0.567	0.501	0.511	0.343
1.0	0.597	0.694	0.699	0.636	0.420	0.489
1.2	0.539	0.604	0.673	0.624	0.442	0.369
1.6	0.566	0.752	0.687	0.636	0.835	0.481
2.0	0.545	0.569	0.542	0.486	0.485	0.482

Table 4.3 D: Mean plus one Standard Deviation of Strong Element Ductility Ratios, Target Ductility of 4

Weak Element Ductility Ratios						
Omega	0.4	0.8	1.0	1.2	1.6	2.0
Period	Case: 0.8 Fy and 1.0 Fy			Mean - 5 Earthquakes		
0.1	1.701	2.160	2.378	2.693	2.684	3.193
0.2	1.709	1.785	2.089	2.211	2.373	2.607
0.3	1.467	1.627	1.713	1.812	2.089	2.339
0.4	1.435	1.678	1.688	1.846	1.964	2.142
0.6	1.297	1.305	1.300	1.362	1.595	1.819
0.8	1.301	1.304	1.354	1.428	1.472	1.636
1.0	1.348	1.400	1.462	1.524	1.543	1.710
1.2	1.408	1.432	1.475	1.481	1.480	1.569
1.6	1.325	1.329	1.343	1.397	1.489	1.515
2.0	1.308	1.284	1.279	1.288	1.322	1.403
	Case: 1.0 Fy and 1.2 Fy			Mean - 5 Earthquakes		
0.1	0.778	0.854	1.001	1.124	1.184	1.392
0.2	0.723	0.845	0.999	1.031	1.141	1.192
0.3	0.879	0.953	1.000	1.025	1.264	1.356
0.4	0.845	0.963	1.002	1.069	1.125	1.236
0.6	0.917	0.968	0.999	1.055	1.111	1.293
0.8	0.930	0.971	0.999	1.024	1.060	1.172
1.0	0.911	0.943	1.000	1.016	1.078	1.170
1.2	1.005	1.017	1.026	1.036	1.097	1.150
1.6	0.970	0.986	1.015	1.071	1.143	1.129
2.0	1.038	1.017	1.016	1.028	1.048	1.120
	Case: 1.0 Fy and 1.5 Fy			Mean - 5 Earthquakes		
0.1	0.655	0.803	1.001	1.027	1.362	1.488
0.2	0.592	0.802	0.999	1.028	1.223	1.320
0.3	0.815	0.929	1.000	1.020	1.571	1.770
0.4	0.759	0.847	1.002	1.064	1.237	1.560
0.6	0.798	0.937	0.999	1.132	1.308	1.330
0.8	0.845	0.956	0.999	1.051	1.152	1.424
1.0	0.824	0.879	1.000	1.013	1.179	1.334
1.2	0.966	1.017	1.026	1.057	1.185	1.317
1.6	0.917	0.971	1.015	1.125	1.284	1.310
2.0	1.050	1.012	1.016	1.045	1.078	1.227
	Case: 1.0 Fy and 2.0 Fy			Mean - 5 Earthquakes		
0.1	0.645	0.767	1.001	0.989	1.384	1.521
0.2	0.606	0.751	0.999	1.060	1.229	1.440
0.3	1.003	0.955	1.000	1.105	1.832	1.846
0.4	0.769	0.871	1.002	1.033	1.432	1.950
0.6	0.716	0.913	0.999	1.187	1.342	1.482
0.8	0.794	0.931	0.999	1.078	1.301	1.632
1.0	0.769	0.845	1.000	1.061	1.329	1.388
1.2	0.919	1.004	1.026	1.124	1.232	1.444
1.6	0.909	0.942	1.015	1.180	1.394	1.534
2.0	1.026	0.994	1.016	1.066	1.145	1.392

Table 4.3 E: Mean of Weak Element Ductility Ratios
Target Ductility of 8

Weak Element Ductility Ratios						
Omega	0.4	0.8	1.0	1.2	1.6	2.0
Period	Case: 0.8 Fy and 1.0 Fy				Mean + 1 Stand. Dev.	
0.1	2.079	2.862	3.153	3.599	3.497	4.166
0.2	2.115	2.276	2.586	2.777	3.142	3.331
0.3	1.658	2.022	2.097	2.224	2.577	2.969
0.4	1.660	2.006	1.964	2.058	2.192	2.457
0.6	1.424	1.490	1.547	1.701	1.911	2.218
0.8	1.389	1.419	1.492	1.548	1.679	1.832
1.0	1.545	1.685	1.754	1.740	1.805	2.048
1.2	1.655	1.718	1.776	1.704	1.620	1.872
1.6	1.475	1.505	1.537	1.641	1.795	1.780
2.0	1.376	1.416	1.431	1.437	1.465	1.472
	Case: 1.0 Fy and 1.2 Fy				Mean + 1 Stand. Dev.	
0.1	0.952	1.023	1.002	1.318	1.424	1.452
0.2	0.850	0.983	1.001	1.149	1.277	1.310
0.3	0.926	1.030	1.000	1.102	1.424	1.731
0.4	0.910	1.060	1.005	1.136	1.281	1.547
0.6	0.957	0.997	1.001	1.133	1.291	1.461
0.8	0.972	1.003	1.001	1.075	1.199	1.391
1.0	0.963	0.983	1.000	1.040	1.124	1.249
1.2	1.093	1.094	1.085	1.054	1.160	1.244
1.6	1.049	1.043	1.080	1.190	1.326	1.348
2.0	1.101	1.051	1.053	1.065	1.117	1.196
	Case: 1.0 Fy and 1.5 Fy				Mean + 1 Stand. Dev	
0.1	0.846	0.997	1.002	1.121	1.554	1.671
0.2	0.804	1.057	1.001	1.116	1.354	1.499
0.3	0.940	1.186	1.000	1.152	1.821	2.215
0.4	0.911	0.992	1.005	1.234	1.484	1.864
0.6	0.878	0.990	1.001	1.266	1.572	1.446
0.8	0.960	1.025	1.001	1.160	1.439	1.696
1.0	0.941	0.986	1.000	1.083	1.358	1.457
1.2	1.142	1.144	1.085	1.118	1.288	1.434
1.6	1.075	1.084	1.080	1.306	1.576	1.687
2.0	1.151	1.051	1.053	1.088	1.164	1.386
	Case: 1.0 Fy and 2.0 Fy				Mean + 1 Stand. Dev.	
0.1	0.860	0.932	1.002	1.096	1.675	1.741
0.2	0.914	1.041	1.001	1.132	1.417	1.698
0.3	1.416	1.414	1.000	1.360	2.507	2.406
0.4	0.901	1.079	1.005	1.225	1.687	2.472
0.6	0.875	1.010	1.001	1.338	1.471	1.793
0.8	0.956	1.042	1.001	1.255	1.602	1.803
1.0	0.941	1.013	1.000	1.205	1.573	1.540
1.2	1.187	1.210	1.085	1.192	1.363	1.641
1.6	1.052	1.101	1.080	1.433	1.791	1.989
2.0	1.100	1.030	1.053	1.122	1.254	1.588

Table 4.3 F: Mean plus one Standard Deviation of Weak Element Ductility Ratios, Target Ductility of 8

Strong Element Ductility Ratios						
Omega	0.4	0.8	1.0	1.2	1.6	2.0
Period	Case: 0.8 Fy and 1.0 Fy			Mean - 5 Earthquakes		
0.1	1.266	1.054	1.001	0.758	0.717	0.633
0.2	1.304	1.244	0.999	0.745	0.714	0.714
0.3	1.221	1.085	1.000	0.925	1.012	0.898
0.4	1.206	1.028	1.002	0.892	0.769	0.779
0.6	1.057	1.041	0.999	0.908	0.688	0.510
0.8	1.068	1.045	0.999	0.972	0.936	0.860
1.0	1.097	1.044	1.000	0.937	0.915	0.792
1.2	1.099	1.061	1.026	1.025	1.052	1.024
1.6	1.052	1.050	1.015	0.999	1.027	1.010
2.0	0.997	1.015	1.016	1.007	0.972	0.905
	Case: 1.0 Fy and 1.2 Fy			Mean - 5 Earthquakes		
0.1	0.532	0.495	0.457	0.434	0.407	0.348
0.2	0.618	0.554	0.462	0.446	0.446	0.435
0.3	0.708	0.737	0.655	0.667	0.719	0.580
0.4	0.748	0.711	0.662	0.679	0.511	0.513
0.6	0.776	0.730	0.688	0.627	0.523	0.431
0.8	0.808	0.779	0.749	0.727	0.754	0.687
1.0	0.793	0.766	0.739	0.730	0.701	0.639
1.2	0.837	0.843	0.824	0.811	0.816	0.744
1.6	0.819	0.813	0.784	0.749	0.782	0.791
2.0	0.827	0.843	0.840	0.829	0.805	0.748
	Case: 1.0 Fy and 1.5 Fy			Mean - 5 Earthquakes		
0.1	0.299	0.272	0.273	0.241	0.178	0.170
0.2	0.382	0.351	0.295	0.297	0.231	0.220
0.3	0.496	0.503	0.540	0.557	0.444	0.312
0.4	0.535	0.533	0.477	0.438	0.403	0.313
0.6	0.581	0.500	0.440	0.432	0.313	0.286
0.8	0.620	0.611	0.592	0.582	0.584	0.413
1.0	0.589	0.551	0.536	0.509	0.522	0.427
1.2	0.672	0.671	0.627	0.607	0.572	0.531
1.6	0.672	0.684	0.643	0.605	0.621	0.579
2.0	0.632	0.633	0.621	0.604	0.571	0.512
	Case: 1.0 Fy and 2.0 Fy			Mean - 5 Earthquakes		
0.1	0.180	0.155	0.171	0.133	0.115	0.109
0.2	0.294	0.272	0.219	0.180	0.144	0.128
0.3	0.378	0.435	0.445	0.391	0.234	0.166
0.4	0.331	0.411	0.340	0.322	0.250	0.194
0.6	0.374	0.326	0.326	0.300	0.215	0.186
0.8	0.455	0.505	0.473	0.471	0.357	0.248
1.0	0.406	0.390	0.380	0.329	0.311	0.275
1.2	0.490	0.522	0.442	0.447	0.394	0.339
1.6	0.511	0.476	0.445	0.442	0.470	0.396
2.0	0.468	0.471	0.465	0.433	0.388	0.384

Table 4.3 G: Mean of Strong Element Ductility Ratios
Target Ductility of 8

Strong Element Ductility Ratios						
Omega	0.4	0.8	1.0	1.2	1.6	2.0
Period	Case: 0.8 Fy and 1.0 Fy			Mean + 1 Stand. Dev.		
0.1	1.490	1.192	1.002	0.889	0.910	0.944
0.2	1.439	1.377	1.001	0.940	0.996	0.934
0.3	1.391	1.114	1.000	1.063	1.712	1.445
0.4	1.306	1.125	1.005	0.955	0.979	1.272
0.6	1.105	1.063	1.001	0.966	0.771	0.633
0.8	1.118	1.086	1.001	1.034	1.102	1.083
1.0	1.204	1.062	1.000	1.030	1.113	1.030
1.2	1.213	1.126	1.085	1.162	1.364	1.248
1.6	1.152	1.151	1.080	1.088	1.241	1.230
2.0	1.083	1.060	1.053	1.045	1.069	1.022
	Case: 1.0 Fy and 1.2 Fy			Mean + 1 Stand. Dev.		
0.1	0.661	0.635	0.594	0.589	0.551	0.464
0.2	0.810	0.748	0.671	0.651	0.679	0.590
0.3	0.775	0.842	0.744	0.885	1.164	0.802
0.4	0.836	0.776	0.769	0.769	0.617	0.779
0.6	0.829	0.781	0.751	0.697	0.568	0.540
0.8	0.874	0.850	0.805	0.794	0.893	0.824
1.0	0.846	0.841	0.812	0.799	0.831	0.808
1.2	0.908	0.950	0.941	0.950	0.996	0.885
1.6	0.929	0.954	0.930	0.899	0.984	0.980
2.0	0.873	0.913	0.905	0.883	0.865	0.812
	Case: 1.0 Fy and 1.5 Fy			Mean + 1 Stand. Dev		
0.1	0.372	0.361	0.383	0.315	0.211	0.215
0.2	0.570	0.511	0.412	0.451	0.344	0.287
0.3	0.626	0.664	0.823	0.971	0.697	0.410
0.4	0.638	0.703	0.626	0.536	0.624	0.425
0.6	0.623	0.542	0.502	0.503	0.358	0.414
0.8	0.704	0.736	0.728	0.724	0.783	0.601
1.0	0.692	0.680	0.716	0.663	0.711	0.661
1.2	0.820	0.857	0.818	0.820	0.765	0.694
1.6	0.818	0.819	0.746	0.701	0.747	0.846
2.0	0.691	0.704	0.685	0.688	0.710	0.617
	Case: 1.0 Fy and 2.0 Fy			Mean + 1 Stand. Dev.		
0.1	0.230	0.197	0.236	0.163	0.130	0.122
0.2	0.456	0.410	0.332	0.262	0.184	0.149
0.3	0.526	0.615	0.748	0.662	0.323	0.221
0.4	0.434	0.593	0.472	0.416	0.374	0.247
0.6	0.418	0.401	0.432	0.345	0.238	0.285
0.8	0.511	0.626	0.573	0.651	0.495	0.362
1.0	0.541	0.512	0.504	0.435	0.437	0.443
1.2	0.683	0.709	0.605	0.674	0.575	0.497
1.6	0.635	0.577	0.549	0.543	0.572	0.537
2.0	0.538	0.557	0.554	0.534	0.502	0.464

Table 4.3 H: Mean plus one Standard Deviation of Strong Element Ductility Ratios, Target Ductility of 8

Gyration Radius x Maximun Angular Response						
Omega	0.4	0.8	1.0	1.2	1.6	2.0
Period	Case: 0.8 Fy and 1.0 Fy			Mean - 5 Earthquakes		
0.1	0.304	0.345	0.347	0.393	0.333	0.307
0.2	0.329	0.247	0.333	0.327	0.298	0.246
0.3	0.244	0.125	0.145	0.187	0.209	0.221
0.4	0.154	0.133	0.150	0.163	0.178	0.184
0.6	0.157	0.115	0.105	0.152	0.163	0.155
0.8	0.149	0.099	0.082	0.096	0.130	0.132
1.0	0.109	0.114	0.125	0.115	0.115	0.115
1.2	0.131	0.091	0.089	0.114	0.104	0.109
1.6	0.108	0.084	0.104	0.119	0.125	0.098
2.0	0.101	0.056	0.053	0.072	0.079	0.088
	Case: 1.0 Fy and 1.2 Fy			Mean - 5 Earthquakes		
0.1	0.156	0.164	0.144	0.133	0.134	0.138
0.2	0.244	0.128	0.137	0.143	0.121	0.102
0.3	0.211	0.094	0.099	0.131	0.148	0.150
0.4	0.121	0.091	0.101	0.108	0.155	0.137
0.6	0.174	0.088	0.087	0.126	0.140	0.127
0.8	0.133	0.088	0.069	0.095	0.118	0.117
1.0	0.093	0.083	0.081	0.082	0.107	0.110
1.2	0.102	0.072	0.073	0.091	0.090	0.090
1.6	0.086	0.059	0.075	0.084	0.101	0.091
2.0	0.101	0.057	0.061	0.078	0.064	0.073
	Case: 1.0 Fy and 1.5 Fy			Mean - 5 Earthquake		
0.1	0.312	0.228	0.201	0.211	0.184	0.155
0.2	0.435	0.175	0.192	0.188	0.165	0.153
0.3	0.426	0.176	0.196	0.205	0.204	0.204
0.4	0.254	0.147	0.185	0.204	0.235	0.223
0.6	0.264	0.187	0.153	0.192	0.192	0.184
0.8	0.285	0.143	0.134	0.167	0.202	0.166
1.0	0.214	0.179	0.156	0.181	0.176	0.167
1.2	0.217	0.139	0.142	0.164	0.159	0.126
1.6	0.173	0.128	0.149	0.157	0.179	0.168
2.0	0.224	0.113	0.116	0.145	0.121	0.139
	Case: 1.0 Fy and 2.0 Fy			Mean - 5 Earthquakes		
0.1	0.431	0.279	0.236	0.225	0.192	0.162
0.2	0.464	0.276	0.232	0.216	0.193	0.171
0.3	0.526	0.247	0.264	0.245	0.212	0.230
0.4	0.368	0.236	0.243	0.294	0.249	0.271
0.6	0.378	0.215	0.219	0.235	0.219	0.202
0.8	0.446	0.218	0.223	0.251	0.229	0.186
1.0	0.334	0.254	0.239	0.234	0.230	0.193
1.2	0.323	0.237	0.214	0.227	0.216	0.173
1.6	0.254	0.228	0.232	0.248	0.269	0.193
2.0	0.307	0.183	0.216	0.236	0.190	0.194

Table 4.3 I: Mean of Radius of Gyration x Maximum Angular Response, Target Ductility of 4

Gyration Radius x Maximun Angular Response						
Omega	0.4	0.8	1.0	1.2	1.6	2.0
Period	Case: 0.8 Fy and 1.0 Fy			Mean + 1 Stand. Dev.		
0.1	0.411	0.589	0.537	0.610	0.479	0.447
0.2	0.495	0.403	0.514	0.503	0.497	0.393
0.3	0.296	0.167	0.212	0.257	0.282	0.284
0.4	0.179	0.186	0.237	0.217	0.243	0.220
0.6	0.222	0.181	0.147	0.199	0.211	0.191
0.8	0.173	0.129	0.115	0.132	0.164	0.172
1.0	0.142	0.161	0.156	0.138	0.145	0.147
1.2	0.201	0.138	0.134	0.159	0.139	0.137
1.6	0.189	0.149	0.190	0.204	0.171	0.137
2.0	0.130	0.076	0.075	0.094	0.116	0.120
	Case: 1.0 Fy and 1.2 Fy			Mean + 1 Stand. Dev.		
0.1	0.179	0.218	0.167	0.162	0.148	0.170
0.2	0.418	0.182	0.160	0.191	0.151	0.136
0.3	0.304	0.155	0.143	0.164	0.195	0.201
0.4	0.181	0.111	0.133	0.143	0.198	0.162
0.6	0.233	0.115	0.144	0.175	0.187	0.155
0.8	0.164	0.112	0.107	0.116	0.144	0.153
1.0	0.122	0.102	0.095	0.107	0.138	0.131
1.2	0.137	0.098	0.098	0.111	0.127	0.131
1.6	0.132	0.070	0.094	0.112	0.125	0.124
2.0	0.141	0.078	0.102	0.111	0.090	0.095
	Case: 1.0 Fy and 1.5 Fy			Mean + 1 Stand. Dev		
0.1	0.409	0.298	0.224	0.260	0.214	0.171
0.2	0.849	0.241	0.239	0.242	0.220	0.203
0.3	0.642	0.271	0.290	0.231	0.251	0.259
0.4	0.305	0.169	0.220	0.258	0.303	0.278
0.6	0.370	0.238	0.208	0.245	0.239	0.237
0.8	0.409	0.197	0.185	0.181	0.256	0.217
1.0	0.269	0.210	0.172	0.250	0.212	0.174
1.2	0.297	0.173	0.180	0.200	0.193	0.150
1.6	0.239	0.159	0.184	0.202	0.233	0.211
2.0	0.296	0.163	0.168	0.200	0.158	0.164
	Case: 1.0 Fy and 2.0 Fy			Mean + 1 Stand. Dev.		
0.1	0.575	0.339	0.271	0.281	0.229	0.186
0.2	0.927	0.413	0.281	0.274	0.258	0.228
0.3	0.725	0.393	0.334	0.276	0.263	0.296
0.4	0.522	0.333	0.298	0.366	0.337	0.352
0.6	0.506	0.263	0.273	0.290	0.239	0.251
0.8	0.693	0.281	0.254	0.287	0.270	0.269
1.0	0.406	0.289	0.299	0.299	0.266	0.232
1.2	0.398	0.257	0.252	0.279	0.262	0.219
1.6	0.299	0.260	0.263	0.295	0.359	0.207
2.0	0.408	0.231	0.274	0.285	0.228	0.222

Table 4.3 J: Mean plus one Standard Deviation of Radius of Gyration x Maximum Angular Response, Target Ductility of 4

Gyration Radius x Maximun Angular Response						
Omega	0.4	0.8	1.0	1.2	1.6	2.0
Period	Case: 0.8 Fy and 1.0 Fy			Mean - 5 Earthquakes		
0.1	0.408	0.622	0.597	0.628	0.504	0.527
0.2	0.389	0.297	0.381	0.476	0.409	0.363
0.3	0.293	0.295	0.310	0.344	0.393	0.361
0.4	0.251	0.263	0.263	0.320	0.287	0.325
0.6	0.188	0.146	0.145	0.199	0.245	0.272
0.8	0.174	0.132	0.134	0.166	0.177	0.205
1.0	0.193	0.200	0.188	0.167	0.161	0.189
1.2	0.166	0.157	0.152	0.135	0.160	0.171
1.6	0.187	0.121	0.115	0.141	0.164	0.130
2.0	0.119	0.086	0.101	0.095	0.104	0.098
	Case: 1.0 Fy and 1.2 Fy			Mean - 5 Earthquakes		
0.1	0.287	0.242	0.297	0.301	0.265	0.251
0.2	0.298	0.253	0.283	0.287	0.249	0.203
0.3	0.243	0.240	0.237	0.267	0.362	0.271
0.4	0.197	0.227	0.233	0.247	0.234	0.253
0.6	0.169	0.123	0.131	0.182	0.192	0.218
0.8	0.166	0.137	0.148	0.129	0.187	0.190
1.0	0.167	0.150	0.164	0.145	0.135	0.160
1.2	0.145	0.149	0.137	0.143	0.157	0.143
1.6	0.172	0.123	0.133	0.155	0.168	0.107
2.0	0.119	0.072	0.077	0.085	0.095	0.087
	Case: 1.0 Fy and 1.5 Fy			Mean - 5 Earthquake		
0.1	0.460	0.348	0.381	0.336	0.368	0.327
0.2	0.524	0.363	0.389	0.394	0.320	0.272
0.3	0.546	0.404	0.420	0.392	0.420	0.406
0.4	0.410	0.390	0.438	0.366	0.371	0.351
0.6	0.312	0.262	0.287	0.353	0.354	0.295
0.8	0.317	0.304	0.310	0.248	0.346	0.308
1.0	0.290	0.278	0.321	0.294	0.253	0.266
1.2	0.389	0.298	0.274	0.295	0.255	0.231
1.6	0.336	0.291	0.285	0.296	0.294	0.234
2.0	0.251	0.172	0.160	0.164	0.186	0.175
	Case: 1.0 Fy and 2.0 Fy			Mean - 5 Earthquakes		
0.1	0.617	0.433	0.434	0.383	0.397	0.356
0.2	0.777	0.453	0.463	0.425	0.354	0.330
0.3	0.801	0.523	0.538	0.466	0.529	0.454
0.4	0.567	0.532	0.531	0.384	0.441	0.483
0.6	0.609	0.422	0.422	0.484	0.405	0.363
0.8	0.483	0.475	0.403	0.372	0.413	0.365
1.0	0.464	0.425	0.470	0.414	0.380	0.321
1.2	0.660	0.464	0.409	0.451	0.363	0.335
1.6	0.425	0.365	0.406	0.392	0.410	0.357
2.0	0.394	0.328	0.318	0.308	0.252	0.310

Table 4.3 K: Mean of Radius of Gyration x Maximum Angular Response, Target Ductility of 8

Gyration Radius x Maximun Angular Response						
Omega	0.4	0.8	1.0	1.2	1.6	2.0
Period	Case: 0.8 Fy and 1.0 Fy			Mean + 1 Stand. Dev.		
0.1	0.560	0.797	0.851	0.909	0.669	0.705
0.2	0.619	0.451	0.570	0.684	0.604	0.537
0.3	0.399	0.415	0.388	0.381	0.508	0.498
0.4	0.309	0.431	0.359	0.407	0.350	0.423
0.6	0.292	0.209	0.193	0.255	0.317	0.363
0.8	0.266	0.158	0.176	0.202	0.214	0.239
1.0	0.278	0.267	0.264	0.222	0.197	0.221
1.2	0.262	0.220	0.204	0.167	0.228	0.189
1.6	0.278	0.169	0.168	0.210	0.240	0.185
2.0	0.178	0.120	0.139	0.123	0.136	0.127
	Case: 1.0 Fy and 1.2 Fy			Mean + 1 Stand. Dev.		
0.1	0.404	0.341	0.394	0.441	0.345	0.288
0.2	0.410	0.388	0.409	0.365	0.322	0.273
0.3	0.295	0.343	0.324	0.315	0.461	0.321
0.4	0.277	0.357	0.330	0.312	0.279	0.308
0.6	0.248	0.178	0.173	0.229	0.250	0.275
0.8	0.206	0.181	0.224	0.182	0.207	0.221
1.0	0.252	0.188	0.210	0.178	0.155	0.192
1.2	0.267	0.194	0.183	0.192	0.220	0.168
1.6	0.248	0.183	0.208	0.245	0.224	0.167
2.0	0.169	0.093	0.099	0.111	0.129	0.122
	Case: 1.0 Fy and 1.5 Fy			Mean + 1 Stand. Dev		
0.1	0.603	0.510	0.436	0.374	0.430	0.371
0.2	0.954	0.503	0.447	0.497	0.396	0.305
0.3	0.708	0.504	0.490	0.450	0.502	0.508
0.4	0.489	0.626	0.673	0.443	0.422	0.443
0.6	0.484	0.349	0.369	0.457	0.414	0.338
0.8	0.375	0.397	0.436	0.365	0.376	0.354
1.0	0.412	0.379	0.387	0.357	0.314	0.323
1.2	0.643	0.383	0.380	0.361	0.328	0.258
1.6	0.513	0.409	0.399	0.429	0.397	0.338
2.0	0.381	0.229	0.217	0.223	0.254	0.235
	Case: 1.0 Fy and 2.0 Fy			Mean + 1 Stand. Dev.		
0.1	0.825	0.566	0.486	0.434	0.491	0.421
0.2	1.510	0.672	0.525	0.481	0.415	0.391
0.3	1.054	0.648	0.595	0.499	0.694	0.585
0.4	0.644	0.874	0.767	0.478	0.530	0.617
0.6	0.919	0.556	0.500	0.593	0.438	0.479
0.8	0.543	0.582	0.592	0.519	0.447	0.454
1.0	0.625	0.526	0.560	0.459	0.472	0.381
1.2	1.051	0.598	0.514	0.546	0.427	0.388
1.6	0.605	0.451	0.517	0.513	0.538	0.446
2.0	0.538	0.462	0.429	0.415	0.305	0.381

Table 4.3 L: Mean plus one Standard Deviation of Radius of Gyration x Maximum Angular Response, Target Ductility of 8

Period	Ductility Level of SDOF at 0.8 Fy	
	Target ductility of 4 at Fy	Target ductility of 8 at Fy
0.1	11.1	19.0
0.2	10.1	16.4
0.3	6.6	13.6
0.4	6.8	13.5
0.6	5.8	10.4
0.8	5.7	10.8
1.0	6.4	11.7
1.2	5.5	11.3
1.6	5.6	10.4
2.0	4.8	10.0

Table 4.4: Mean of the ductilities (5 earthquakes) for SDOF systems yielding at 0.8 Fy and subjected to the same scaled earthquakes that create uniform ductility demand on SDOFs yielding at 1.0 Fy.

Omega (Ω)	e/r	
	0.1	0.3
0.4	0.25	0.75
0.8	0.125	0.375
1.0	0.1	0.3
1.2	0.0833	0.25
1.6	0.0625	0.1875
2.0	0.05	0.15

Table 5.1: Value of e/d as a function of Ω and e/r

Weak Element Ductility Ratios						
Omega	0.4	0.8	1.0	1.2	1.6	2.0
Period	Case: e/r = 0.1 Mean of 5 Earthquake					
0.1	0.899	1.380	1.001	0.956	1.143	1.278
0.2	1.070	1.407	1.000	0.750	1.047	1.159
0.3	1.008	1.029	0.991	0.939	1.118	1.383
0.4	1.032	1.536	1.000	0.934	1.202	1.256
0.6	0.998	1.586	0.977	0.875	1.191	1.176
0.8	1.120	1.012	1.000	0.897	1.105	1.215
1.0	1.034	1.437	1.000	0.785	0.938	1.152
1.2	1.024	1.401	1.000	0.858	0.985	1.052
1.6	1.060	1.254	1.000	0.803	1.020	1.140
2.0	1.042	1.165	1.000	0.926	1.073	1.018
	Case: e/r = 0.3 Mean of 5 Earthquake					
0.1	0.475	0.563	1.000	0.878	1.044	1.309
0.2	0.666	1.098	1.000	0.916	1.164	1.258
0.3	0.723	0.839	0.998	0.896	1.102	1.583
0.4	1.159	2.794	1.000	0.956	1.105	1.692
0.6	0.925	1.194	0.992	0.785	1.159	1.447
0.8	0.809	1.296	1.000	0.835	1.007	1.262
1.0	0.835	1.053	1.000	0.826	1.039	1.143
1.2	1.154	1.170	1.000	0.868	0.953	1.085
1.6	1.164	1.151	1.000	0.860	1.102	1.129
2.0	1.424	1.515	1.000	0.909	1.029	1.014

Strong Element Ductility Ratios						
Omega	0.4	0.8	1.0	1.2	1.6	2.0
Period	Case: e/r = 0.1 Mean of 5 Earthquake					
0.1	0.678	0.890	0.536	0.392	0.537	0.566
0.2	0.941	0.938	0.584	0.478	0.504	0.592
0.3	0.899	0.941	0.639	0.514	0.620	0.658
0.4	1.142	1.232	0.730	0.645	0.680	0.647
0.6	1.034	1.096	0.740	0.578	0.651	0.635
0.8	1.060	1.027	1.002	0.769	0.868	0.687
1.0	1.049	1.198	0.880	0.669	0.766	0.752
1.2	1.107	1.265	0.882	0.648	0.766	0.742
1.6	1.086	1.143	0.967	0.756	0.897	0.755
2.0	1.056	1.155	0.873	0.785	0.788	0.835
	Case: e/r = 0.3 Mean of 5 Earthquake					
0.1	0.098	0.209	0.211	0.204	0.269	0.283
0.2	0.315	0.368	0.335	0.233	0.275	0.338
0.3	0.376	0.528	0.628	0.367	0.413	0.407
0.4	0.792	1.932	0.705	0.488	0.406	0.410
0.6	0.774	0.817	0.573	0.384	0.390	0.431
0.8	0.998	0.835	0.727	0.493	0.493	0.438
1.0	1.002	1.061	0.744	0.593	0.448	0.472
1.2	1.177	0.946	0.762	0.545	0.466	0.524
1.6	1.225	1.018	1.004	0.762	0.734	0.544
2.0	1.376	1.398	0.826	0.555	0.601	0.664

Table 5.2: Mean of Weak and Strong Element Ductility Ratios Case of Target Ductility of 4

Weak Element Ductility Ratios						
Omega	0.4	0.8	1.0	1.2	1.6	2.0
Period	Case: e/r = 0.1 Mean + 1 Stand. Dev.					
0.1	1.501	2.057	1.001	1.103	1.224	1.400
0.2	1.655	1.696	1.000	0.946	1.281	1.270
0.3	1.351	1.481	1.046	1.126	1.323	1.540
0.4	1.284	2.269	1.000	1.020	1.326	1.492
0.6	1.310	2.032	0.992	0.997	1.393	1.409
0.8	1.343	1.299	1.000	1.093	1.311	1.397
1.0	1.187	1.704	1.000	0.879	1.051	1.316
1.2	1.110	1.687	1.000	0.949	1.028	1.127
1.6	1.138	1.565	1.000	0.904	1.170	1.240
2.0	1.105	1.453	1.000	1.057	1.220	1.235
	Case: e/r = 0.3 Mean + 1 Stand. Dev.					
0.1	0.607	0.661	1.001	1.064	1.104	1.471
0.2	1.030	1.739	1.000	1.128	1.425	1.374
0.3	1.099	1.192	1.010	1.164	1.256	2.061
0.4	1.752	6.077	1.000	1.076	1.347	2.067
0.6	1.371	1.870	1.004	0.879	1.606	2.173
0.8	0.952	2.146	1.000	1.002	1.299	1.591
1.0	1.040	1.489	1.000	0.891	1.108	1.263
1.2	1.677	1.562	1.000	1.051	1.093	1.335
1.6	1.598	1.749	1.000	0.975	1.378	1.329
2.0	1.814	2.389	1.000	1.022	1.296	1.186

Strong Element Ductility Ratios						
Omega	0.4	0.8	1.0	1.2	1.6	2.0
Period	Case: e/r = 0.1 Mean + 1 Stand. Dev.					
0.1	1.064	1.312	0.729	0.520	0.682	0.722
0.2	1.450	1.612	0.818	0.745	0.653	0.754
0.3	1.266	1.460	0.890	0.642	0.864	0.800
0.4	1.393	1.772	0.780	0.745	0.836	0.811
0.6	1.233	1.505	0.908	0.681	0.763	0.768
0.8	1.271	1.136	1.147	0.932	1.038	0.789
1.0	1.254	1.495	1.031	0.765	0.890	0.883
1.2	1.139	1.400	1.180	0.727	0.868	0.836
1.6	1.133	1.335	1.099	0.884	1.042	0.811
2.0	1.109	1.505	1.000	0.922	0.897	0.984
	Case: e/r = 0.3 Mean + 1 Stand. Dev.					
0.1	0.146	0.259	0.241	0.230	0.303	0.326
0.2	0.488	0.472	0.435	0.295	0.353	0.393
0.3	0.536	0.792	1.042	0.629	0.660	0.535
0.4	1.086	4.300	0.886	0.678	0.582	0.500
0.6	0.973	1.281	0.643	0.422	0.459	0.660
0.8	1.200	1.374	0.995	0.693	0.615	0.577
1.0	1.237	1.529	1.103	0.701	0.559	0.588
1.2	1.459	1.291	1.112	0.722	0.586	0.743
1.6	1.442	1.488	1.297	1.029	1.141	0.696
2.0	1.619	2.151	0.902	0.646	0.757	0.853

Table 5.3: Mean-plus-one-standard-deviation of Weak and Strong Element Ductility Ratios Case of Target Ductility of 4

Weak Element Ductility Ratios						
Omega	0.4	0.8	1.0	1.2	1.6	2.0
Period	Case: e/r = 0.1 Mean of 5 Earthquake					
0.1	0.751	1.314	1.000	0.842	1.072	1.169
0.2	0.766	1.134	1.000	0.705	1.015	1.146
0.3	1.041	0.892	0.975	0.813	1.172	1.204
0.4	1.059	1.388	1.000	0.766	0.997	1.119
0.6	0.945	1.253	0.990	0.844	1.017	1.184
0.8	1.045	1.171	1.000	0.836	0.993	1.079
1.0	0.964	1.300	1.000	0.770	0.961	1.080
1.2	1.065	1.414	1.000	0.862	0.947	1.017
1.6	1.114	1.209	1.000	0.824	0.981	0.996
2.0	1.061	1.051	1.000	0.884	0.969	1.014
	Case: e/r = 0.3 Mean of 5 Earthquake					
0.1	0.273	0.394	1.000	0.832	1.069	1.256
0.2	0.443	0.880	1.000	0.782	1.030	1.192
0.3	0.509	0.772	1.019	0.805	1.148	1.370
0.4	0.935	2.031	1.000	0.814	0.976	1.317
0.6	0.725	1.062	0.989	0.826	0.962	1.074
0.8	0.910	1.203	1.000	0.775	0.993	1.226
1.0	1.008	0.994	1.000	0.728	0.887	1.093
1.2	1.049	1.002	1.000	0.834	0.851	1.077
1.6	1.318	1.193	1.000	0.794	0.914	1.004
2.0	1.256	1.343	1.000	0.791	0.862	1.009

Strong Element Ductility Ratios						
Omega	0.4	0.8	1.0	1.2	1.6	2.0
Period	Case: e/r = 0.1 Mean of 5 Earthquake					
0.1	0.698	0.690	0.501	0.331	0.472	0.503
0.2	0.665	0.892	0.414	0.350	0.482	0.614
0.3	0.987	0.837	0.747	0.698	0.765	0.711
0.4	1.082	1.100	0.692	0.564	0.557	0.609
0.6	1.048	1.139	0.683	0.513	0.564	0.524
0.8	1.079	1.010	0.841	0.725	0.806	0.795
1.0	1.007	1.194	0.882	0.626	0.781	0.741
1.2	1.097	1.289	0.880	0.725	0.879	0.818
1.6	1.083	1.118	0.829	0.751	0.869	0.859
2.0	1.064	1.057	1.007	0.835	0.870	0.834
	Case: e/r = 0.3 Mean of 5 Earthquake					
0.1	0.055	0.125	0.136	0.133	0.157	0.199
0.2	0.218	0.320	0.297	0.168	0.188	0.270
0.3	0.338	0.574	0.567	0.488	0.414	0.335
0.4	0.696	1.031	0.481	0.401	0.365	0.353
0.6	0.713	0.791	0.649	0.334	0.303	0.329
0.8	0.967	0.926	0.805	0.650	0.517	0.490
1.0	0.969	0.890	0.791	0.581	0.556	0.454
1.2	1.060	0.960	0.803	0.596	0.624	0.633
1.6	1.228	1.129	0.802	0.684	0.738	0.623
2.0	1.224	1.111	0.923	0.678	0.618	0.628

Table 5.4: Mean of Weak and Strong Element Ductility Ratios Case of Target Ductility of 8

Weak Element Ductility Ratios						
Omega	0.4	0.8	1.0	1.2	1.6	2.0
Period	Case: e/r = 0.1 Mean + 1 Stand. Dev.					
0.1	1.326	2.437	1.001	0.969	1.281	1.264
0.2	1.138	1.433	1.000	0.846	1.112	1.300
0.3	1.480	1.223	1.040	0.899	1.336	1.369
0.4	1.288	1.742	1.000	0.926	1.156	1.400
0.6	1.174	1.595	1.000	0.930	1.144	1.284
0.8	1.207	1.451	1.000	1.055	1.177	1.251
1.0	1.080	1.590	1.000	0.910	1.045	1.140
1.2	1.153	1.775	1.000	0.932	1.005	1.070
1.6	1.201	1.403	1.000	0.958	1.108	1.119
2.0	1.091	1.135	1.000	0.994	1.072	1.103
	Case: e/r = 0.3 Mean + 1 Stand. Dev.					
0.1	0.363	0.533	1.001	0.914	1.148	1.362
0.2	0.677	1.255	1.000	0.869	1.202	1.309
0.3	0.763	1.186	1.040	0.949	1.307	1.592
0.4	1.218	4.323	1.000	0.964	1.199	1.628
0.6	0.961	1.654	0.993	0.984	1.192	1.213
0.8	1.032	2.015	1.000	0.957	1.285	1.467
1.0	1.438	1.324	1.000	0.946	1.078	1.242
1.2	1.465	1.356	1.000	0.919	0.946	1.177
1.6	1.705	1.680	1.000	0.898	1.161	1.119
2.0	1.481	1.990	1.000	0.871	1.009	1.193

Strong Element Ductility Ratios						
Omega	0.4	0.8	1.0	1.2	1.6	2.0
Period	Case: e/r = 0.1 Mean + 1 Stand. Dev.					
0.1	1.227	1.054	0.700	0.432	0.603	0.650
0.2	1.023	1.628	0.637	0.511	0.753	0.830
0.3	1.490	1.212	0.972	1.134	1.248	0.951
0.4	1.290	1.465	0.876	0.698	0.705	0.873
0.6	1.236	1.408	0.822	0.619	0.627	0.654
0.8	1.237	1.193	0.981	0.895	0.967	0.909
1.0	1.148	1.440	1.012	0.738	0.974	0.895
1.2	1.140	1.408	1.061	0.897	1.004	0.945
1.6	1.140	1.304	1.044	0.917	1.072	0.945
2.0	1.110	1.166	1.125	0.964	0.936	0.884
	Case: e/r = 0.3 Mean + 1 Stand. Dev.					
0.1	0.082	0.162	0.160	0.163	0.185	0.260
0.2	0.327	0.539	0.475	0.236	0.258	0.372
0.3	0.490	0.914	0.979	0.837	0.587	0.432
0.4	0.999	2.063	0.626	0.555	0.587	0.513
0.6	0.934	1.248	0.848	0.404	0.315	0.513
0.8	1.142	1.581	1.204	1.012	0.698	0.699
1.0	1.180	1.384	1.152	0.834	0.852	0.658
1.2	1.260	1.361	0.994	0.877	0.837	0.876
1.6	1.431	1.493	1.050	0.972	0.982	0.814
2.0	1.347	1.489	1.110	0.792	0.805	0.731

Table 5.5: Mean-plus-one-standard-deviation of the Weak and Strong Element Ductility Ratios Case of Target Ductility of 8

Table 5.6:

1) Initially Eccentric Systems Results Diskettes:

File Name	Location A:	Description	Format
eccdraec.4 eccdraol.4 eccdrapd.4 eccdrapk.4 eccdratf.4	\duct4ecc\.	Ductility of 4 Ratios of ductilities for both elements.	1
eccdraec.8 eccdraol.8 eccdrapd.8 eccdrapk.8 eccdratf.8	\duct8ecc\.	Same as above but Ductility of 8	1
weakec4x.dat weakol4x.dat weakpd4x.dat weakpk4x.dat weaktf4x.dat	\duct4ecc\.	Bloc Comparisons of Omega values For weak elements Ductility of 4	2
weakec8x.dat weakol8x.dat weakpd8x.dat weakpk8x.dat weaktf8x.dat	\duct8ecc\.	Bloc Comparisons of Omega values For weak elements Ductility of 8	2
strgec4x.dat strgol4x.dat strgpd4x.dat strgpk4x.dat strgtf4x.dat	\duct4ecc\.	Bloc Comparisons of Omega values For Strong elements Ductility of 4	2
strgec8x.dat strgol8x.dat strgpd8x.dat strgpk8x.dat strgtf8x.dat	\duct8ecc\.	Bloc Comparisons of Omega values For Strong elements Ductility of 8	2

Where the labels ec, ol, pd, pk and tf relate the each individual earthquake records used to generate those results, that is:

ec : El Centro 1940
ol : Olympia 1949
pd : Pacoima Dam 1971
pk : Parkfield 1966
tf : Taft 1952

Table 5.6 (continued):

Furthermore, the files calculating the mean for the five earthquake used (as well as the mean plus one standard deviation) are labeled as follow:

For the means (all located in a:\eccstats, except for the files meanangx.all, mndv2ya1.dat, mp1sangx.all and mpdv2ya1.dat, which are stored in a:\angleecc):

File Name	Mean of	Ductility of	Format
meandecc.4	eccdra--.4 files	4	1
meandecc.8	eccdra--.8 files	8	1
meanangx.all	allangle files	4 & 8	3
mndv2ya1.dat	d*angle/δy files	4 & 8	4
meanwk4x.dat	weak....files	4	2
meanwk8x.dat	weak... files	8	2
meansg4x.dat	strg... files	4	2
meansg8x.dat	strg... files	8	2

For the means-plus-one-standard-deviations (all located in a:\stats):

File Name	Mean + 1 SDV	Ductility of	Format
mp1sdecc.4	eccdra--.4 files	4	1
mp1sdecc.8	eccdra--.8 files	8	1
mp1sangx.all	allangle files	4 & 8	3
mpdv2ya1.dat	d*angle/δy files	4 & 8	4
mp1swk4x.dat	weak....files	4	2
mp1swk8x.dat	weak... files	8	2
mp1ssg4x.dat	strg... files	4	2
mp1ssg8x.dat	strg... files	8	2

Table 5.6 (continued):

To Read any file:

All files presented above are wide files (more than 80 columns wide; refer to format list for details). Refer to Table 4.2 for instructions on how to easily read these files. Format 1 & 4:

List of Formats:

The files under format 1 and 3 are 132 columns wide. They can therefore be printed on wide-carriage printers (or printer that can emulate wide-printing) without undesirable line folding. The columns are organized as follow (after some brief comment lines):

Columns 1 and 2 respectively contain the period and omega (Ω) values for that given set of analyses. For format 1, the following 4 columns are related (two-by-two) to the 2 different levels of normalized eccentricity studied (i.e. e/r=0.1 and e/r=0.3). The columns 3 and 5 contain the ductility ratios results for the strong element (stiffer), and columns 4 and 6 hold the results for the weak elements. Thus, the proper heading could read: Period, Omega, Strong & Weak for e/r=0.1, Weak & Strong for e/r=0.3. For format 3, the following 8 columns are also related (two-by-two) to the two different levels of ductility and normalized eccentricity studied. Columns 3, 5, 7 and 9 contain the maximum angular responses (in radians), and columns 4, 6, 8 and 10 contain the values in their respective previous column multiplied by the edge distance and divided by the yield displacement (let's call these normalized). Therefore, the proper heading could read: Period, Omega, (Ductility = 4: Max. Angle and Normalized Max. Angle for e/r=0.1, then for e/r=0.3), (Ductility = 8: Max. Angle and Normalized Max. Angle for e/r=0.1 and e/r=0.3).

The files under format 2 and 4 are more than 132 characters long (but less than 250). These files are formatted with current standards for ASCII file-reading by spreadsheet programs like LOTUS 1-2-3. After a few heading lines, the first column is always blank, and the second contains the periods. The format 2 columns are grouped as follow: For each of the 2 normalized eccentricity combinations studied, the columns represent the ductility ratios for omega values increasing from 0.4 to 2.0. For format 4, for each of the two ductility and normalized eccentricity studied, the columns represent normalized maximum angles for omega values increasing from 0.4 to 2.0, in the following order: Ductility of 4: e/r=0.1 and e/r=0.3; then ductility of 8: e/r=0.1 and e/r=0.3. Column of zeros separates all the 10x6 "blocs".

Period	Duct.	Omega	e/r	Ductility Ratios	
				With Proposed Scaling	Without Proposed Scaling
0.1	4	0.4	0.3	0.48	3.46
0.1	4	0.8	0.3	0.62	2.32
0.1	4	1.0	0.3	1.00	1.00
0.1	4	1.2	0.3	0.93	1.65
0.1	4	1.6	0.3	1.10	2.38
0.1	4	2.0	0.3	1.40	2.55
0.2	4	0.4	0.3	0.48	1.21
0.3	4	0.4	0.3	0.70	2.07

Table 5.7: Comparison of ductility ratios obtained with and without the proposed scaling of the seismic excitation to match the elastic responses.

Reference Two Element System Weak Element Ductility Ratio Case 1.0 Fy and 1.5 Fy	
Ω	Weak El. Ratio
0.4	0.84
0.8	0.90
1.0	1.00
1.2	1.25
1.6	1.80
2.0	1.94

Four Element Systems			
Ω	WSSS	WWSS	WWWS
0.4	0.81	0.85	0.87
0.8	0.76	0.88	1.02
1.0	0.91	1.06	1.11
1.2	1.17	1.34	1.36
1.6	1.37	1.64	1.63
2.0	1.38	1.64	1.68

Six Element Systems					
Ω	WSSSSS	WWSSSS	WWWSSS	WWWWSS	WWWWWS
0.4	0.88	0.79	0.85	0.87	0.93
0.8	0.75	0.78	0.89	1.02	1.04
1.0	0.89	0.98	1.09	1.14	1.10
1.2	1.13	1.27	1.39	1.43	1.30
1.6	1.22	1.56	1.71	1.73	1.58
2.0	1.26	1.54	1.64	1.76	1.55

Eight Element Systems							
Ω	WSSSSSSS	WWSSSSSS	WWWSSSSS	WWWWSSSS	WWWWWSSS	WWWWWWSS	WWWWWWWS
0.4	0.92	0.81	0.81	0.84	0.87	0.88	0.96
0.8	0.74	0.77	0.80	0.90	1.02	1.07	1.06
1.0	0.86	0.94	1.02	1.10	1.14	1.14	1.11
1.2	1.06	1.25	1.30	1.41	1.46	1.42	1.25
1.6	1.12	1.44	1.64	1.74	1.77	1.72	1.50
2.0	1.23	1.46	1.61	1.67	1.75	1.73	1.49

Table 6.1: Weak Element Ductility Ratios for Initially Symmetric Multi-Element Systems; Equaly spaced Elements of Equal Stiffness. Weak element (1.0 Fy) represented by W and Strong element (1.5 Fy) represented by S.

Reference Two Element System Strong Element Ductility Ratio Case 1.0 Fy and 1.5 Fy	
Ω	Strong El. Ratio
0.4	0.59
0.8	0.57
1.0	0.73
1.2	0.69
1.6	0.34
2.0	0.45

Four Element Systems			
Ω	WSSS	WWSS	WWWS
0.4	0.55	0.61	0.66
0.8	0.59	0.59	0.63
1.0	0.72	0.57	0.55
1.2	0.82	0.70	0.55
1.6	0.39	0.34	0.41
2.0	0.39	0.47	0.49

Six Element Systems					
Ω	WSSSSS	WWSSSS	WWWSSS	WWWWSS	WWWWWS
0.4	0.55	0.57	0.61	0.64	0.67
0.8	0.66	0.55	0.60	0.63	0.64
1.0	0.78	0.68	0.57	0.53	0.58
1.2	0.77	0.80	0.71	0.61	0.47
1.6	0.42	0.37	0.36	0.38	0.45
2.0	0.37	0.46	0.48	0.45	0.76

Eight Element Systems							
Ω	WSSSSSSS	WWSSSSSS	WWWSSSSS	WWWWSSSS	WWWWWSSS	WWWWWWSS	WWWWWWWS
0.4	0.59	0.55	0.58	0.61	0.64	0.66	0.68
0.8	0.69	0.60	0.57	0.60	0.63	0.63	0.65
1.0	0.79	0.74	0.65	0.57	0.53	0.56	0.59
1.2	0.74	0.83	0.79	0.72	0.65	0.54	0.51
1.6	0.42	0.40	0.37	0.37	0.38	0.41	0.47
2.0	0.38	0.40	0.46	0.49	0.47	0.40	0.50

Table 6.2: Strong Element Ductility Ratios for Initially Symmetric Multi-Element Systems; Equaly spaced Elements of Equal Stiffness. Weak element (1.0 Fy) represented by W and Strong element (1.5 Fy) represented by S.

Reference Two Element System Weak Element Ductility Ratio Case 1.0 Fy and 1.5 Fy	
Ω	Weak El. Ratio
0.4	0.84
0.8	0.90
1.0	1.00
1.2	1.25
1.6	1.80
2.0	1.94

Outside (edge) Weak Element Ductility Ratio							
K_1/K_2 Values from 1/16 to 4							
Ω	1/16	1/8	1/4	1/2	1	2	4
D_1/D_2 value of 2							
0.4	0.88	0.88	0.85	0.84	0.84	0.84	0.84
0.8	1.03	1.00	0.97	0.92	0.89	0.88	0.88
1.0	1.23	1.18	1.15	1.10	1.06	1.03	1.02
1.2	1.65	1.57	1.49	1.41	1.35	1.30	1.28
1.6	2.22	1.98	1.85	1.74	1.65	1.73	1.75
2.0	2.43	2.21	1.95	1.81	1.80	1.81	1.84
D_1/D_2 value of 3							
0.4	1.00	0.93	0.86	0.84	0.85	0.84	0.84
0.8	1.14	1.04	0.95	0.90	0.88	0.87	0.87
1.0	1.40	1.35	1.20	1.10	1.06	1.03	1.02
1.2	1.83	1.66	1.52	1.41	1.34	1.30	1.28
1.6	2.39	2.10	1.88	1.73	1.64	1.63	1.70
2.0	2.46	2.10	1.81	1.66	1.64	1.70	1.76
D_1/D_2 value of 4							
0.4	1.08	0.95	0.85	0.84	0.85	0.84	0.84
0.8	1.21	1.02	0.93	0.88	0.86	0.86	0.87
1.0	1.60	1.40	1.16	1.10	1.05	1.03	1.02
1.2	1.86	1.65	1.50	1.40	1.33	1.29	1.27
1.6	2.46	2.06	1.84	1.71	1.62	1.60	1.69
2.0	2.43	2.02	1.80	1.65	1.57	1.66	1.74

Table 6.3: Outside (edge) Weak Element Ductility Ratios for Initially Symmetric Multi-Element Systems; Various Stiffness and geometric distribution.

Reference Two Element System Weak Element Ductility Ratio Case 1.0 Fy and 1.5 Fy	
Ω	Weak El. Ratio
0.4	0.84
0.8	0.90
1.0	1.00
1.2	1.25
1.6	1.80
2.0	1.94

Inside (near C.M.) Weak Element Ductility Ratio							
K_1/K_2 Values from 1/16 to 4							
Ω	1/16	1/8	1/4	1/2	1	2	4
D_1/D_2 value of 2							
0.4	0.84	0.84	0.84	0.84	0.85	0.84	0.84
0.8	0.87	0.86	0.85	0.84	0.83	0.83	0.83
1.0	1.03	1.02	1.01	0.98	0.95	0.95	0.95
1.2	1.19	1.15	1.11	1.08	1.05	1.03	1.02
1.6	1.56	1.41	1.32	1.26	1.26	1.34	1.36
2.0	1.65	1.53	1.39	1.33	1.34	1.36	1.40
D_1/D_2 value of 3							
0.4	0.84	0.85	0.85	0.85	0.85	0.85	0.85
0.8	0.84	0.82	0.82	0.82	0.82	0.81	0.81
1.0	1.03	1.01	0.94	0.89	0.88	0.90	0.92
1.2	1.10	1.05	1.02	0.99	0.96	0.95	0.94
1.6	1.31	1.22	1.16	1.11	1.08	1.16	1.21
2.0	1.33	1.20	1.14	1.09	1.10	1.15	1.20
D_1/D_2 value of 4							
0.4	0.85	0.85	0.85	0.85	0.85	0.85	0.85
0.8	0.82	0.82	0.82	0.82	0.82	0.81	0.81
1.0	1.01	0.94	0.88	0.87	0.86	0.87	0.90
1.2	1.03	0.99	0.96	0.94	0.92	0.91	0.90
1.6	1.20	1.12	1.07	1.04	1.01	1.09	1.15
2.0	1.20	1.11	1.06	1.02	1.00	1.07	1.12

Table 6.4: Inside (near C.M.) Weak Element Ductility Ratios for Initially Symmetric Multi-Element Systems; Various Stiffness and geometric distribution.

Reference Two Element System Element Ductility Ratio Case e/r=0.3 and Tx=0.4		
Ω	Strong	Weak
0.4	1.06	0.83
0.8	0.98	0.78
1.0	0.93	1.00
1.2	0.48	0.89
1.6	0.38	1.53
2.0	0.53	1.88

Four-Element Linear Stiffness Variation Systems						
	Edge Strong Element			Edge Weak Element		
	D_1/D_2 value			D_1/D_2 value		
Ω	2	3	4	2	3	4
0.4	1.09	-	-	0.74	-	-
0.8	1.07	1.06	1.05	0.74	0.75	0.82
1.0	0.87	0.82	0.85	1.07	1.15	1.22
1.2	0.46	0.44	0.41	0.83	0.77	0.75
1.6	0.35	0.32	0.31	1.20	1.18	1.17
2.0	0.54	0.51	0.49	1.68	1.56	1.53

Four-Element Step Stiffness Variation Systems				
	Edge Strong Element		Edge Weak Element	
	Step Configuration		Step Configuration	
Ω	Single	Double	Single	Double
0.4	1.10	-	0.68	-
0.8	1.06	1.06	0.72	0.76
1.0	0.86	0.89	1.05	1.10
1.2	0.47	0.45	0.83	0.82
1.6	0.35	0.35	1.20	1.20
2.0	0.54	0.54	1.66	1.71

Table 6.5: Element Ductility Ratios for Initially Eccentric Multi-Element Systems with e/r=0.3 and Tx=0.4; Linear Stiffness Distribution, Single Step and Double Step Distribution.

Reference Two Element System Element Ductility Ratio Case e/r=0.3 and Tx=0.4		
Ω	Strong	Weak
0.4	1.06	0.83
0.8	0.98	0.78
1.0	0.93	1.00
1.2	0.48	0.89
1.6	0.38	1.53
2.0	0.53	1.88

Six-Element Linear Stiffness Variation Systems		
Ω	Edge Strong Element	Edge Weak Element
0.4	-	-
0.8	1.06	0.74
1.0	0.90	1.26
1.2	0.44	0.75
1.6	0.30	1.18
2.0	0.52	1.53

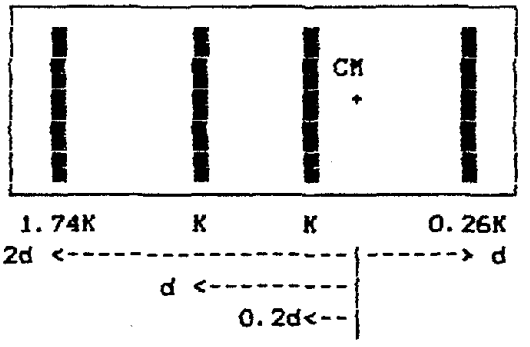

< Totally Irregular
< Four-Element System
< (Plan View)

Totally Irregular Four-Element System (one case)		
Ω	Edge Strong Element	Edge Weak Element
0.4	1.02	1.14

Table 6.6: Element Ductility Ratios for Initially Eccentric Multi-Element Systems with e/r=0.3 and Tx=0.4; Six-Element Systems with Linear Stiffness Distribution and Equally Spaced Elements, and One Case of Totally Irregular (Geometry and Stiffness Distribution) Four-Element System.

Elastic Buckling Element : Yield = Fy Buckling = Fy						
	Strong Element Ductility Ratios			Weak Element Ductility Ratios		
Ω	Y = 1.50 B = 1.50	Y = 2.00 B = 1.00	Y = 2.50 B = 0.50	Y = 1.50 B = 1.50	Y = 2.00 B = 1.00	Y = 2.50 B = 0.50
0.4	0.30	0.23	0.41	0.45	0.56	1.10
0.8	0.30	0.22	0.47	0.46	0.52	0.97
1.0	0.32	0.22	0.35	1.00	1.00	1.00
1.2	0.25	0.19	0.39	0.28	1.24	0.89
1.6	0.22	0.18	0.20	1.50	1.48	1.39
2.0	0.28	0.23	0.21	1.56	1.65	1.19

Elastic Buckling Element : Yield=1.25 Fy Buckling=0.75 Fy						
	Strong Element Ductility Ratios			Weak Element Ductility Ratios		
Ω	Y =1.875 B =1.125	Y = 2.25 B = 0.75	Y =2.625 B =0.375	Y =1.875 B =1.125	Y = 2.25 B = 0.75	Y =2.625 B =0.375
0.4	0.66	0.46	0.52	0.92	0.82	0.79
0.8	0.67	0.60	0.55	1.03	0.79	0.87
1.0	0.75	0.57	0.44	1.00	1.00	1.00
1.2	0.37	0.25	0.41	1.60	1.21	1.25
1.6	0.24	0.24	0.33	1.35	1.33	1.86
2.0	0.25	0.25	0.28	1.22	1.20	1.55

Elastic Buckling Element : Yield=1.50 Fy Buckling=0.50 Fy						
	Strong Element Ductility Ratios			Weak Element Ductility Ratios		
Ω	Y = 2.25 B = 0.75	Y = 2.50 B = 0.50	Y = 2.75 B = 0.25	Y = 2.25 B = 0.75	Y = 2.50 Y = 0.50	Y = 2.75 Y = 0.25
0.4	0.50	0.58	0.62	0.62	0.88	1.01
0.8	0.55	0.68	0.60	0.66	0.71	1.01
1.0	0.45	0.40	0.52	1.00	1.00	1.00
1.2	0.47	0.37	0.43	1.24	1.43	1.67
1.6	0.40	0.32	0.31	1.27	1.70	1.98
2.0	0.24	0.38	0.24	1.18	1.58	1.99

Table 6.7: Element Ductility Ratios for Initially Symmetric Two-Element Braced Frame Systems with Tx=0.4 and Three Cases of Weak Elements; Elastic Buckling Element Model. Y = Yield and B = Buckling Stresses (Fy) of Strong Element.

Physical Brace Element Model Weak Element: Yield = 1.25 Fy Buckling = 0.75 Fy Strong Element: Yield = 1.50 Fy Buckling = 0.50 Fy		
Ω	Strong Element Ductility Ratios	Weak Element Ductility Ratios
0.4	0.82	1.08
0.8	0.88	1.13
1.0	0.89	0.99
1.2	0.87	1.14
1.6	0.57	1.65
2.0	0.71	1.35

Table 6.8: Element Ductility Ratios for Initially Symmetric Two-Element Braced Frame Systems with Tx=0.4; Physical Brace Element Model.

Reference Two Element System Element Ductility Ratio Case e/r=0.3 and Tx=0.4		
Ω	Strong	Weak
0.4	1.06	0.83
0.8	0.98	0.78
1.0	0.93	1.00
1.2	0.48	0.89
1.6	0.38	1.53
2.0	0.53	1.88

Elastic Buckling Element -- Initially Eccentric Systems						
	Strong Element Ductility Ratios			Weak Element Ductility Ratios		
Ω	Y = 1.00 B = 1.00	Y = 1.25 B = 0.75	Y = 1.50 B = 0.50	Y = 1.00 B = 1.00	Y = 1.25 B = 0.75	Y = 1.50 B = 0.50
0.4	0.61	0.95	0.63	0.59	0.85	0.71
0.8	0.43	0.32	0.69	0.98	1.04	1.00
1.0	0.24	0.27	0.37	1.00	1.00	1.00
1.2	0.22	0.20	0.20	0.79	0.74	0.76
1.6	0.30	0.32	0.38	1.45	0.99	1.08
2.0	0.26	0.30	0.35	1.20	0.99	1.09

Physical Brace Element Model Initially Eccentric Systems				
	Strong Element Ductility Ratios		Weak Element Ductility Ratios	
Ω	Y = 1.25 B = 0.75	Y = 1.50 B = 0.50	Y = 1.25 B = 0.75	Y = 1.50 B = 0.50
0.4	0.87	0.81	0.73	0.71
0.8	0.78	0.80	0.48	0.83
1.0	0.91	0.78	1.00	1.00
1.2	0.47	0.85	0.89	0.61
1.6	0.27	0.99	1.39	1.60
2.0	0.25	0.60	1.82	1.56

Table 6.9: Element Ductility Ratios for Initially Eccentric Two-Element Braced Frame Systems with e/r=0.3 and Tx=0.4; Elastic Buckling Element and Physical Brace Element Model. Y = Yield, B = Buckling Stresses (in Fy) for both Strong and Weak Element.

Initially Eccentric Two-Story System ---- K_{TOP}/K_{BOT} = 2/3						
	Strong Element Ductility Ratios			Weak Element Ductility Ratios		
	Interstory		Total	Interstory		Total
(Ω)	0 to 1	1 to 2	Roof	0 to 1	1 to 2	Roof
(0.4)	0.33	0.35	0.19	0.57	0.45	0.36
(0.8)	0.69	1.28	0.84	2.36	0.95	1.57
(1.0)	0.61	0.50	0.49	1.35	0.82	0.79
(1.2)	0.30	0.33	0.31	1.33	0.39	0.83
(1.6)	0.39	0.16	0.24	1.75	0.51	0.87
(2.0)	0.52	0.20	0.34	1.83	0.53	0.94

Initially Eccentric Two-Story System ---- K_{TOP}/K_{BOT} = 1/3						
	Strong Element Ductility Ratios			Weak Element Ductility Ratios		
	Interstory		Total	Interstory		Total
(Ω)	0 to 1	1 to 2	Roof	0 to 1	1 to 2	Roof
(0.4)	0.09	0.55	0.29	0.41	0.77	0.39
(0.8)	0.25	2.52	1.26	0.67	3.14	1.72
(1.0)	0.13	1.08	0.56	0.50	2.05	0.98
(1.2)	0.10	0.81	0.43	0.24	1.32	0.66
(1.6)	0.17	0.81	0.45	0.28	2.52	1.26
(2.0)	0.20	0.53	0.33	0.27	3.28	1.67

Note: As explained in Chapter 6, the Ω presented here are simply an indicator of the ratios of strong/weak stiffness ratios on a given story; the relationship is as follows:

(Ω)	Strong/weak Stiffness Ratio
(0.4)	7.00
(0.8)	2.20
(1.0)	1.86
(1.2)	1.67
(1.6)	1.46
(2.0)	1.35

Table 6.10: Interstory and Total Element Ductility Ratios for Initially Eccentric Two-Story Systems.

Initially Symmetric Two-Story System ---- K_{Top}/K_{Bot} = 2/3						
	Strong Element Ductility Ratios			Weak Element Ductility Ratios		
	Interstory		Total	Interstory		Total
(Ω)	0 to 1	1 to 2	Roof	0 to 1	1 to 2	Roof
(0.4)	0.37	0.66	0.75	0.41	0.91	0.83
(0.8)	0.33	0.82	0.79	0.81	0.72	0.86
(1.0)	0.37	0.63	0.76	0.99	1.00	0.99
(1.2)	0.33	0.61	0.71	1.09	1.05	1.30
(1.6)	0.28	0.27	0.44	1.14	1.36	1.20
(2.0)	0.20	0.29	0.37	1.28	1.23	1.26

Note: As explained in Chapter 6, the Ω presented here are simply an indicator of the ratios edge distance over radius of gyration (d/r) which is constant here for both stories.

Table 6.11: Interstory and Total Element Ductility Ratios for Initially Symmetric Two-Story Systems.

IRREGULAR CONFIGURATION SYSTEM

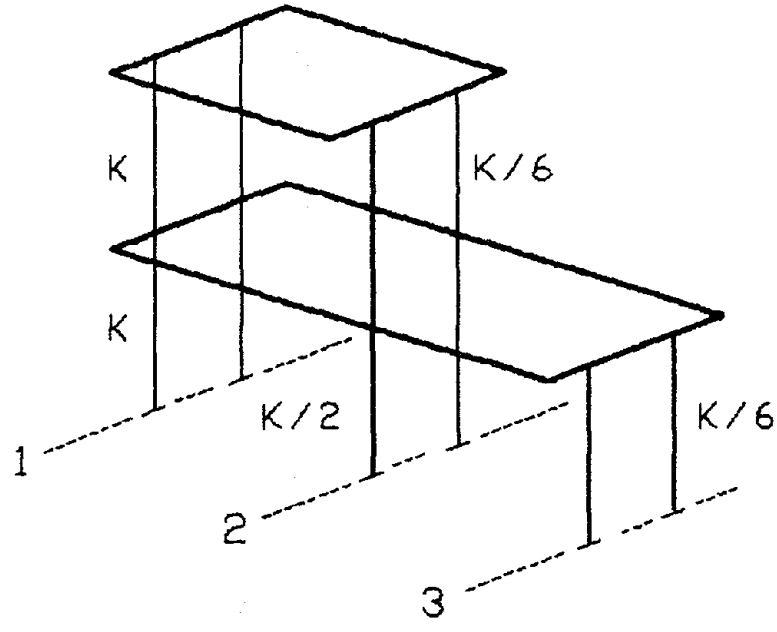

Irregular Configuration System					
Interstory Ductility Ratios					
Ground to First Story Ductility Ratios			First to Second Story Ductility Ratios		
Design Line (/Stiffness)			Design Line (/Stiffness)		
1 K	2 K/2	3 K/6	1 K	2 K/6	3 -
1.58	0.74	1.76	0.31	1.33	-

Total Ductility Ratios	
Top of Second Story (roof)	
Design Line (/Stiffness)	
1 K	2 K/6
0.92	0.49

Table 6.12: Interstory and Total Element Ductility Ratios for Two-Story System with Irregular Configuration.

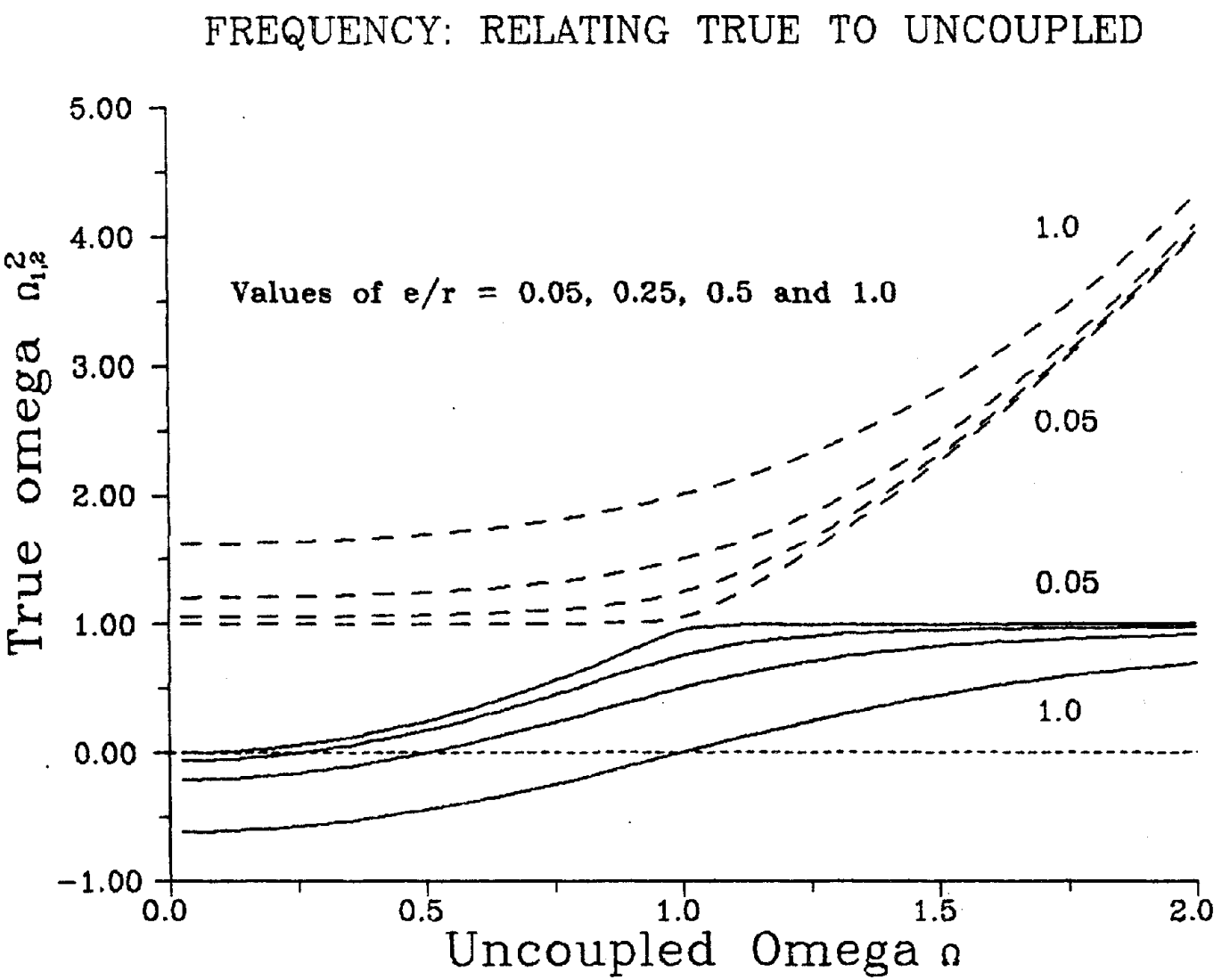

Figure 2.1 Relation Between the True and Uncoupled Frequencies as Expressed by the Omega Ratios

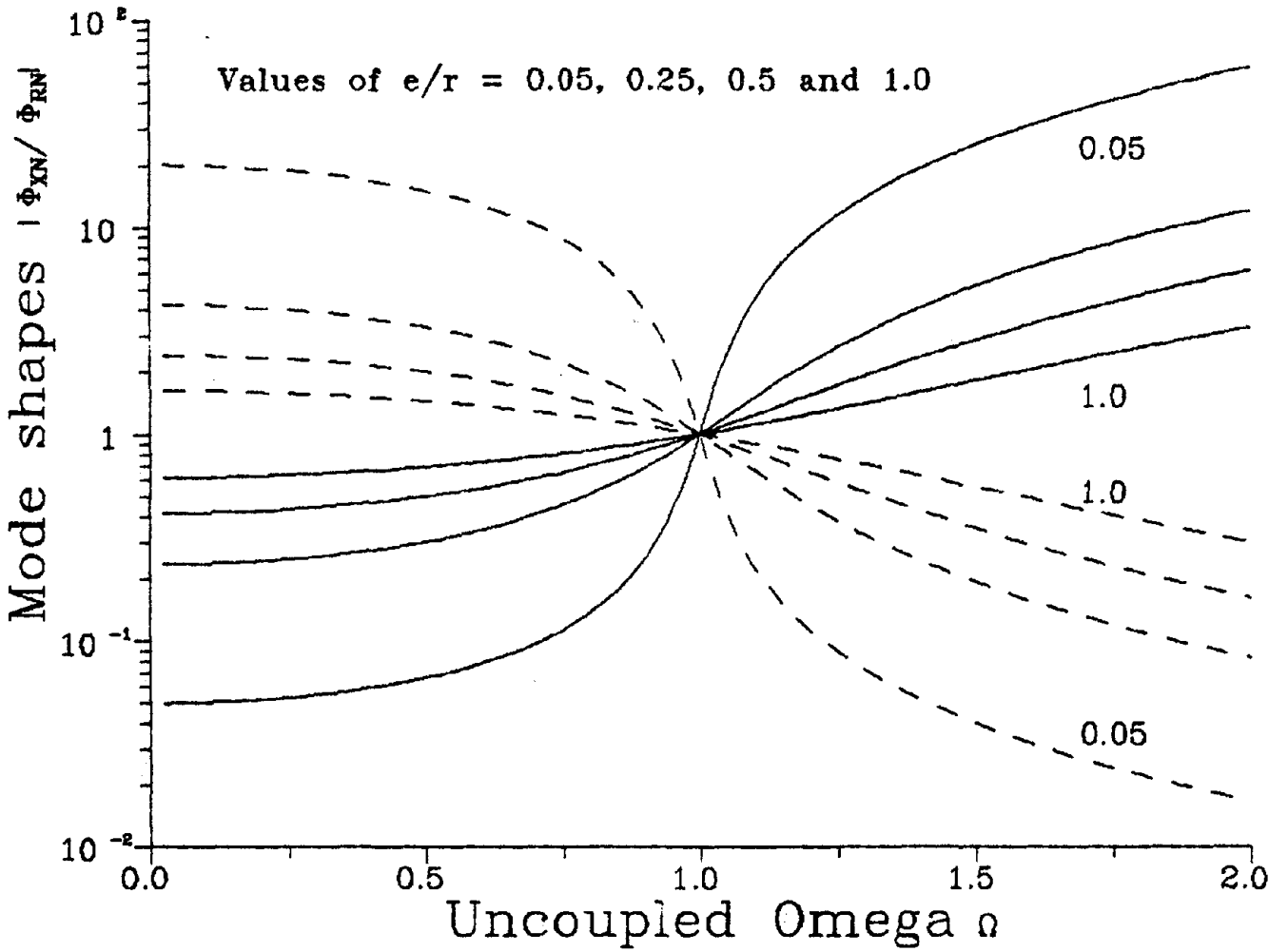

Figure 2.2 True Mode Shapes in Function of the Uncoupled Frequency Ratio

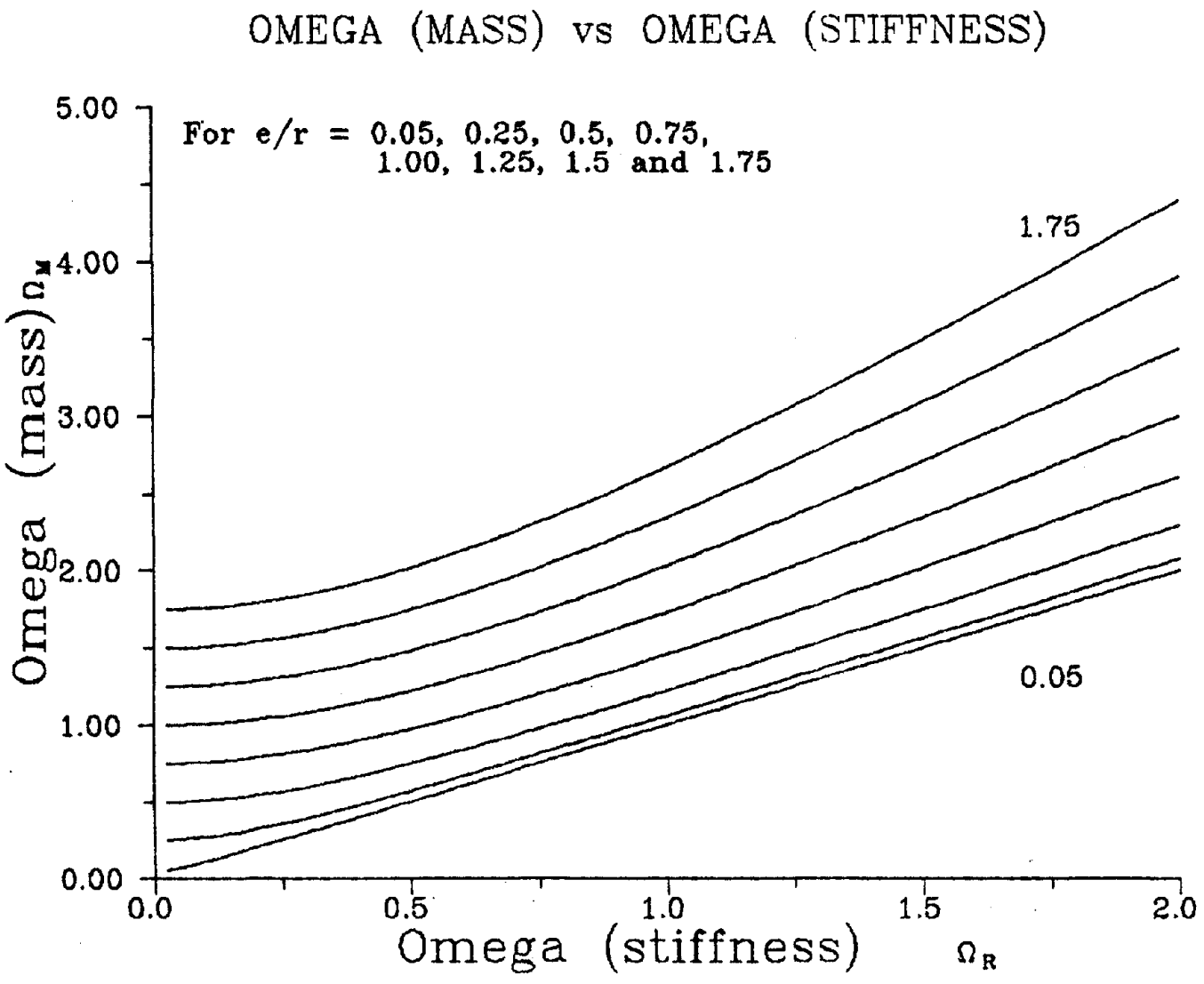

Figure 2.3 Relation Between the Uncoupled Frequency Ratios Derived Around the Centers of Mass and Stiffness

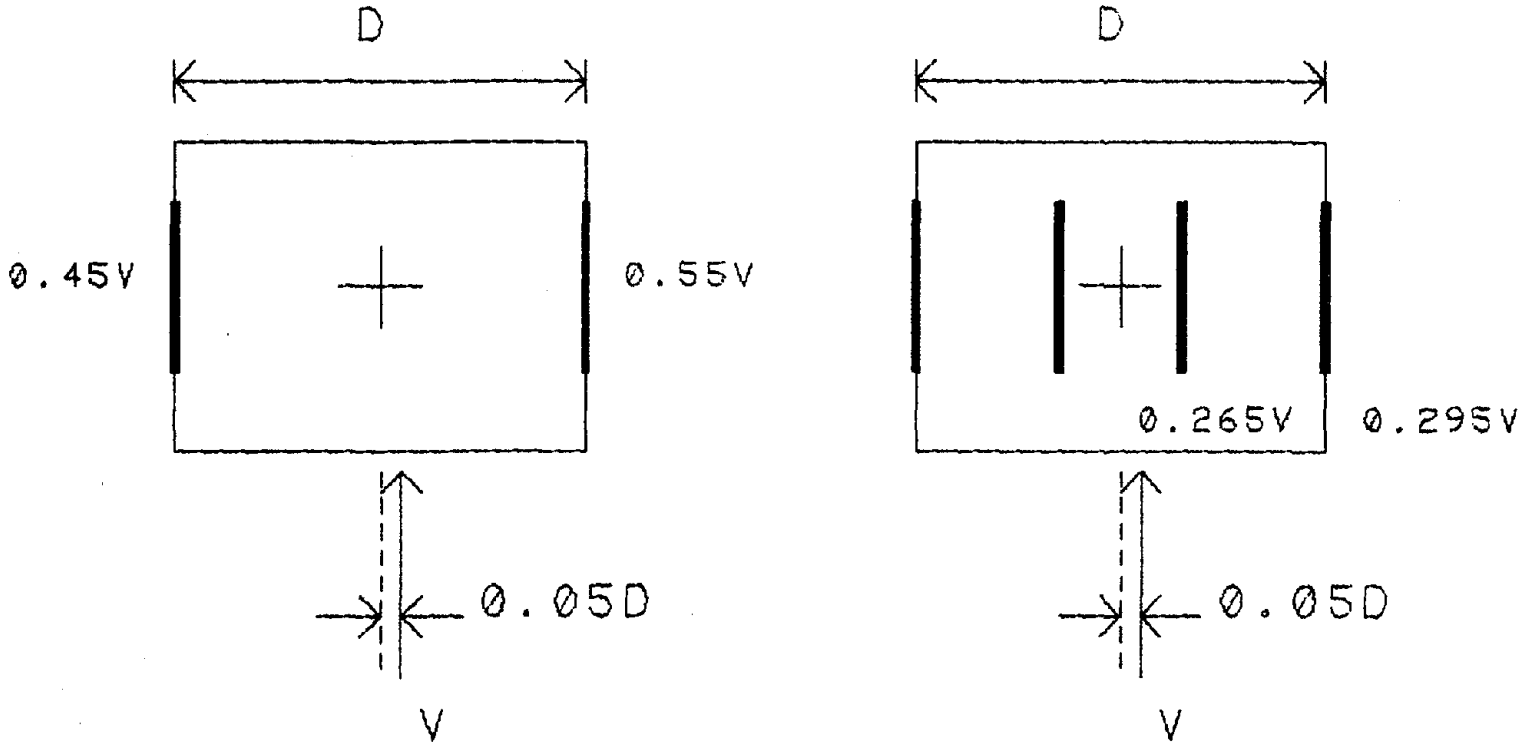

REDUNDANCY AND ACCIDENTAL ECCENTRICITY

Figure 3.1 Effect of Redundancy and Code Specified Accidental Eccentricity on Element Design

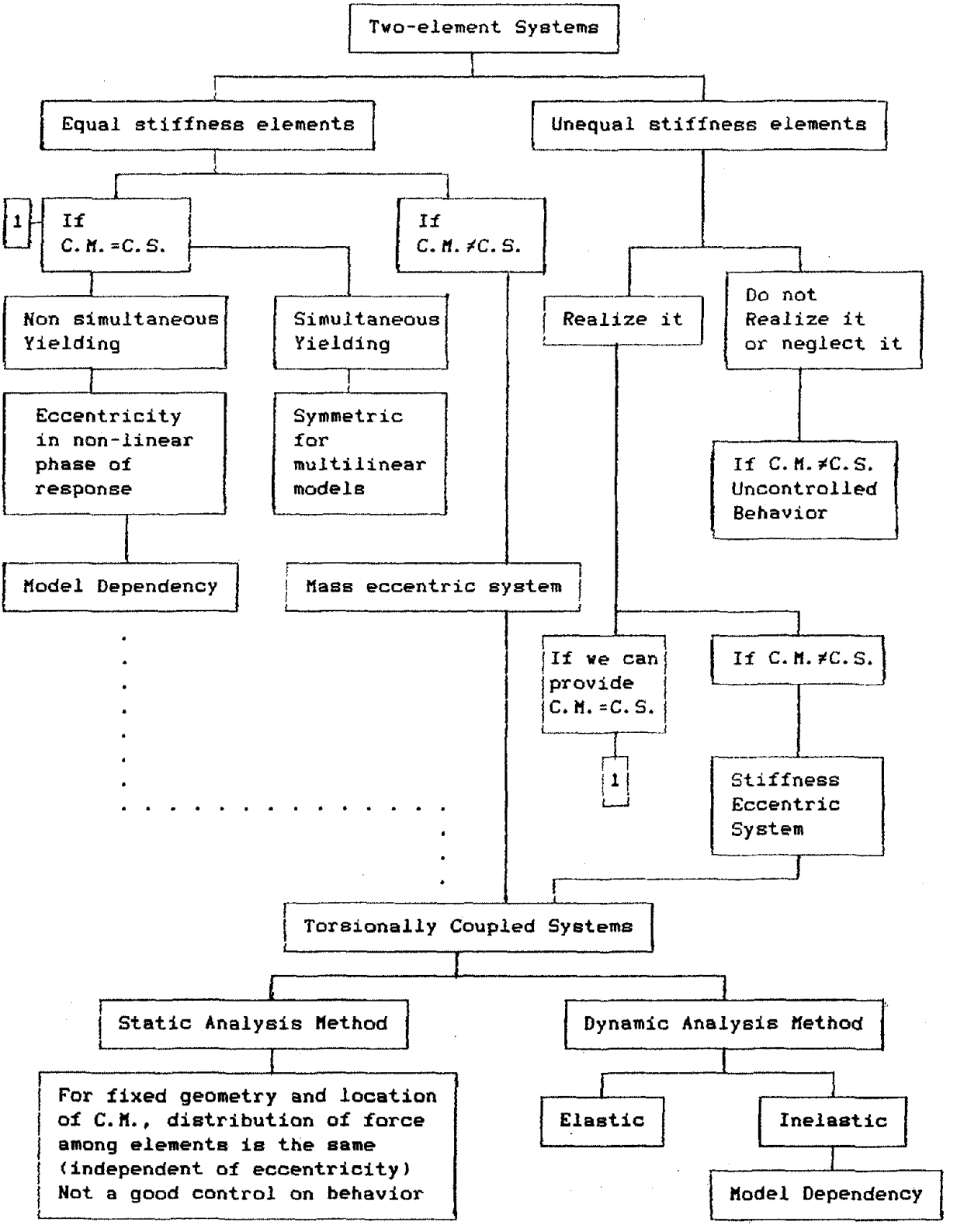

Figure 3.2: Possible Design Options for a Two-Element System

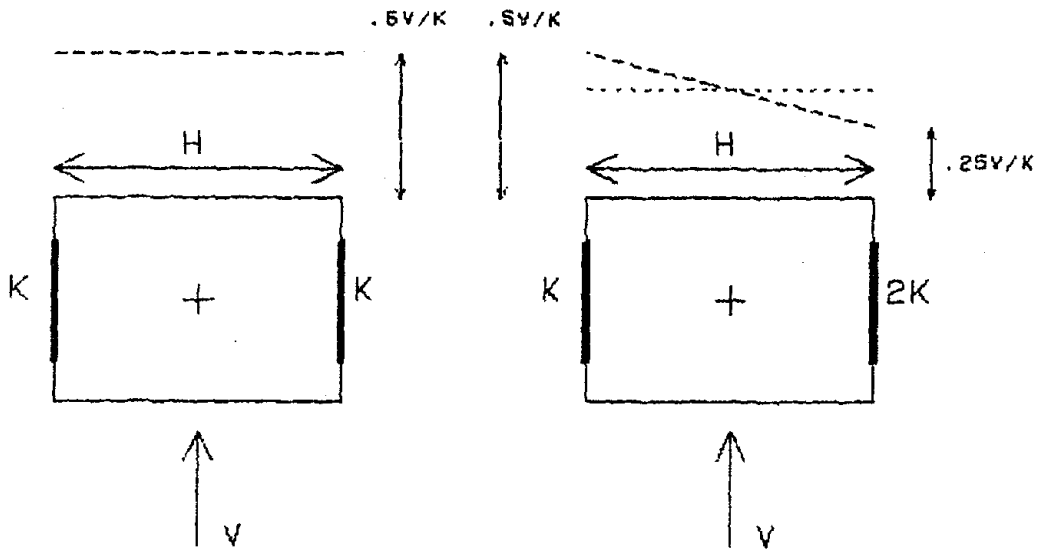

Equal stiffness

$V = 2(K)\ \delta$

Thus simply:

$\delta = 0.5\ V/K$

Unequal stiffness

$$\underline{V} = \underline{K}\ \underline{\delta}$$

$$\underline{K} = \begin{bmatrix} 3 & 0.5h \\ 0.5h & 0.75h^2 \end{bmatrix} K$$

$$\underline{K}^{-1} = \begin{bmatrix} 0.375 & -0.25/h \\ -0.25/h & 1.5/h^2 \end{bmatrix} \frac{1}{K}$$

$$\underline{\delta} = \underline{K}^{-1} \begin{bmatrix} V \\ 0 \end{bmatrix} = \begin{bmatrix} 0.375 \\ -0.25/h \end{bmatrix} \frac{\underline{V}}{K}$$

$\delta_{LEFT} = \delta_1 - (\delta_2 * h/2) = 0.5\ V/K$
$\delta_{RIGHT} = \delta_1 + (\delta_2 * h/2) = 0.25\ V/K$

Note: Degrees of freedom are taken as translation (1) and rotation (2) around center of mass.

Figure 3.3 Edge Displacements from Static Analyses Considering Equal and Unequal Element Stiffnesses

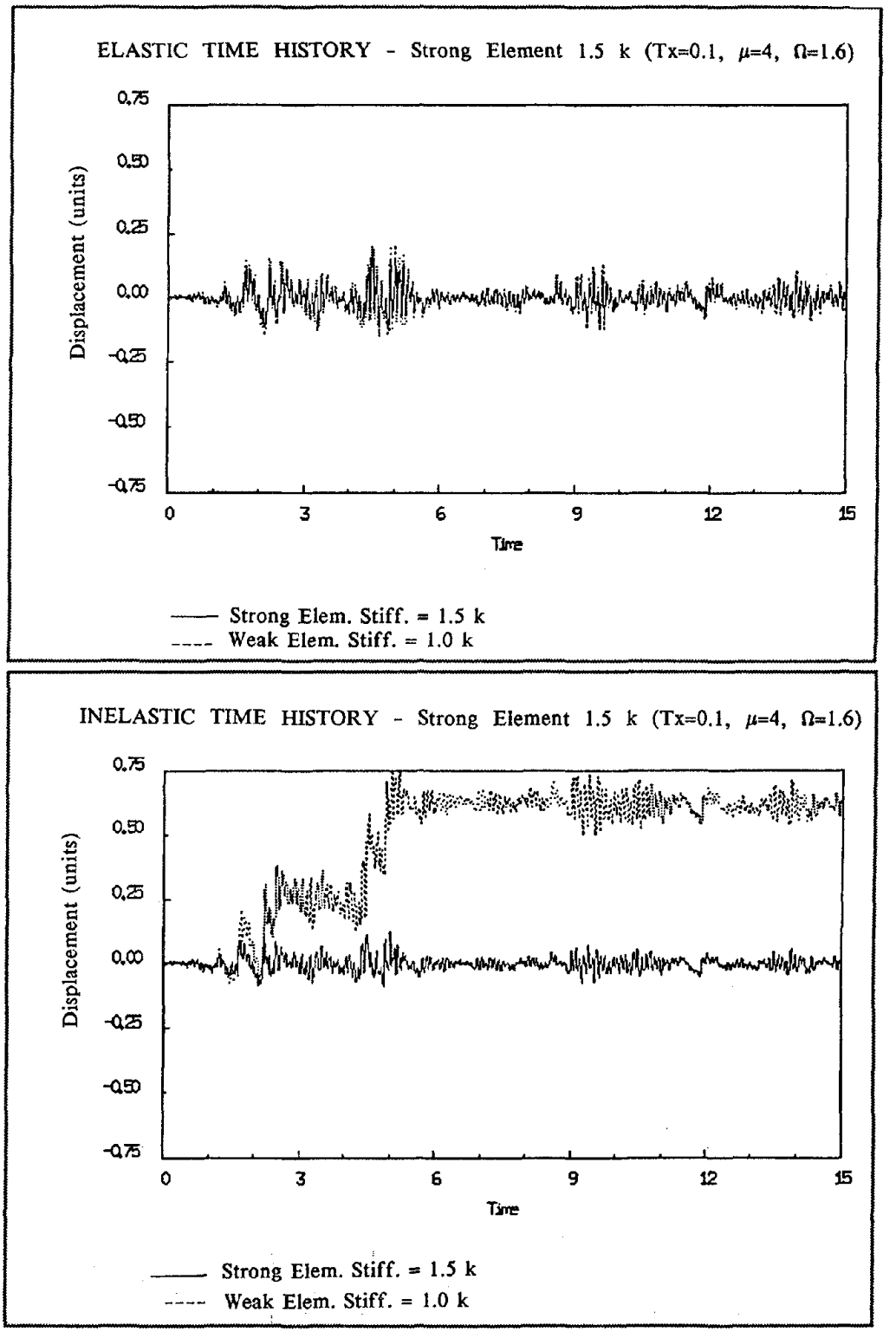

Figure 3.4 Elastic (top) and Inelastic (bottom) Analysis of A Structural System Having One Element 50% Stiffer than the Other (Yield Displacement = 0.12 units)

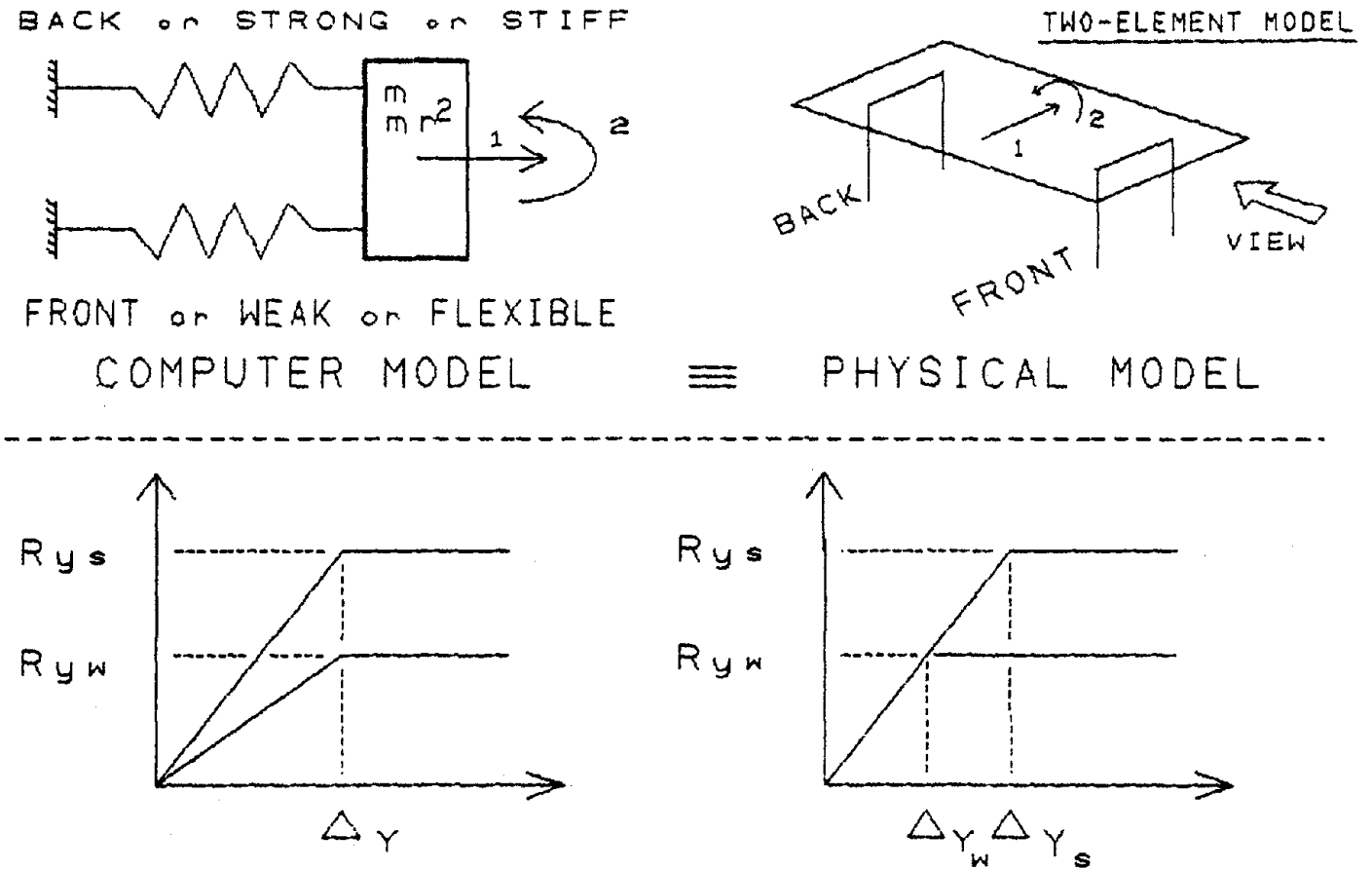

Figure 3.5 Element Models Used for this Research Program

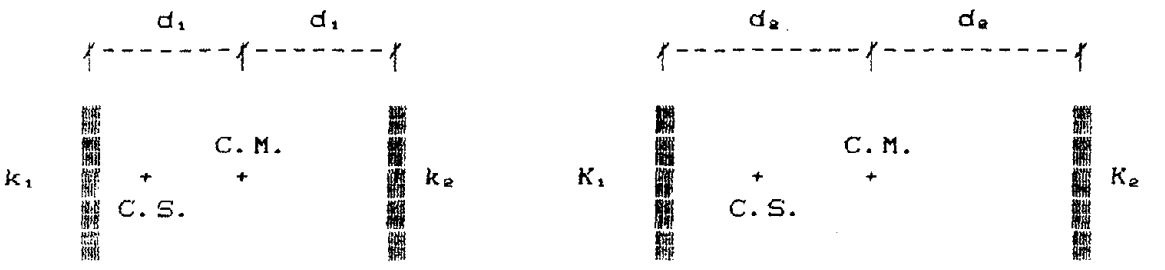

Assume in this example (for simplicity) that all elements are bi-linear with no strain hardening.

Now, we want the two systems to have the same ω_x, ω_x', ω_θ, ω_θ', (e/r) and (e'/r).

Therefore:

$$\omega_x^2{}_1 = \frac{k_1 + k_2}{m} = \omega_x^2{}_2 = \frac{K_1 + K_2}{M}$$

$$\omega_x^2{}_1' = k_1/m = \omega_x^2{}_2' = K_1/M$$

Thus $k_1/m = K_1/M$ and $k_2/m = K_2/M$

$\omega_{\theta 1} = \omega_{\theta 2}$ implies $[(K_1+K_2)/M][d_2/r_2]^2 = [(k_1+k_2)/m][d_1/r_1]^2$

and therefore $d_1/r_1 = d_2/r_2 = D$ = constant

(Note that d/r is more restrictive than e/r in general. If the center of mass is not equidistant to each element, we will have different values of d_i's (i being index for i-th element), and thus different D_i's too, whereas the e/r values may be similar. Also, the D value for a system is constant even through the different yielding phases, whereas (e'/r) will vary with the instantaneous eccentricities e'.)

Numerically, the above has been verified for large values of inelastic demand and all systems produced similar results. For example, for a system with period of 0.1 seconds, (e/r)=0.3, Ω=0.5, one element yielding at 28.8 ksi and the other at 36 ksi, 0.005 strain hardening, 2% damping, excited by the first 15 seconds of the N-S component of the 1940 El Centro record (scaled arbitrarily to produce excessively large displacement), we obtained the following displacement:

Case 1:	d=50	(e=30)	r=100	D=0.5
Case 2:	d=100	(e=60)	r=200	D=0.5

Max. Response: (both systems)	First element: 1.429 (δ_y=0.096)	Second element: 4.324 (δ_y=0.12)

Figure 3.6: Example of Geometric Independence

1) Initially symmetric systems with following properties:

$\omega_x^2 = 800$ $\omega_\theta^2 = 400$ $(e/r)=0$

A) Two-element system:

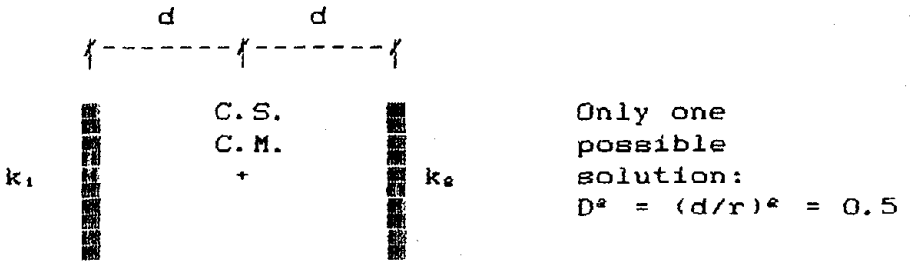

B) Four-element systems:

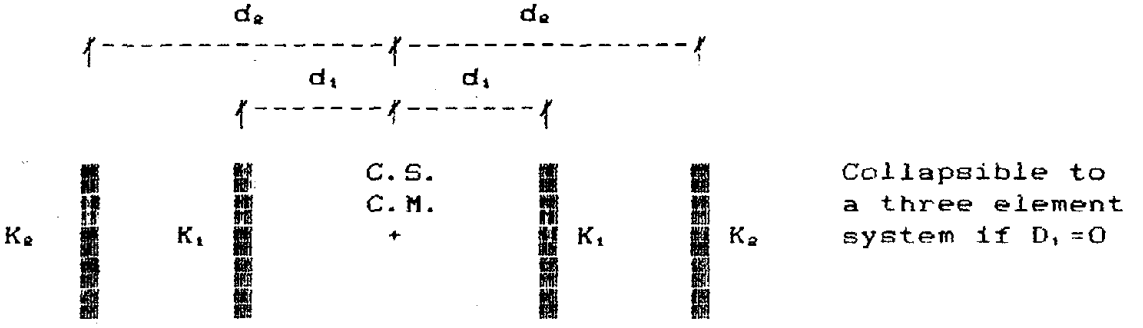

The effect of parametric variations on D_1 and D_2 is plotted in part b of this Figure.

2) Generally eccentric two-element system with following properties:

m=10 (to express stiffnesses in numbers instead of ratios K/M)
$\omega_x^2 = 400$, $\omega_\theta^2 = 43.2$ $(e/r)=0.3$

If the center of mass is not within the resisting element, but lies on the outside of both element:

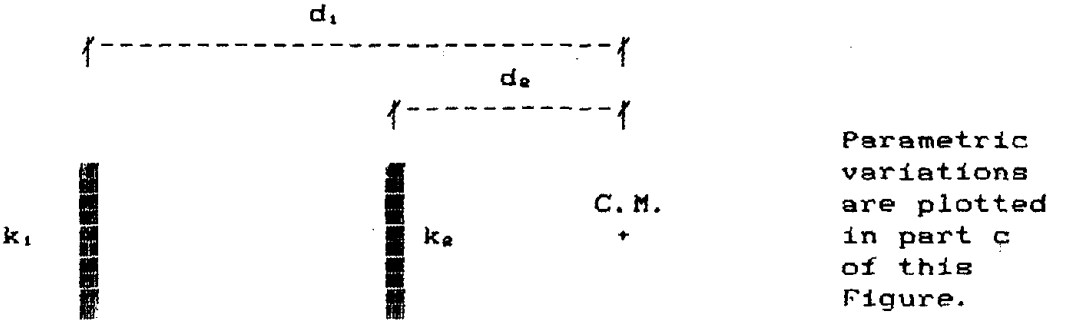

Figure 3.7a Geometric Dependence Examples

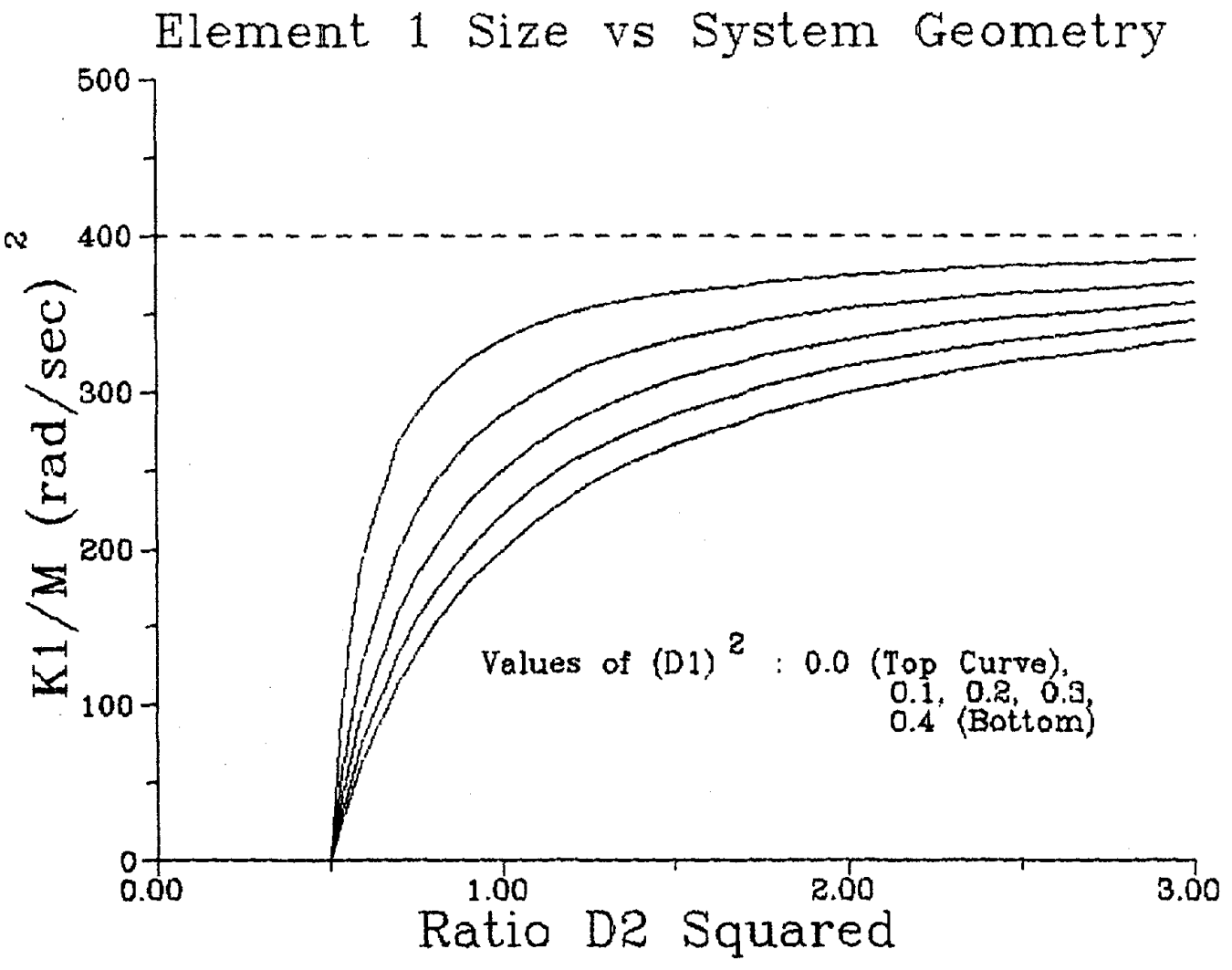

Figure 3.7b Stiffness of Interior Elements in Four Element System as Affected by the System Geometry

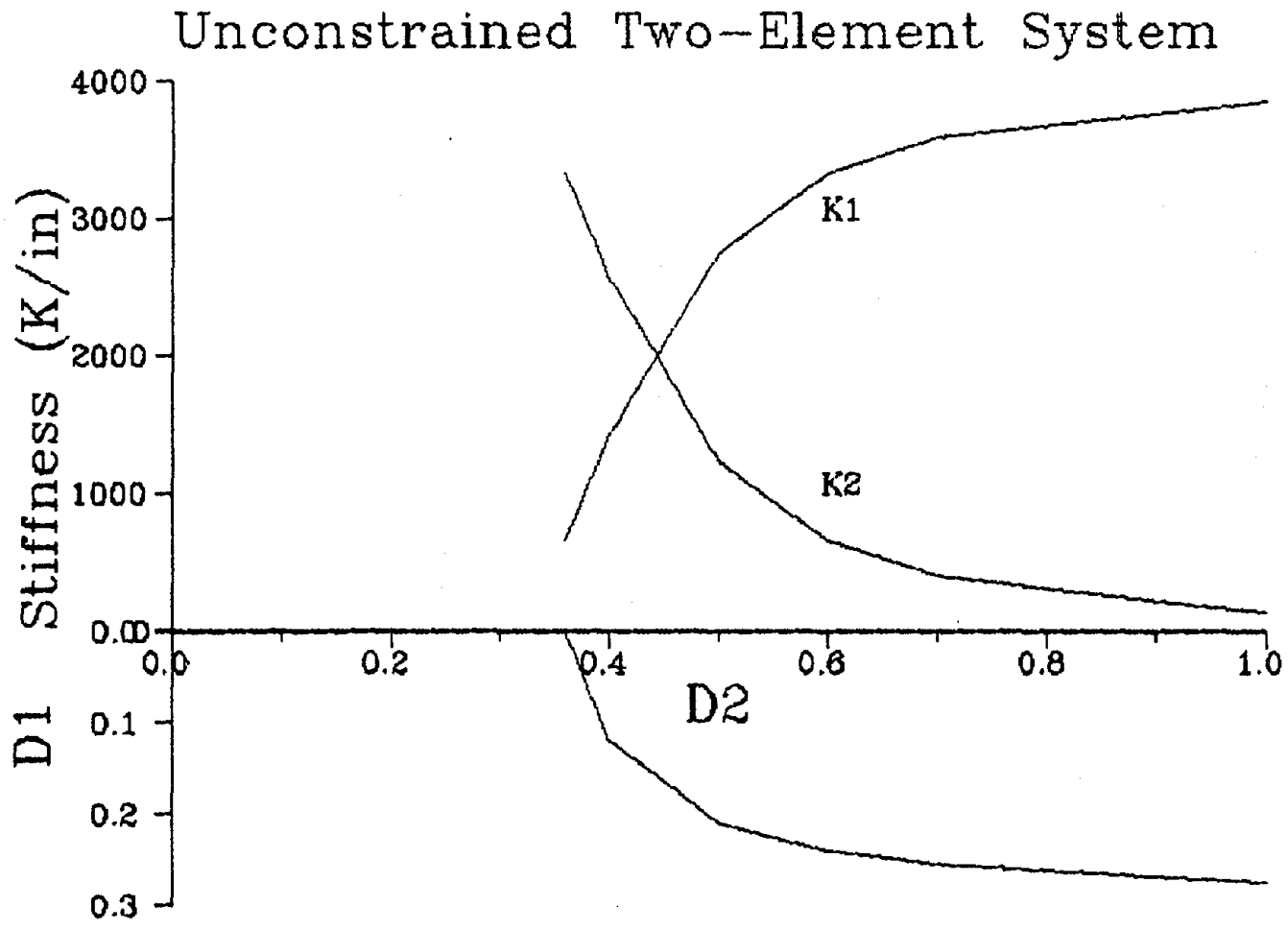

Figure 3.7c Stiffness and Geometric Dependance for an Uncontrained Two Element System with Center of Mass Lying Outside Both Resisting Elements

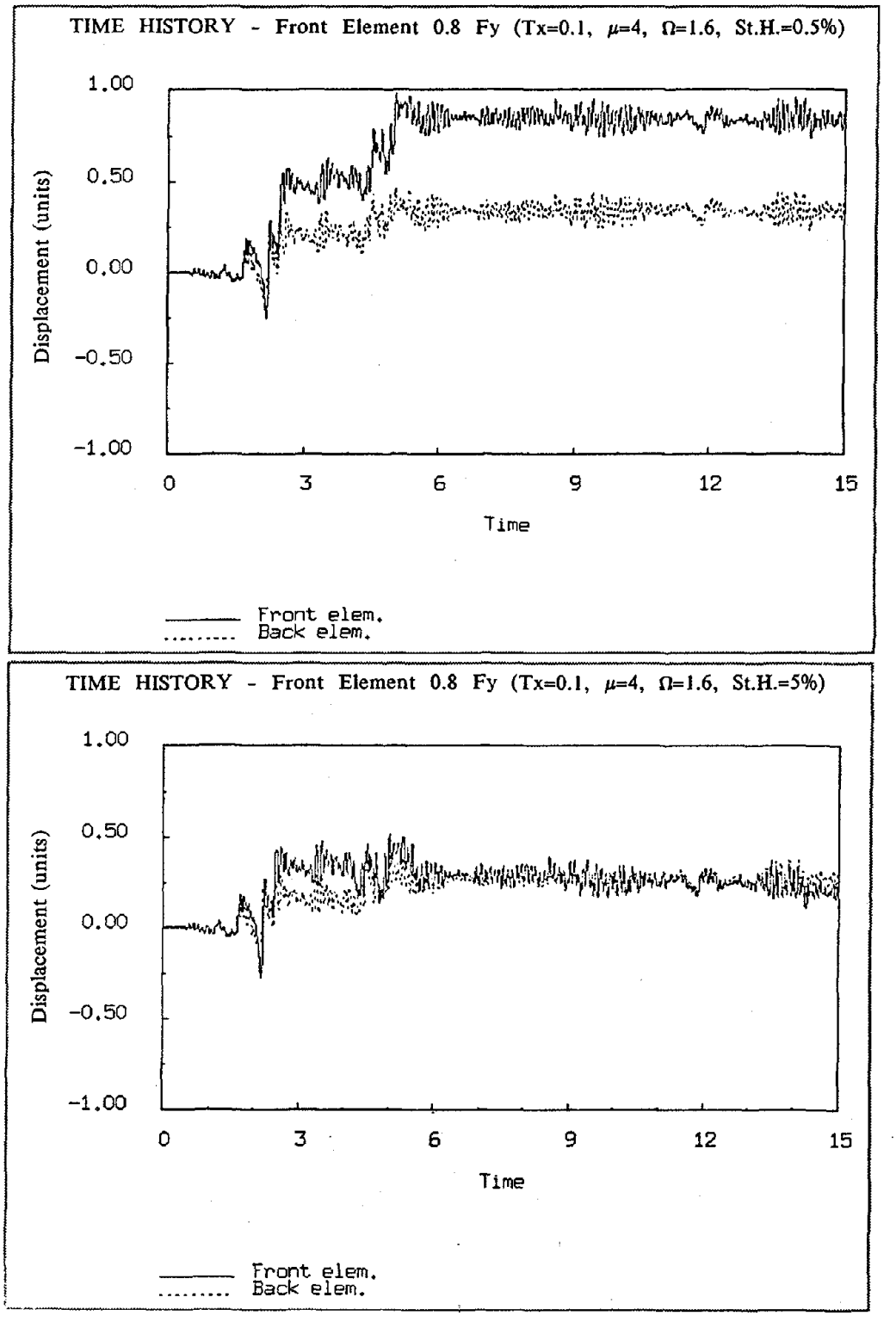

Figure 3.8 Investigation of the Effect of Strain Hardening on an Initially Symmetric System (Case 0.8 Fy and Fy - Yield Displacement of Front Element = 0.096 units, Back Element = 0.12 units)

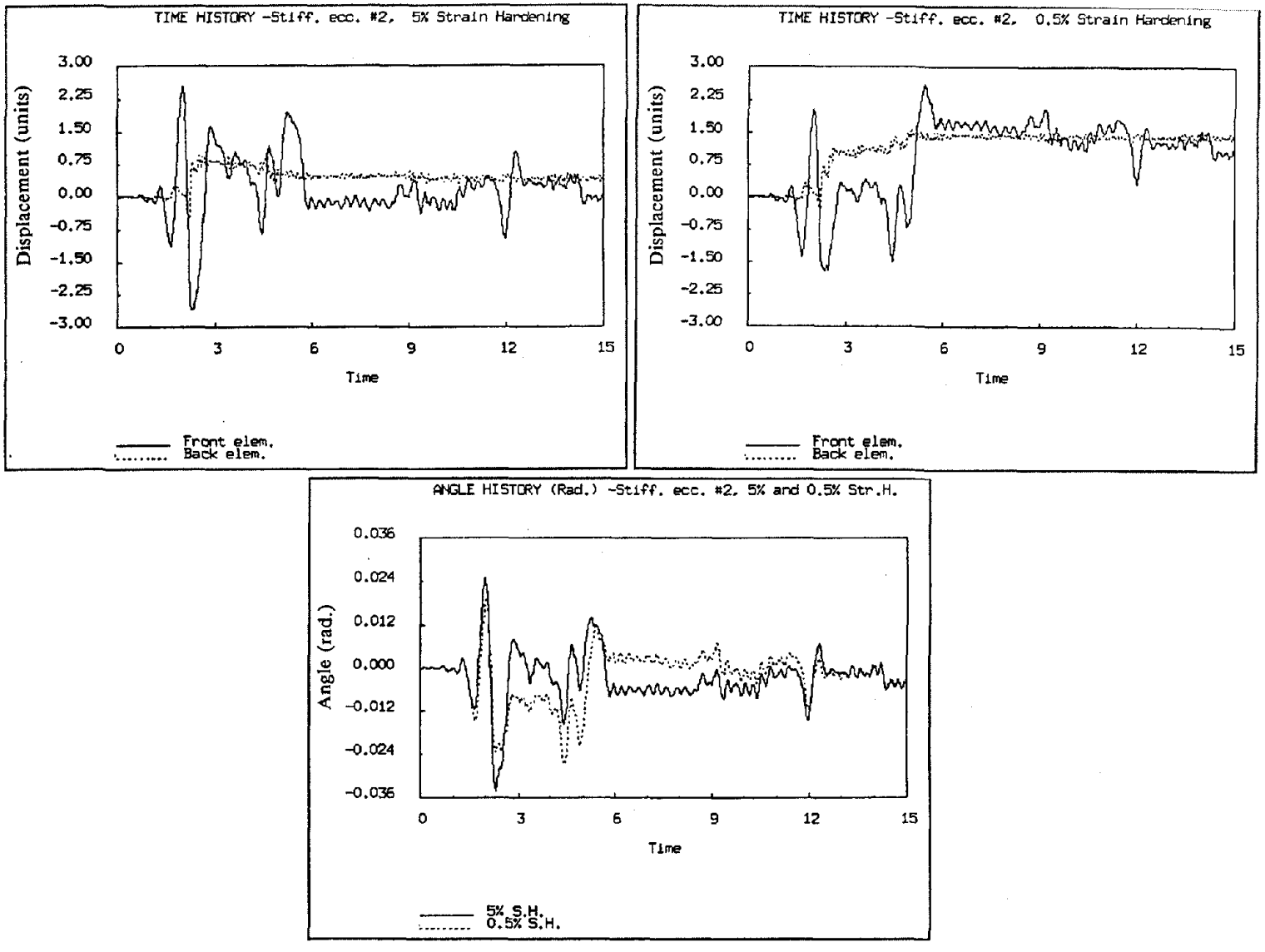

Figure 3.9a Illustration of a Case of Initially Eccentric System where an Increase in Strain Hardening Increases the Response (Yield Displacement = 0.12 units)

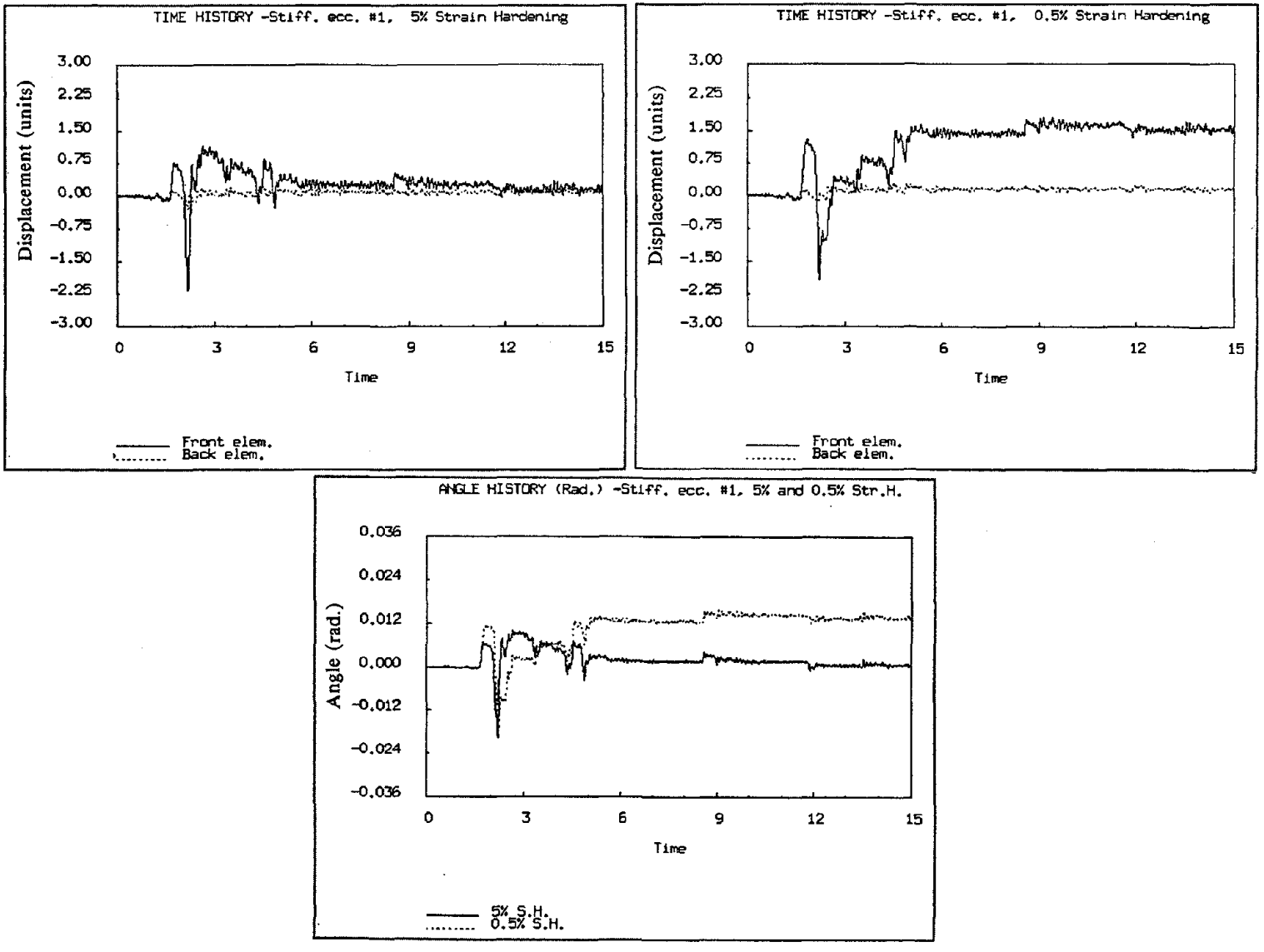

Figure 3.9b Illustration of a Case of Initially Eccentric System where an Increase in Strain Hardening Decreases the Response (Yield Displacement = 0.12 units)

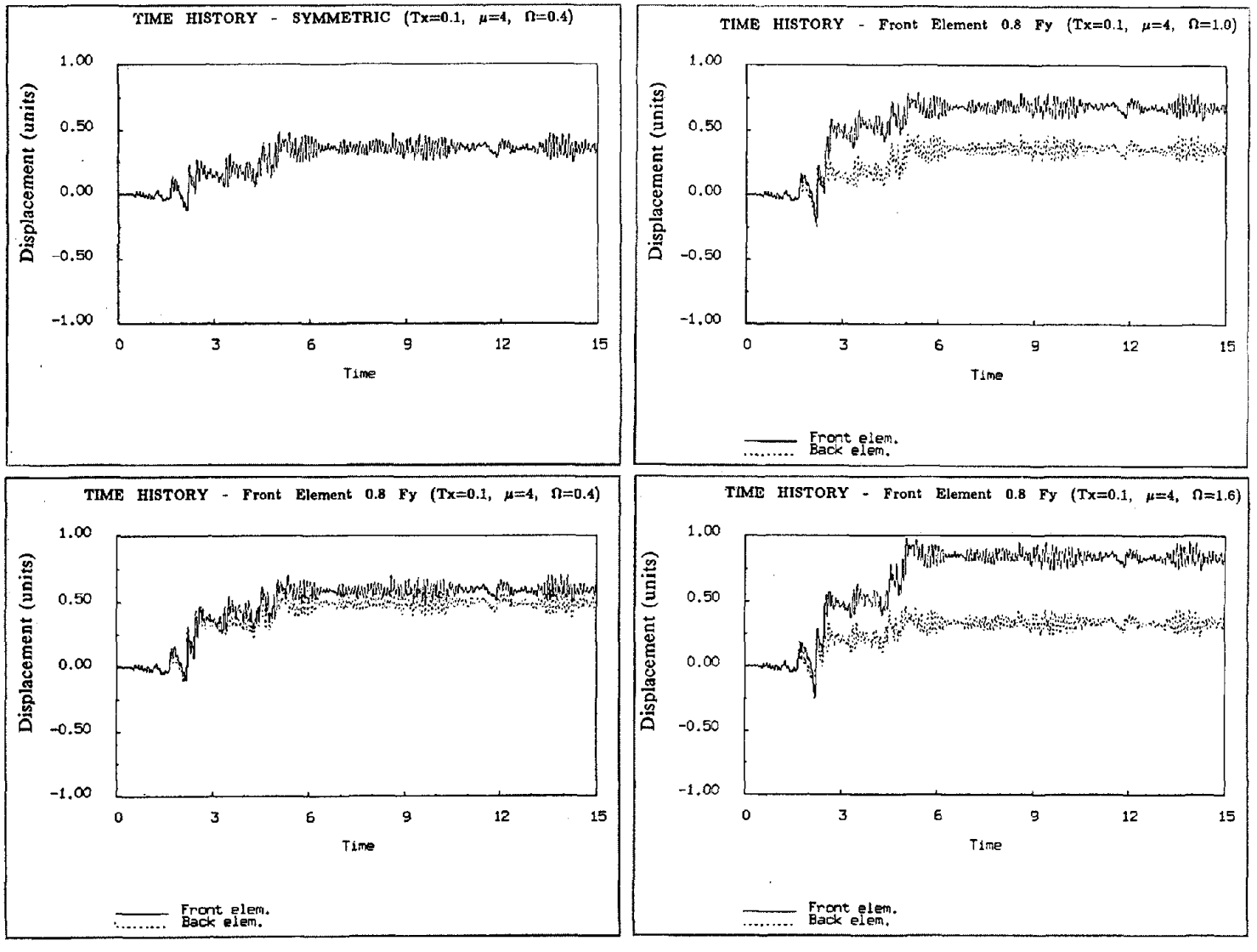

Figure 3.10a Effect of Change in Rotational Inertia on the Response of an Initially Symmetric System (Case 0.8 Fy and Fy) - High Omega Values Correspond to Low Rotational Inertia (Yield Displacement of Front Element = 0.096 units, Back Element = 0.12 units)

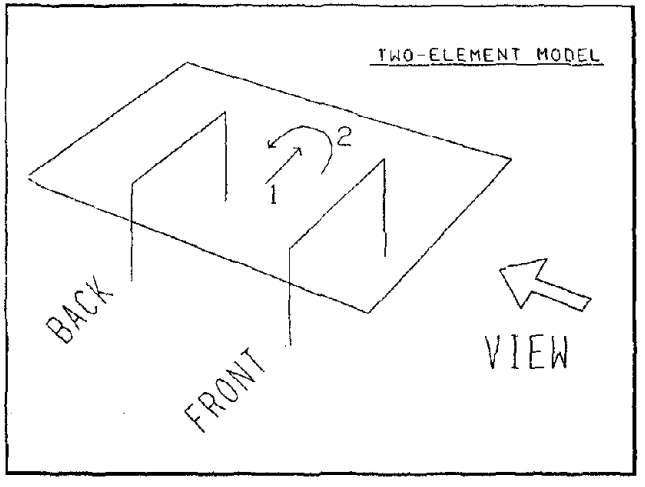

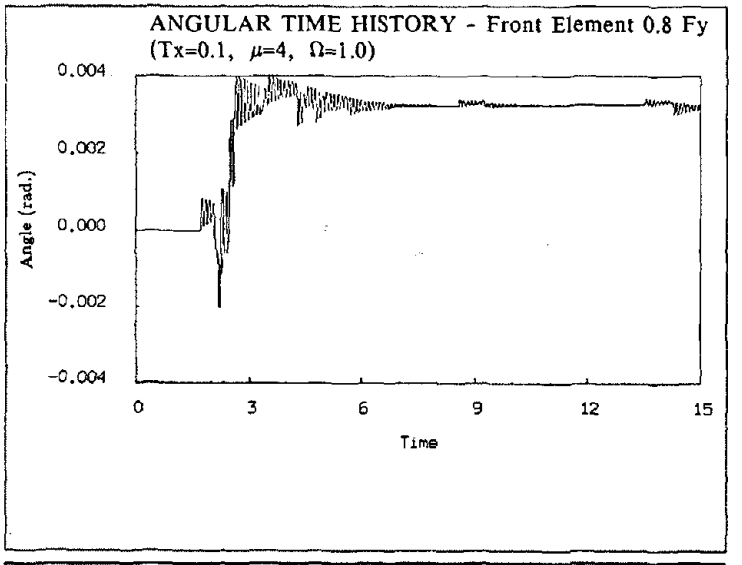

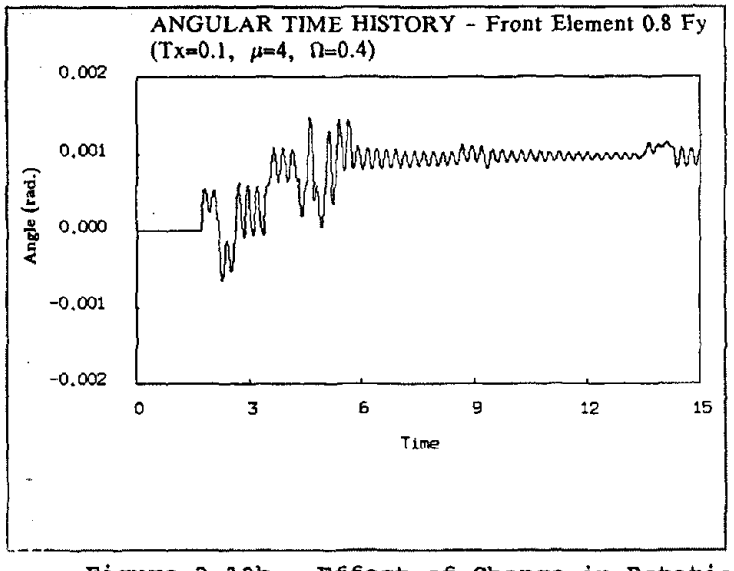

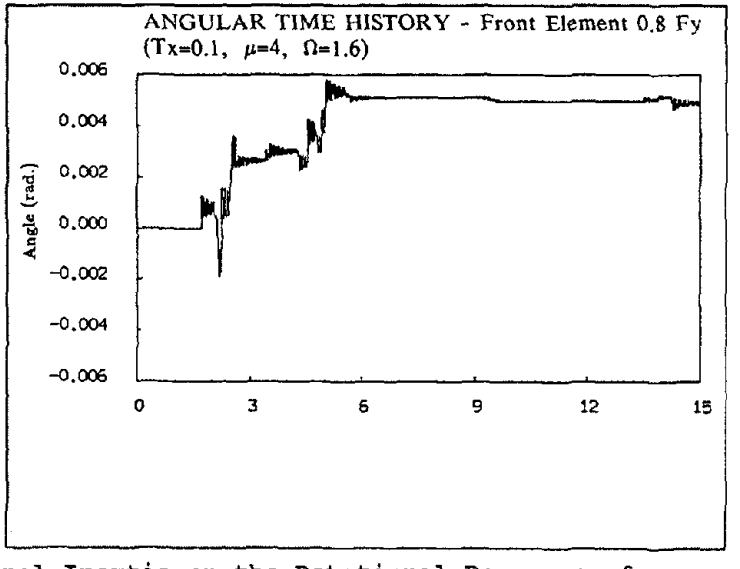

Figure 3.10b Effect of Change in Rotational Inertia on the Rotational Response of an Initially Symmetric System (Case 0.8 Fy and Fy) - High Omega Values Correspond to Low Rotational Inertia - All Plots at Different Scale - (Also Shown in Upper Left Corner, Schematic Representation of Two Element Model)

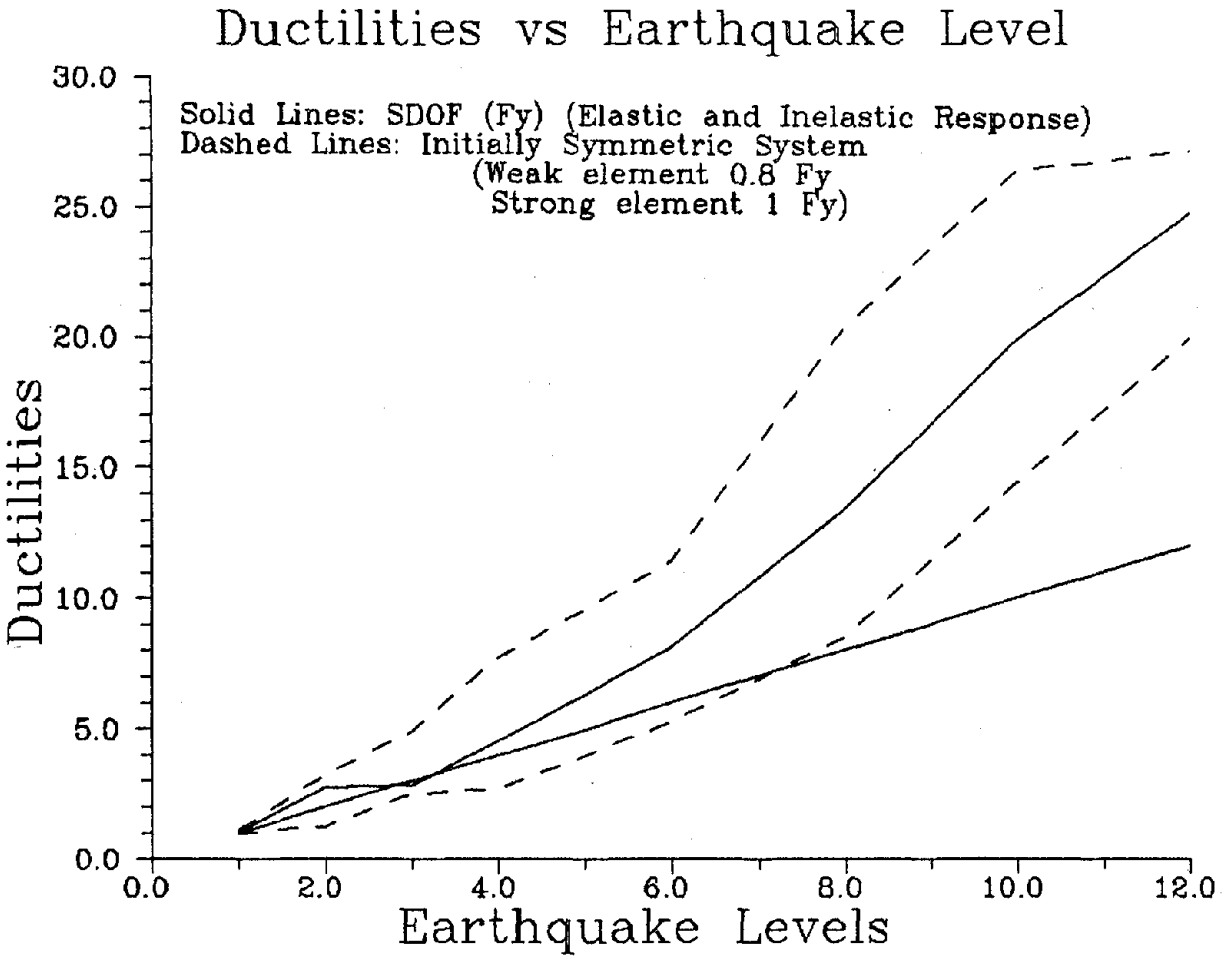

Figure 3.11 Effect of Various Earthquake Intensities on the Response of Initially Symmetric Systems - Maximum Displacement Ductility ratios

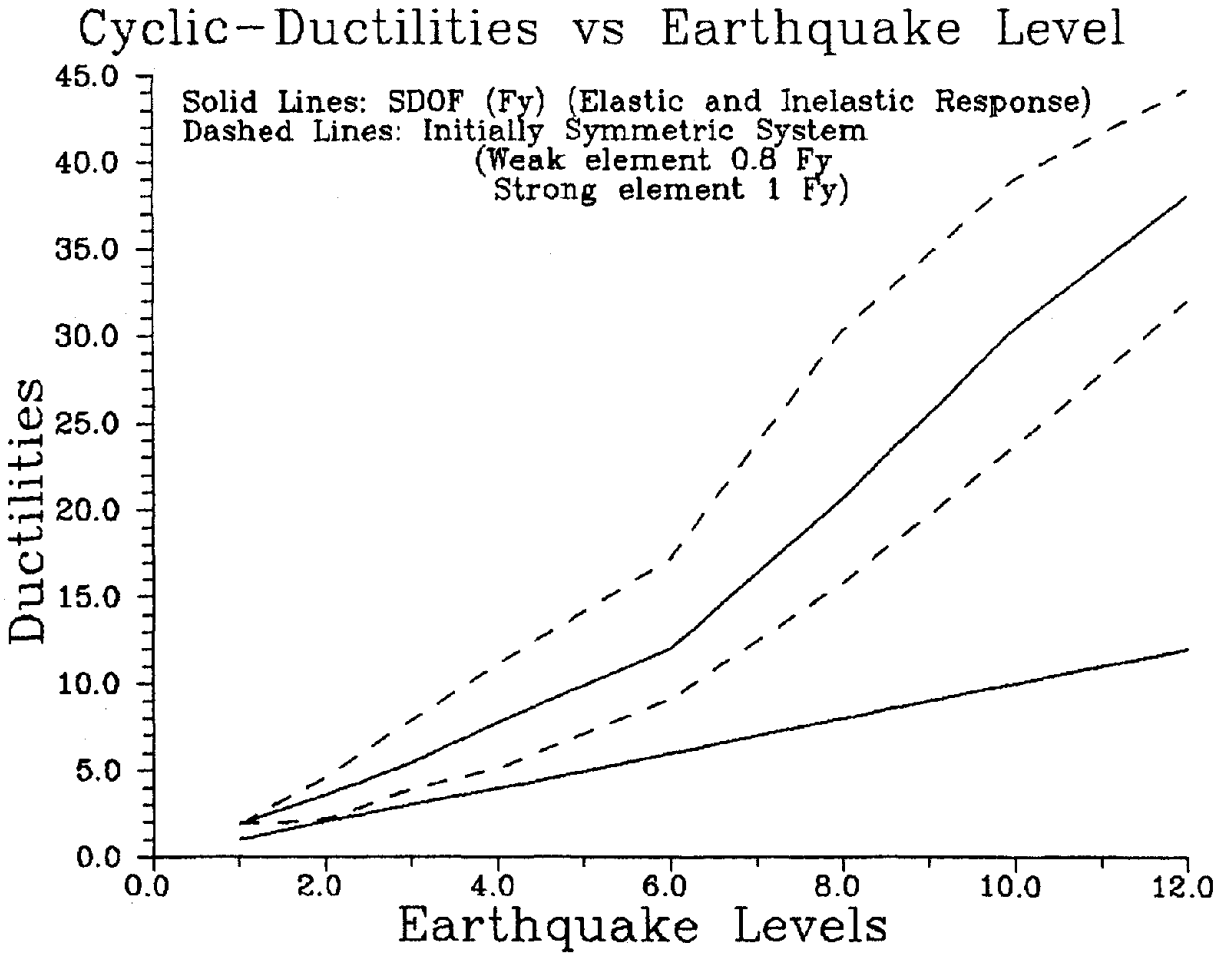

Figure 3.12 Effect of Various Earthquake Intensities on the Response of Initially Symmetric Systems - Cyclic Ductility ratios

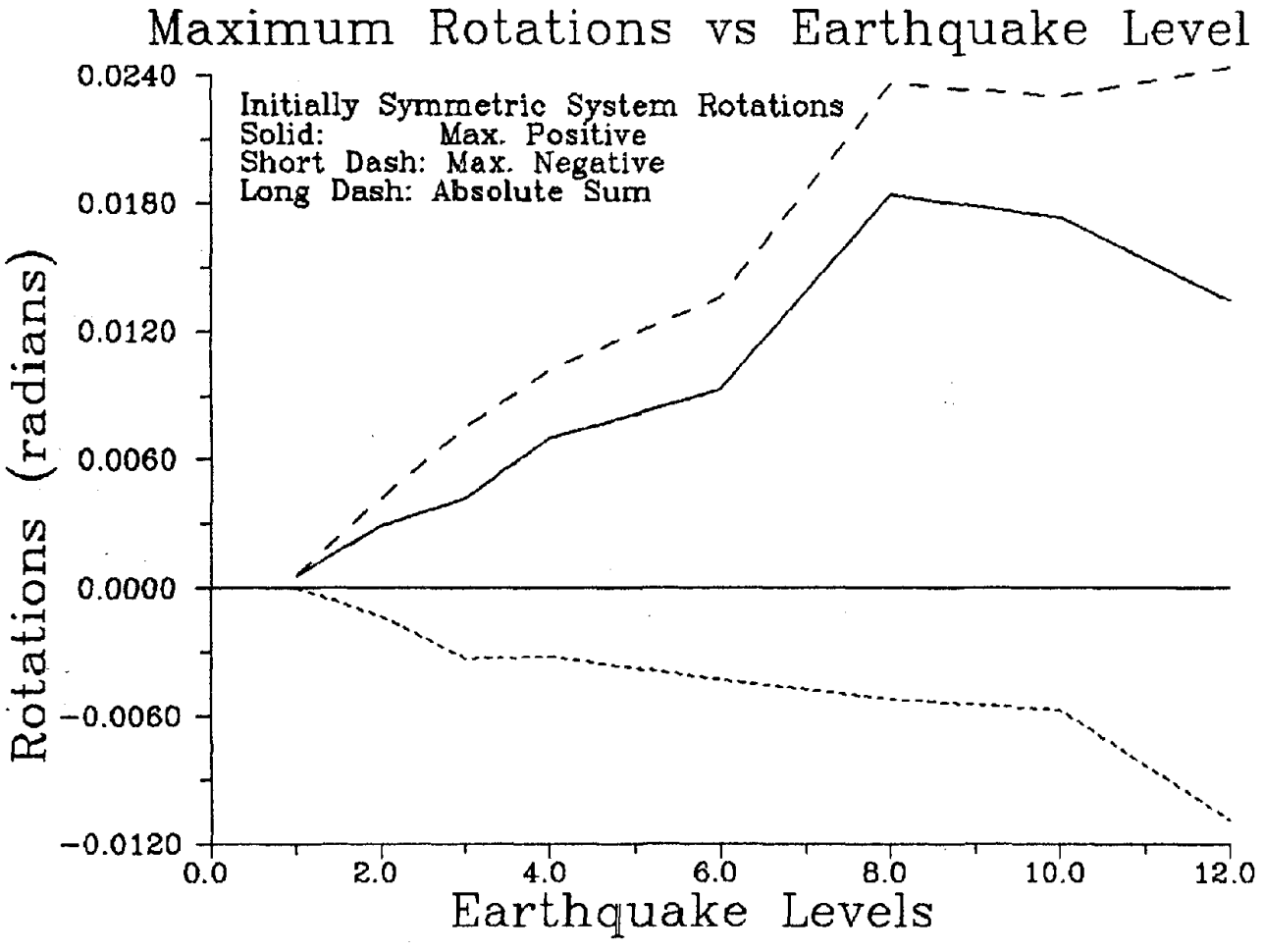

Figure 3.13 Effect of Various Earthquake Intensities on the Response of Initially Symmetric Systems - Maximum Rotations

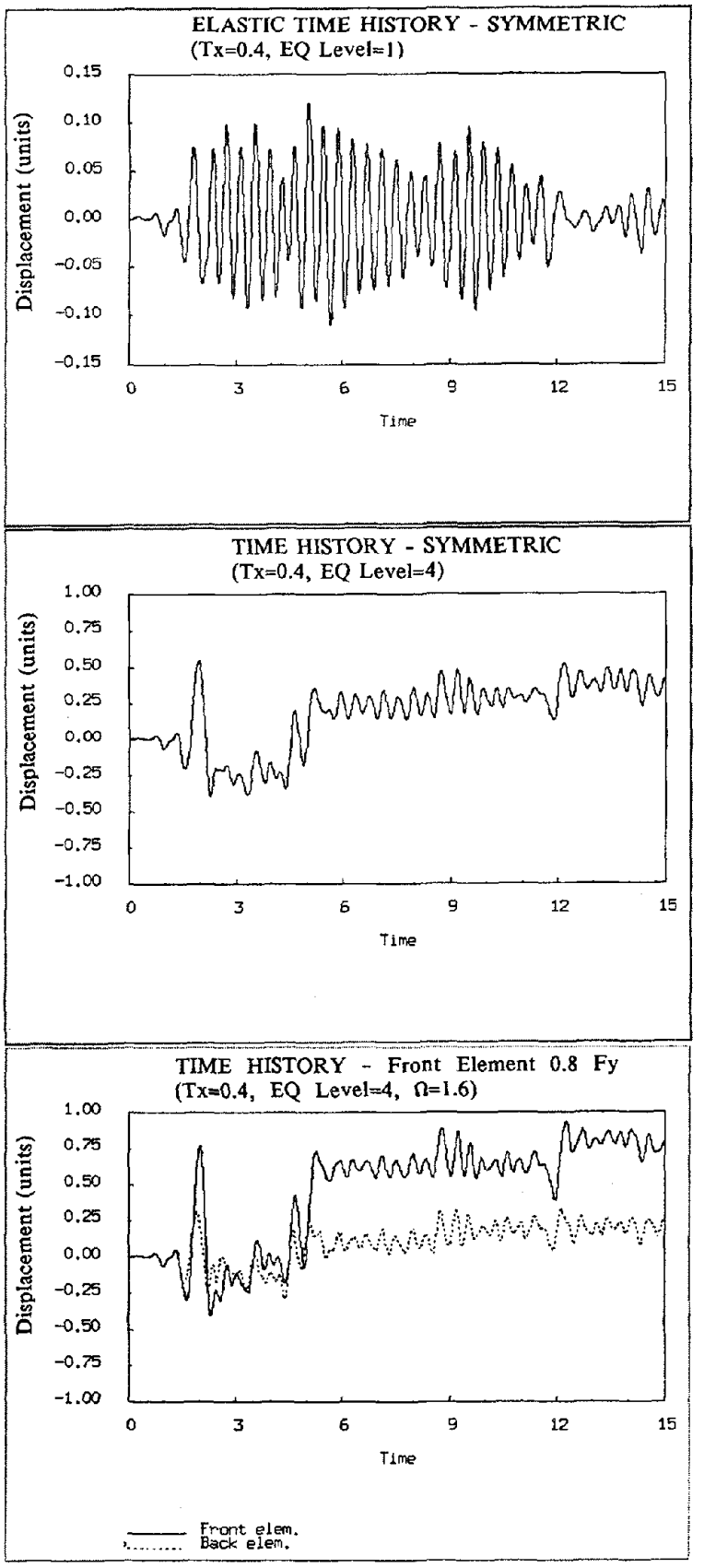

Figure 3.14a Comparison of Single Degree of Freedom System and Initially Symmetric System Time Histories for Various Earthquake Intensities (Part 1) - Plots at Different Scales (Yield Displacement of Front Element = 0.096 units, Back Element = 0.12 units, SDOF = 0.12 units)

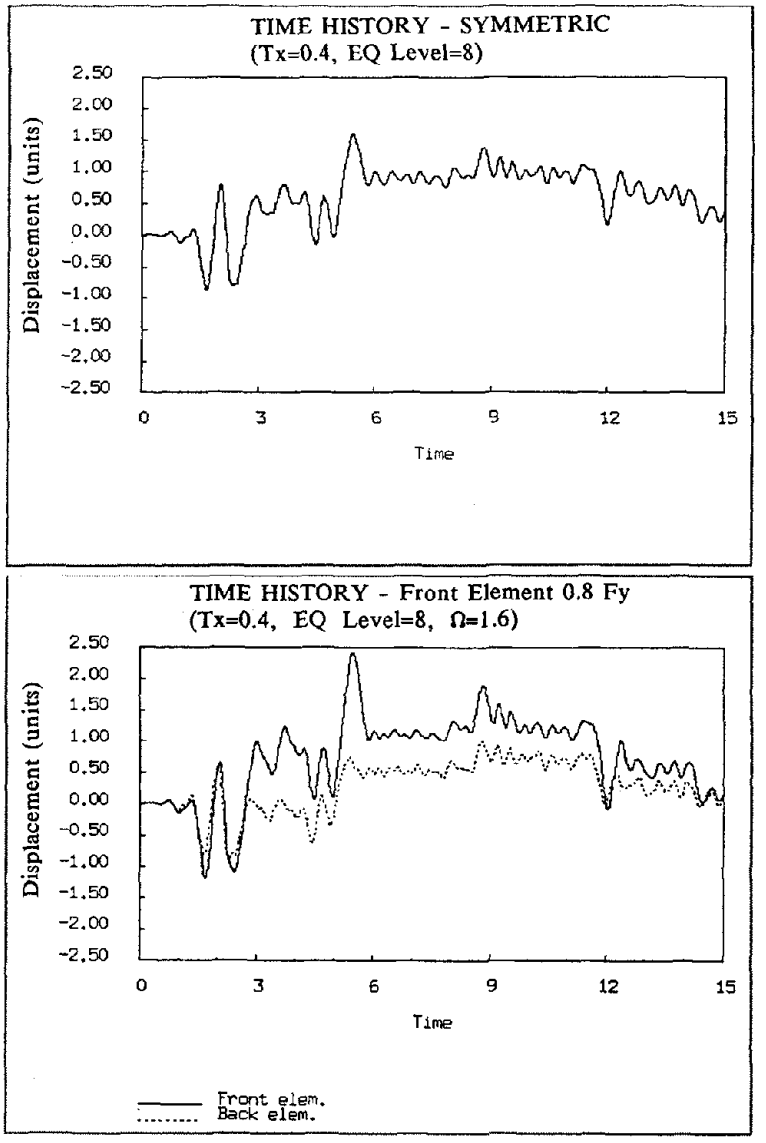

Figure 3.14b Comparison of Single Degree of Freedom System and Initially Symmetric System Time Histories for Various Earthquake Intensities (Part 2) (Yield Displacement of Front Element = 0.096 units, Back Element = 0.12 units, SDOF = 0.12 units)

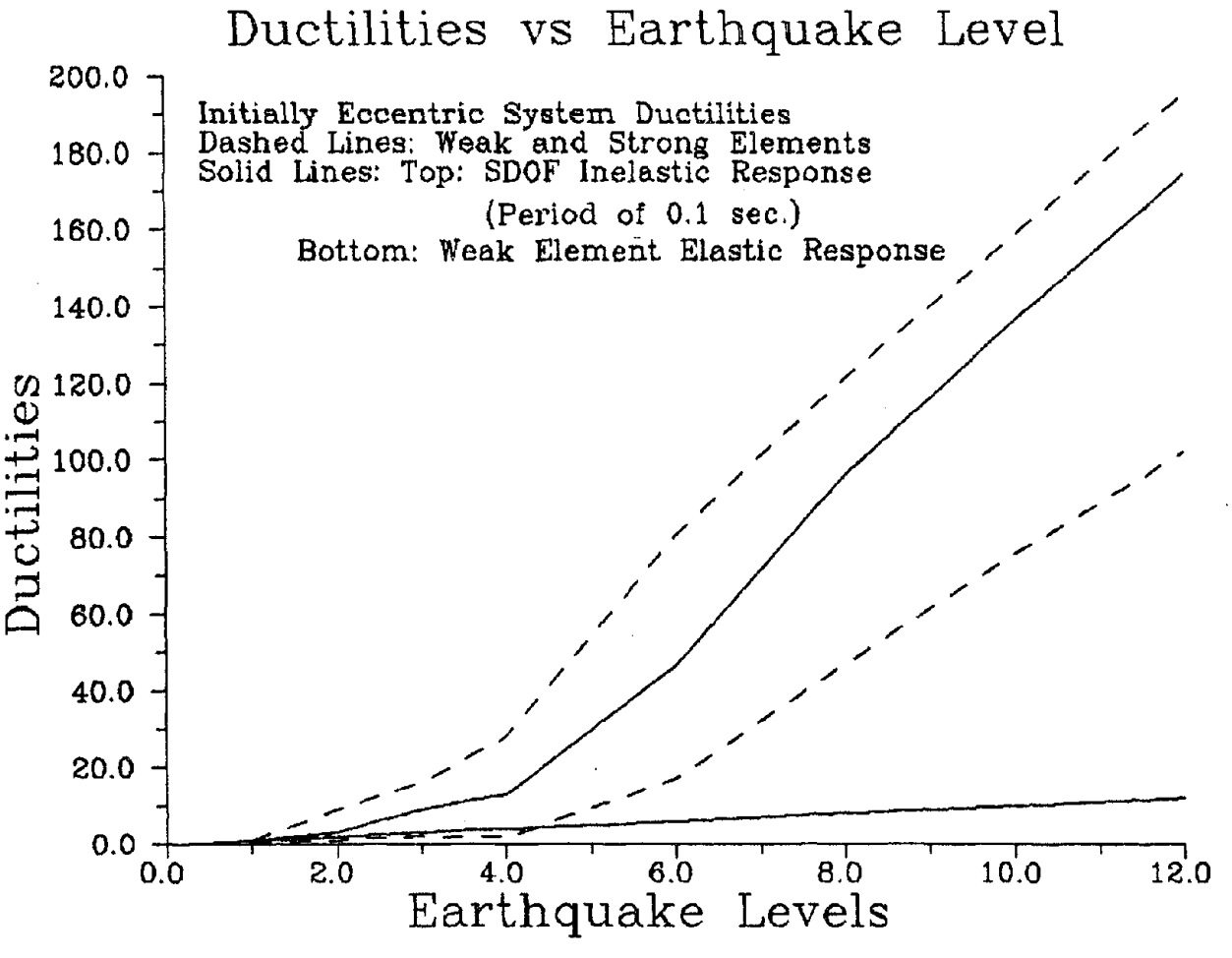

Figure 3.15 Effect of Various Earthquake Intensities on the Response of Initially Eccentric Systems - Maximum Displacement Ductility ratios

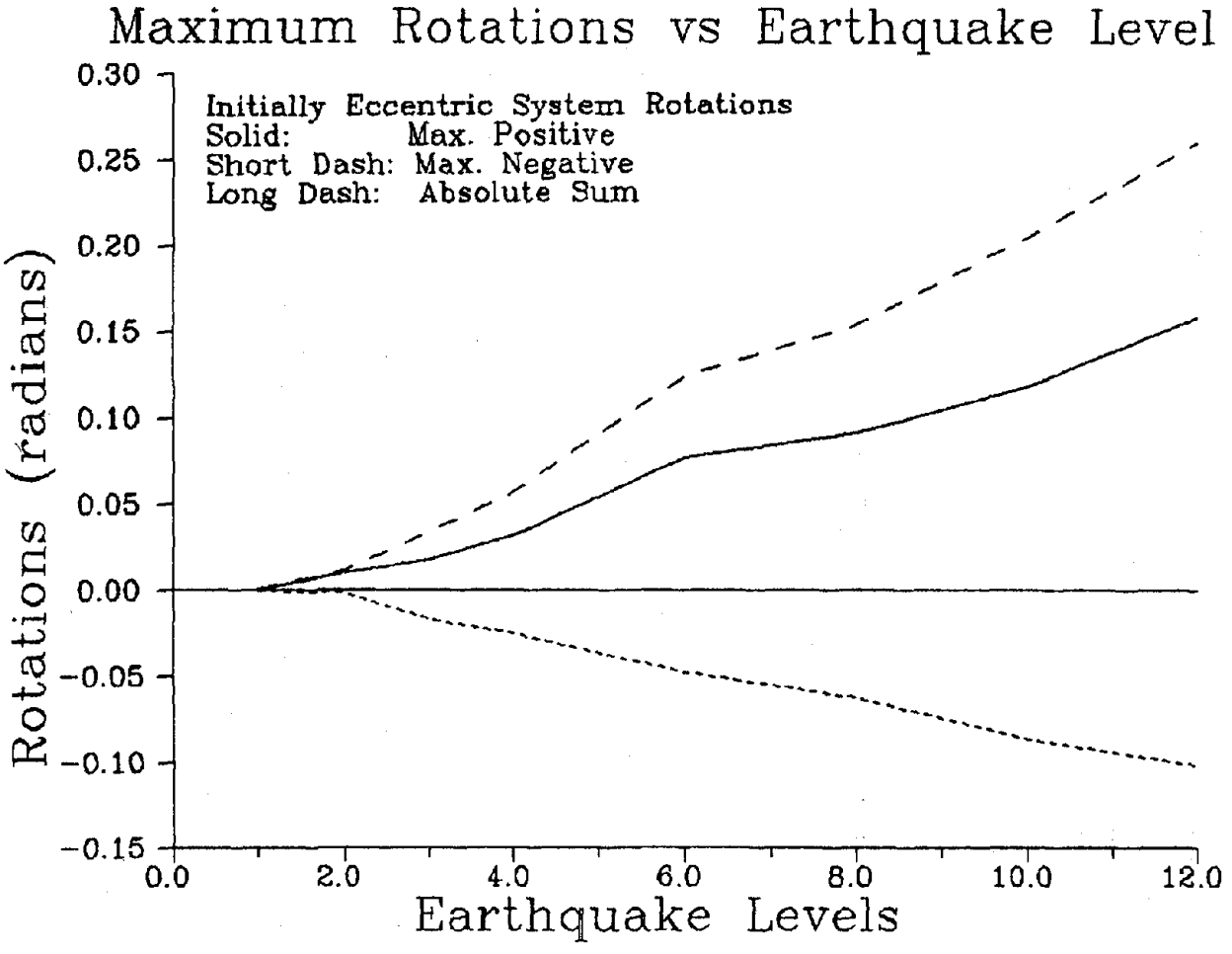

Figure 3.16 Effect of Various Earthquake Intensities on the Response of Initially Eccentric Systems - Maximum Rotations

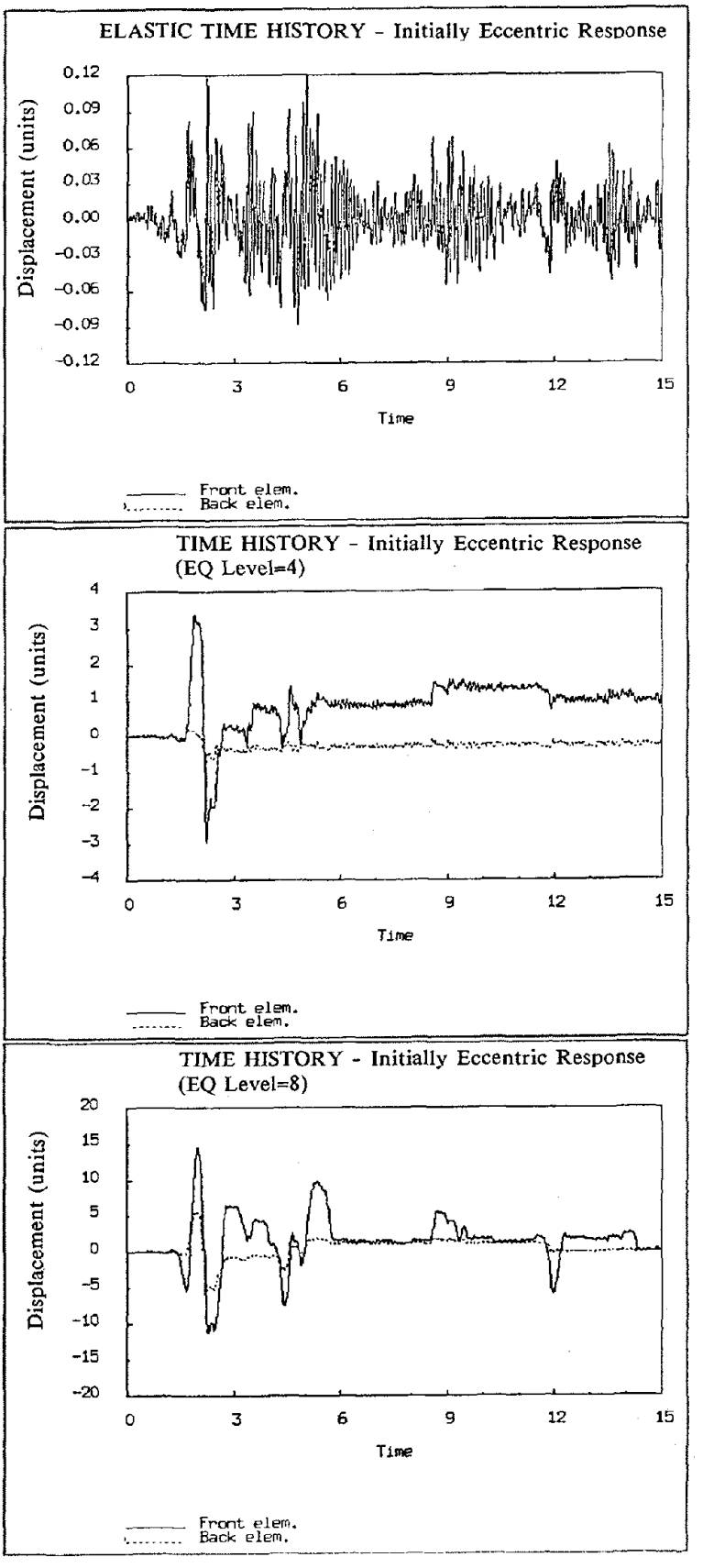

Figure 3.17 Time Histories of Element Response of Initially Eccentric System Various Earthquake Intensities. Top: Excitation Level of One (Elastic at the Onset of Yield); Middle: Excitation Level of Four; Bottom: Excitation Level of Eight - All Plots at Different Scale (Yield Displacement = 0.12 units)

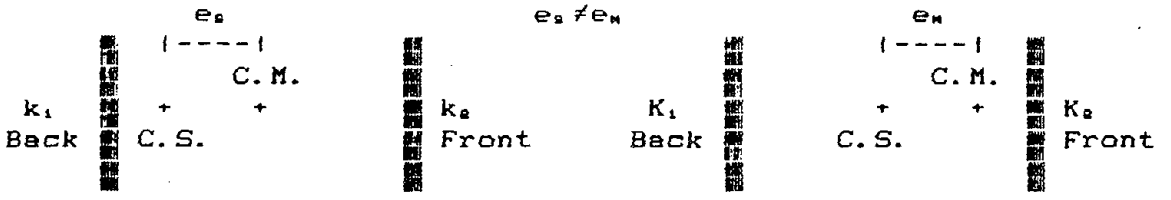

Stiffness Eccentric Mass Eccentric

Case 1: T_x=0.1s, Ω=1.5, (e/r)=0.3, 2% damping, 5% str.hrd.

Response (*)	Back Element	C.M.	Front Element
Elastic			
Mass Ecc.	0.2049	0.3070	0.3744
	-0.1486	-0.2145	-0.2730
Stiff. Ecc.	0.2204	0.3070	0.3935
	-0.1564	-0.2145	-0.2895
Inelastic			
Mass Ecc.	0.2393	0.7010	1.0465
	-0.1967	-1.1939	-1.8795
Stiff. Ecc.	0.2116	0.6550	1.1531
	-0.2941	-1.2117	-2.1501

	Maximum rθ	Minimum rθ
Elastic		
Mass.Ecc.	0.058	-0.051
Stiff. Ecc.	0.058	-0.051
Inelastic		
Mass Ecc.	0.303	-0.602
Stiff. Ecc.	0.340	-0.640

Case 2: T_x=0.1s, Ω=0.5, (e/r)=0.3, 2% damping, 5% str.hrd.

Response (*)	Back Element	C.M.	Front Element
Elastic			
Mass Ecc.	0.424	0.481	0.593
	-0.458	-0.397	-0.501
Stiff. Ecc.	0.282	0.481	1.065
	-0.234	-0.397	-0.916
Inelastic			
Mass Ecc.	1.463	1.079	1.237
	-0.366	-1.712	-1.962
Stiff. Ecc.	0.978	1.289	2.541
	-0.512	-1.238	-2.608

	Maximum rθ	Minimum rθ
Elastic		
Mass.Ecc.	1.22	-1.04
Stiff. Ecc.	1.22	-1.04
Inelastic		
Mass Ecc.	1.58	-3.55
Stiff. Ecc.	2.51	-3.41

(*) Positive and Negative Values from Response Envelope

Figure 3.18 Mass vs Stiffness Eccentricity

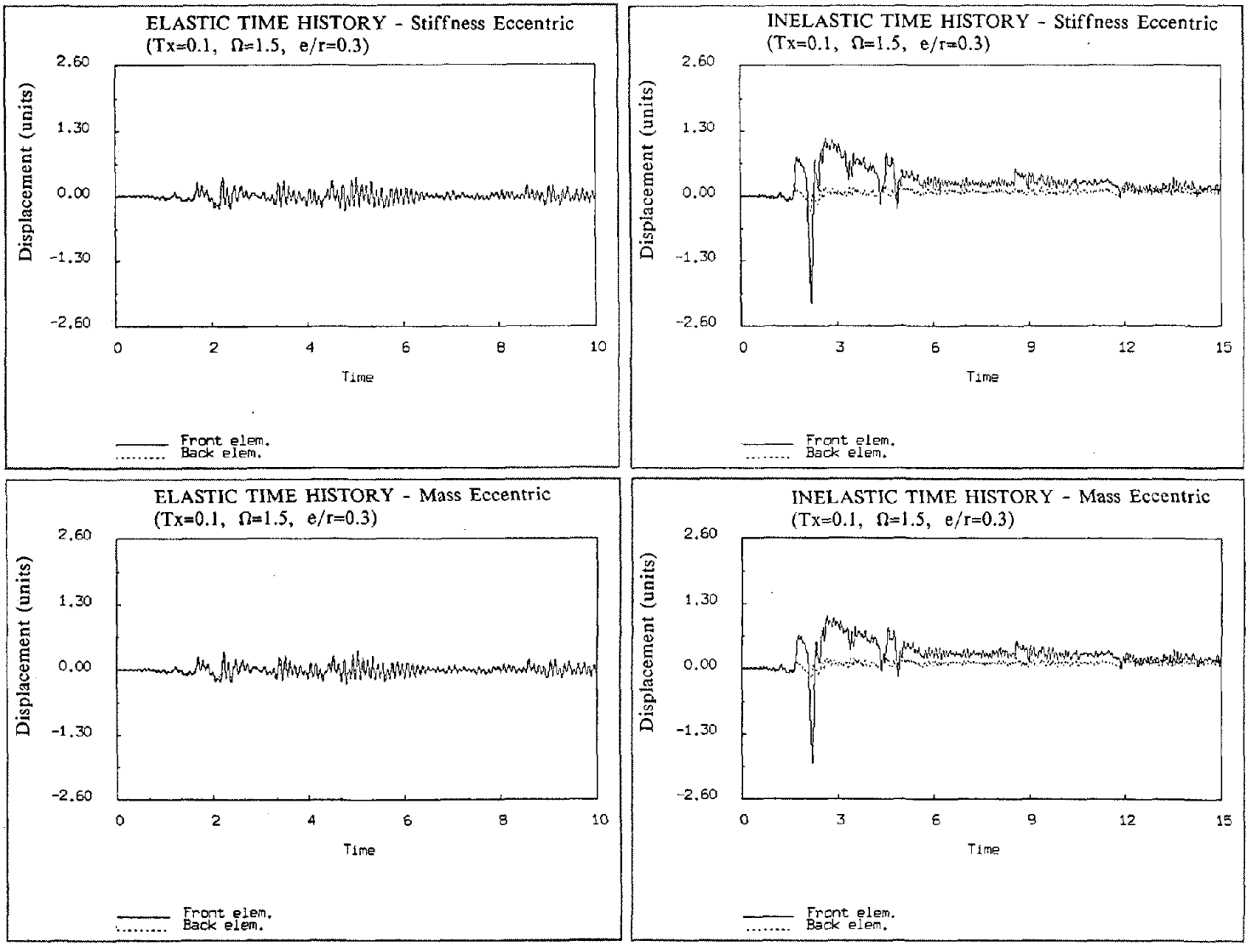

Figure 3.19a Mass Eccentric (bottom) vs Stiffness (top) Eccentric Systems (Large Omega Case) - Elastic Response (right) and Inelastic Response (left) (Yield Displacement = 0.12 units)

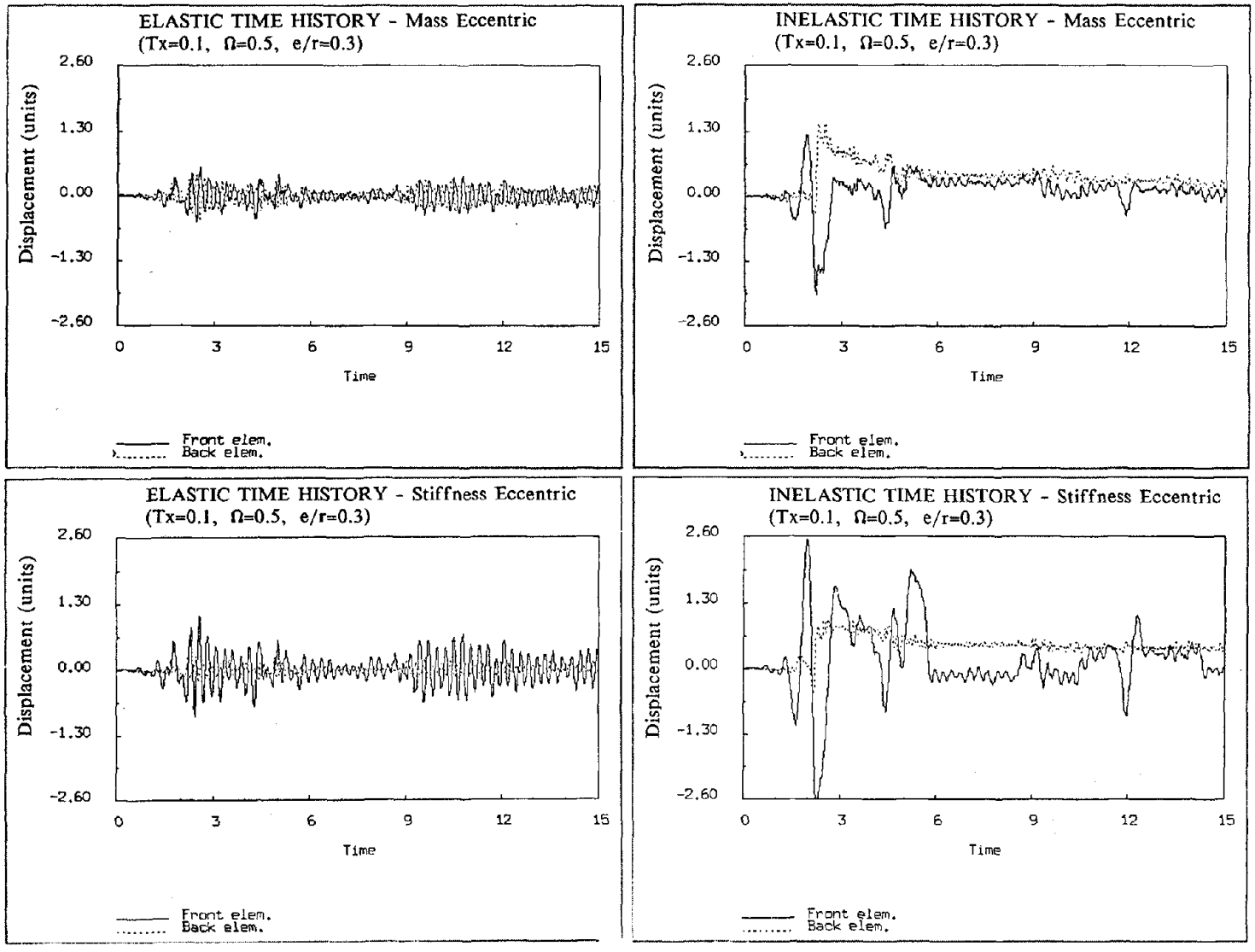

Figure 3.19b Mass Eccentric (top) vs Stiffness (bottom) Eccentric Systems (Small Omega Case) - Elastic Response (right) and Inelastic Response (left) (Yield Displacement = 0.12 units)

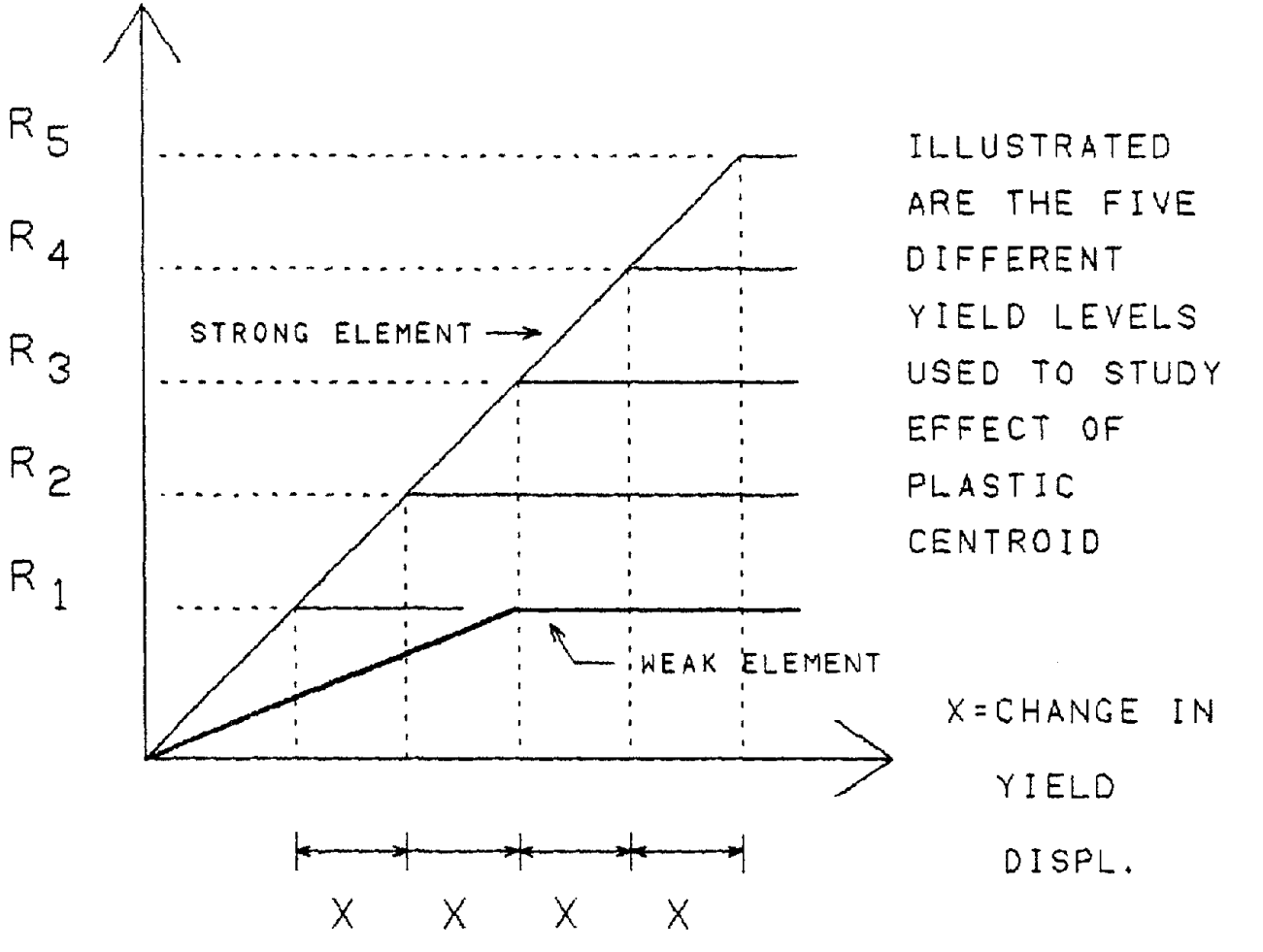

Figure 3.20 Inter-Element Relation Cases Studied for Initially Eccentric Systems

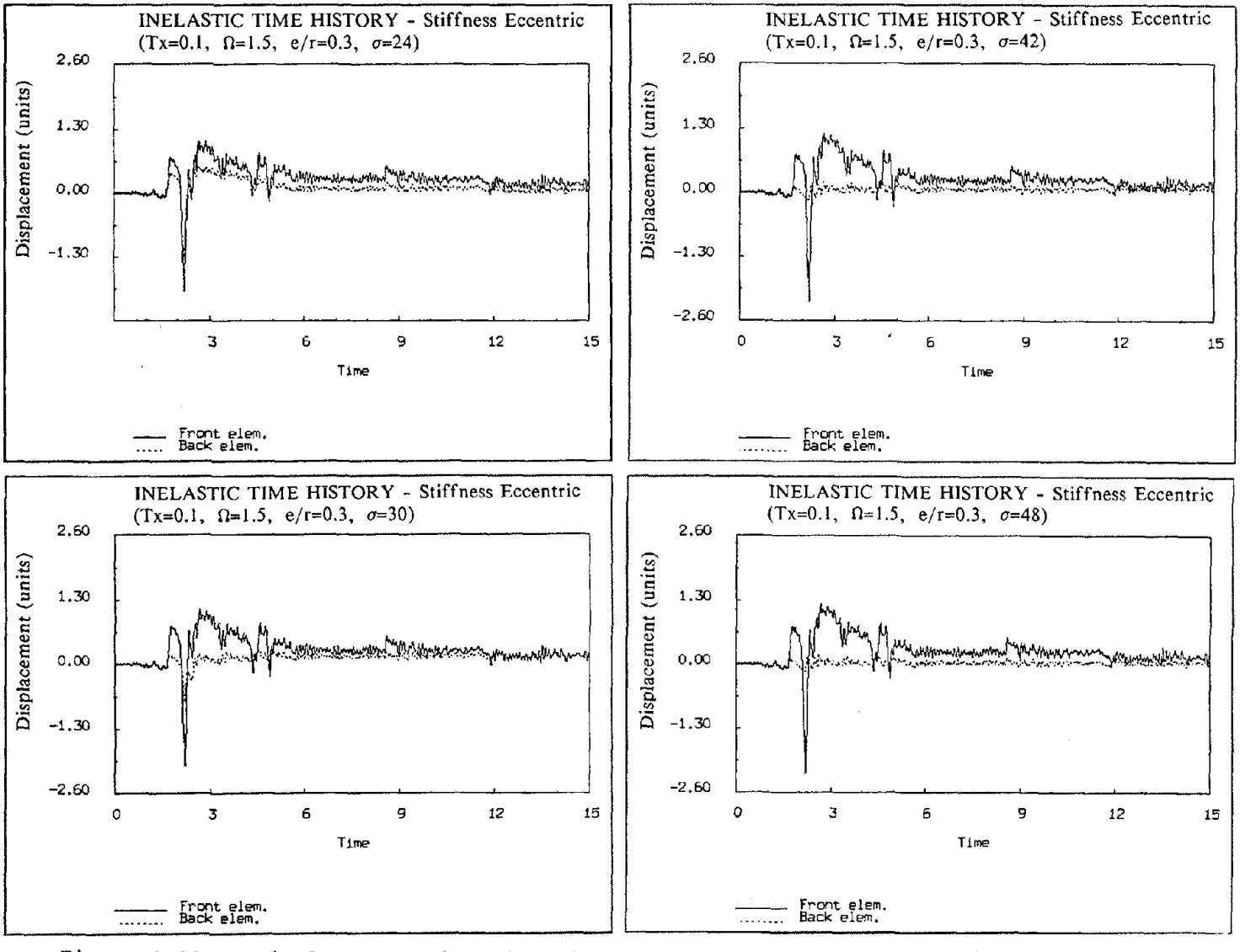

Figure 3.21a Displacement Time Histories for the Inter-Element Relation Cases Studied for Initially Eccentric Systems (Large Omega Case) - Also Refer to Table 3.2 (Yield Displacement = 0.12 units)

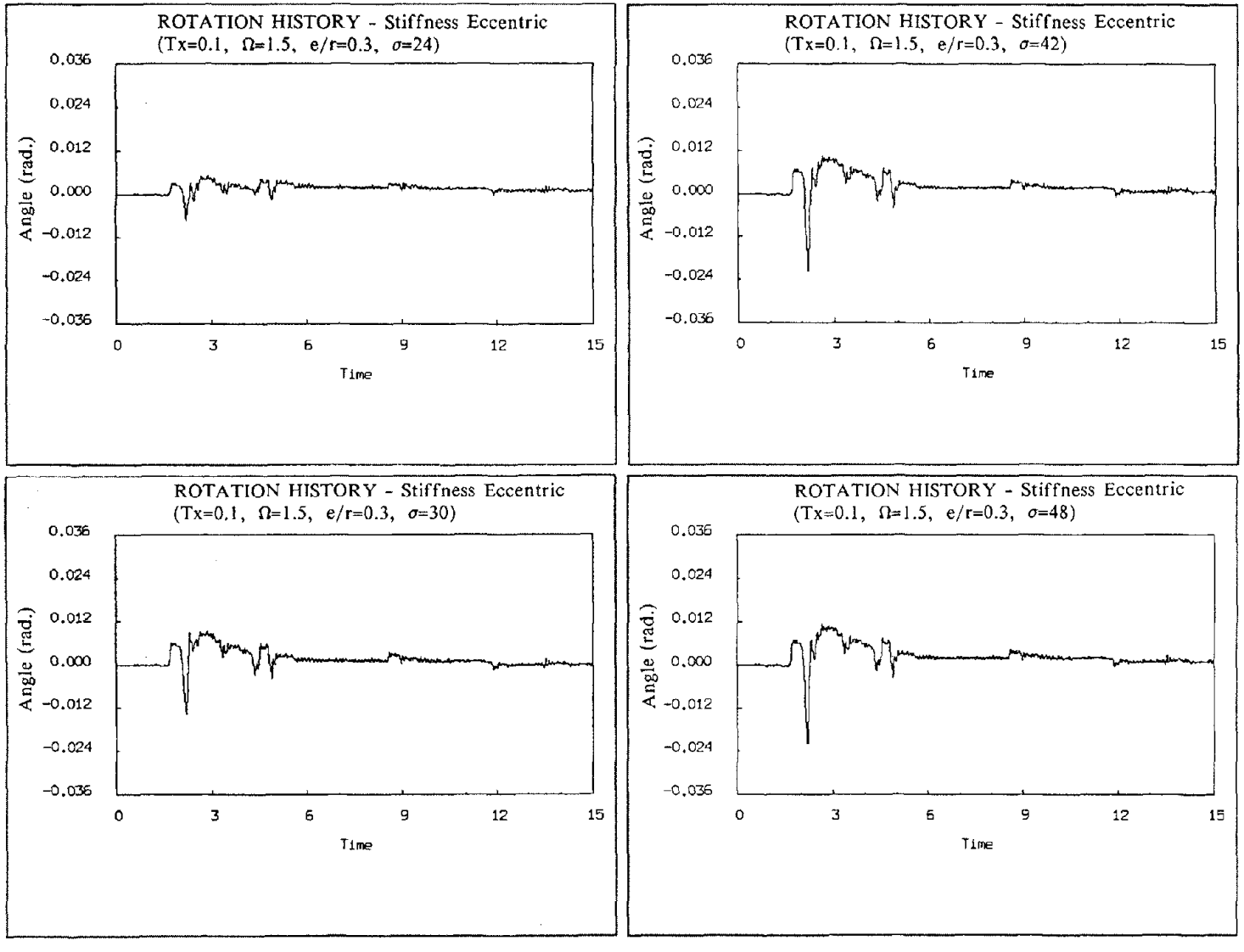

Figure 3.21b Rotation Time Histories for the Inter-Element Relation Cases Studied for Initially Eccentric Systems (Large Omega Case) - Also Refer to Table 3.2 (Yield Displacement = 0.12 units)

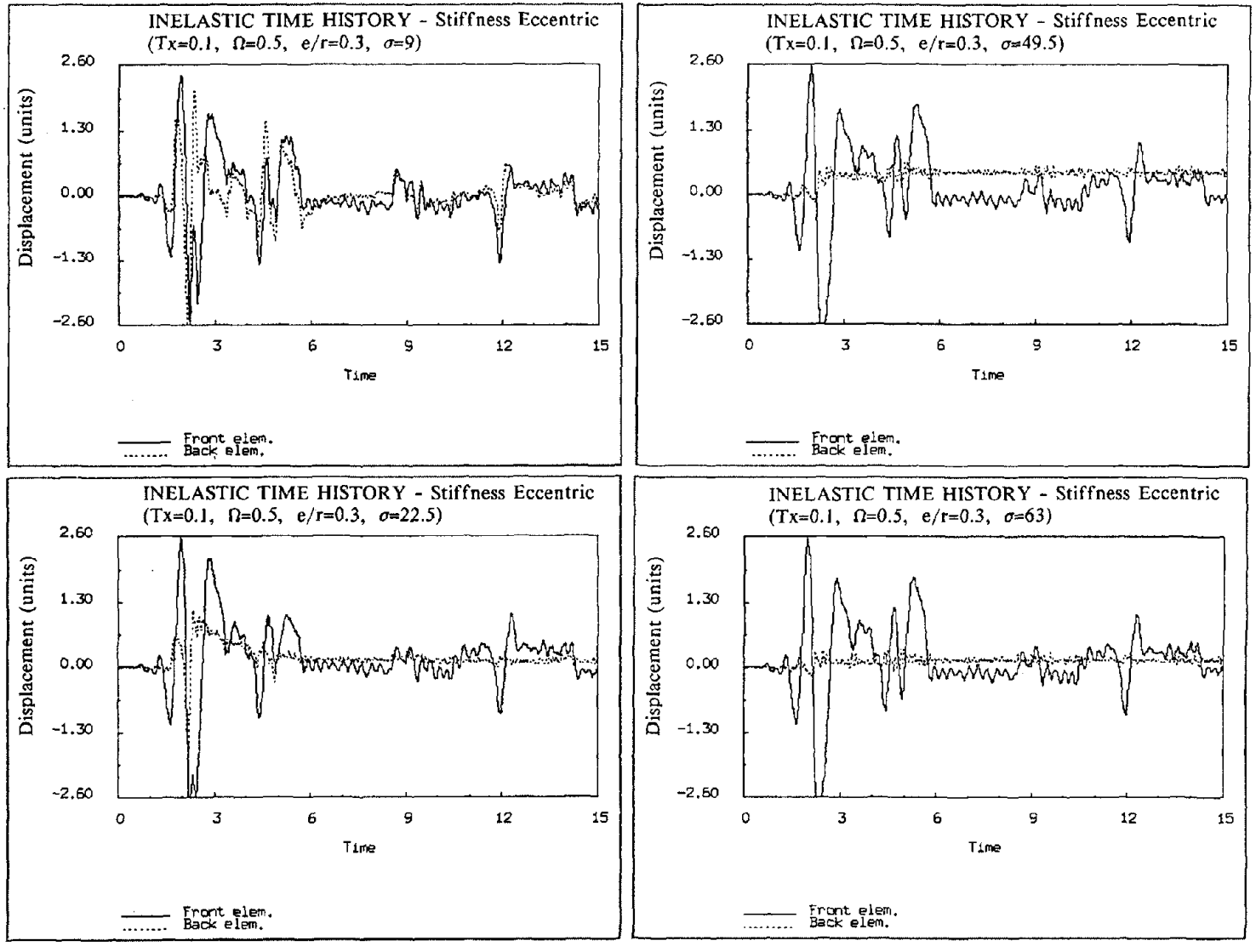

Figure 3.21c Displacement Time Histories for the Inter-Element Relation Cases Studied for Initially Eccentric Systems (Small Omega Case) - Also Refer to Table 3.2 (Yield Displacement = 0.12 units)

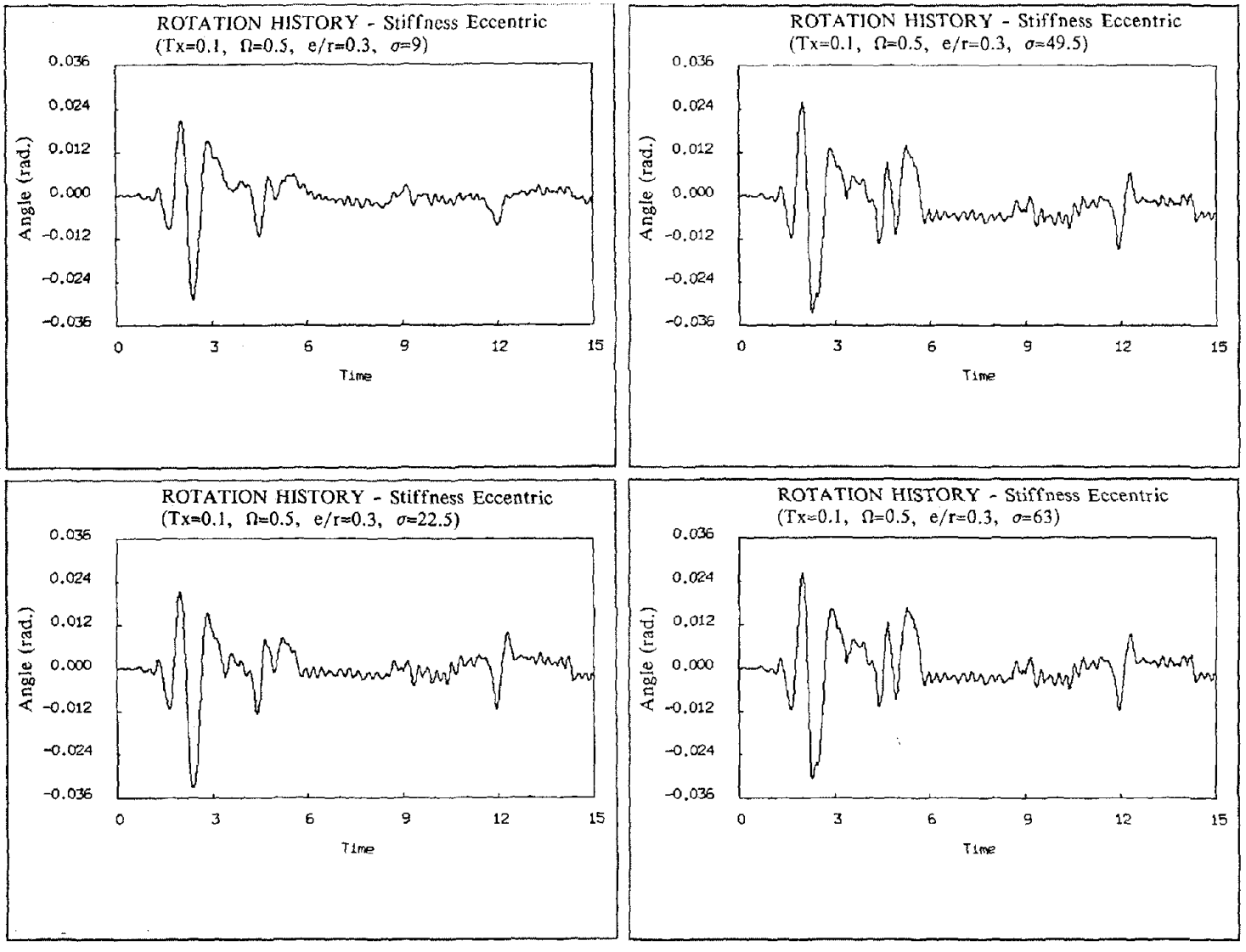

Figure 3.21d Rotation Time Histories for the Inter-Element Relation Cases Studied for Initially Eccentric Systems (Small Omega Case) - Also Refer to Table 3.2 (Yield Displacement = 0.12 units)

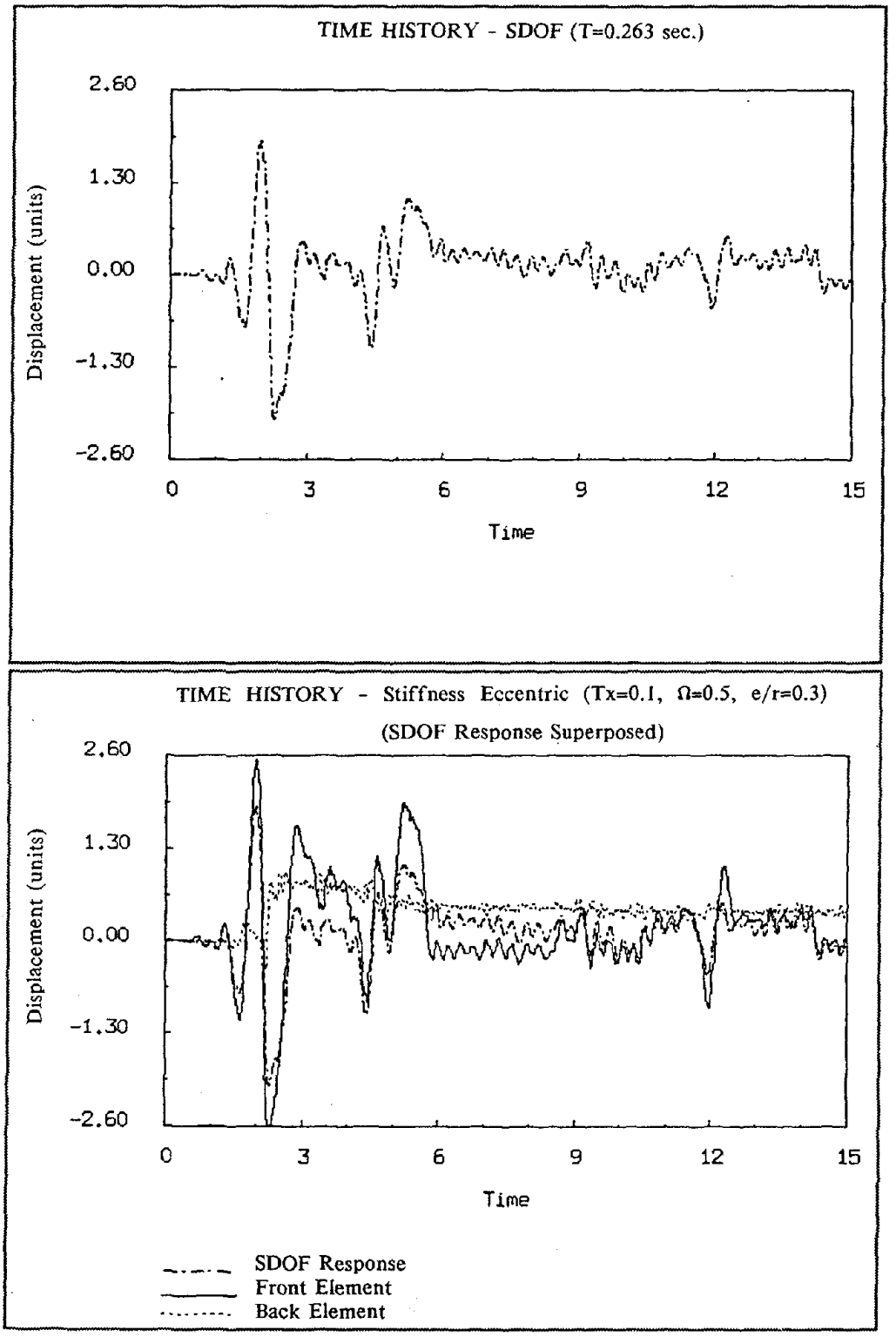

Figure 3.22 Inelastic Responses of Initially Eccentric System and SDOF System (Period Equal to the True First Period of the Eccentric System) where Elastic Responses Were Matches (Yield Displacement = 0.12 units)

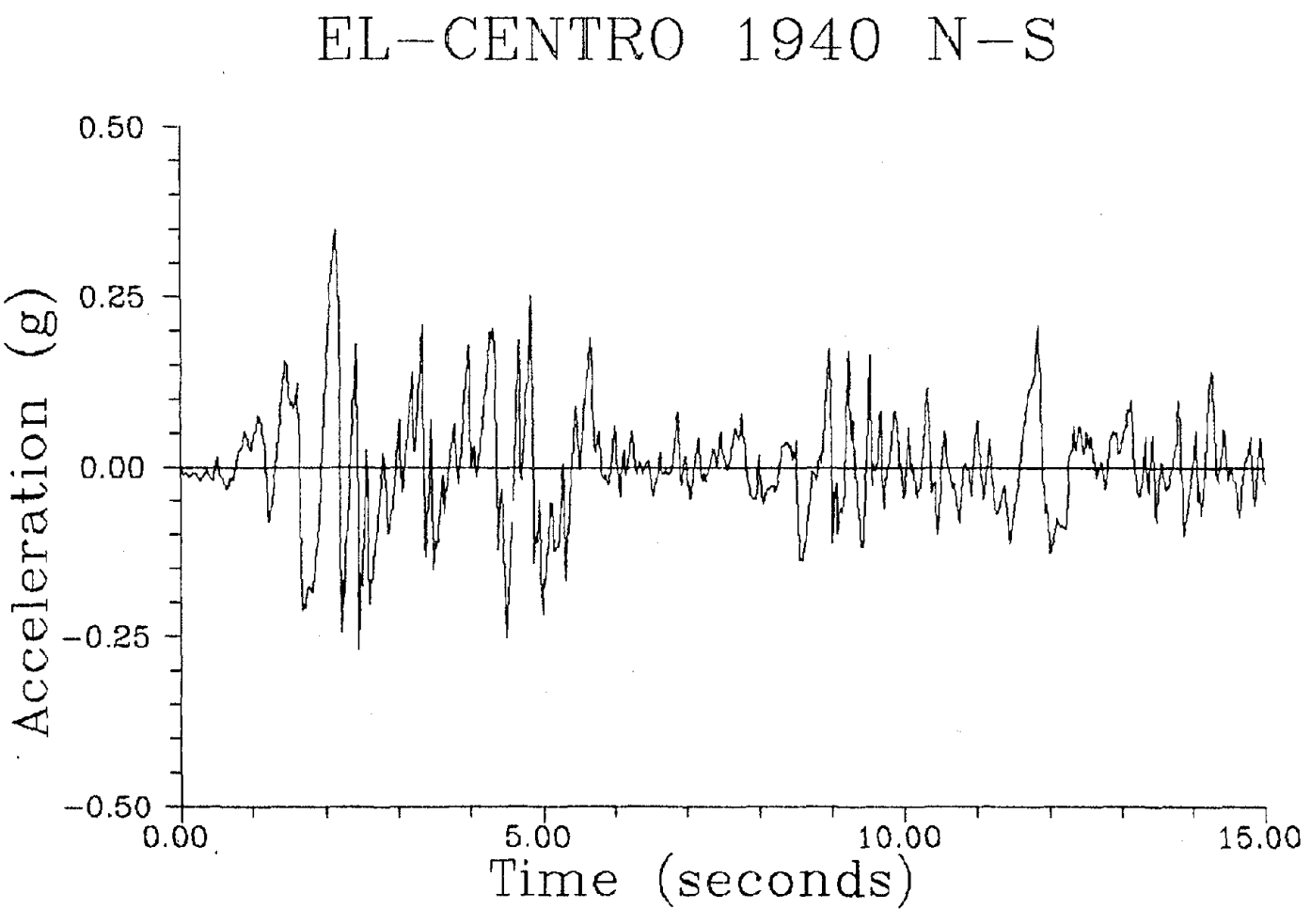

Figure 4.1a N-S Component of 1940 El Centro Earthquake Record Used for the Parametric Study

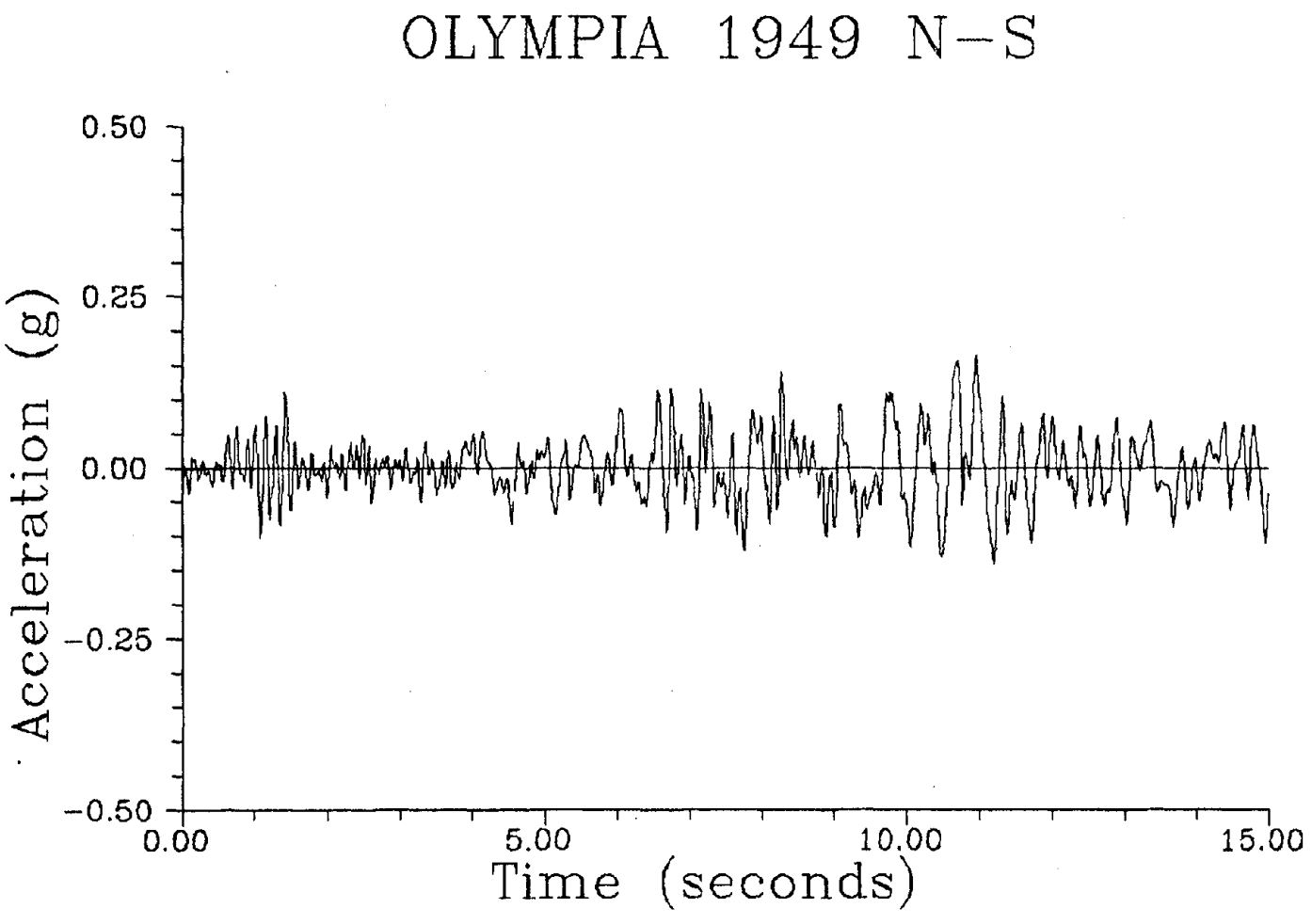

Figure 4.1b N-S Component of 1949 Olympia Earthquake Record Used for the Parametric Study

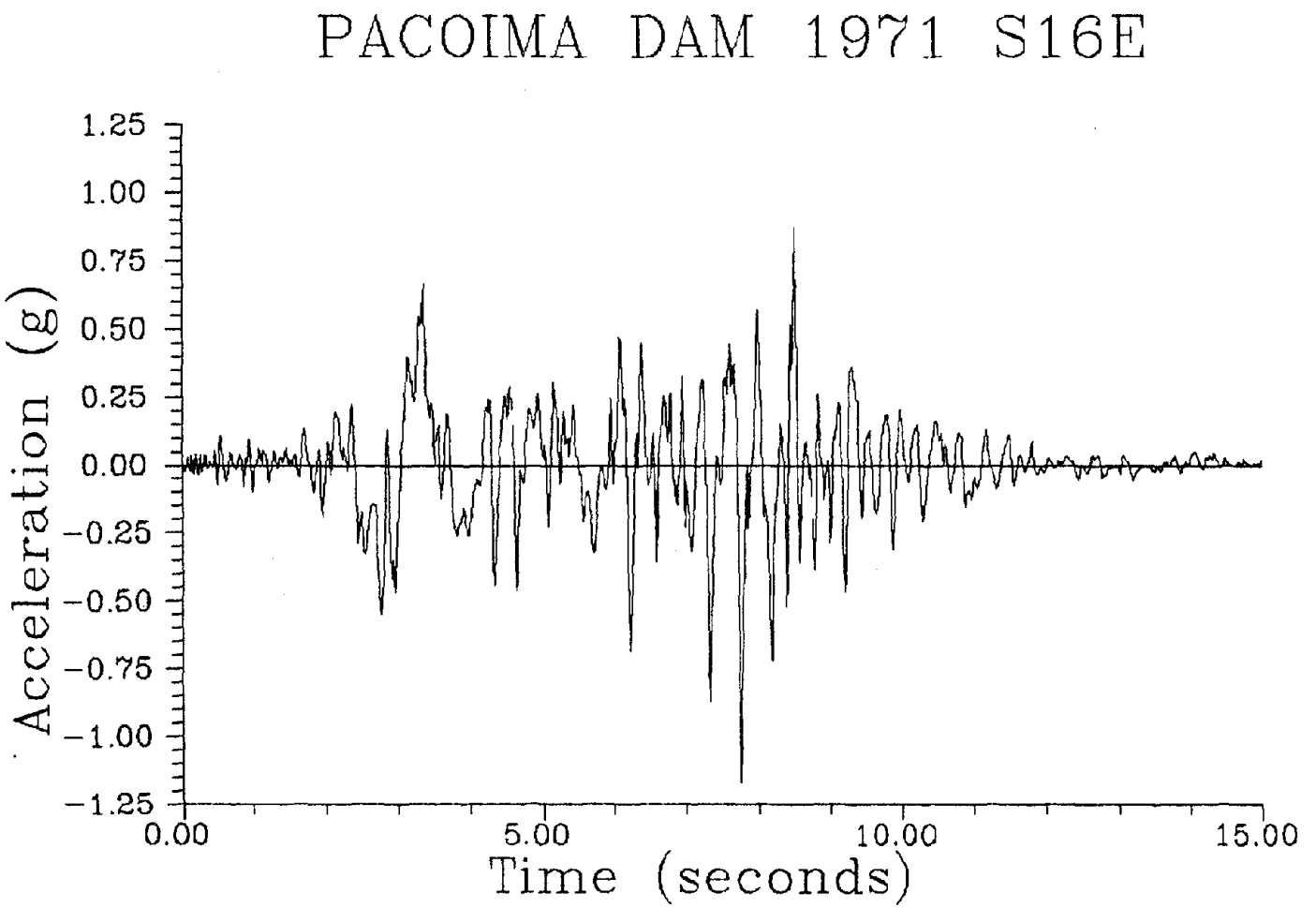

Figure 4.1c S16E Component of 1971 Pacoima Dam Earthquake Record Used for the Parametric Study

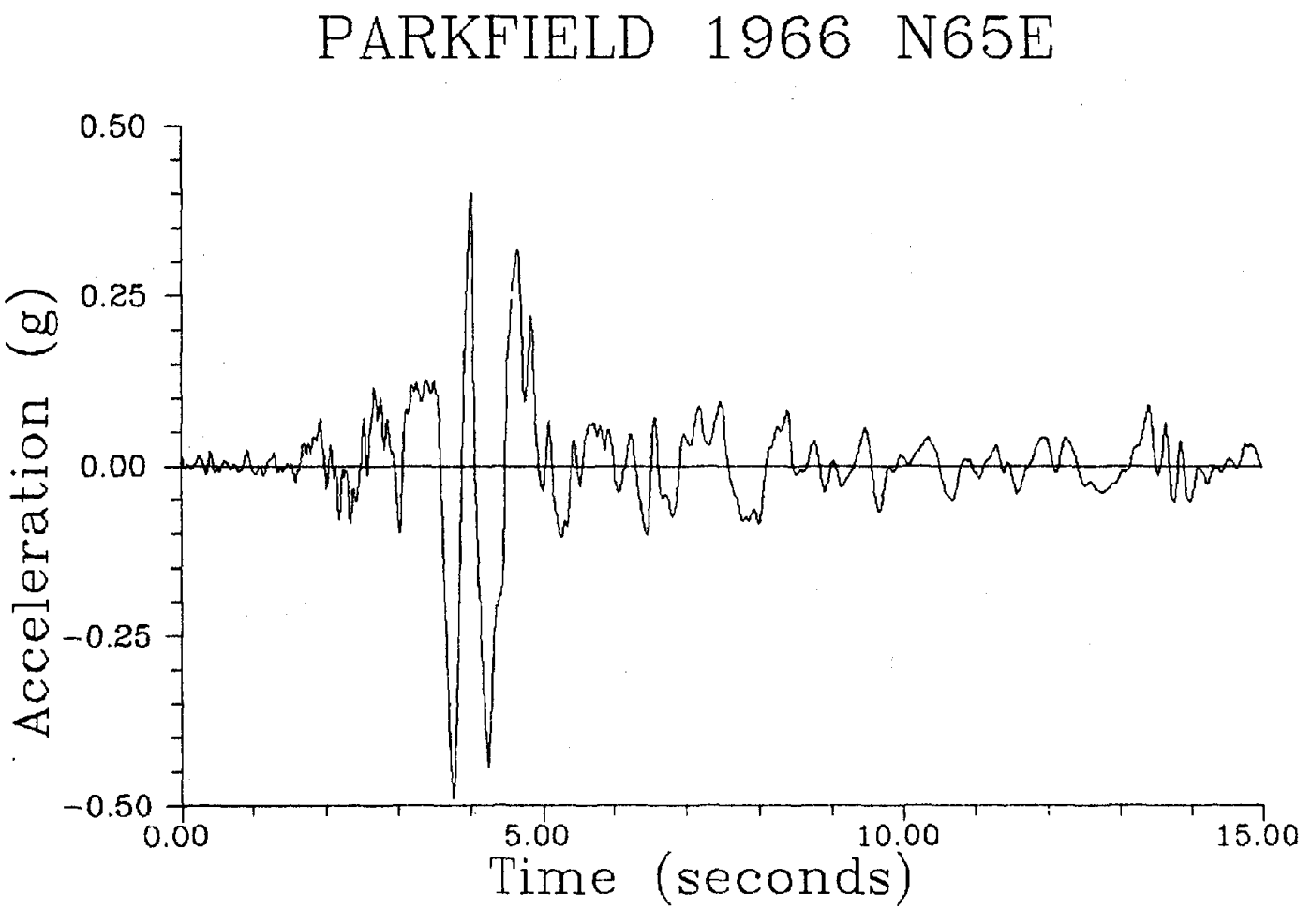

Figure 4.1d N65E Component of 1966 Parkfield Earthquake Record Used for the Parametric Study

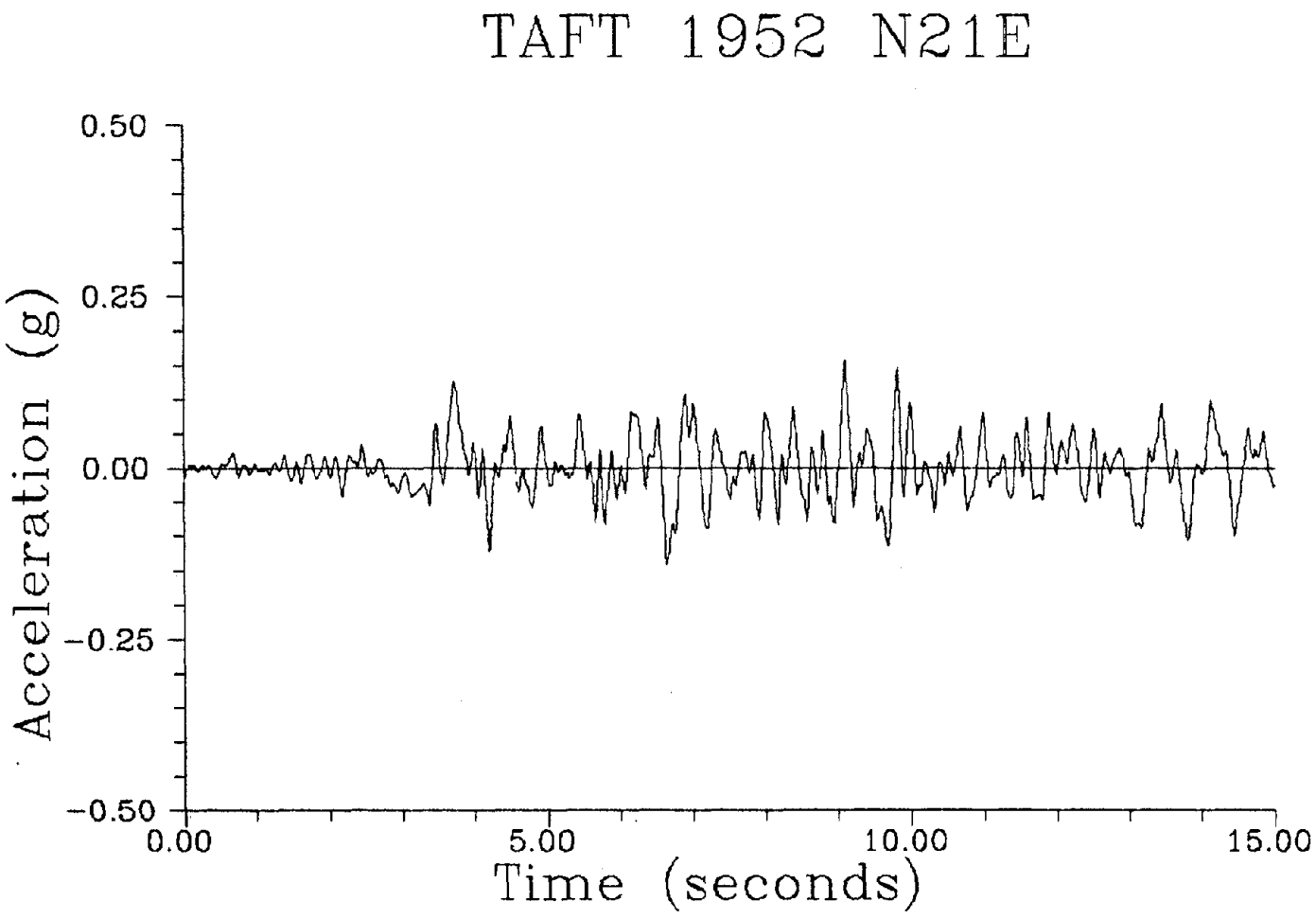

Figure 4.1e N21E Component of 1952 Taft Earthquake Record Used for the Parametric Study

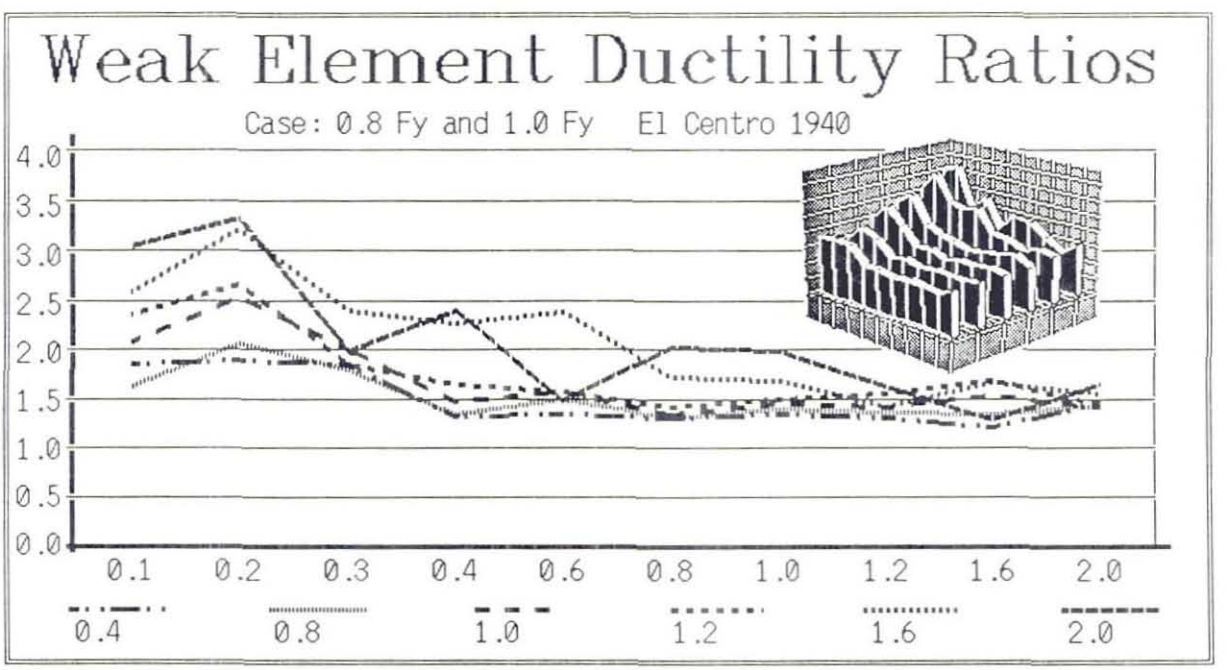

Figure 4.2 Comparison of Two-Dimensional and Three-Dimensional Presentation of Results

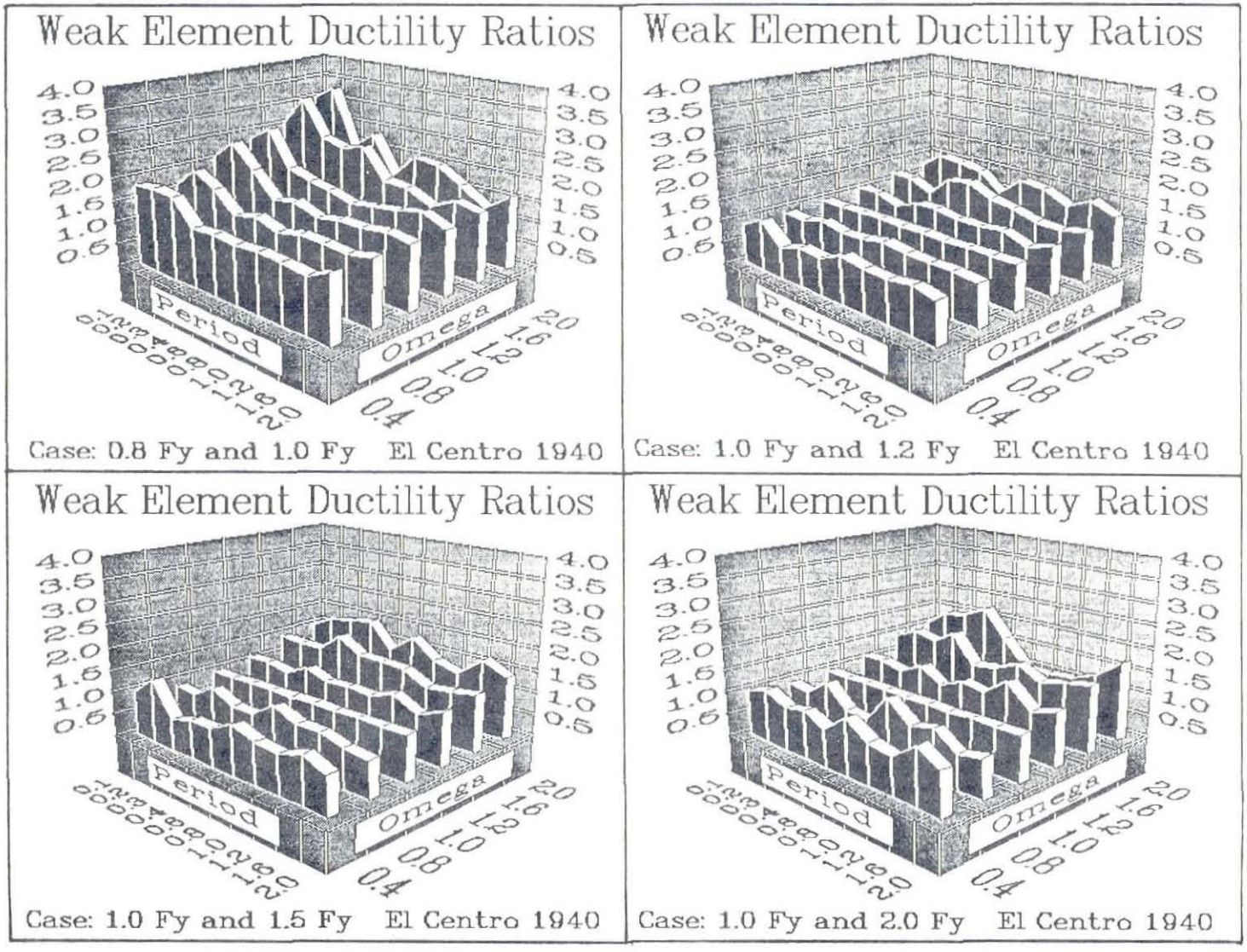

Figure 4.3 Weak Element Ductility Ratios for Target Ductility of 4 and El Centro Earthquake Record

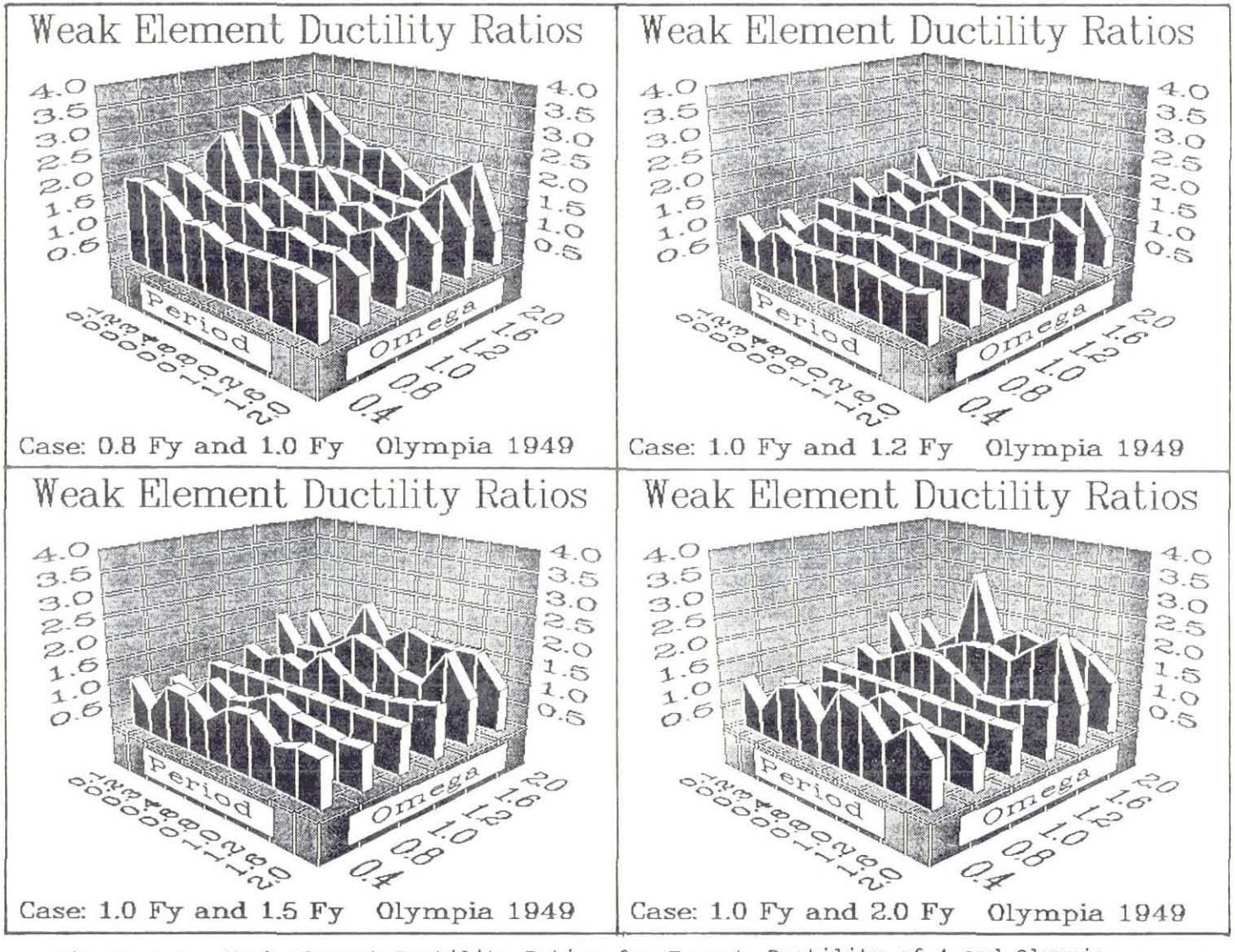

Figure 4.4 Weak Element Ductility Ratios for Target Ductility of 4 and Olympia Earthquake Record

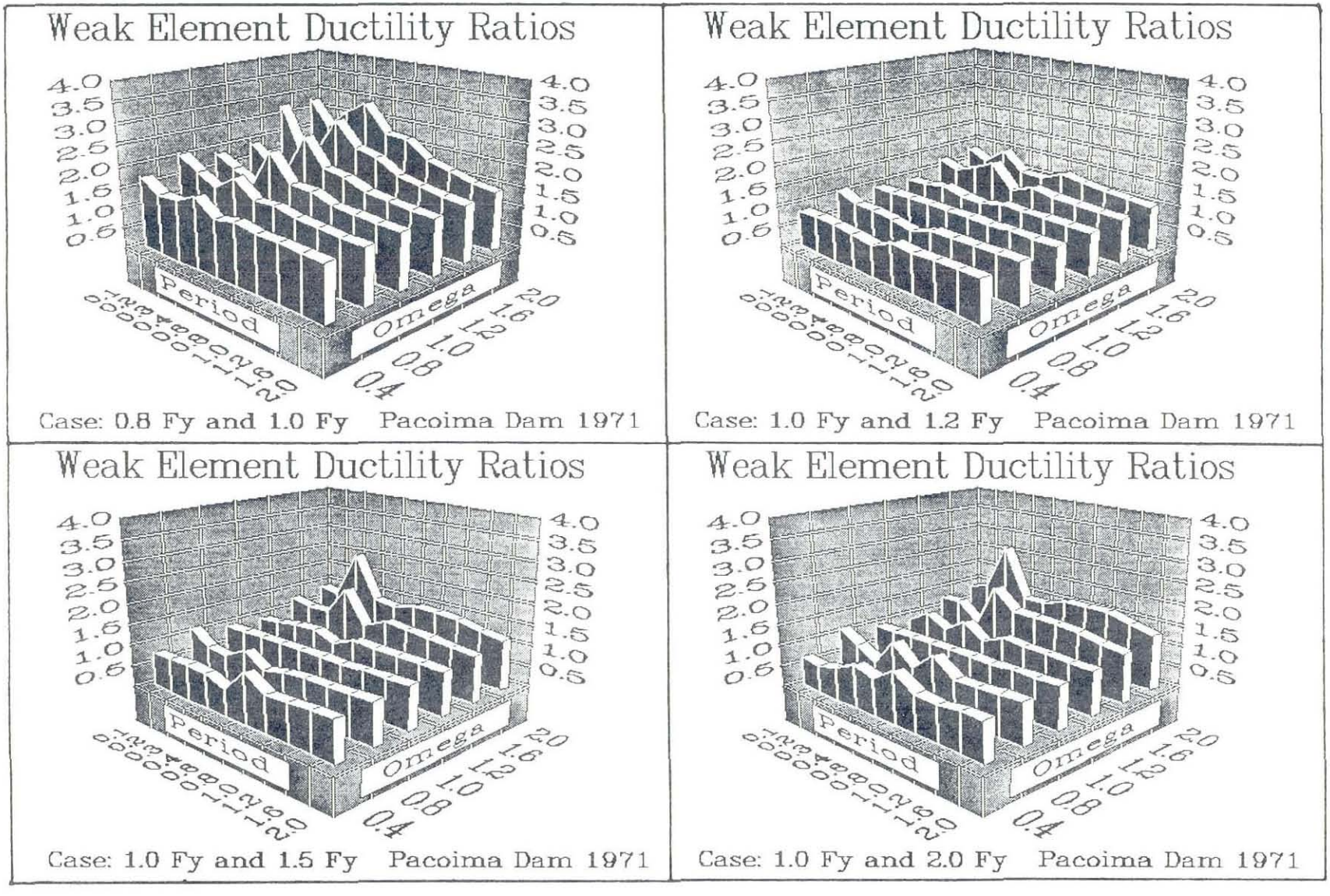

Figure 4.5 Weak Element Ductility Ratios for Target Ductility of 4 and Pacoima Dam Earthquake Record

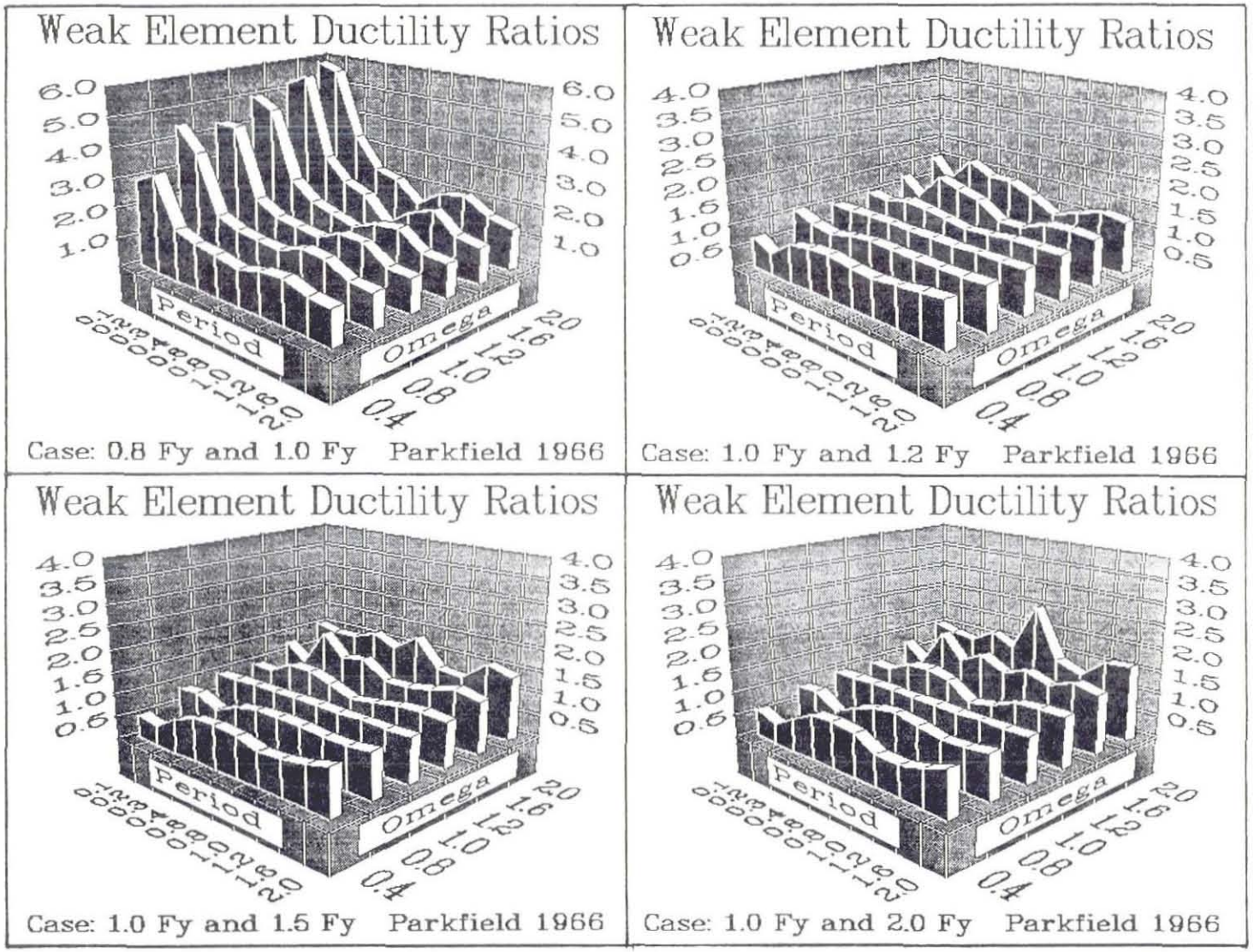

Figure 4.6 Weak Element Ductility Ratios for Target Ductility of 4 and Parkfield Earthquake Record

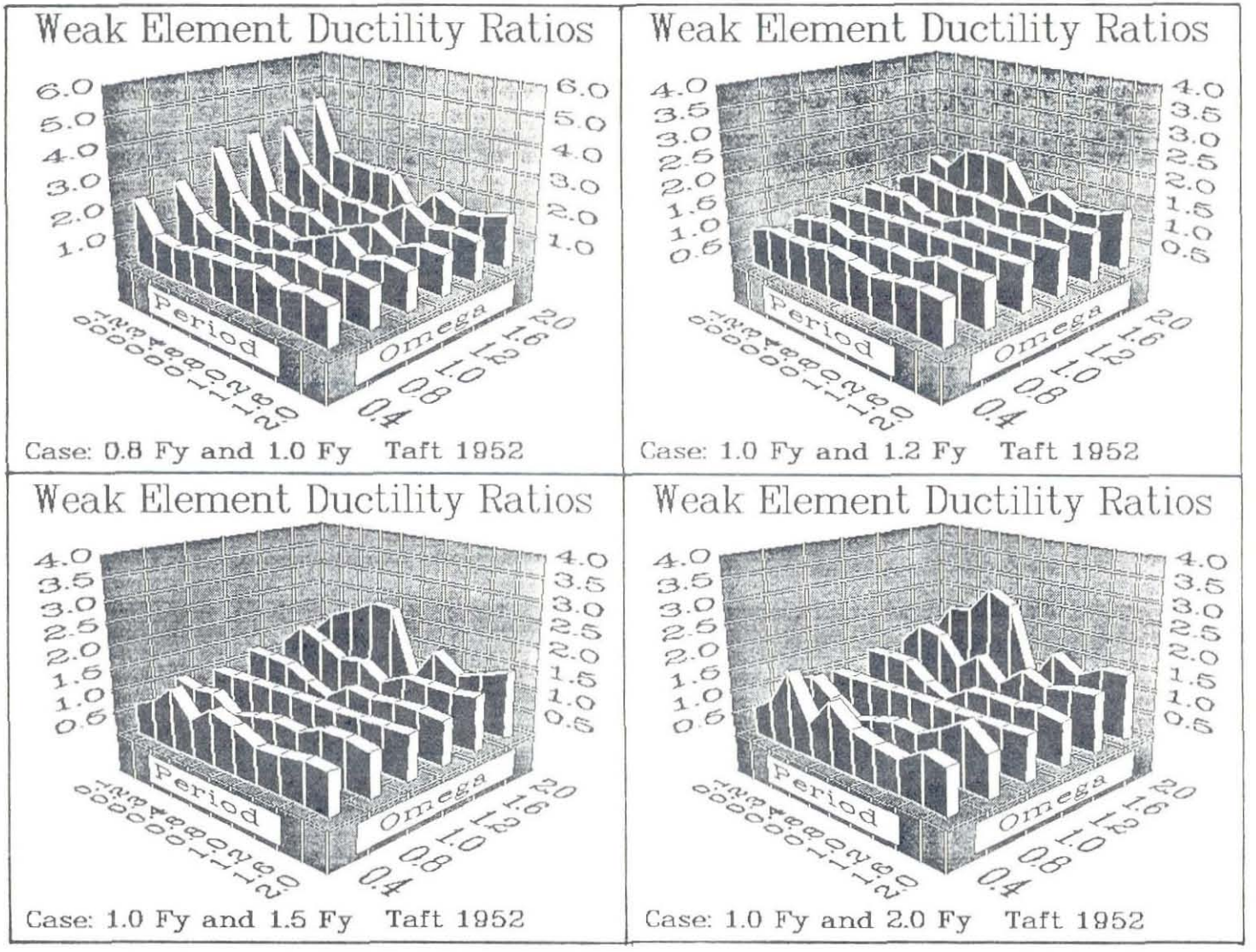

Figure 4.7 Weak Element Ductility Ratios for Target Ductility of 4 and Taft Earthquake Record

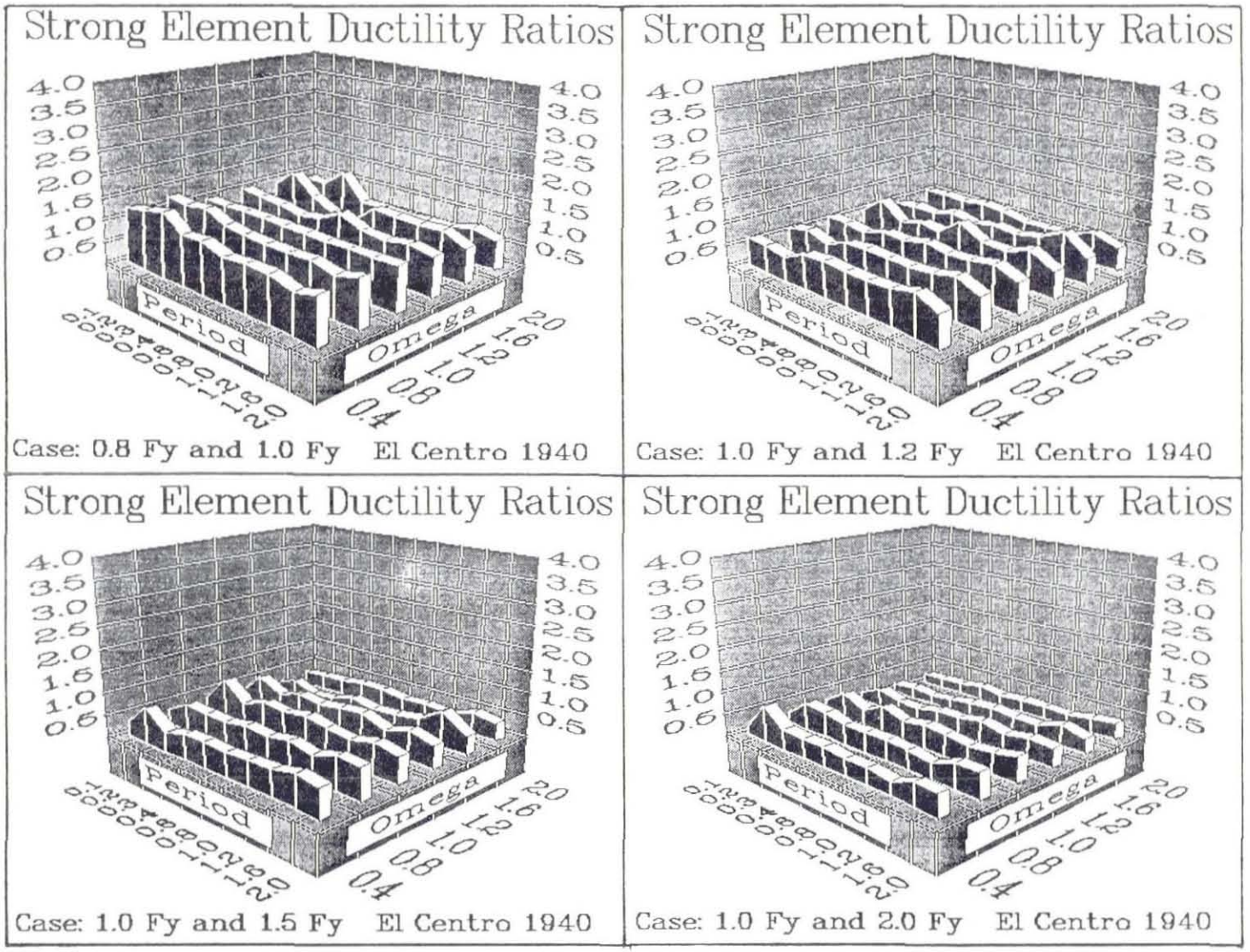

Figure 4.8 Strong Element Ductility Ratios for Target Ductility of 4 and El Centro Earthquake Record

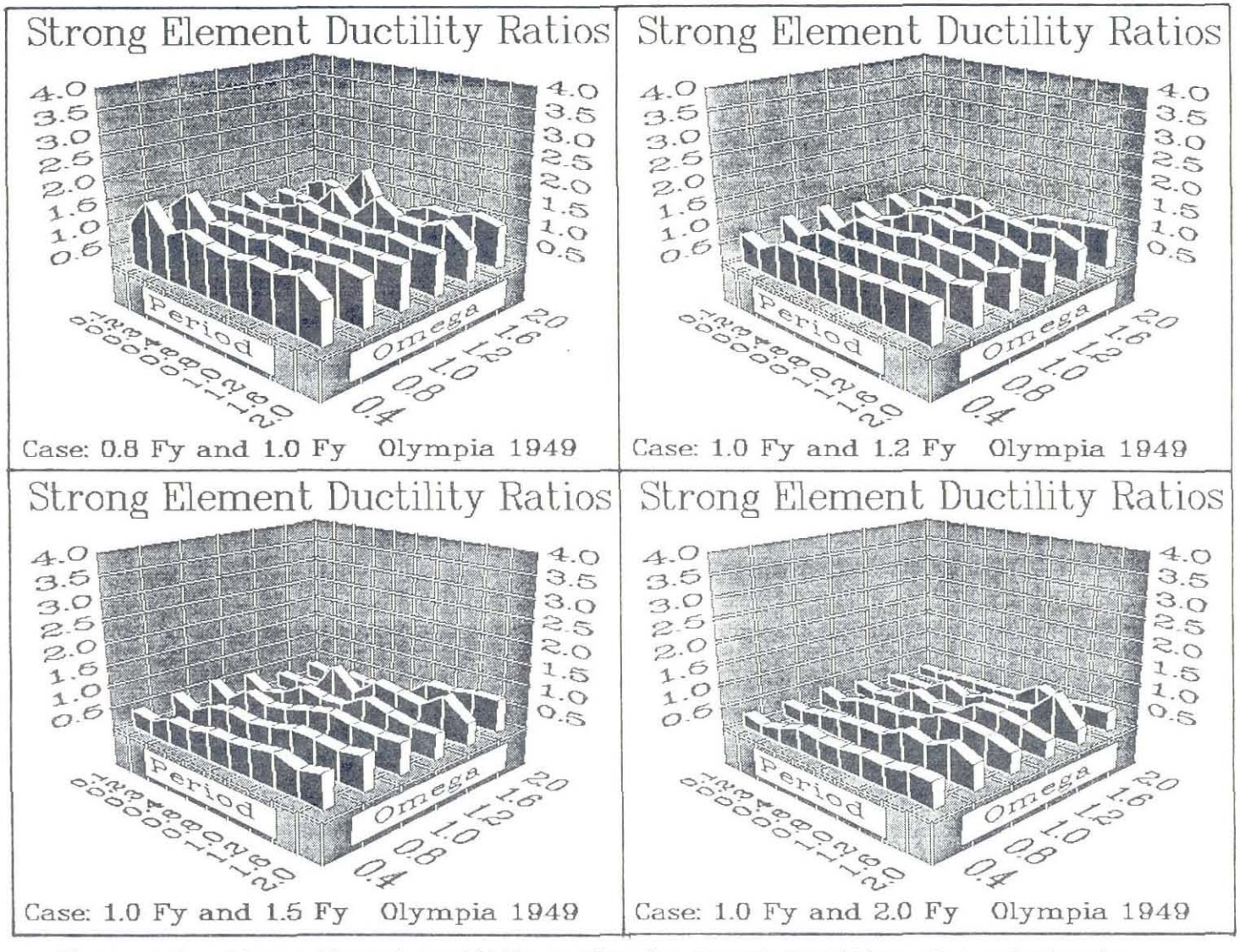

Figure 4.9 Strong Element Ductility Ratios for Target Ductility of 4 and Olympia Earthquake Record

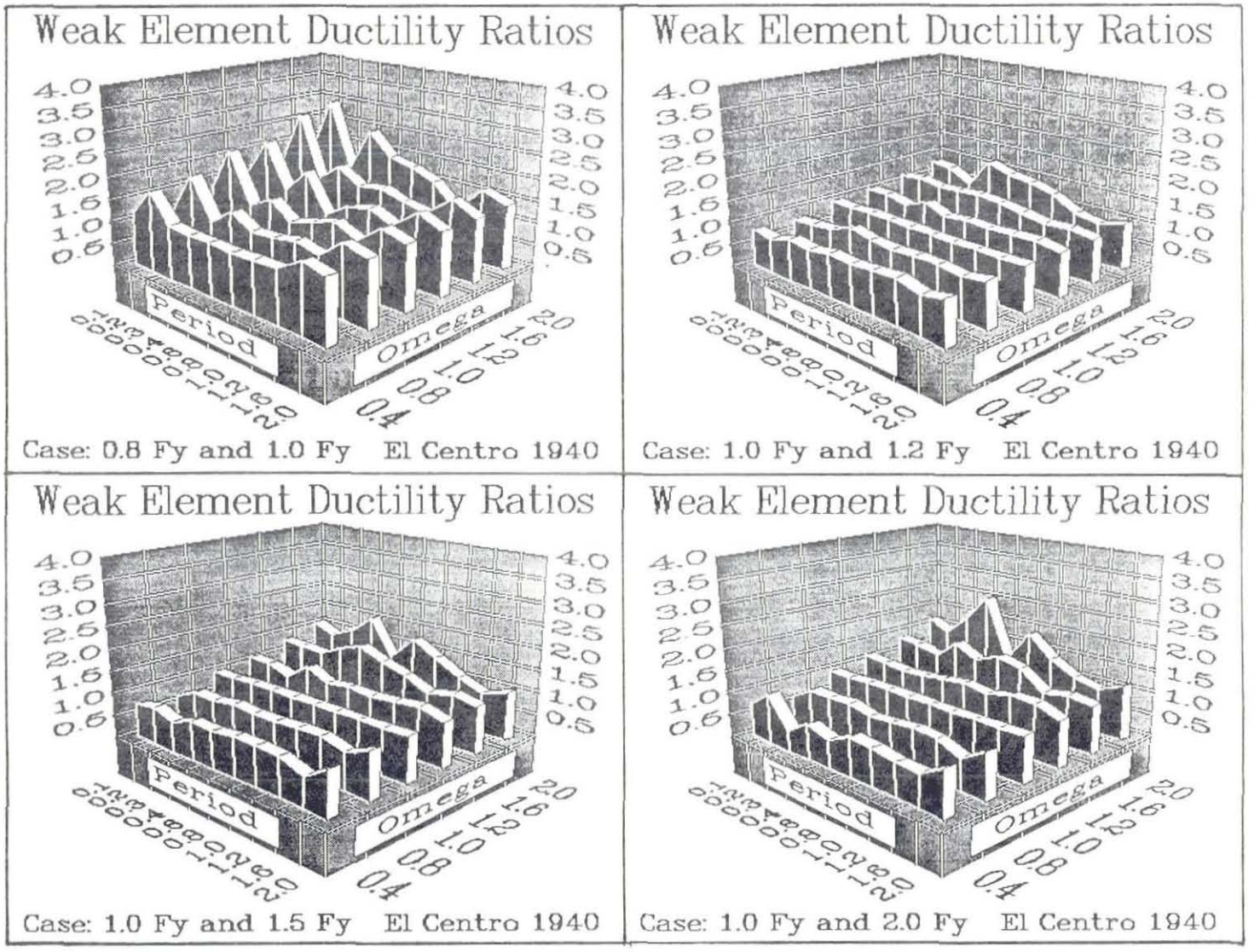

Figure 4.10 Weak Element Ductility Ratios for Target Ductility of 8 and El Centro Earthquake Record

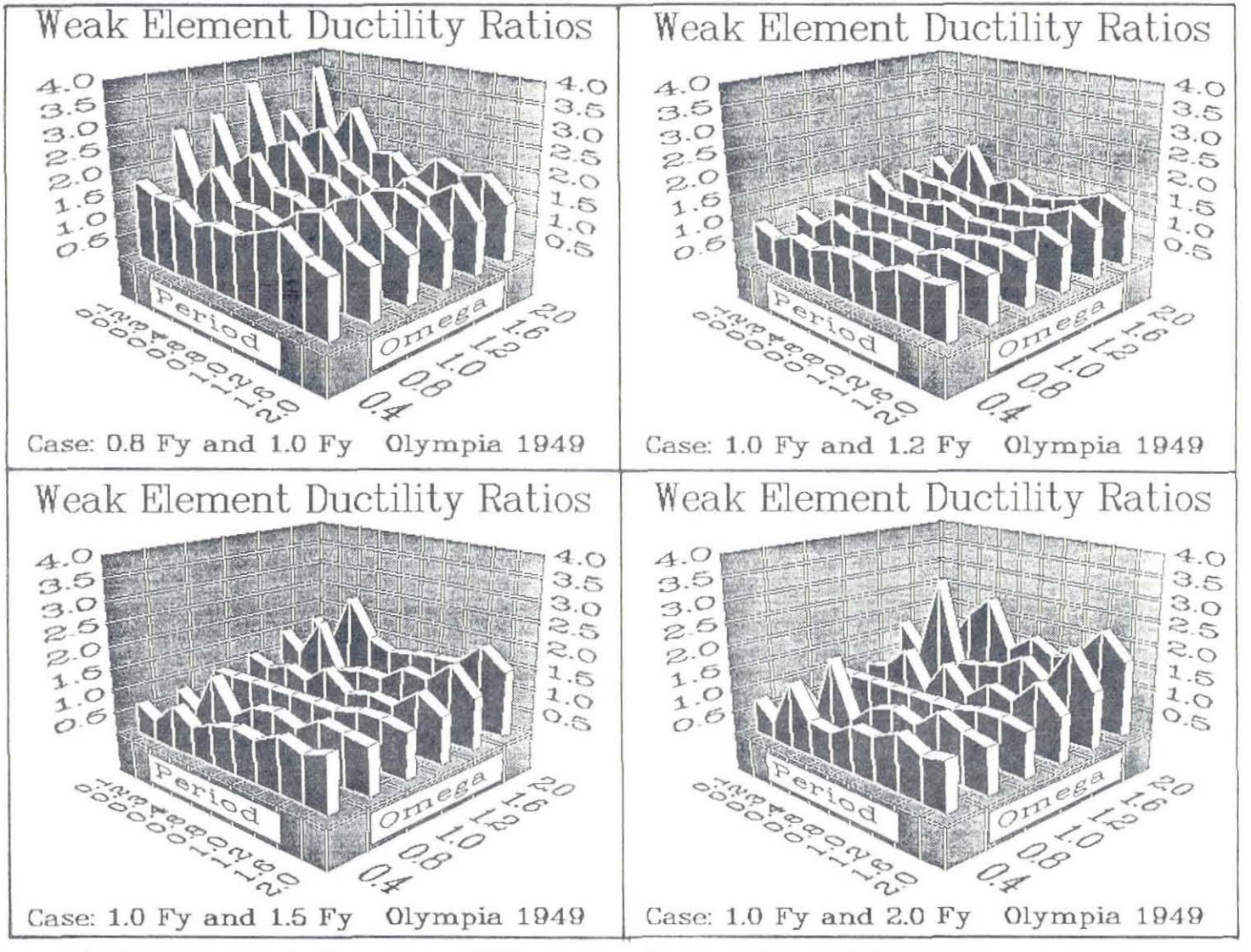

Figure 4.11 Weak Element Ductility Ratios for Target Ductility of 8 and Olympia Earthquake Record

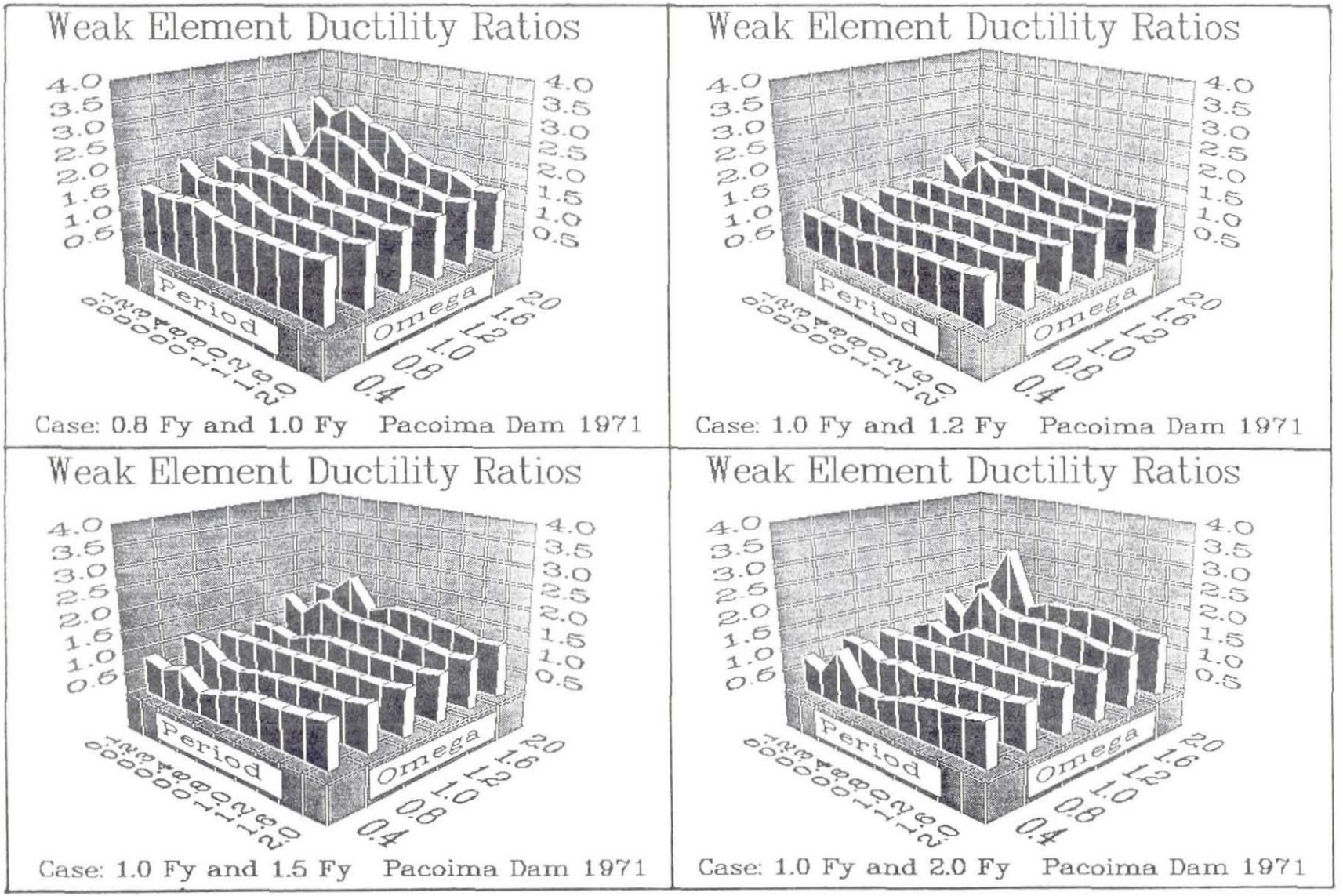

Figure 4.12 Weak Element Ductility Ratios for Target Ductility of 8 and Pacoima Dam Earthquake Record

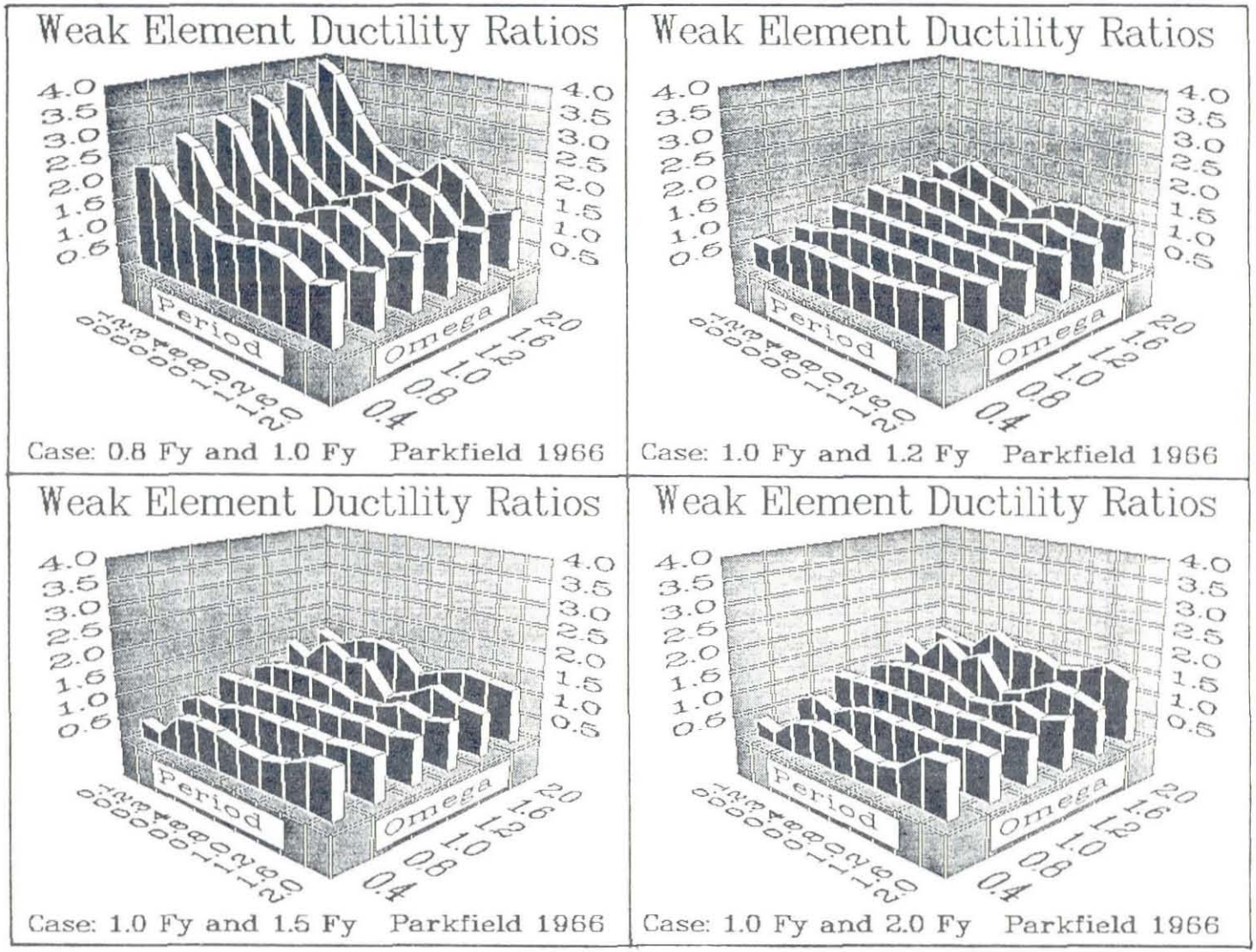

Figure 4.13 Weak Element Ductility Ratios for Target Ductility of 8 and Parkfield Earthquake Record

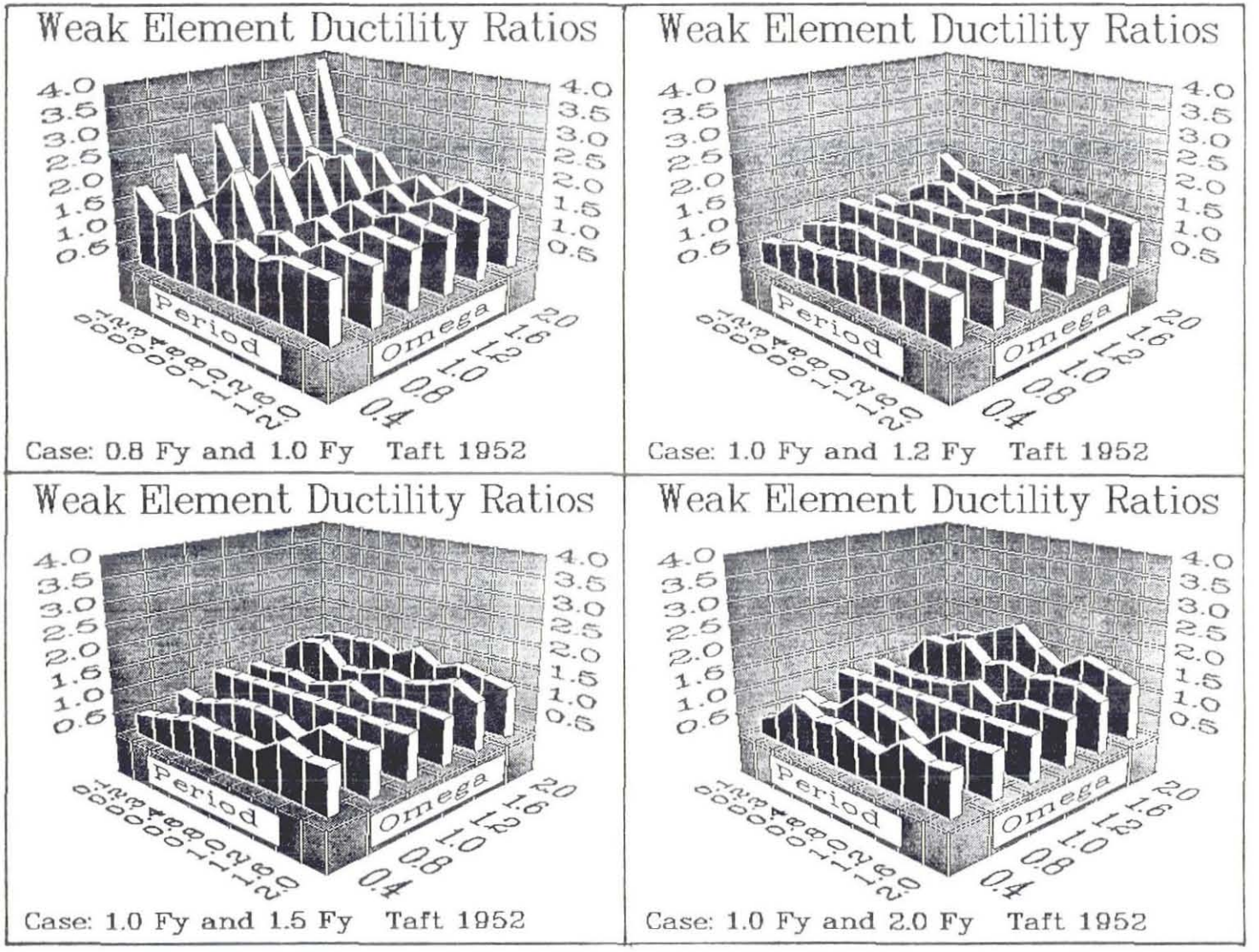

Figure 4.14 Weak Element Ductility Ratios for Target Ductility of 8 and Taft Earthquake Record

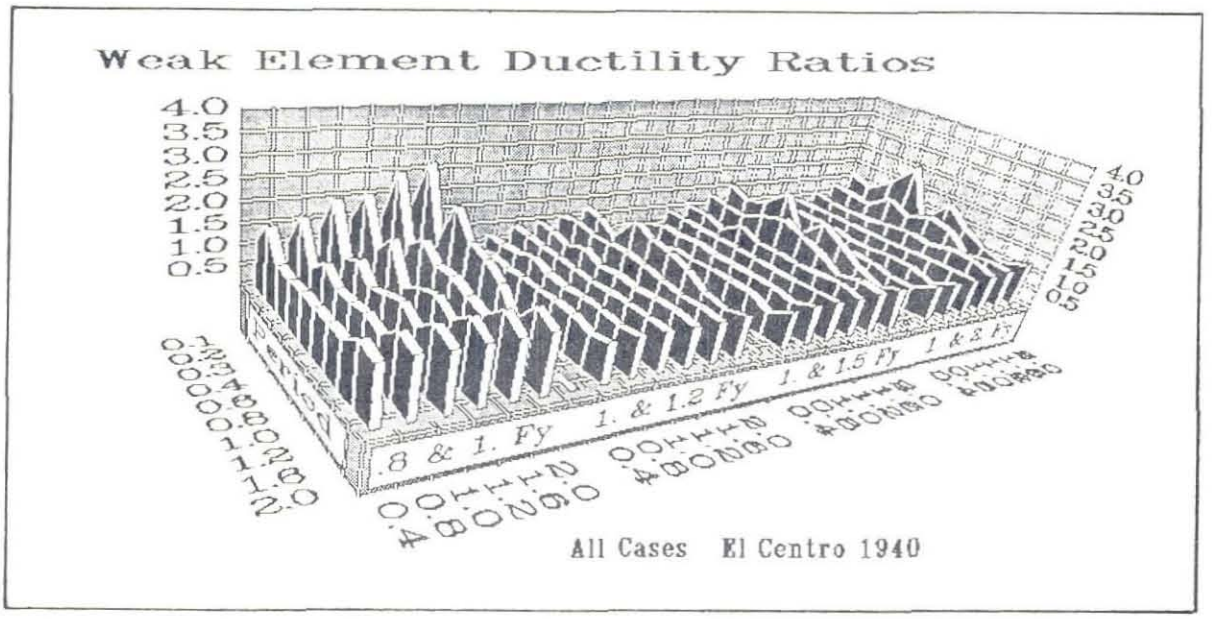

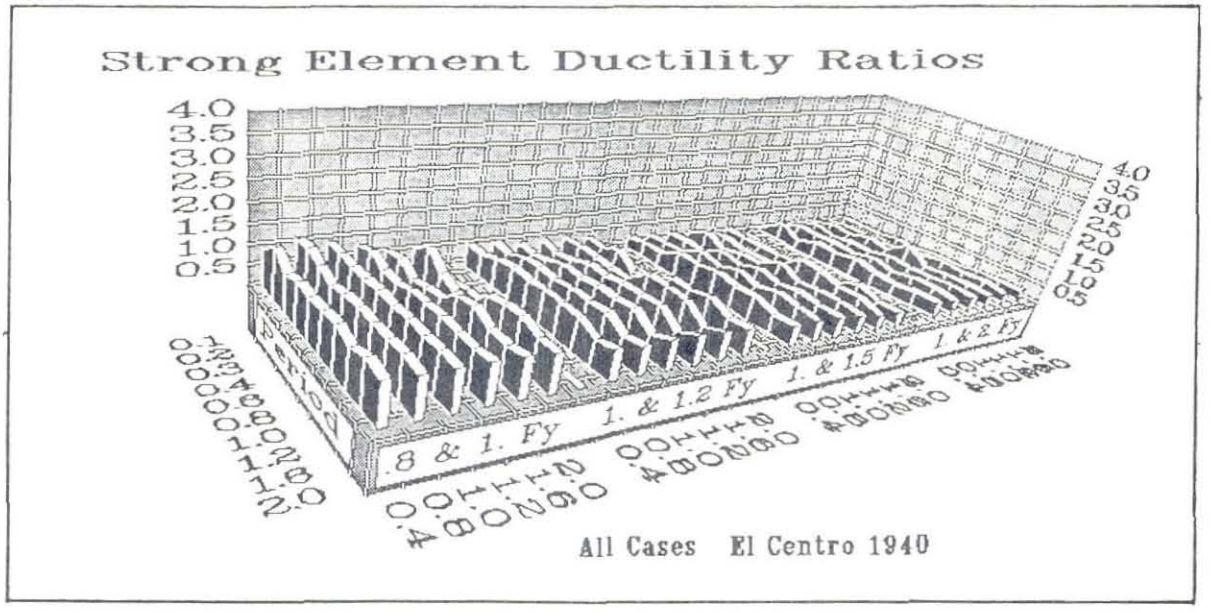

Figure 4.15 Global Graphs of Element Ductility Ratios for Target Ductility of 8 and El Centro Earthquake Record

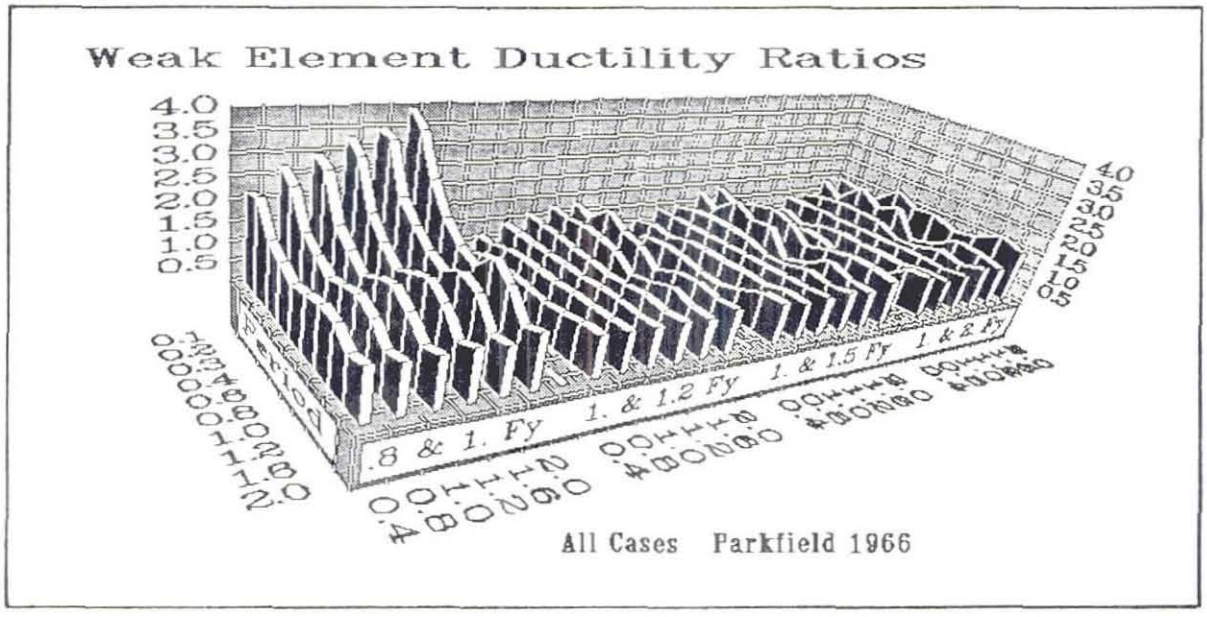

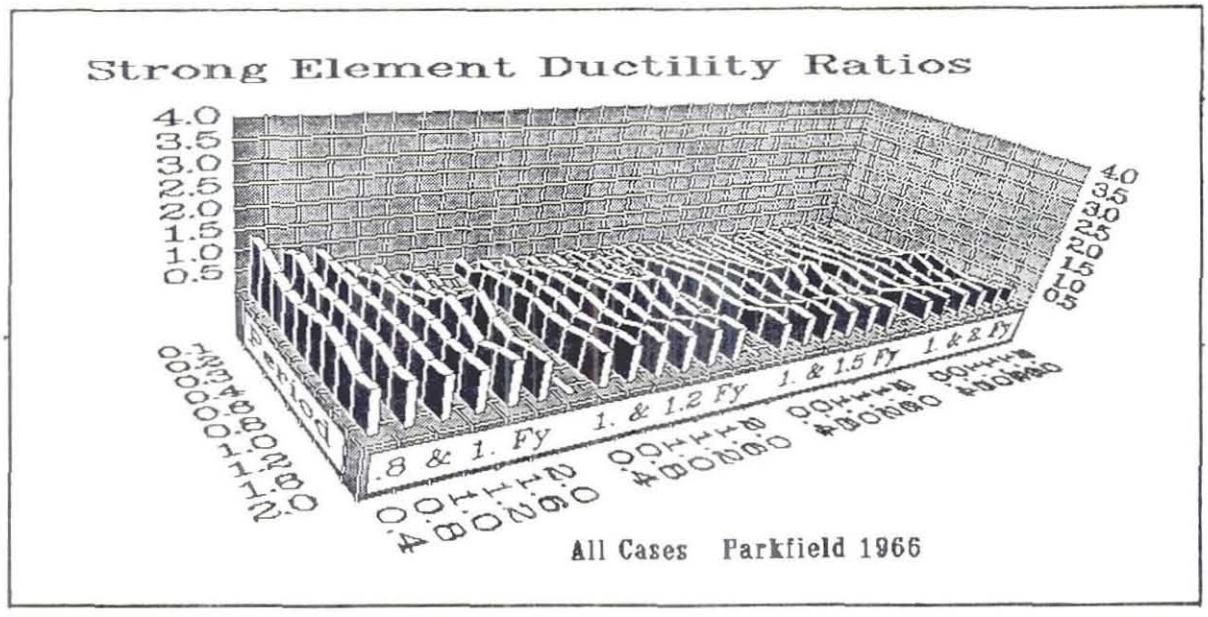

Figure 4.16 Global Graphs of Element Ductility Ratios for Target Ductility of 8 and Parkfield Earthquake Record

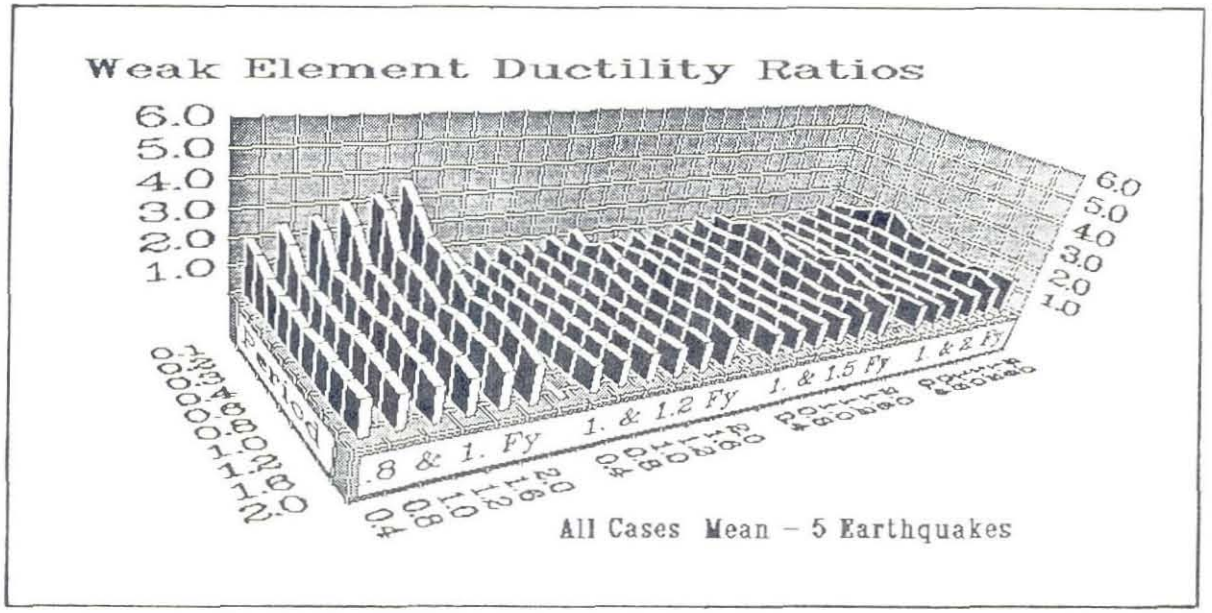

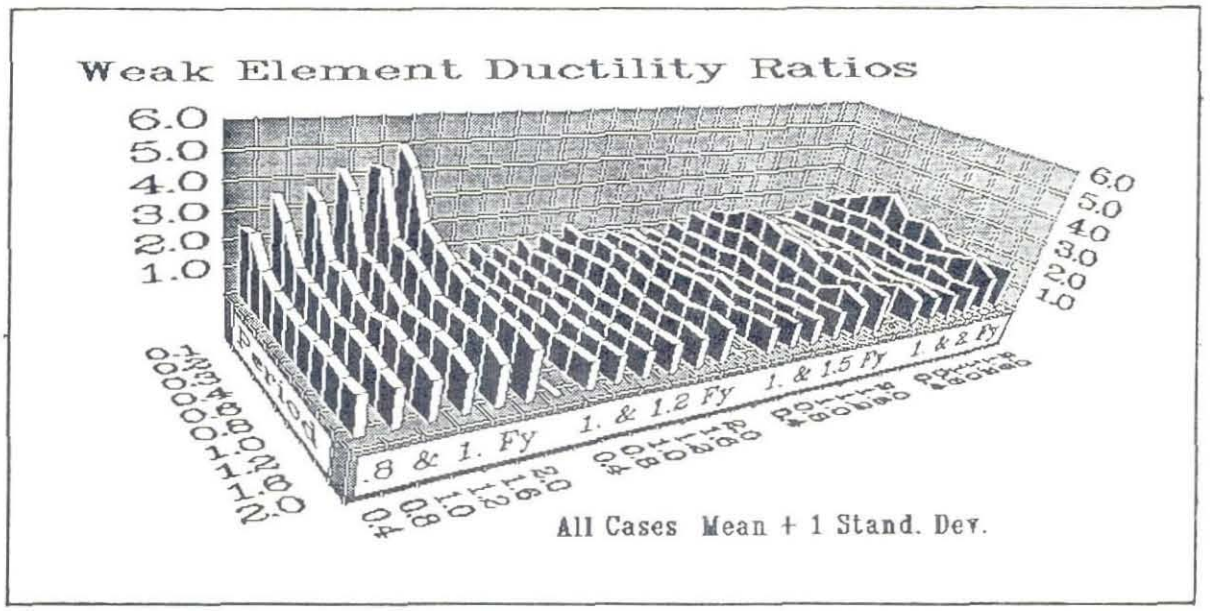

Figure 4.17 Mean and Mean-Plus-One-Standard-Deviation (Five Earthquake Records) of Weak Element Ductility Ratios for Target Ductility of 4 (Grouped by Yield Cases)

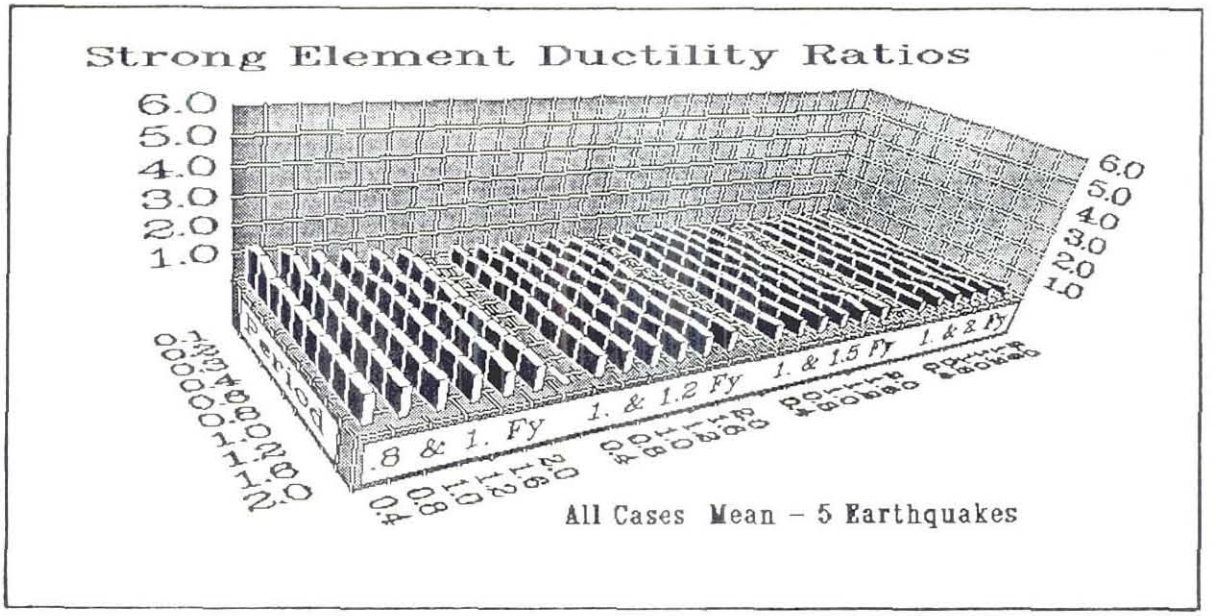

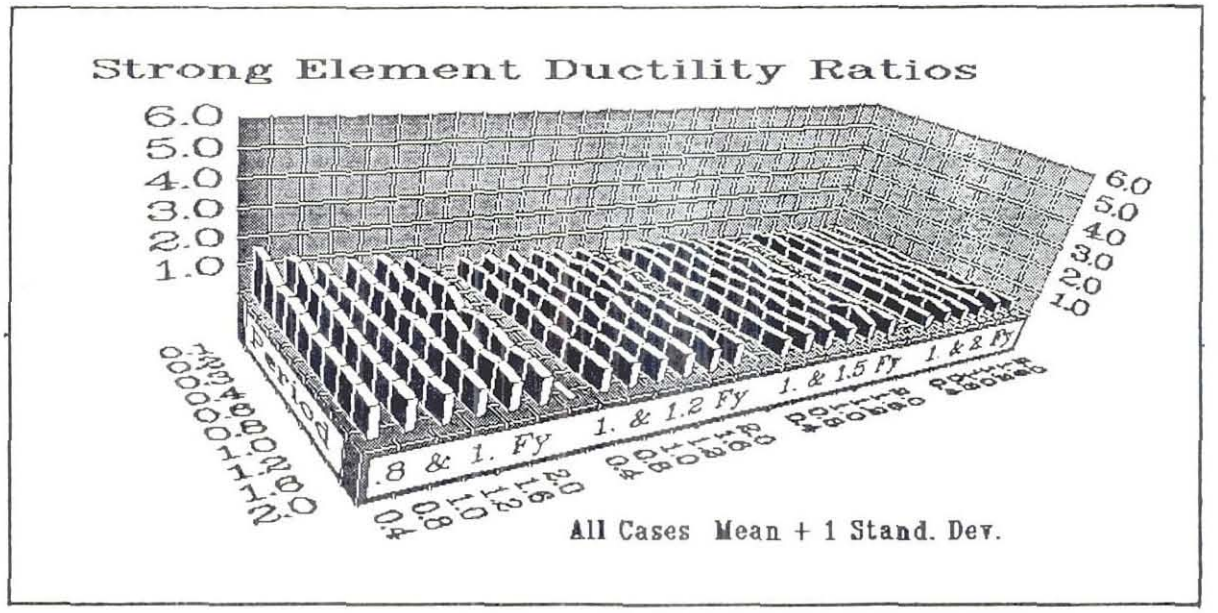

Figure 4.18 Mean and Mean-Plus-One-Standard-Deviation (Five Earthquake Records) of Strong Element Ductility Ratios for Target Ductility of 4 (Grouped by Yield Cases)

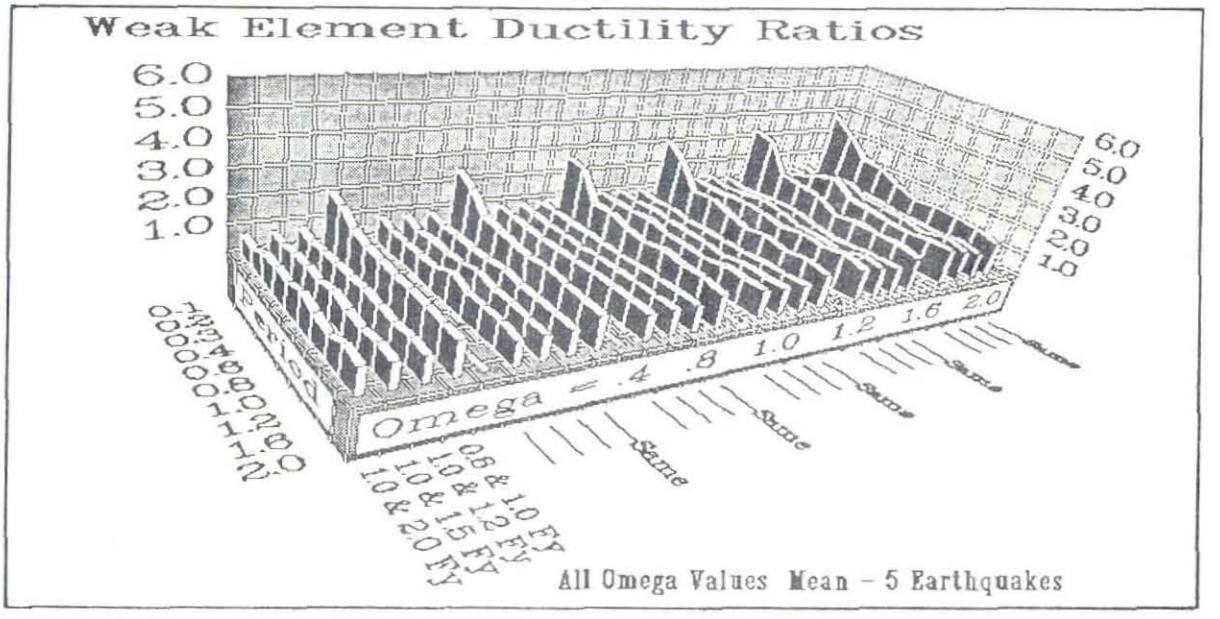

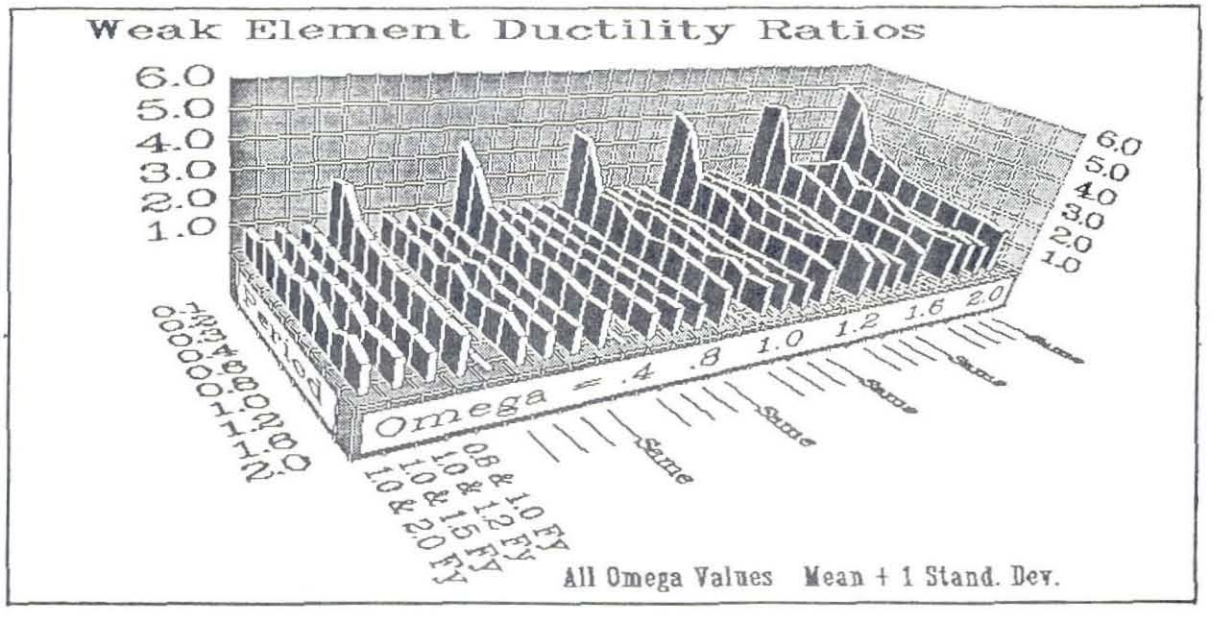

Figure 4.19 Mean and Mean-Plus-One-Standard-Deviation (Five Earthquake Records) of Weak Element Ductility Ratios for Target Ductility of 4 (Grouped by Omega Values)

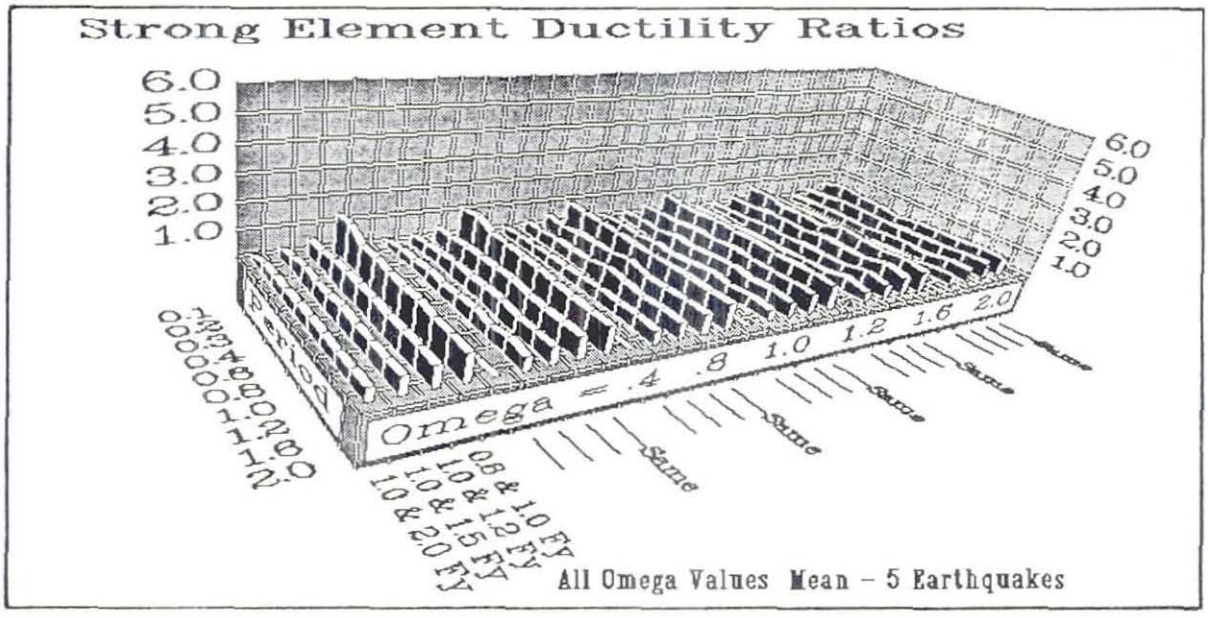

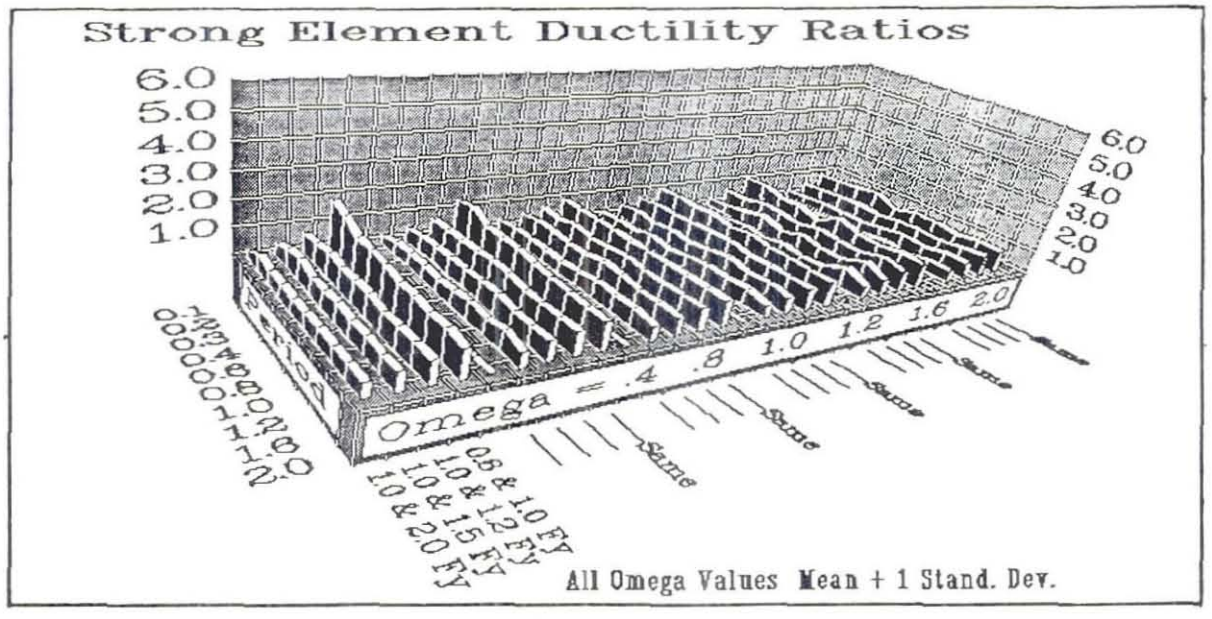

Figure 4.20 Mean and Mean-Plus-One-Standard-Deviation (Five Earthquake Records) of Strong Element Ductility Ratios for Target Ductility of 4 (Grouped by Omega Values)

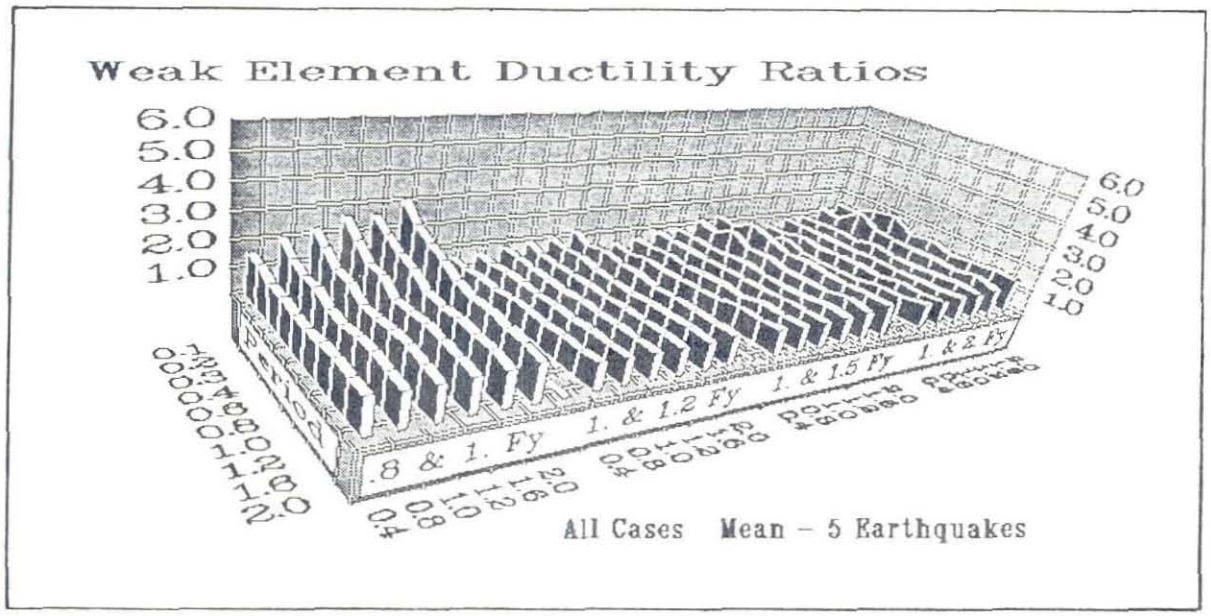

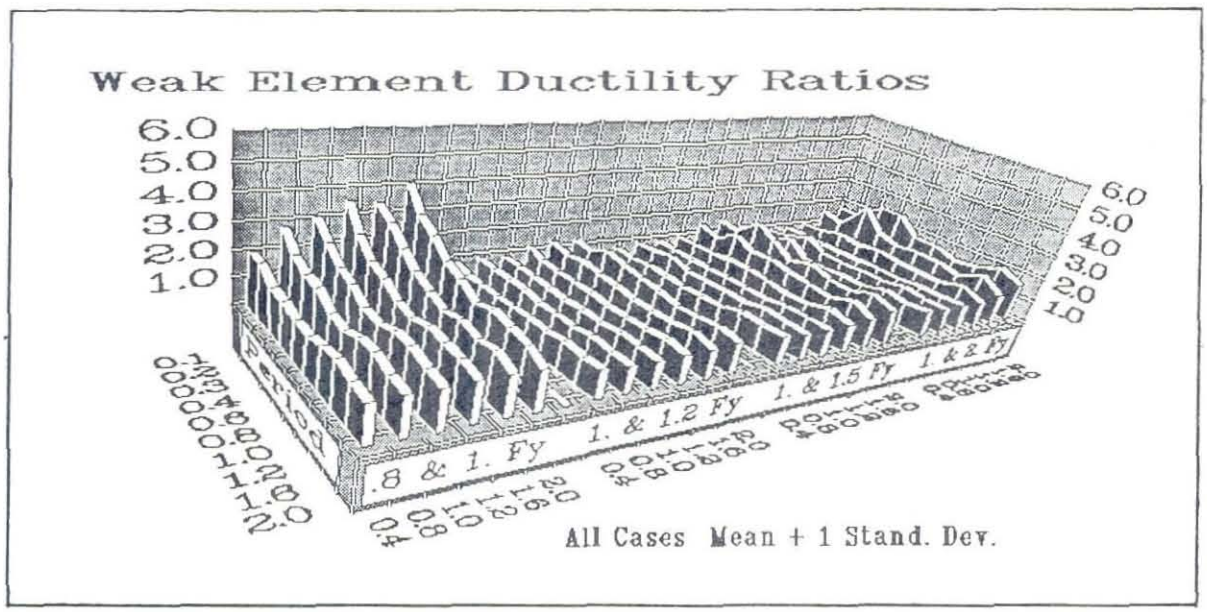

Figure 4.21 Mean and Mean-Plus-One-Standard-Deviation (Five Earthquake Records) of Weak Element Ductility Ratios for Target Ductility of 8 (Grouped by Yield Cases)

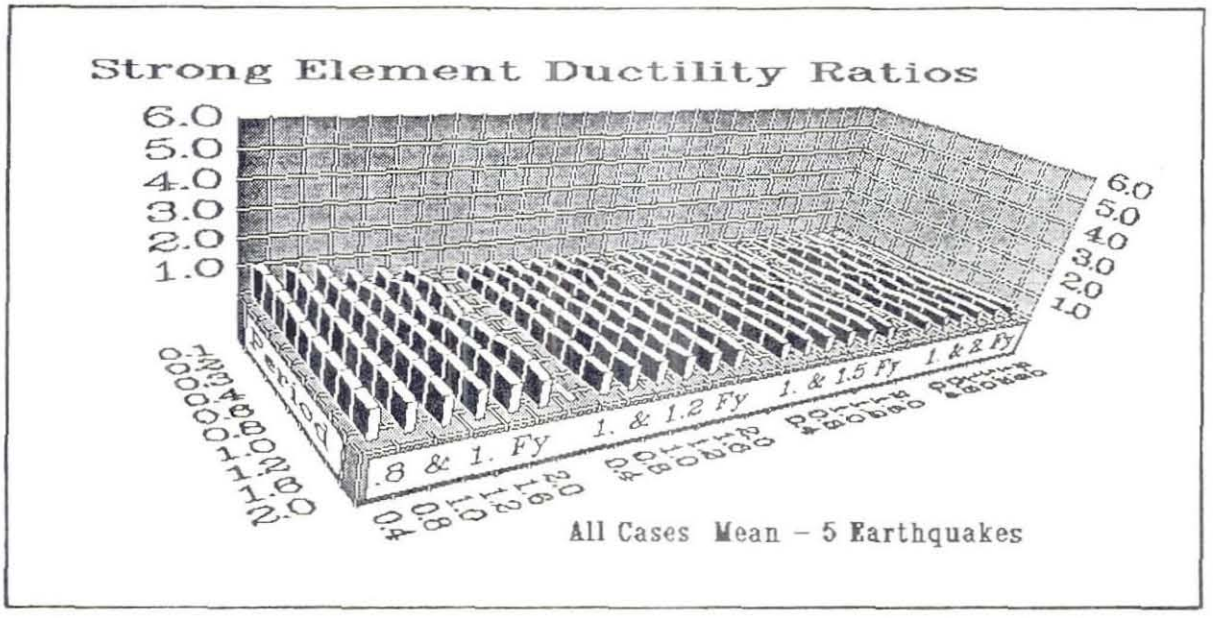

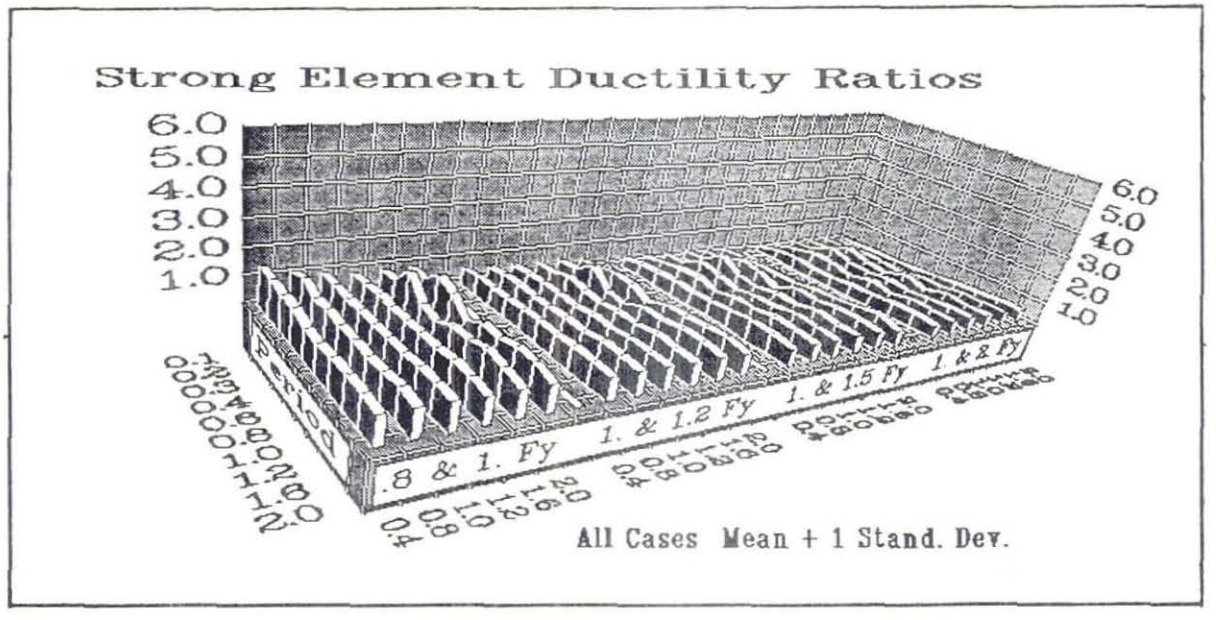

Figure 4.22 Mean and Mean-Plus-One-Standard-Deviation (Five Earthquake Records) of Strong Element Ductility Ratios for Target Ductility of 8 (Grouped by Yield Cases)

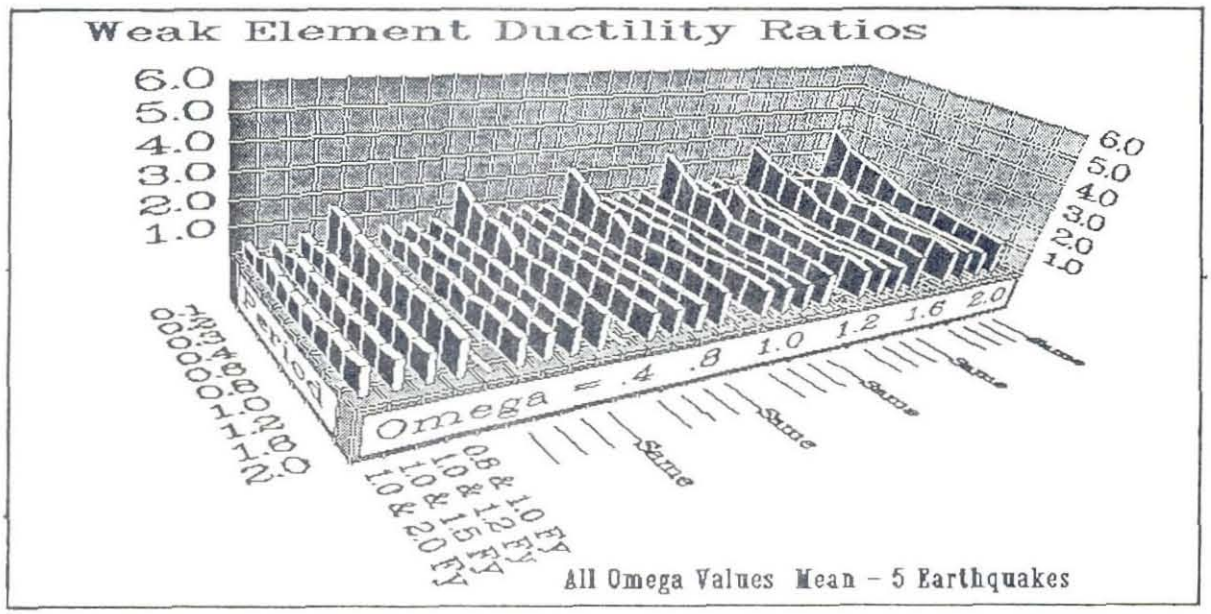

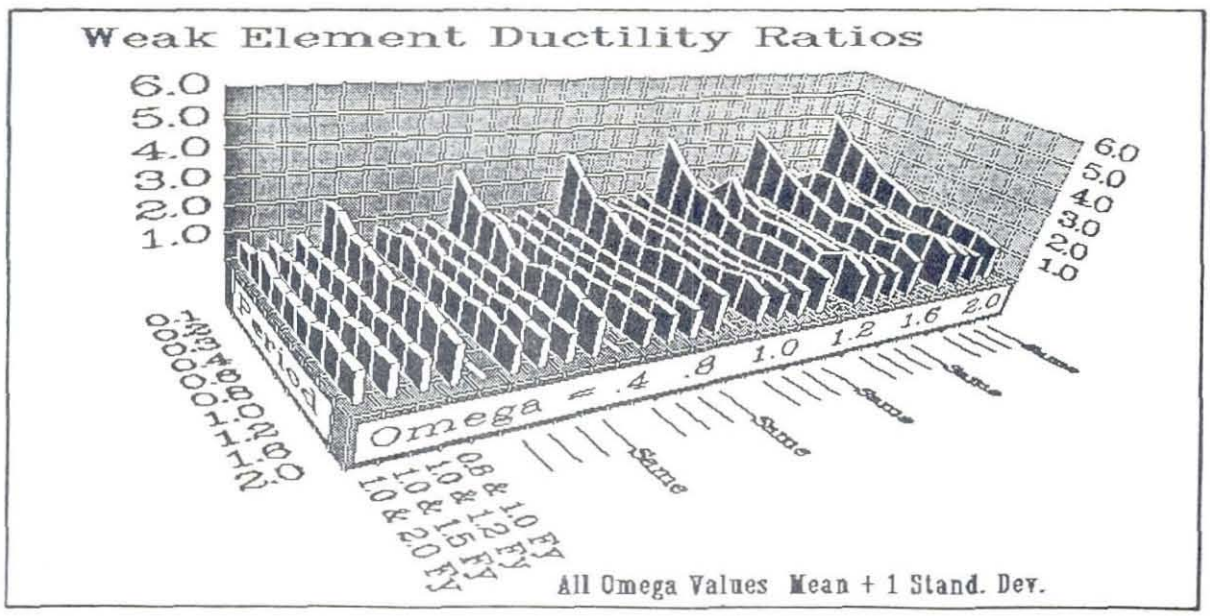

Figure 4.23 Mean and Mean-Plus-One-Standard-Deviation (Five Earthquake Records) of Weak Element Ductility Ratios for Target Ductility of 8 (Grouped by Omega Values)

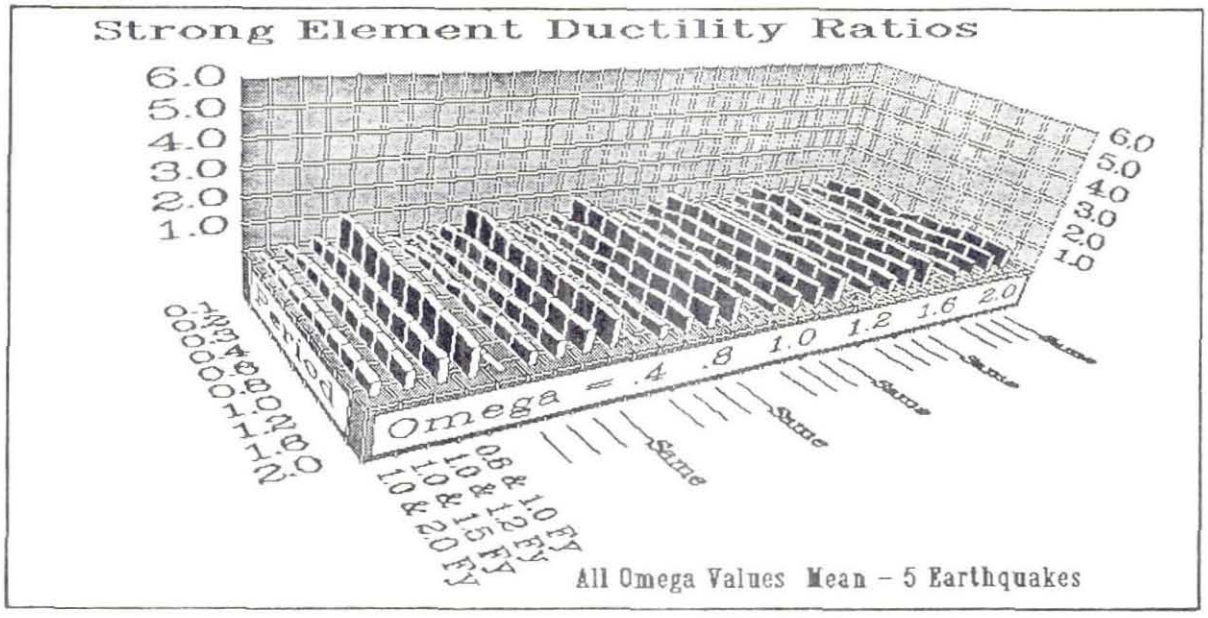

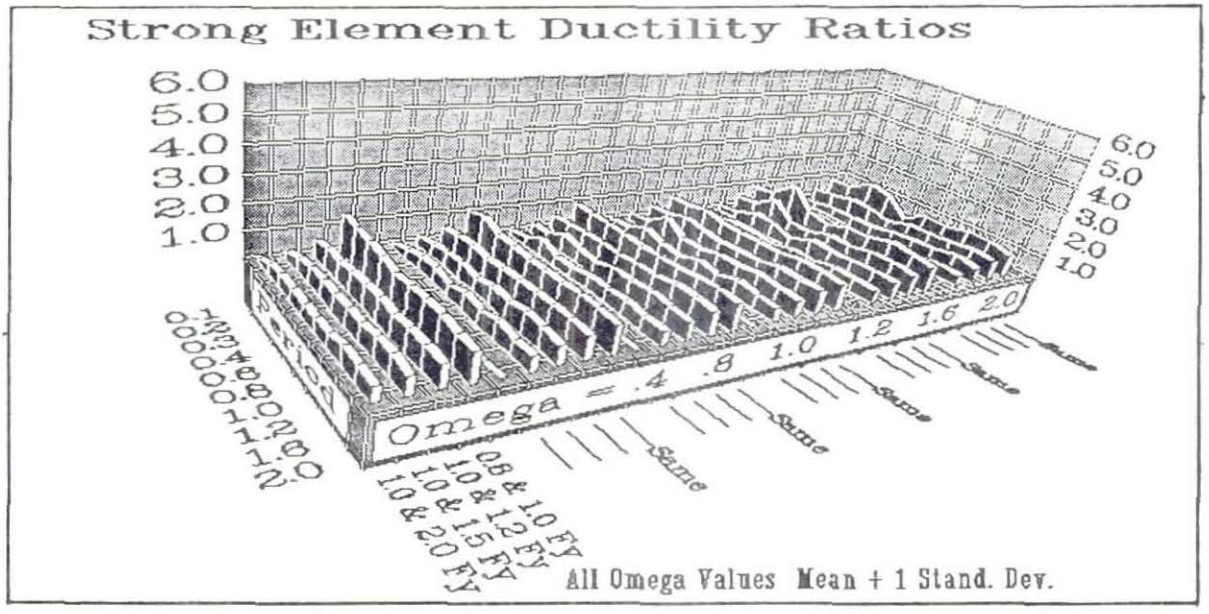

Figure 4.24 Mean and Mean-Plus-One-Standard-Deviation (Five Earthquake Records) of Strong Element Ductility Ratios for Target Ductility of 8 (Grouped by Omega Values)

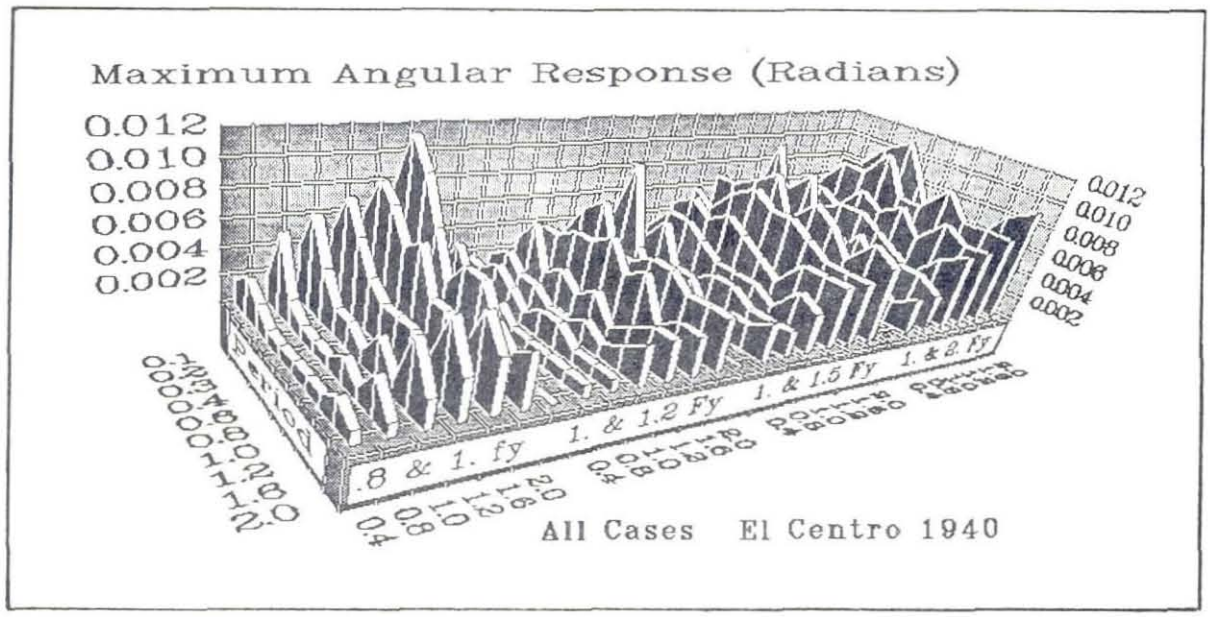

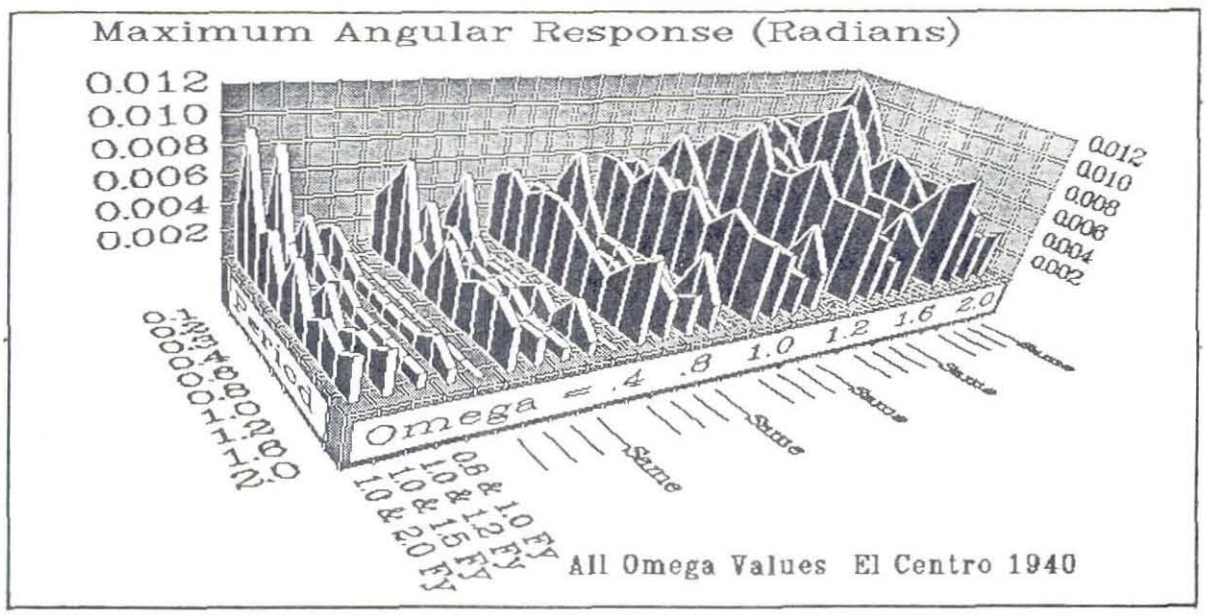

Figure 4.25 Maximum Angular Response of Systems for Target Ductility of 4 and El Centro Earthquake Record

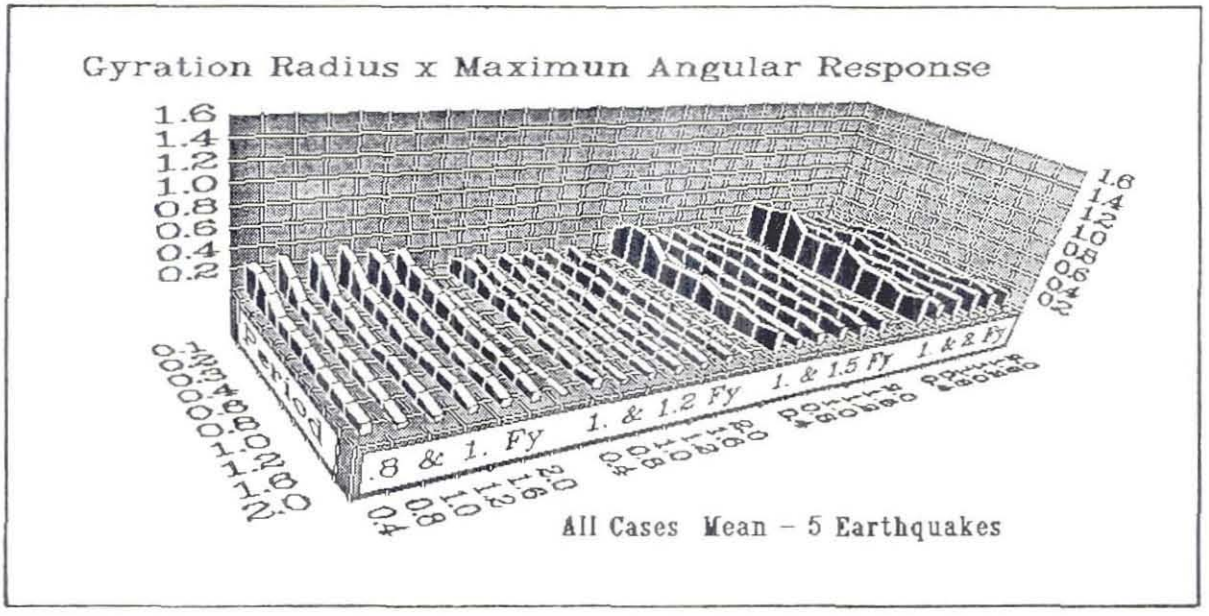

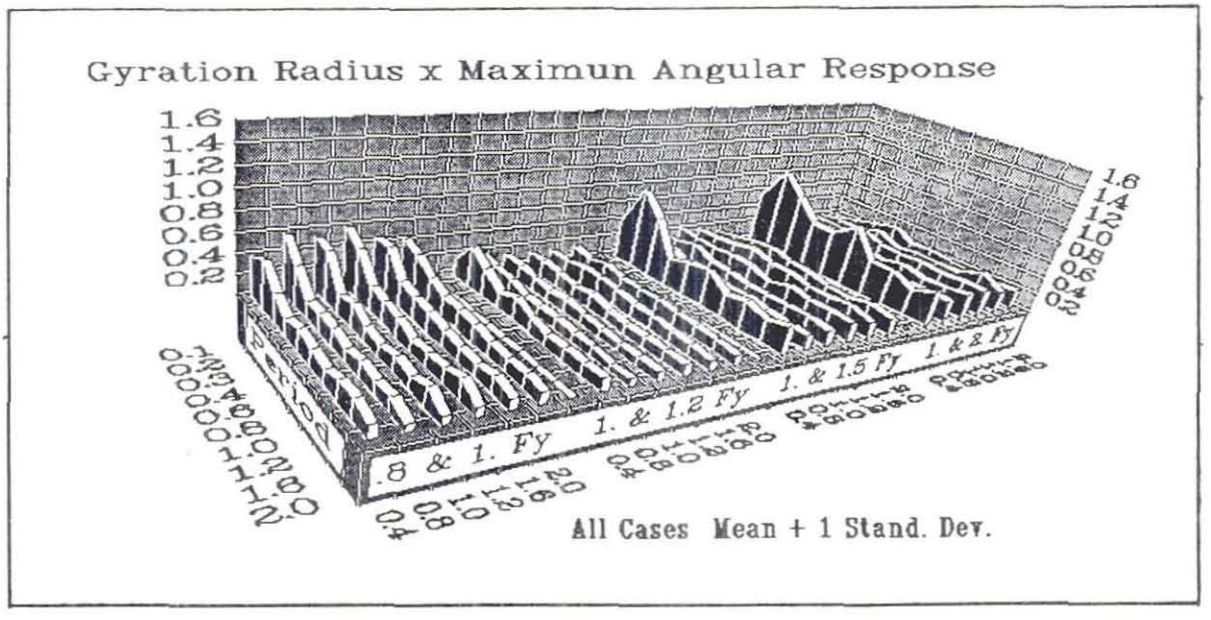

Figure 4.26 Mean and Mean-Plus-One-Standard-Deviation (Five Earthquake Records) of Gyration Radius Multiplied by the Maximum Angular Response of Systems for Target Ductility of 4

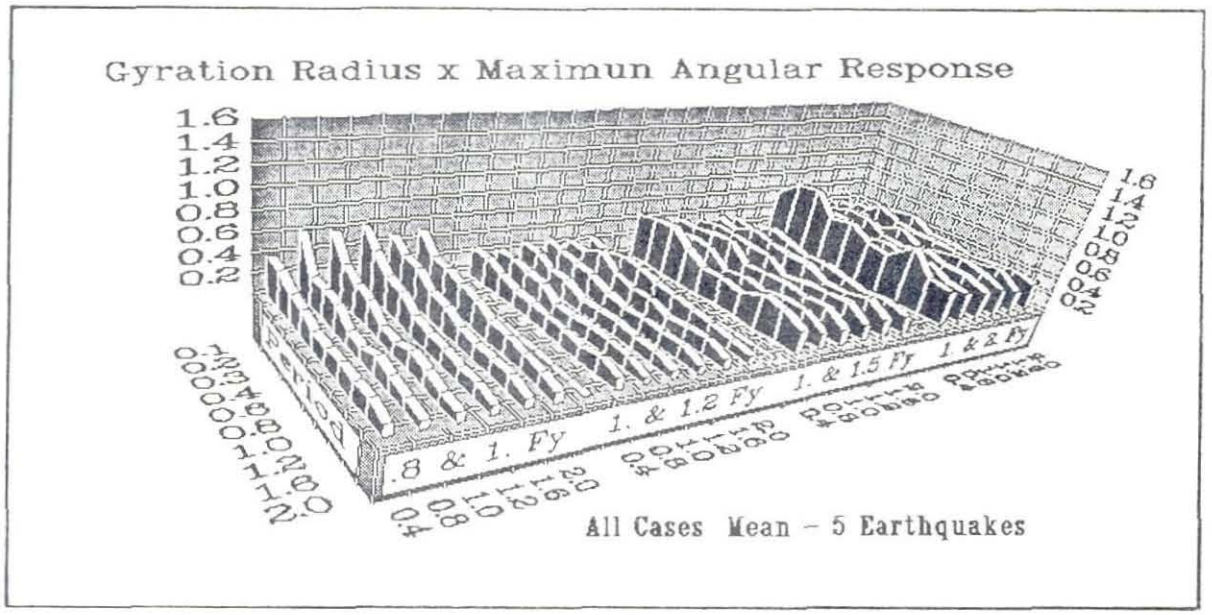

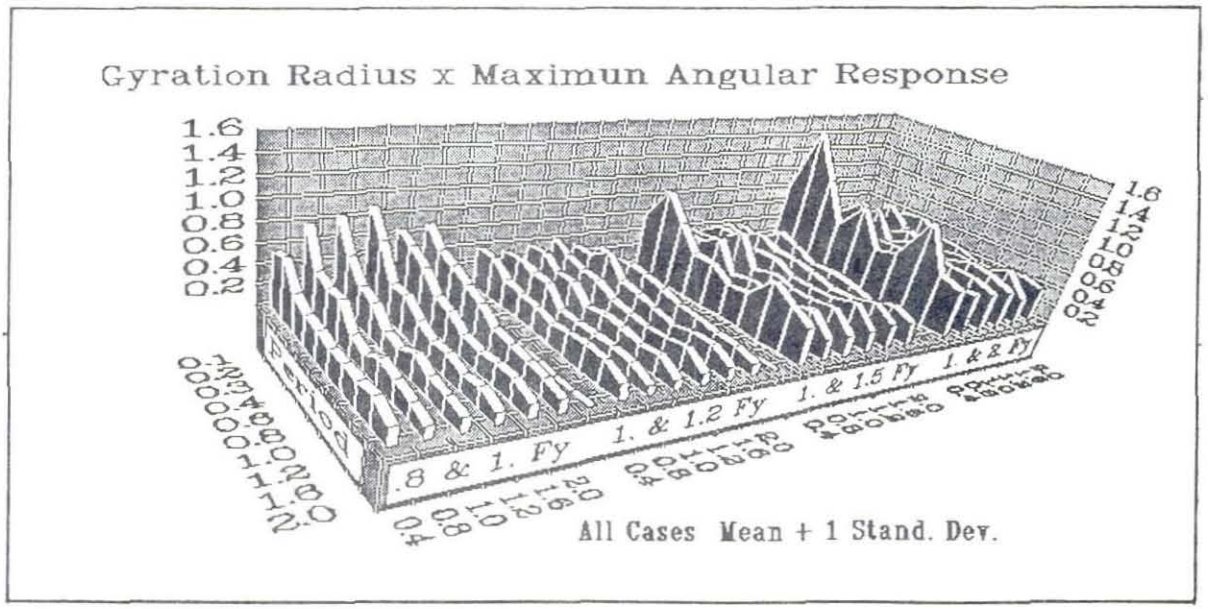

Figure 4.27 Mean and Mean-Plus-One-Standard-Deviation (Five Earthquake Records) of Gyration Radius Multiplied by the Maximum Angular Response of Systems for Target Ductility of 8

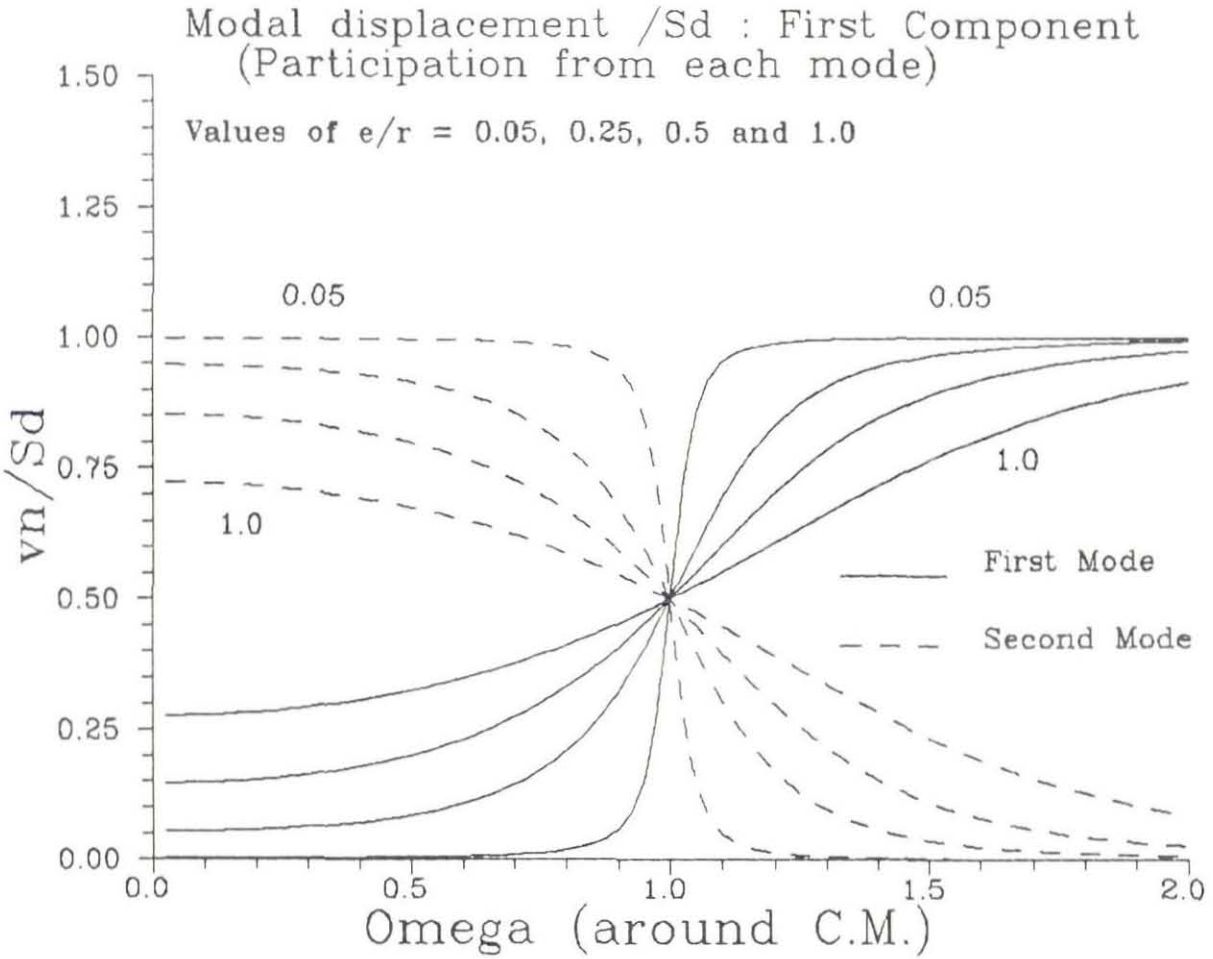

Figure 5.1 Participation from Each Mode to the First Component of the Modal Displacement

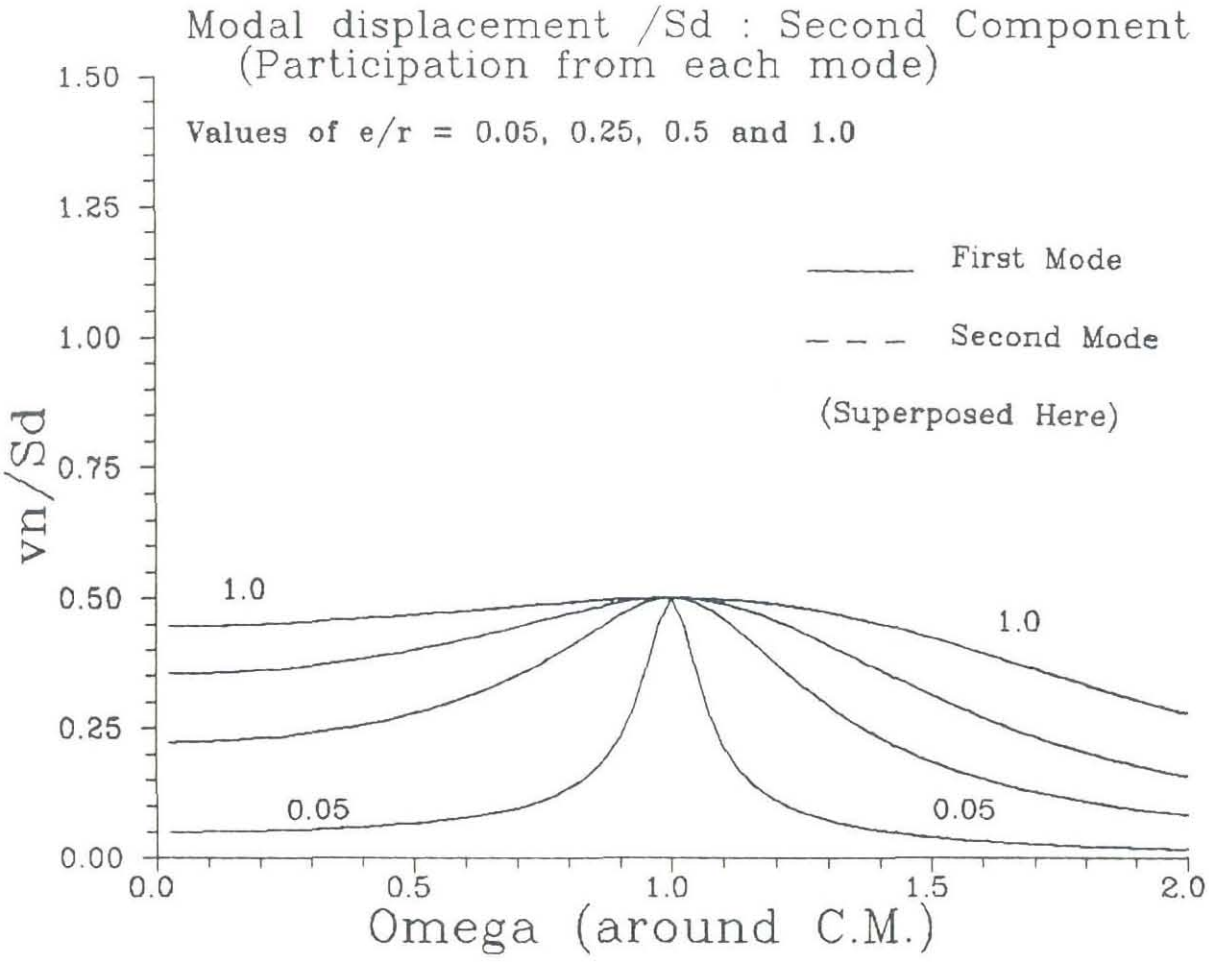

Figure 5.2 Participation from Each Mode to the Second Component of the Modal Displacement

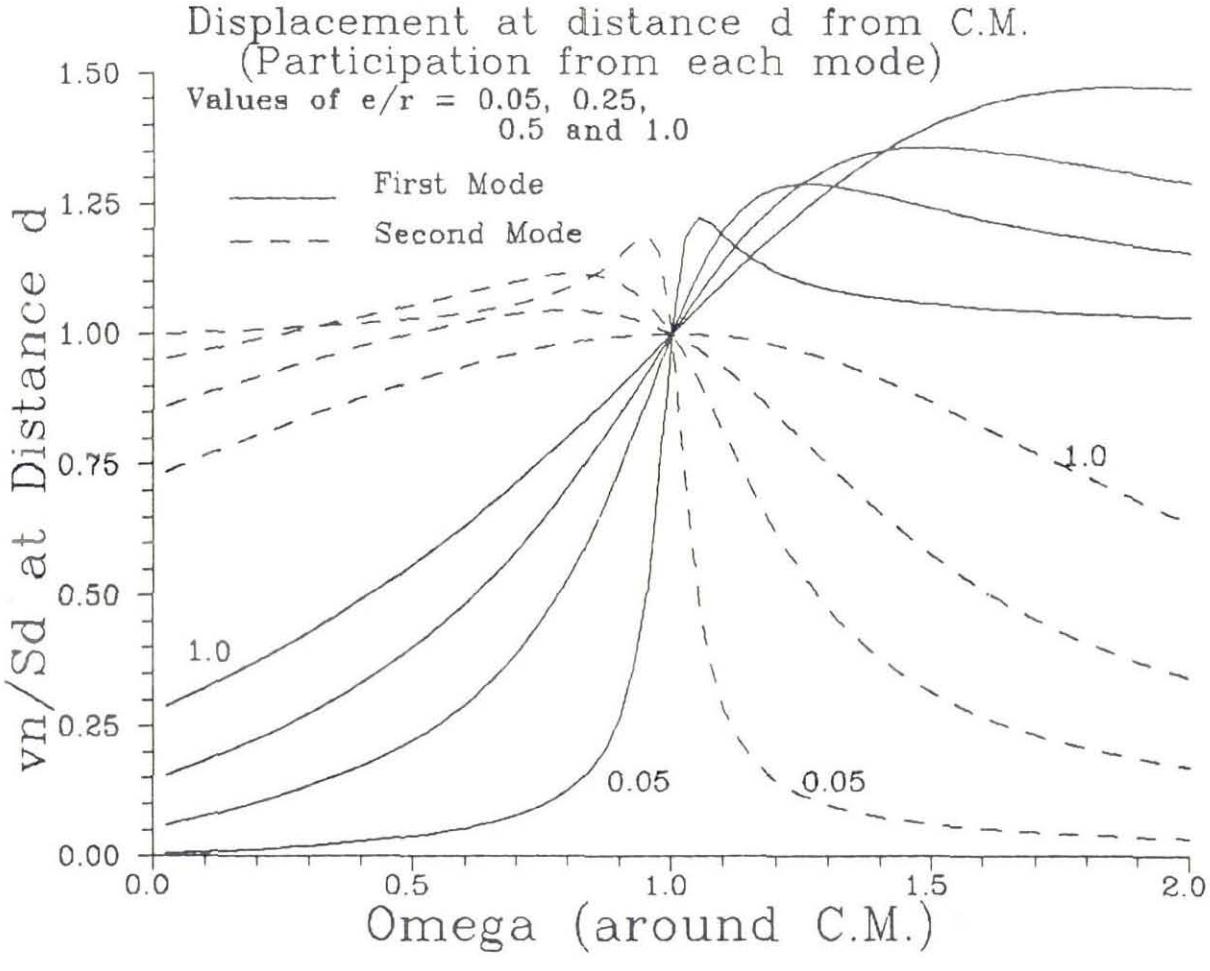

Figure 5.3 Participation from Each Mode to the Displacement at a Distance d from the Center of Mass

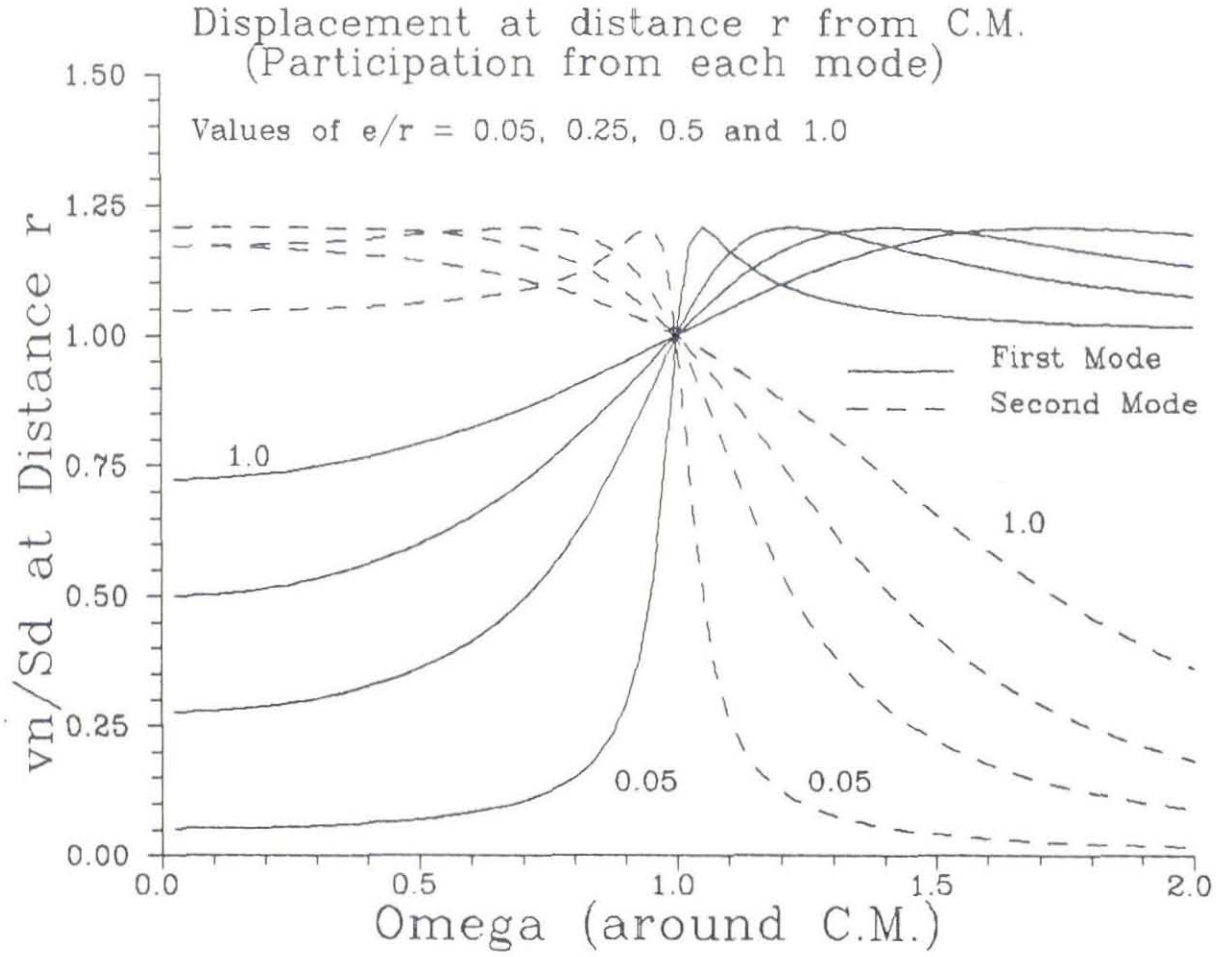

Figure 5.4 Participation from Each Mode to the Displacement at a Distance r from the Center of Mass

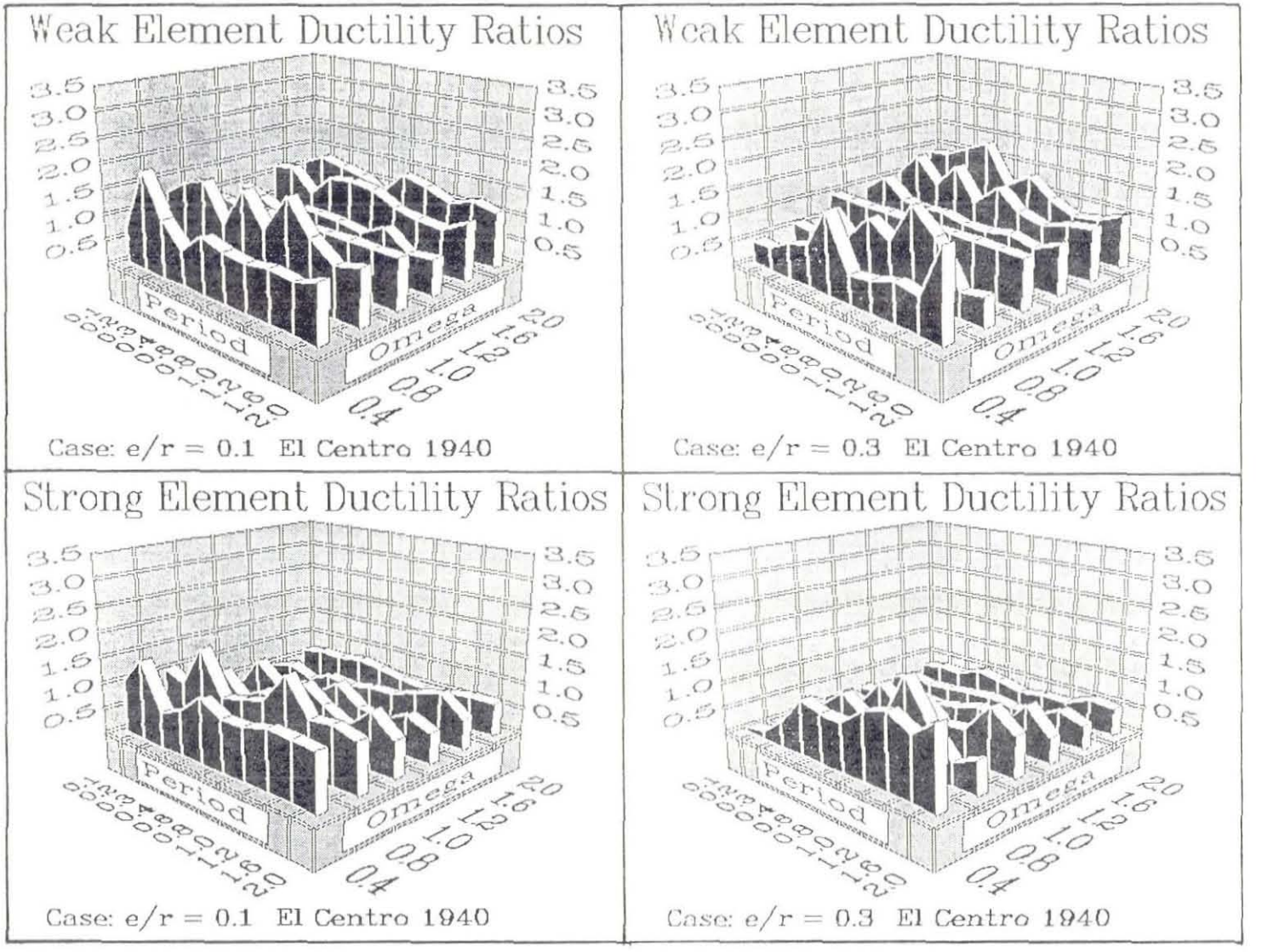

Figure 5.5 Weak and Strong Element Ductility Ratios for Target Ductility of 4 and El Centro Earthquake Record

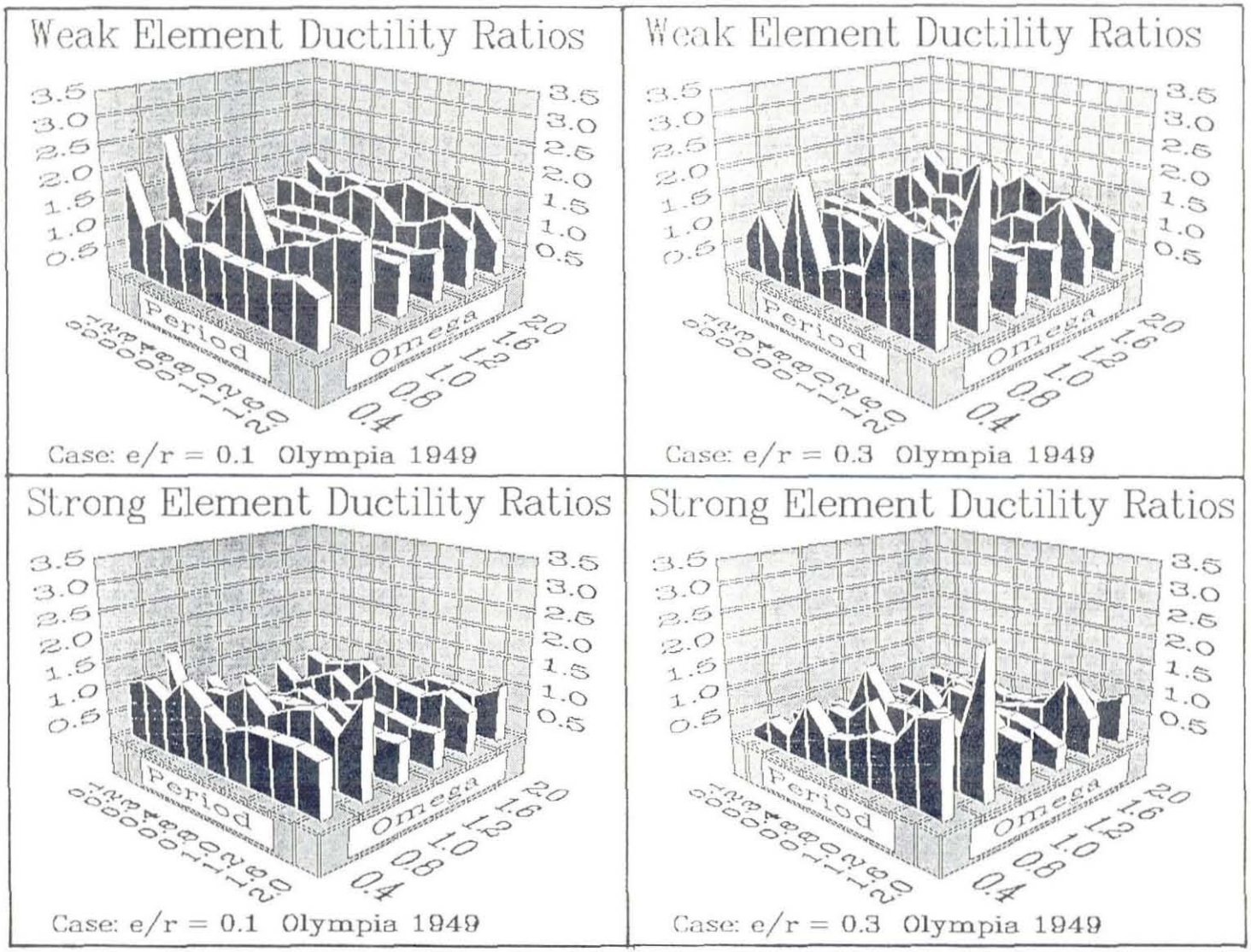

Figure 5.6 Weak and Strong Element Ductility Ratios for Target Ductility of 4 and Olympia Earthquake Record

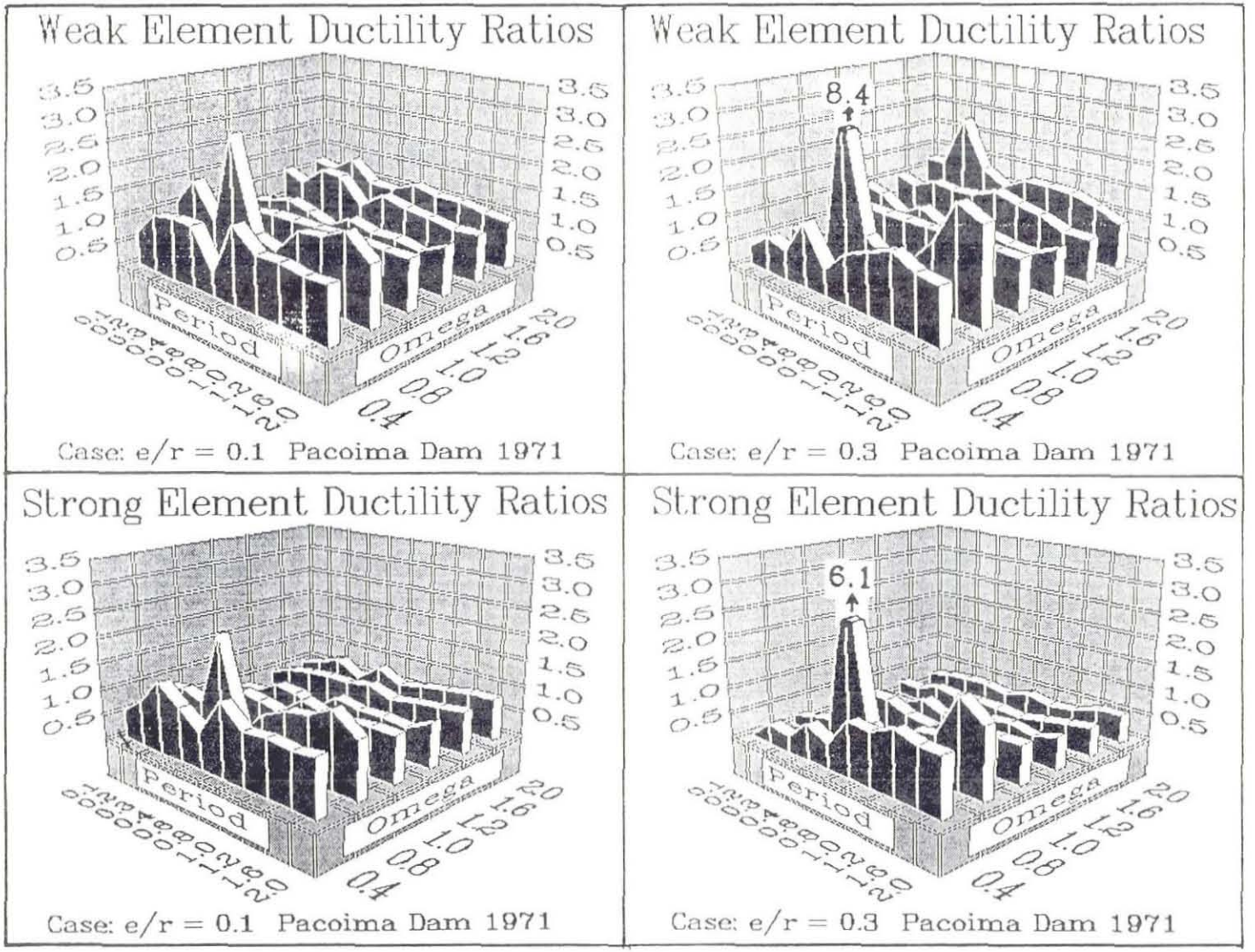

Figure 5.7 Weak and Strong Element Ductility Ratios for Target Ductility of 4 and Pacoima Dam Earthquake Record

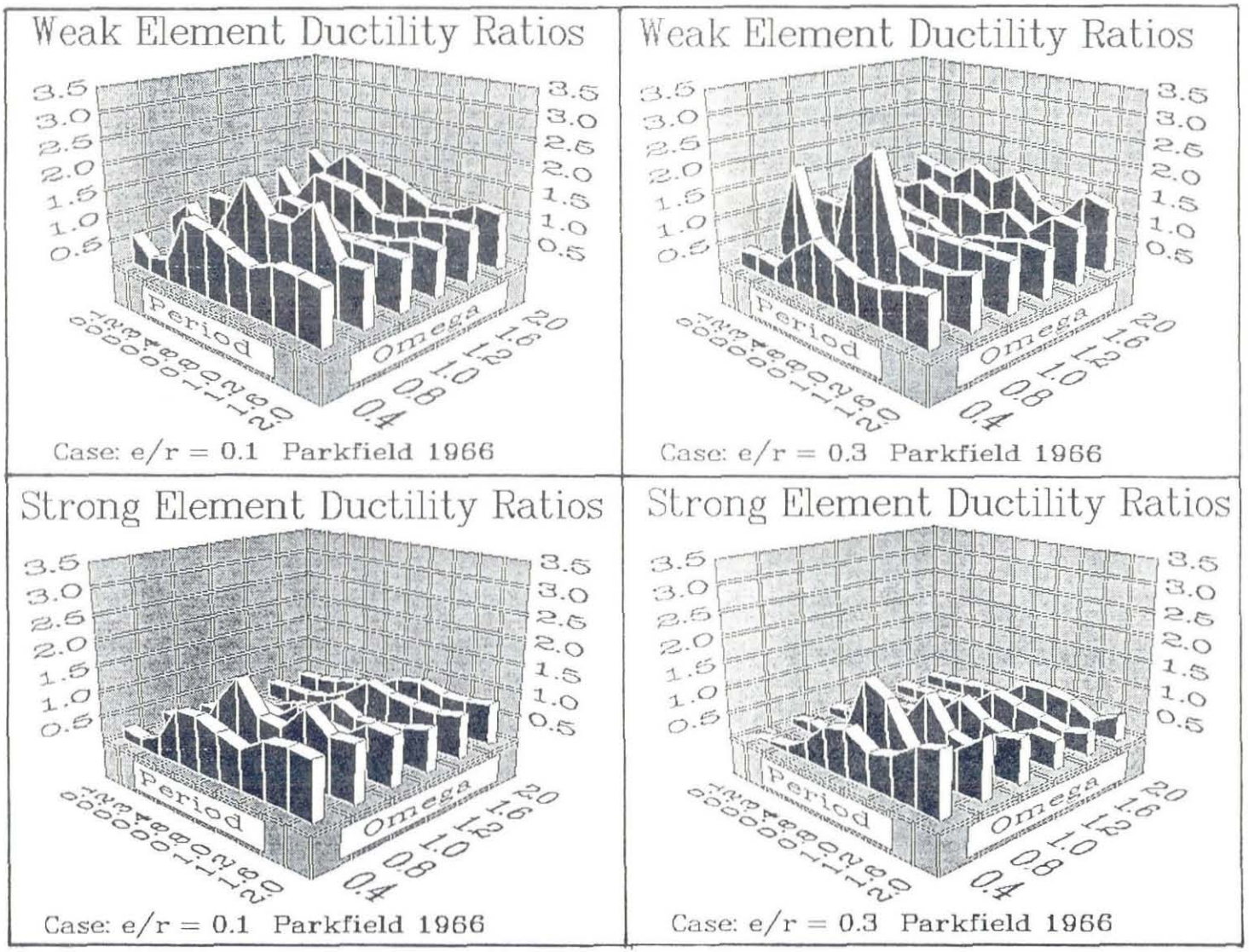

Figure 5.8 Weak and Strong Element Ductility Ratios for Target Ductility of 4 and Parkfield Earthquake Record

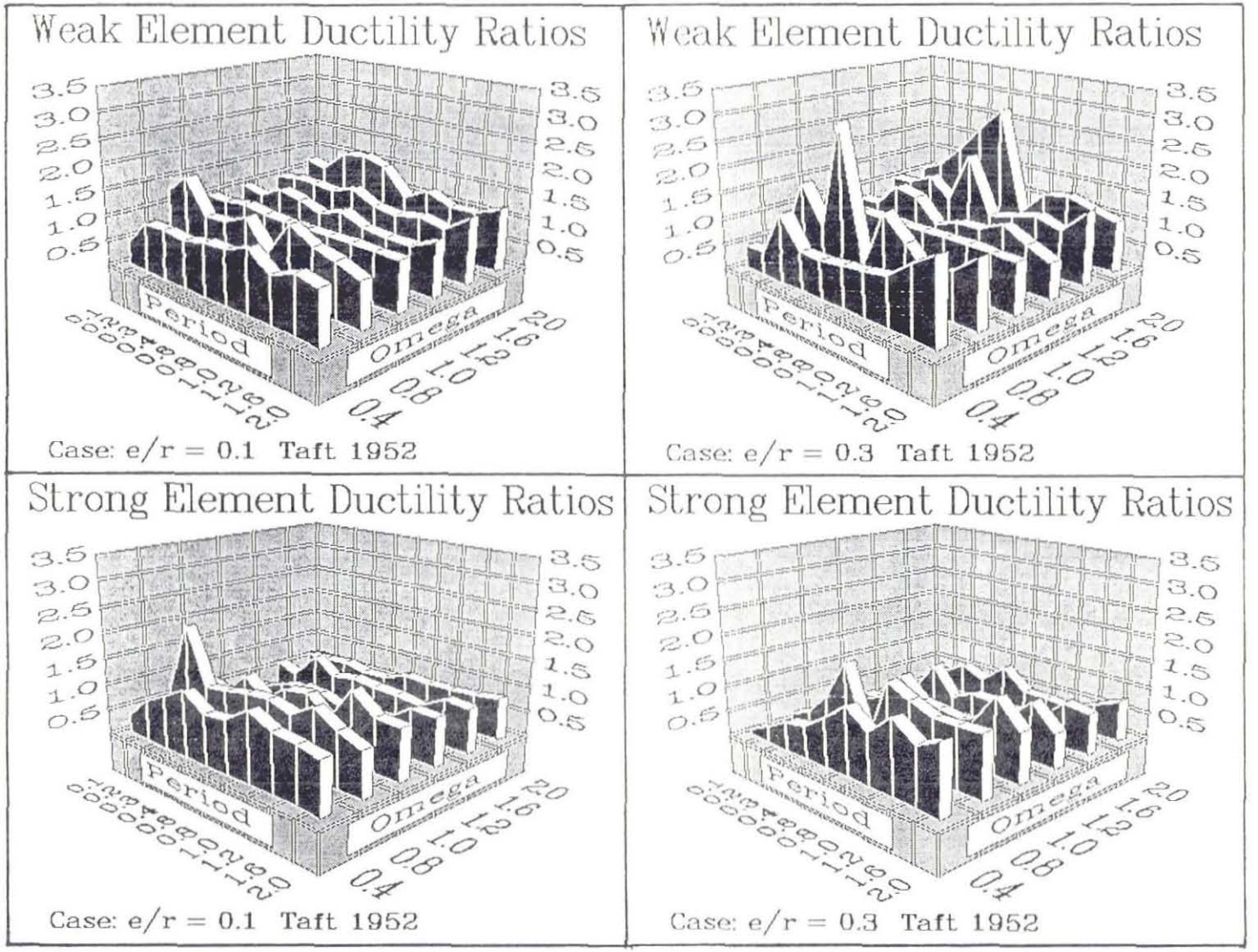

Figure 5.9 Weak and Strong Element Ductility Ratios for Target Ductility of 4 and Taft Earthquake Record

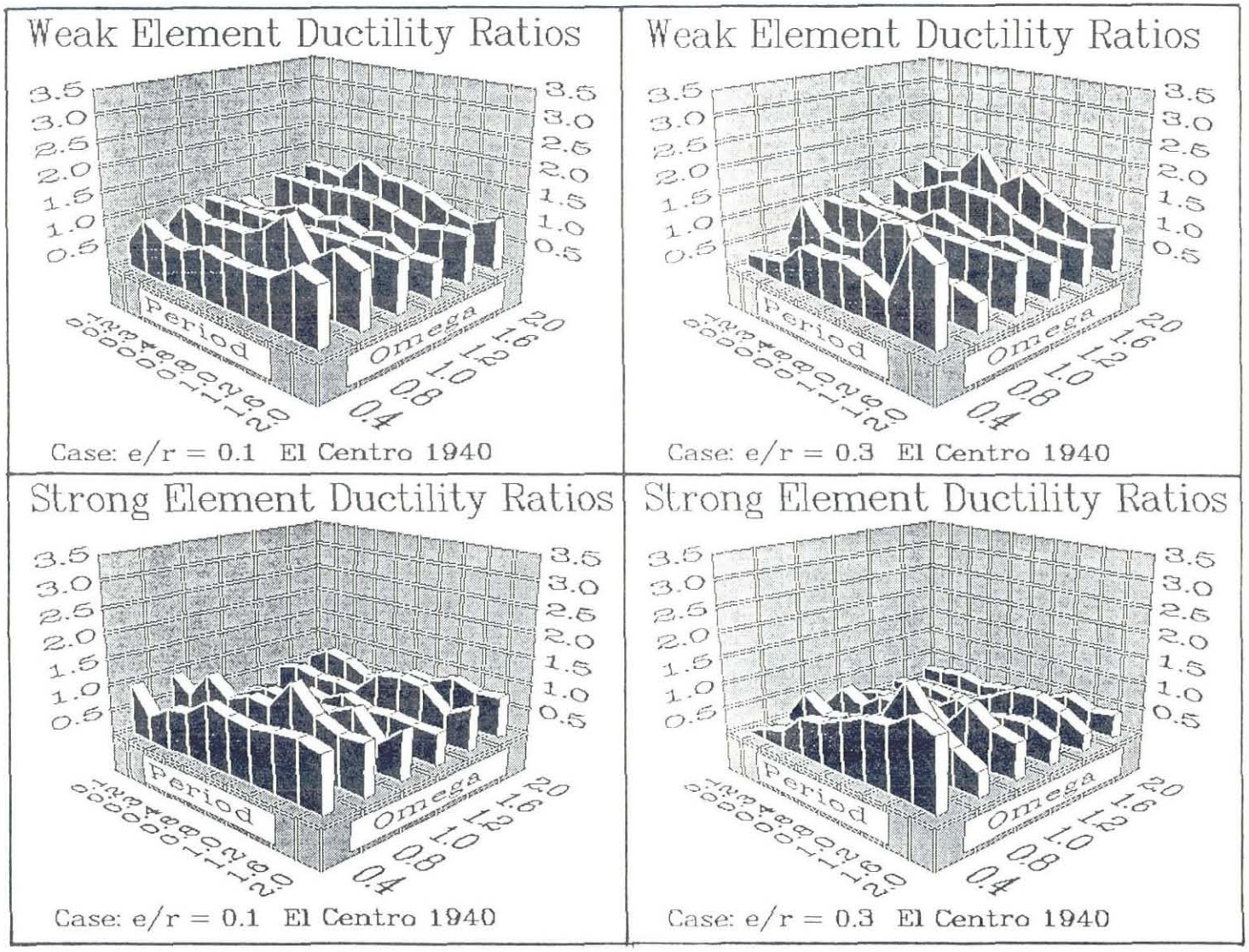

Figure 5.10 Weak and Strong Element Ductility Ratios for Target Ductility of 8 and El Centro Earthquake Record

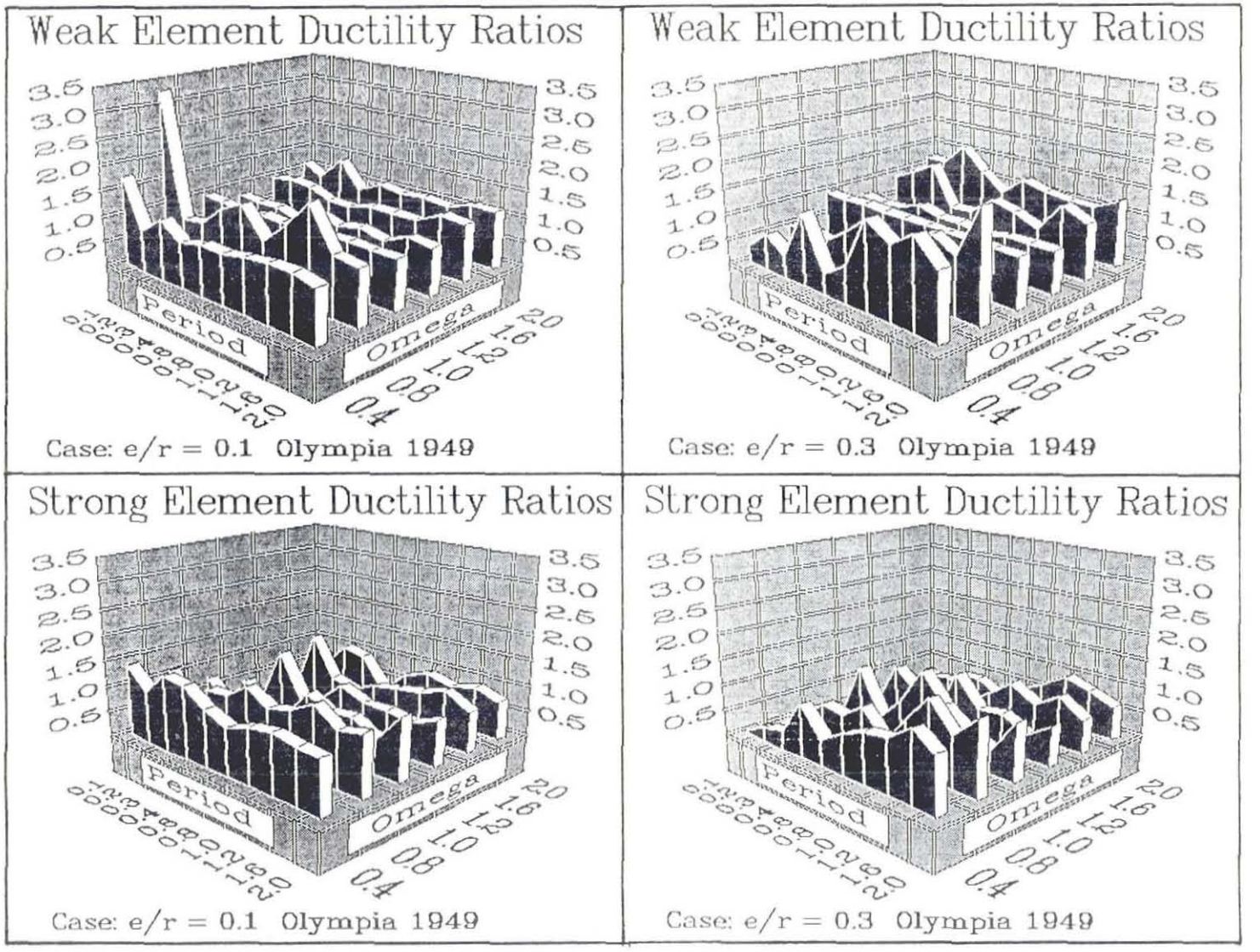

Figure 5.11 Weak and Strong Element Ductility Ratios for Target Ductility of 8 and Olympia Earthquake Record

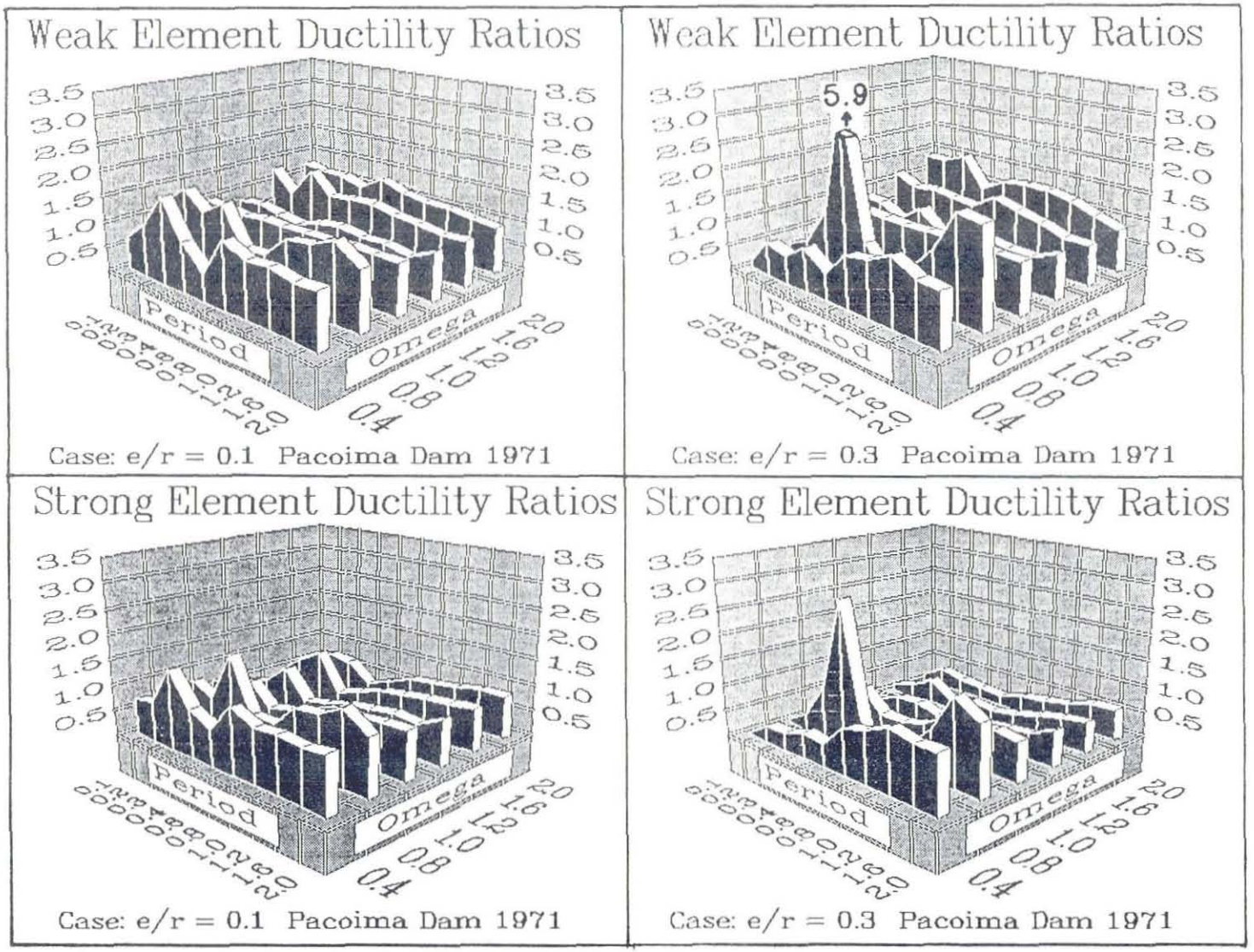

Figure 5.12 Weak and Strong Element Ductility Ratios for Target Ductility of 8 and Pacoima Dam Earthquake Record

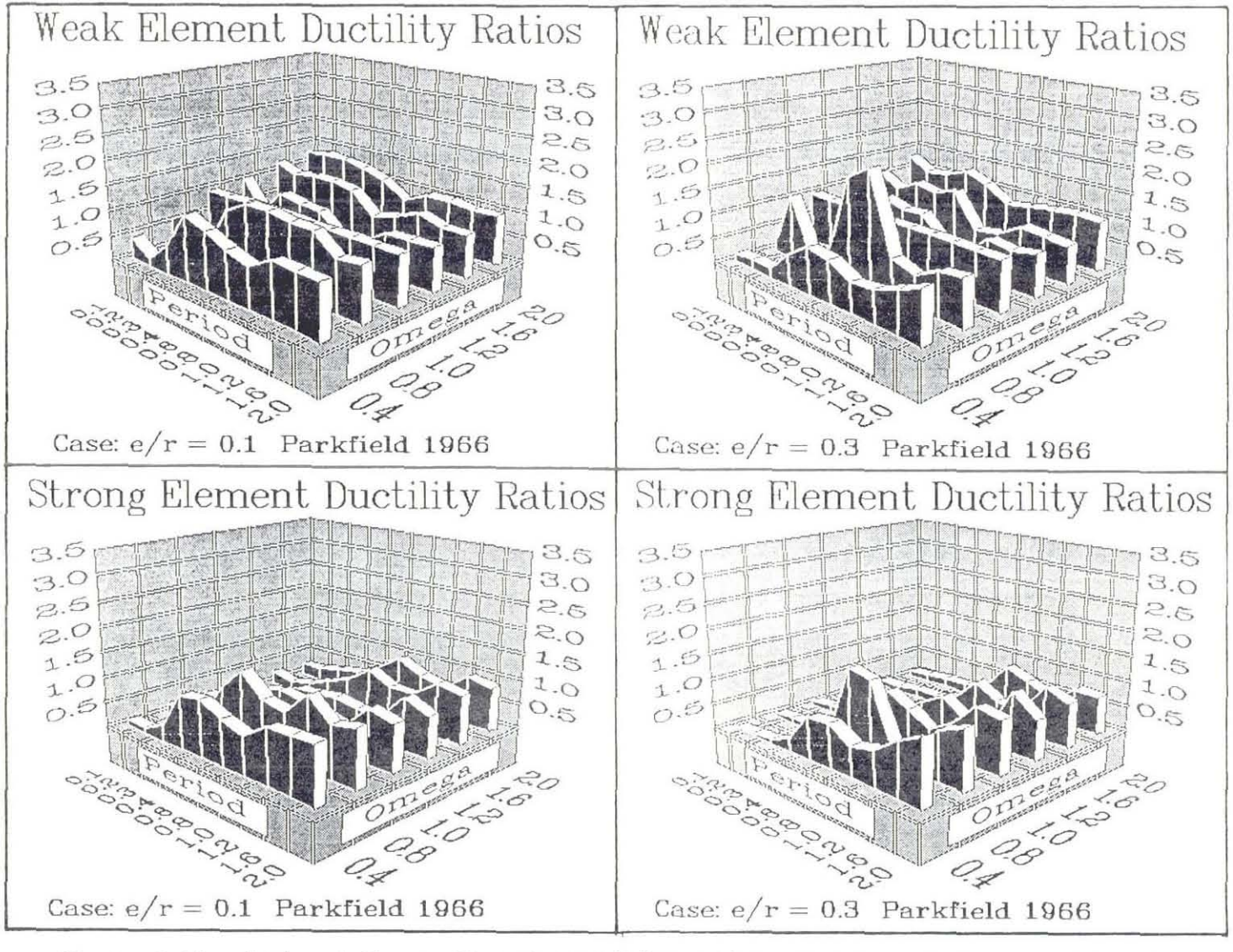

Figure 5.13 Weak and Strong Element Ductility Ratios for Target Ductility of 8 and Parkfield Earthquake Record

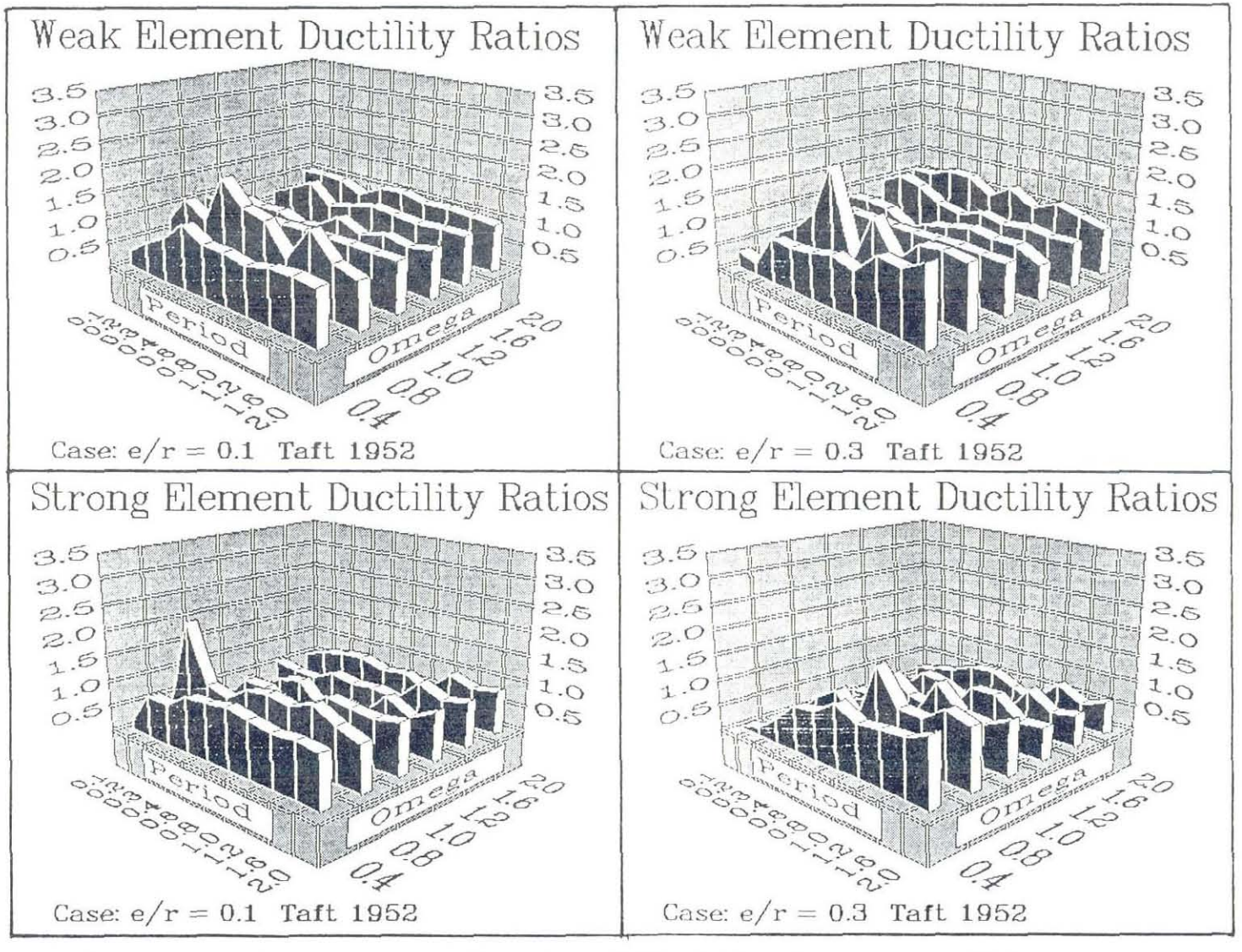

Figure 5.14 Weak and Strong Element Ductility Ratios for Target Ductility of 8 and Taft Earthquake Record

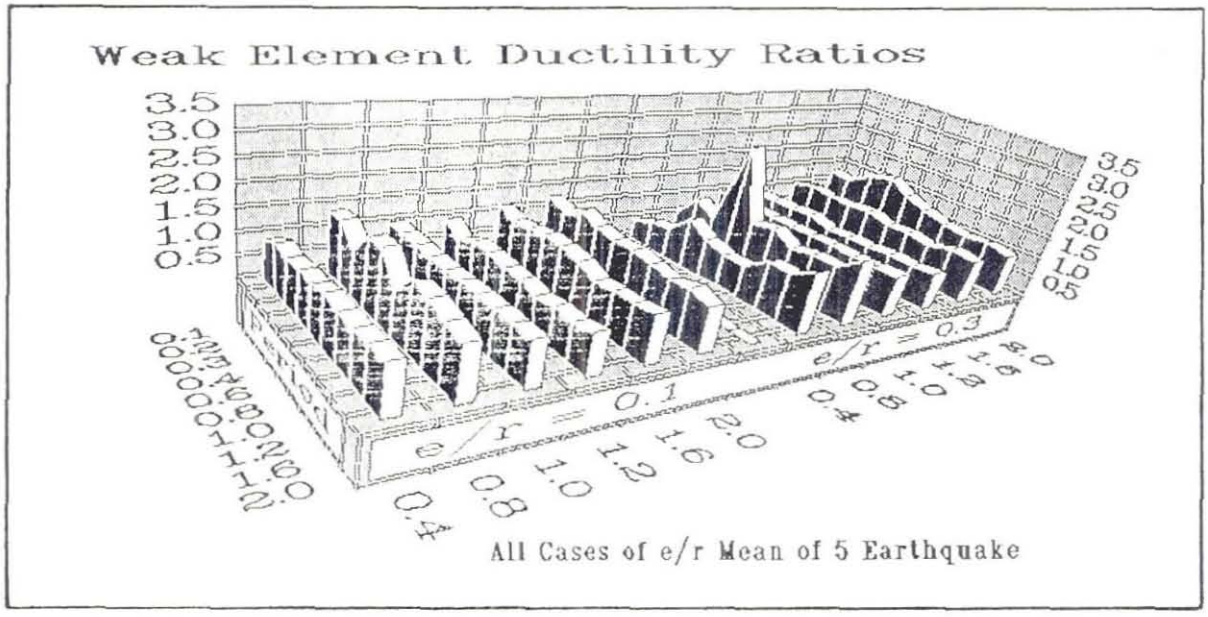

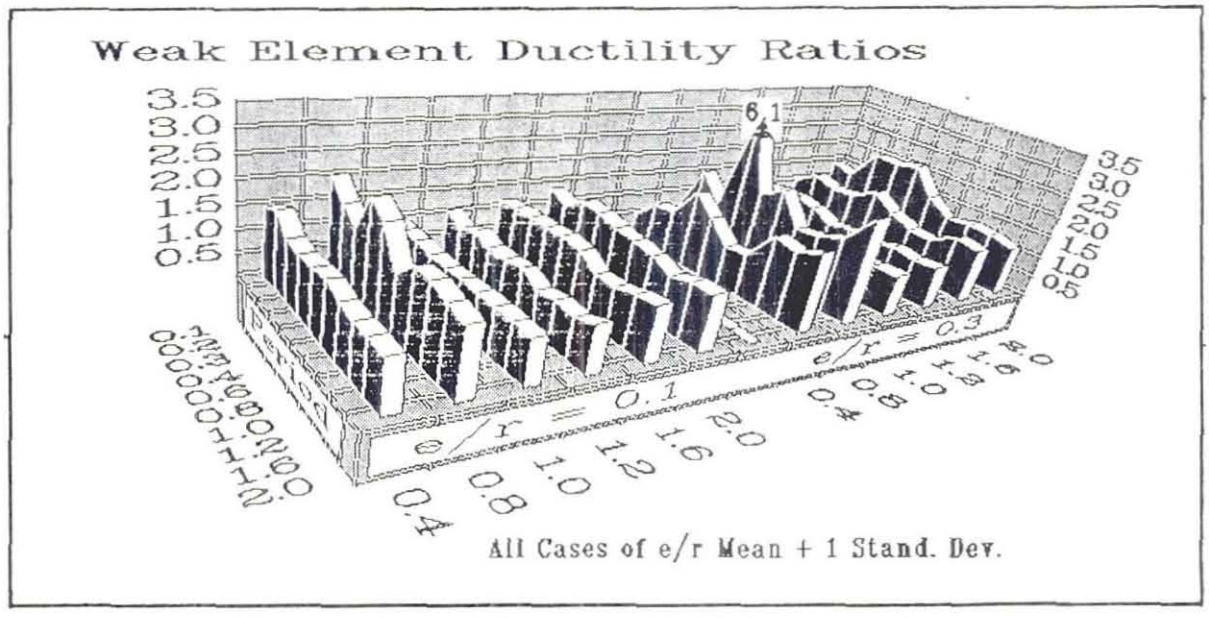

Figure 5.15 Mean and Mean-Plus-One-Standard-Deviation (Five Earthquake Records) of Weak Element Ductility Ratios for Target Ductility of 4

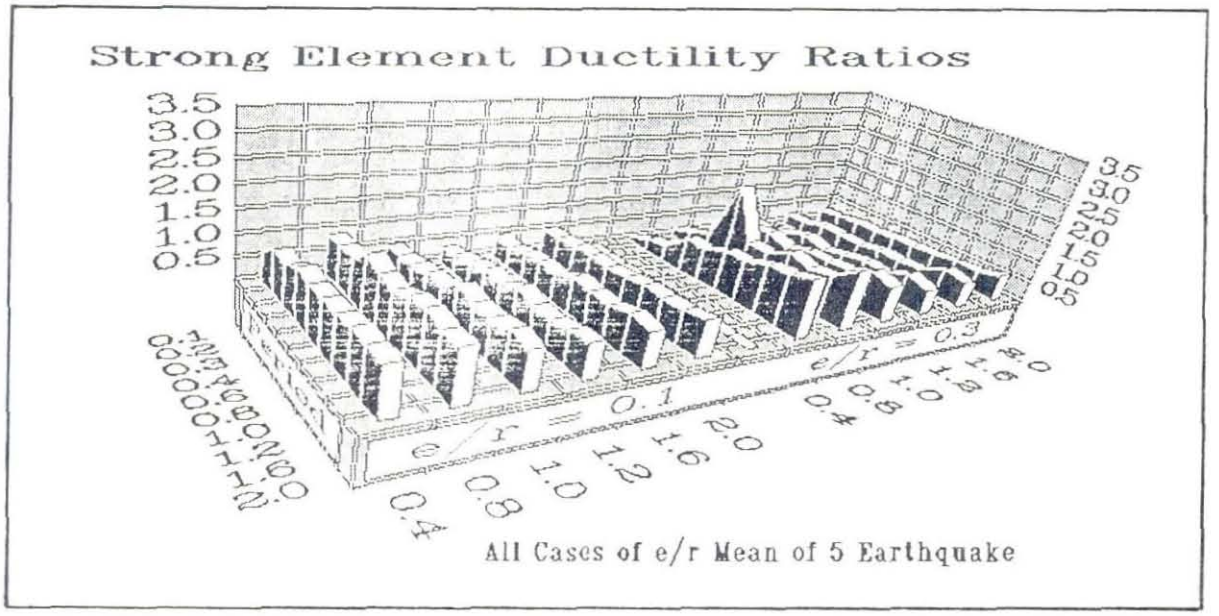

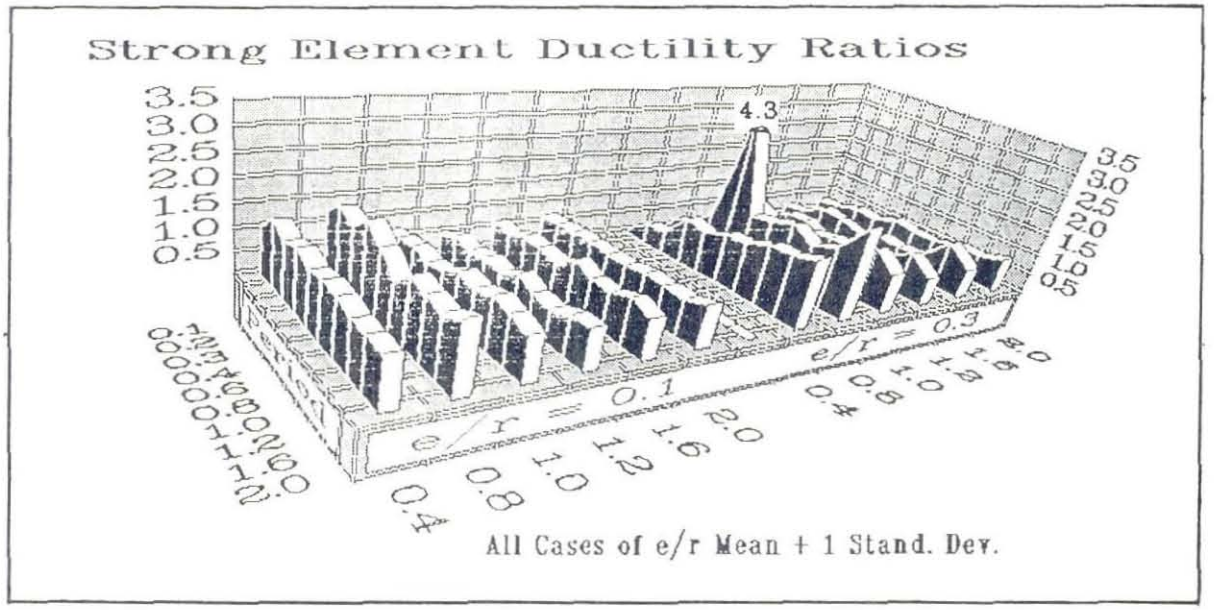

Figure 5.16 Mean and Mean-Plus-One-Standard-Deviation (Five Earthquake Records) of Strong Element Ductility Ratios for Target Ductility of 4

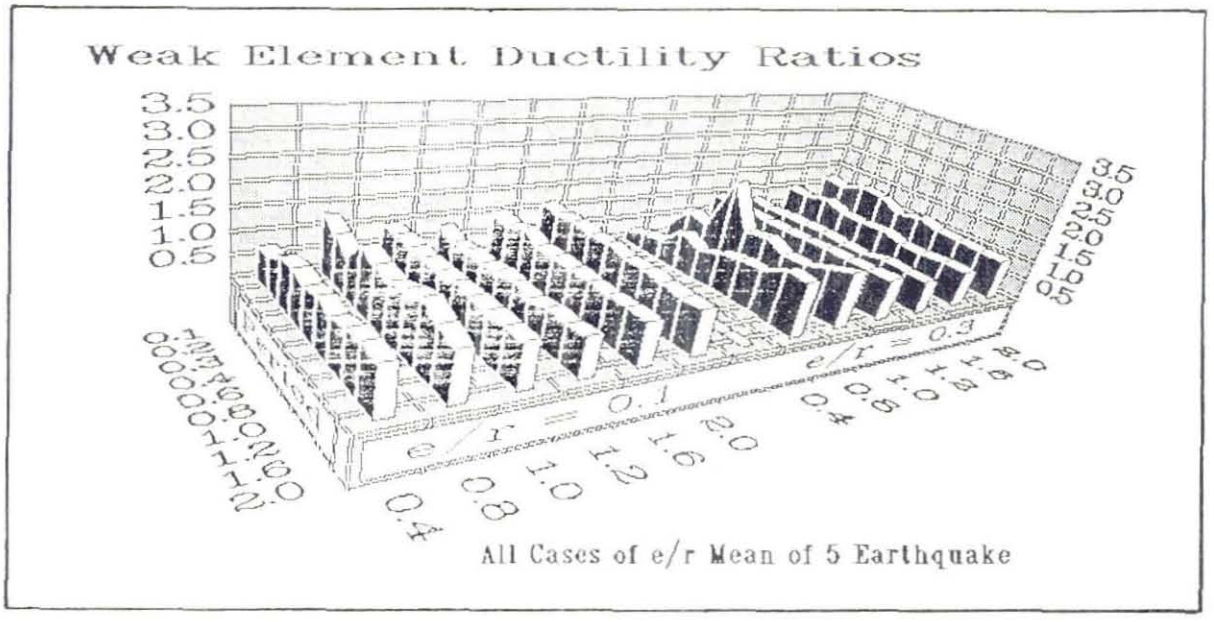

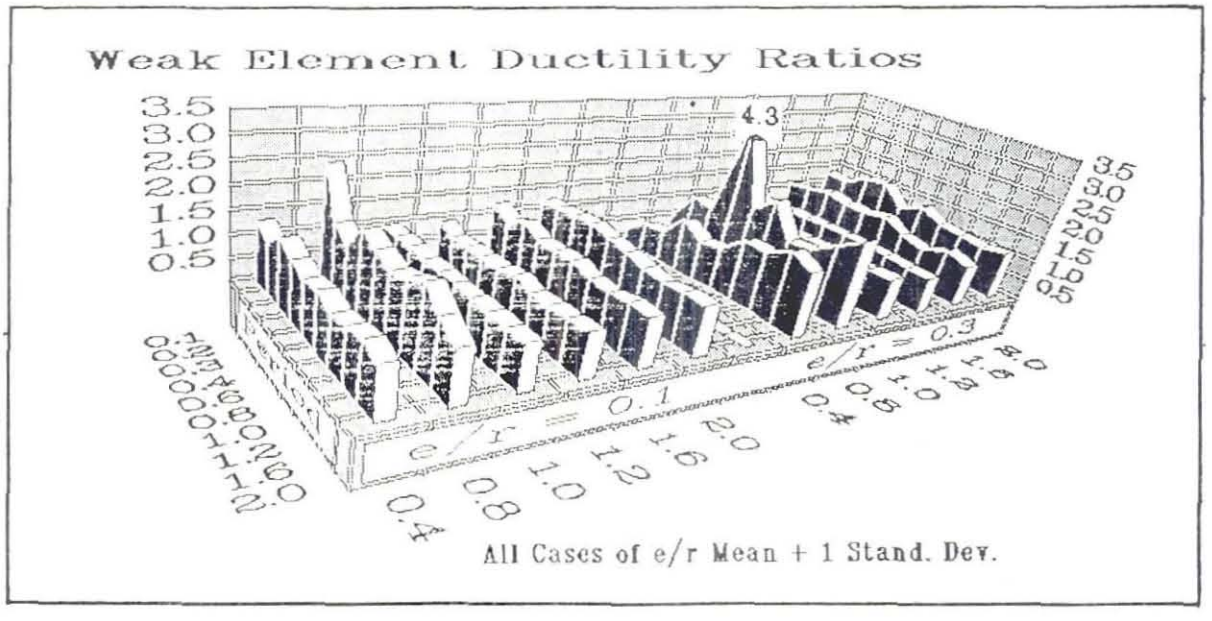

Figure 5.17 Mean and Mean-Plus-One-Standard-Deviation (Five Earthquake Records) of Weak Element Ductility Ratios for Target Ductility of 8

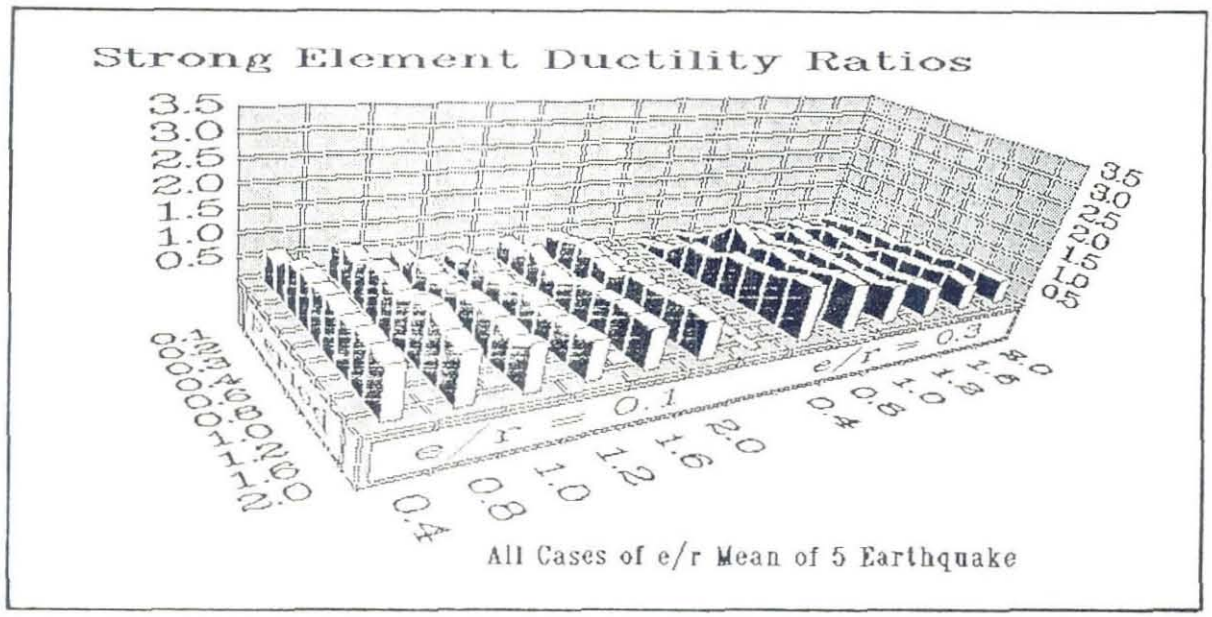

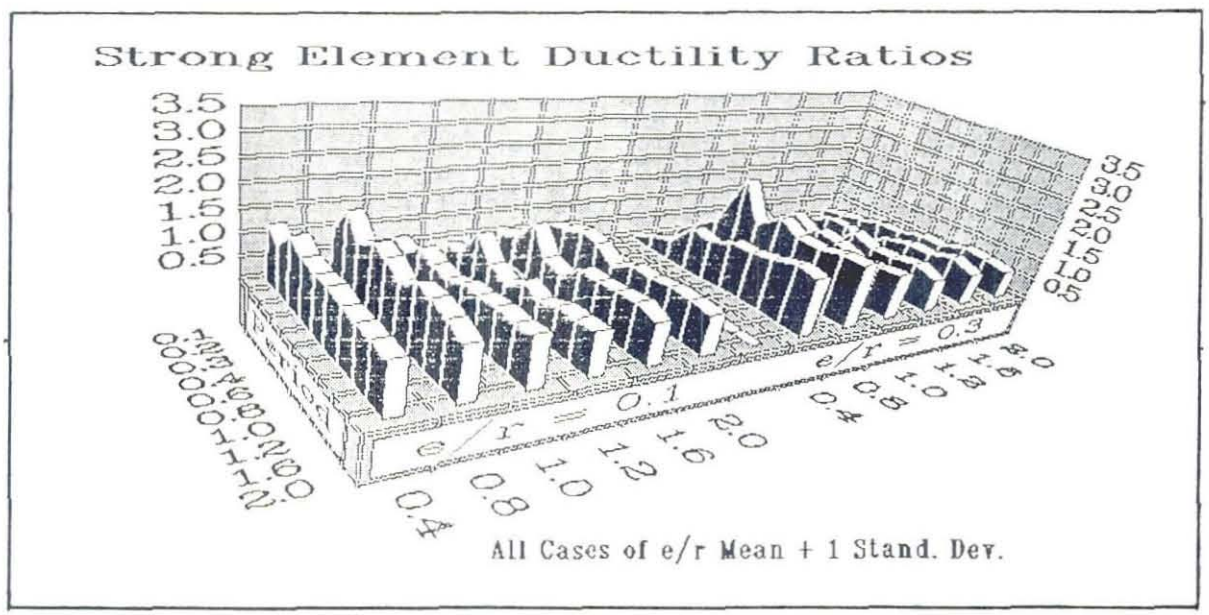

Figure 5.18 Mean and Mean-Plus-One-Standard-Deviation (Five Earthquake Records) of Strong Element Ductility Ratios for Target Ductility of 8

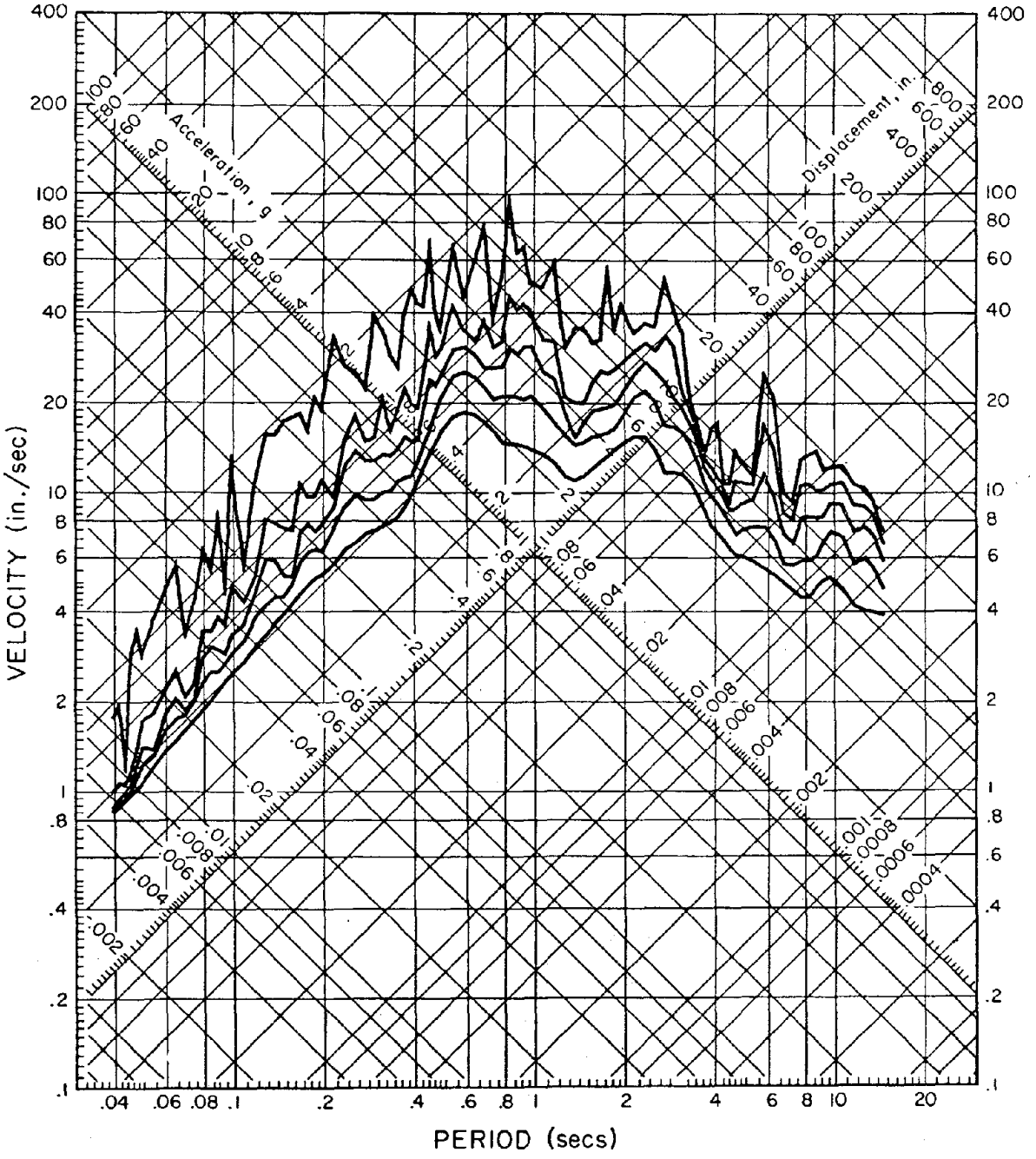

Figure 5.19: Response Spectrum - Imperial Valley Earthquake, May 18 1940 - 2037 PST, Comp S00E, Damping values of 0, 2, 5, 10 and 20 percent of critical (From Caltech Strong Motion Database Volume III).

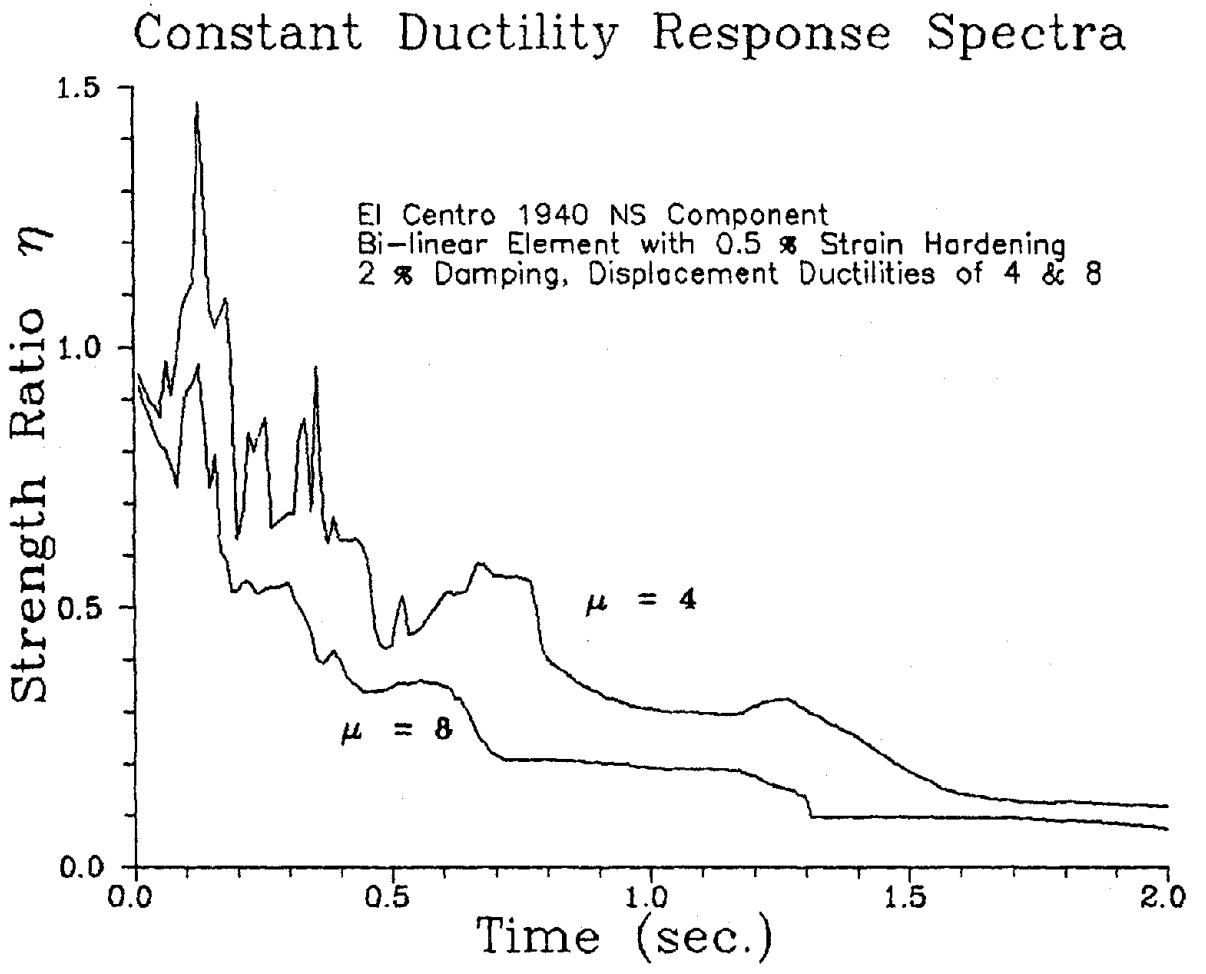

Figure 5.20 Constant Ductility Response Spectra for the N-S Component of the El Centro Earthquake, for Bi-Linear Element Model with 0.5% Strain Hardening and 2% Damping

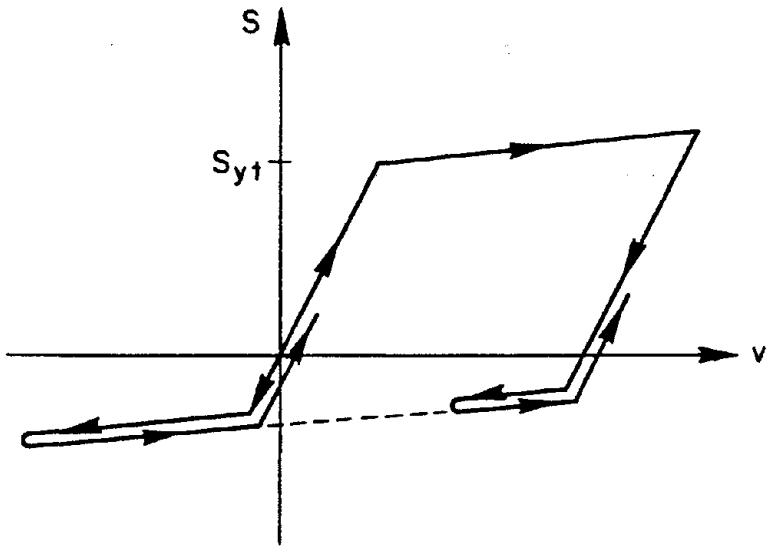

Figure 6.1: Inelastic Truss Element Model with Elastic Buckling (Yielding in Tension, Buckling in Compression) - From Mondkar & Powell (1975)

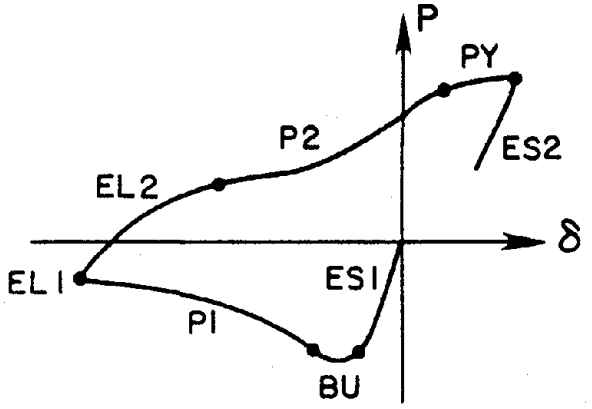

ES1 = Elastic Shortening Zone in Compression
BU = Buckling Zone
P1 = Plastic Zone in Compression
EL1 = Elastic Elongation Zone in Compression
EL2 = Elastic Elongation Zone in Tension
P2 = Plastic Zone in Tension
PY = Yielding Zone
ES2 = Elastic Shortening Zone in Tension

(a) P-δ Curve

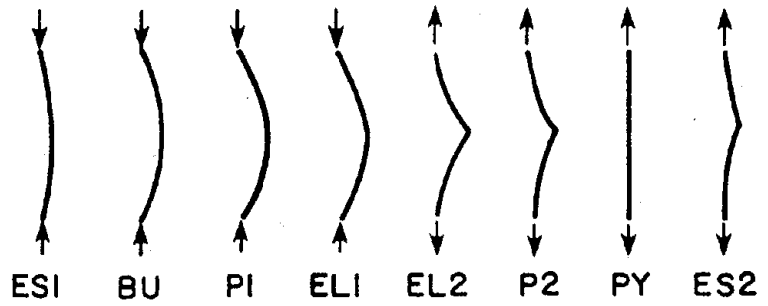

(b) Basic Behavior of a Brace associated with each Zone

Figure 6.2: Physical Brace Element Model - From Mahin & Ikeda (1984).

Appendix A:

Expansion of the step-by-step method for torsionnally coupled system:

A Newmark β-γ step-by-step method at a given step is usually described as follows (see Clough & Penzien (1975) [R?] for derivation of this results):

$$K^*(t) * \Delta v(t) = \Delta p^*(t)$$

where

$$K^*(t) = K(t) + \frac{1}{(\beta(\Delta t)^2)} m + \frac{\gamma}{(\beta\ \Delta t)} c(t)$$

and

$$\Delta p^*(t) = \Delta p(t) + m \left[\frac{1}{\beta \Delta t} \dot{v}(t) + \frac{1}{2\ \beta} \ddot{v}(t) \right]$$

$$+ c(t) \left[(\gamma/\beta)\ \dot{v}(t) + \Delta t\ (\gamma/2\beta - 1)\ \ddot{v}(t) \right]$$

For Constant Avereage Acceleration Method: $\beta = 1/4$ & $\gamma = 1/2$ (Unconditionally stable method)

For Linear Acceleration Method: $\beta = 1/6$ & $\gamma = 1/2$

Once $\Delta v(t)$ has been found, all other quantities can be easily calculated. For example, for the linear acceleration method, we would get:

$$\Delta \dot{v}(t) = \frac{3}{\Delta t} \Delta v(t) - 3\ \dot{v}(t) - \frac{\Delta t}{2} \ddot{v}(t)$$

$$v(t+\Delta t) = v(t) + \Delta v(t)$$

$$\dot{v}(t+\Delta t) = \dot{v}(t) + \Delta \dot{v}(t)$$

and $\ddot{v}(t+\Delta t)$ is calculated from the condition of dynamic equibrilium at time $t+\Delta t$

$$\ddot{v}(t+\Delta t) = m^{-1} \left[p(t+\Delta t) - f_D(t+\Delta t) - f_S(t+\Delta t) \right]$$

Specific Case of Two DOF Response for Torsionnally Coupled System:

As demonstrated previously, for a two DOF torsionnally coupled system, with the degrees of freedom located at the center of mass, the mass and stiffness matrices can be expanded as follow:

$$M = \begin{bmatrix} m & 0 \\ 0 & mr^2 \end{bmatrix} \qquad K = \begin{bmatrix} K_x & K_x e \\ K_x e & K_\theta \end{bmatrix}$$

and for typical Rayleigh Damping

$C(t) = a\,M + b\,K_i$ where K_i is the initial stiffness

When yielding of an element occurs, the state of the system is changed. In this case, the mass and damping matrices will not change but the stiffness matrix will.

Typically, the tangeant stiffness can be expressed as follow:

$$K_T = \begin{bmatrix} K_x' & K_x'e' \\ K_x'e' & K_\theta' \end{bmatrix}$$ where the primes (') indicate instantaneous properties!

Substituing this into the step-by-step equation, we get:

$$K^*(t) = \begin{bmatrix} K_x' & K_x'e' \\ K_x'e' & K_\theta' \end{bmatrix} + (C_1 + a\,C_2) \begin{bmatrix} m & 0 \\ 0 & mr^2 \end{bmatrix} + b\,C_2 \begin{bmatrix} K_x & K_x e \\ K_x e & K_\theta \end{bmatrix}$$

where $C_1 = \dfrac{1}{\beta(\Delta t)^2}$ and $C_2 = \gamma / (\beta \Delta t)$

are constants dependant on the Newmark method used.

Thus,

$$K^*(t) = \begin{bmatrix} K_x' + C_3 & K_x'e' + B_3 \\ K_x'e' + B_3 & K_\theta' + C_4 \end{bmatrix}$$

where

$$C_3 = (C_1 + a\,C_2)\,m + b\,C_2\,K_x$$
$$C_4 = (C_1 + a\,C_2)\,m + b\,C_2\,K_\theta$$
$$B_3 = b\,C_2\,K_x\,e$$

We can similarly expand and regroup the second term:

$$\Delta p^*(t) = \begin{bmatrix} \Delta p_1(t) \\ \Delta p_2(t) \end{bmatrix} + \begin{bmatrix} m\,[(B_4+B_6)\dot{v}_1(t) + (B_5+B_7)\ddot{v}_1(t)] \\ mr^2[(B_4+B_6)\dot{v}_2(t) + (B_5+B_7)\ddot{v}_2(t)] \end{bmatrix}$$

$$+ \begin{bmatrix} K_x\{B_8[\dot{v}_1(t)+e\dot{v}_2(t)] + B_9[\ddot{v}_1(t) + e\ddot{v}_2(t)]\} \\ K_\theta\{B_8[(K_x e/K_\theta)\dot{v}_1(t)+\dot{v}_2(t)] + B_9[(K_x e/K_\theta)\ddot{v}_1(t) + \ddot{v}_2(t)]\} \end{bmatrix}$$

Thus,

$$\Delta p^*(t) = \begin{bmatrix} \Delta p_1(t) \\ \Delta p_2(t) \end{bmatrix} + \begin{bmatrix} m\,C_8(t) \\ mr^2 C_9(t) \end{bmatrix} + \begin{bmatrix} K_x C_{10}(t) \\ K_\theta C_{11}(t) \end{bmatrix}$$

where

$B_4 = 1 / \beta\Delta t$ $\quad B_6 = \gamma a / \beta$ $\quad B_8 = \Delta t[(\gamma/2\beta)-1]a$

$B_5 = 1 / 2\beta$ $\quad B_7 = \gamma b / \beta$ $\quad B_9 = \Delta t[(\gamma/2\beta)-1]b$

$$C_8(t) = (B_4+B_6)\dot{v}_1(t) + (B_5+B_7)\ddot{v}_1(t)$$
$$C_9(t) = (B_4+B_6)\dot{v}_2(t) + (B_5+B_7)\ddot{v}_2(t)$$
$$C_{10}(t) = B_8[\dot{v}_1(t)+e\dot{v}_2(t)] + B_9[\ddot{v}_1(t)+e\ddot{v}_2(t)]$$
$$C_{11}(t) = B_8[(K_x e/K_\theta)e\dot{v}_1(t)+\dot{v}_2(t)] + B_9[(K_x e/K_\theta)\ddot{v}_1(t)+\ddot{v}_2(t)]$$

Now solving for a particular step of the step-by-step method, we will get:

$$\Delta v(t) = \begin{bmatrix} \Delta v_1(t) \\ \Delta v_2(t) \end{bmatrix} = [K^*(t)]^{-1}\,\Delta p^*(t)$$

$$[K^*(t)]^{-1} = \frac{1}{DET}\begin{bmatrix} K_\theta' + C_4 & -(K_x' e' + B_3) \\ \text{sym.} & (K_x' + C_3) \end{bmatrix}$$

$$DET = K_x' K_\theta' + C_3 K_\theta' + K_x' C_4 + C_3 C_4 - K_x' e'^2 - 2K_x' e' B_3 - B_3^2$$

$$\begin{aligned} DET/(m^2 r^2) = {} & \omega_x^2{}'\omega_\theta^2{}' \\ & + [C_1 + aC_2 + bC_2\omega_x^2]\omega_\theta^2{}' \\ & + [C_1 + aC_2 + bC_2\omega_\theta^2]\omega_x^2{}' \\ & + [C_1 + aC_2 + bC_2\omega_\theta^2][C_1 + aC_2 + bC_2\omega_x^2] \\ & - \omega_x^4{}'(e'/r)^2 \\ & - 2\omega_x^2\omega_x^2{}'(e'/r)(e/r)bC_2 \\ & - b^2 C_2\omega_x^4(e/r)^2 \end{aligned}$$

$$DET = m^2 r^2 \ \text{function}[\omega_x, \omega_\theta, (e/r), \omega_x', \omega_\theta', (e'/r)]$$

And now,

$$\Delta v_1(t) = \frac{1}{DET}\,[K_\theta' + C_4]\Delta p''_1(t) - [K_x' e' + B_3]\Delta p''_2(t)$$

$$\Delta v_2(t) = \frac{1}{DET}\,[K_x' + C_3]\Delta p''_2(t) - [K_x' e' + B_3]\Delta p''_1(t)$$

Expanding these values:

$$[K_x' e' + B_3] = mr\,[\omega_x^2{}'(e'/r) + bC_2\,\omega_x^2(e/r)]$$

$$[K_x' + C_3] = m\,[\omega_x^2{}' + C_1 + aC_2 + bC_2\,\omega_x^2]$$

$$[K_\theta' + C_4] = mr^2\,[\omega_\theta^2{}' + C_1 + aC_2 + bC_1\,\omega_\theta^2]$$

$$\Delta p''_1(t) = m\,\{\Delta\ddot{v}_g(t) + (B_4 + B_6)\dot{v}_1(t) + (B_5 + B_7)\ddot{v}_1(t) + \omega_x^2[B_8(\dot{v}_1(t) + (e/r)r\dot{v}_2(t)) + B_9(\ddot{v}_1(t) + (e/r)r\ddot{v}_2(t))]\}$$

$$\Delta p''_2(t) = mr\,[(B_4 + B_6)r\dot{v}_2(t) + (B_5 + B_7)r\ddot{v}_2(t) + B_8(\omega_x^2(e/r)\dot{v}_1(t) + \omega_\theta^2 r\dot{v}_2(t)) + B_9(\omega_x^2(e/r)\ddot{v}_1(t) + \omega_\theta^2 r\ddot{v}_2(t))]$$

if $\Delta p_1(t) = m\ddot{v}_g(t)$ and $\Delta p_2(t) = 0$

By doing the direct combination of the terms above, we demonstrate that the terms $\Delta v_1(t)$ and $r\Delta v_2(t)$ are a direct function of the following variables:

$$\Delta v_1(t) = \text{function}[\omega_x^2, \omega_\theta^2, (e/r), \omega_x^2{}', \omega_\theta^2{}', (e'/r), \Delta\ddot{v}_g(t), \dot{v}_1(t), r\dot{v}_2(t), \ddot{v}_1(t) \text{ and } r\ddot{v}_2(t)]$$

$$r\Delta v_2(t) = \text{function}[\omega_x^2, \omega_\theta^2, (e/r), \omega_x^2{}', \omega_\theta^2{}', (e'/r), \Delta\ddot{v}_g(t), \dot{v}_1(t), r\dot{v}_2(t), \ddot{v}_1(t) \text{ and } r\ddot{v}_2(t)]$$

This implies that if two systems have the same initial properties ω_x^2, ω_θ^2, and (e/r), are modelled with the same Rayleigh-type damping, and are submitted to the same earthquake excitation, in order for them to have the same dynamic response $v_1(t)$ and $rv_2(t)$ (even in the inelastic range), they must change to the same tangeant properties $\omega_x^2{}'$, $\omega_\theta^2{}'$, and (e'/r) simultaneously all the time. This can

be achieved only if both systems are of the same type of element modeling with same defining parameters (strain hardening, etc.).

It is interesting to assemble the equations for the second response parameter (i.e. $r\nu_2(t)$).

There is no loss of generality in neglecting damping for that purpose, and it will greatly simplify the final expression.

Thus, we obtain:

$$r\Delta\nu_2(t) = \left[\frac{[\omega_x^{2\prime} + C_1][B_4 r\dot{\nu}_2(t) + B_5 r\ddot{\nu}_2(t)] - \omega_x^{2\prime}(e'/r)[\Delta\ddot{\nu}_e(t) + B_4\dot{\nu}_1(t) + B_5\ddot{\nu}_1(t)]}{\omega_x^{2\prime}\omega_e^{2\prime} + C_1[\omega_x^{2\prime}+\omega_e^{2\prime}] + C_1^2 - \omega_x^4(e'/r)^2} \right]$$

It is interesting to note that if we set the initial values of $\dot{\nu}_1(t) = \dot{\nu}_2(t) = \ddot{\nu}_1(t) = \ddot{\nu}_2(t) = 0$, then we have the simplified hypothetical result :

$$r\Delta\nu_2(t) = \frac{-\omega_x^{2\prime}(e'/r)\ \Delta\ddot{\nu}_e(t)}{\omega_x^{2\prime}\omega_e^{2\prime} + C_1[\omega_x^{2\prime}+\omega_e^{2\prime}] + C_1^2 - \omega_x^4(e'/r)^2}$$

$$= \frac{-(e'/r)\ \Delta\ddot{\nu}_e(t)}{\omega_e^{2\prime} + C_1[1+\Omega_e^{2\prime}] + [C_1^2/\omega_x^{2\prime}) - \omega_x^{2\prime}(e'/r)^2}$$

where $\Omega_e' = (\omega_e'/\omega_x')$

and $\Omega_e' = \Omega_e$ if the two resisting elements are equidistant to the center of mass.

Therefore, it is apparent that an increase in (e'/r) is bound to increase the torsionnal effect as the numerator increase and the denominator decrease in the previous equation.

It also appears that an increase in ω_e' will decrease the torsional response. This can be done by increasing the torsional stiffness K_e. One could be induced to think that reducing the mass rotational inertia could also be an affective way to modify ω_e' but one must not only realise the difficulty in controling the term mr^2 in practice, but more important, the fact that reducing r actually affects more the term (e'/r) on the numerator than the term mr^2 in the denominateur.

The effect of changing the frequency ω_x' is not as clear. By doing a partial derivative of the denominator (in the case where $\Omega_e' = \Omega_e$), we get:

$$\frac{\partial(\text{Denominateur})}{\partial\, \omega_x^{2\prime}} = (C_1^2 + C_1\, \omega_e^{2\prime}) \frac{\partial\ (1/\omega_x^{2\prime})}{\partial\ \omega_x^{2\prime}} - (e'/r)^2 \frac{\partial\ (\omega_x^{2\prime})}{\partial\ \omega_x^{2\prime}}$$

$$= \frac{-(C_1^2 + C_1\, \omega_e^{2\prime})}{\omega_x^{4\prime}} - (e'/r)^2$$

Therefore, it seems that an increase in $\omega_x^{2\prime}$ will decrease the denominator, and therefore increase the torsional response $rv_2(t)$. Thus a high frequency (low period) system is expected to have a larger torsional response!

EARTHQUAKE ENGINEERING RESEARCH CENTER REPORT SERIES

EERC reports are available from the National Information Service for Earthquake Engineering(NISEE) and from the National Technical Information Service(NTIS). Numbers in parentheses are Accession Numbers assigned by the National Technical Information Service; these are followed by a price code. Contact NTIS, 5285 Port Royal Road, Springfield Virginia, 22161 for more information. Reports without Accession Numbers were not available from NTIS at the time of printing. For a current complete list of EERC reports (from EERC 67-1) and availablity information, please contact University of California, EERC, NISEE, 1301 South 46th Street, Richmond, California 94804.

UCB/EERC-80/01 "Earthquake Response of Concrete Gravity Dams Including Hydrodynamic and Foundation Interaction Effects," by Chopra, A.K., Chakrabarti, P. and Gupta, S., January 1980, (AD-A087297)A10.

UCB/EERC-80/02 "Rocking Response of Rigid Blocks to Earthquakes," by Yim, C.S., Chopra, A.K. and Penzien, J., January 1980, (PB80 166 002)A04.

UCB/EERC-80/03 "Optimum Inelastic Design of Seismic-Resistant Reinforced Concrete Frame Structures," by Zagajeski, S.W. and Bertero, V.V., January 1980, (PB80 164 635)A06.

UCB/EERC-80/04 "Effects of Amount and Arrangement of Wall-Panel Reinforcement on Hysteretic Behavior of Reinforced Concrete Walls," by Iliya, R. and Bertero, V.V., February 1980, (PB81 122 525)A09.

UCB/EERC-80/05 "Shaking Table Research on Concrete Dam Models," by Niwa, A. and Clough, R.W., September 1980, (PB81 122 368)A06.

UCB/EERC-80/06 "The Design of Steel Energy-Absorbing Restrainers and their Incorporation into Nuclear Power Plants for Enhanced Safety (Vol 1a): Piping with Energy Absorbing Restrainers: Parameter Study on Small Systems," by Powell, G.H., Oughourlian, C. and Simons, J., June 1980.

UCB/EERC-80/07 "Inelastic Torsional Response of Structures Subjected to Earthquake Ground Motions," by Yamazaki, Y., April 1980, (PB81 122 327)A08.

UCB/EERC-80/08 "Study of X-Braced Steel Frame Structures under Earthquake Simulation," by Ghanaat, Y., April 1980, (PB81 122 335)A11.

UCB/EERC-80/09 "Hybrid Modelling of Soil-Structure Interaction," by Gupta, S., Lin, T.W. and Penzien, J., May 1980, (PB81 122 319)A07.

UCB/EERC-80/10 "General Applicability of a Nonlinear Model of a One Story Steel Frame," by Sveinsson, B.I. and McNiven, H.D., May 1980, (PB81 124 877)A06.

UCB/EERC-80/11 "A Green-Function Method for Wave Interaction with a Submerged Body," by Kioka, W., April 1980, (PB81 122 269)A07.

UCB/EERC-80/12 "Hydrodynamic Pressure and Added Mass for Axisymmetric Bodies.," by Nilrat, F., May 1980, (PB81 122 343)A08.

UCB/EERC-80/13 "Treatment of Non-Linear Drag Forces Acting on Offshore Platforms," by Dao, B.V. and Penzien, J., May 1980, (PB81 153 413)A07.

UCB/EERC-80/14 "2D Plane/Axisymmetric Solid Element (Type 3-Elastic or Elastic-Perfectly Plastic)for the ANSR-II Program," by Mondkar, D.P. and Powell, G.H., July 1980, (PB81 122 350)A03.

UCB/EERC-80/15 "A Response Spectrum Method for Random Vibrations," by Der Kiureghian, A., June 1981, (PB81 122 301)A03.

UCB/EERC-80/16 "Cyclic Inelastic Buckling of Tubular Steel Braces," by Zayas, V.A., Popov, E.P. and Mahin, S.A., June 1981, (PB81 124 885)A10.

UCB/EERC-80/17 "Dynamic Response of Simple Arch Dams Including Hydrodynamic Interaction," by Porter, C.S. and Chopra, A.K., July 1981, (PB81 124 000)A13.

UCB/EERC-80/18 "Experimental Testing of a Friction Damped Aseismic Base Isolation System with Fail-Safe Characteristics," by Kelly, J.M., Beucke, K.E. and Skinner, M.S., July 1980, (PB81 148 595)A04.

UCB/EERC-80/19 "The Design of Steel Energy-Absorbing Restrainers and their Incorporation into Nuclear Power Plants for Enhanced Safety (Vol.1B): Stochastic Seismic Analyses of Nuclear Power Plant Structures and Piping Systems Subjected to Multiple Supported Excitations," by Lee, M.C. and Penzien, J., June 1980, (PB82 201 872)A08.

UCB/EERC-80/20 "The Design of Steel Energy-Absorbing Restrainers and their Incorporation into Nuclear Power Plants for Enhanced Safety (Vol 1C): Numerical Method for Dynamic Substructure Analysis," by Dickens, J.M. and Wilson, E.L., June 1980.

UCB/EERC-80/21 "The Design of Steel Energy-Absorbing Restrainers and their Incorporation into Nuclear Power Plants for Enhanced Safety (Vol 2): Development and Testing of Restraints for Nuclear Piping Systems," by Kelly, J.M. and Skinner, M.S., June 1980.

UCB/EERC-80/22 "3D Solid Element (Type 4-Elastic or Elastic-Perfectly-Plastic) for the ANSR-II Program," by Mondkar, D.P. and Powell, G.H., July 1980, (PB81 123 242)A03.

UCB/EERC-80/23 "Gap-Friction Element (Type 5) for the Ansr-II Program," by Mondkar, D.P. and Powell, G.H., July 1980, (PB81 122 285)A03.

UCB/EERC-80/24 "U-Bar Restraint Element (Type 11) for the ANSR-II Program," by Oughourlian, C. and Powell, G.H., July 1980, (PB81 122 293)A03.

UCB/EERC-80/25 "Testing of a Natural Rubber Base Isolation System by an Explosively Simulated Earthquake," by Kelly, J.M., August 1980, (PB81 201 360)A04.

UCB/EERC-80/26 "Input Identification from Structural Vibrational Response," by Hu, Y., August 1980, (PB81 152 308)A05.

UCB/EERC-80/27 "Cyclic Inelastic Behavior of Steel Offshore Structures," by Zayas, V.A., Mahin, S.A. and Popov, E.P., August 1980, (PB81 196 180)A15.

UCB/EERC-80/28 "Shaking Table Testing of a Reinforced Concrete Frame with Biaxial Response," by Oliva, M.G., October 1980, (PB81 154 304)A10.

UCB/EERC-80/29 "Dynamic Properties of a Twelve-Story Prefabricated Panel Building," by Bouwkamp, J.G., Kollegger, J.P. and Stephen, R.M., October 1980, (PB82 138 777)A07.

UCB/EERC-80/30 "Dynamic Properties of an Eight-Story Prefabricated Panel Building," by Bouwkamp, J.G., Kollegger, J.P. and Stephen, R.M., October 1980, (PB81 200 313)A05.

UCB/EERC-80/31 "Predictive Dynamic Response of Panel Type Structures under Earthquakes," by Kollegger, J.P. and Bouwkamp, J.G., October 1980, (PB81 152 316)A04.

UCB/EERC-80/32 "The Design of Steel Energy-Absorbing Restrainers and their Incorporation into Nuclear Power Plants for Enhanced Safety (Vol 3): Testing of Commercial Steels in Low-Cycle Torsional Fatigue," by Spanner, P., Parker, E.R., Jongewaard, E. and Dory, M., 1980.

UCB/EERC-80/33 "The Design of Steel Energy-Absorbing Restrainers and their Incorporation into Nuclear Power Plants for Enhanced Safety (Vol 4): Shaking Table Tests of Piping Systems with Energy-Absorbing Restrainers," by Stiemer, S.F. and Godden, W.G., September 1980, (PB82 201 880)A05.

UCB/EERC-80/34 "The Design of Steel Energy-Absorbing Restrainers and their Incorporation into Nuclear Power Plants for Enhanced Safety (Vol 5): Summary Report," by Spencer, P., 1980.

UCB/EERC-80/35 "Experimental Testing of an Energy-Absorbing Base Isolation System," by Kelly, J.M., Skinner, M.S. and Beucke, K.E., October 1980, (PB81 154 072)A04.

UCB/EERC-80/36 "Simulating and Analyzing Artificial Non-Stationary Earth Ground Motions," by Nau, R.F., Oliver, R.M. and Pister, K.S., October 1980, (PB81 153 397)A04.

UCB/EERC-80/37 "Earthquake Engineering at Berkeley - 1980," by , September 1980, (PB81 205 674)A09.

UCB/EERC-80/38 "Inelastic Seismic Analysis of Large Panel Buildings," by Schricker, V. and Powell, G.H., September 1980, (PB81 154 338)A13.

UCB/EERC-80/39 "Dynamic Response of Embankment, Concrete-Gavity and Arch Dams Including Hydrodynamic Interation," by Hall, J.F. and Chopra, A.K., October 1980, (PB81 152 324)A11.

UCB/EERC-80/40 "Inelastic Buckling of Steel Struts under Cyclic Load Reversal.," by Black, R.G., Wenger, W.A. and Popov, E.P., October 1980, (PB81 154 312)A08.

UCB/EERC-80/41 "Influence of Site Characteristics on Buildings Damage during the October 3,1974 Lima Earthquake," by Repetto, P., Arango, I. and Seed, H.B., September 1980, (PB81 161 739)A05.

UCB/EERC-80/42 "Evaluation of a Shaking Table Test Program on Response Behavior of a Two Story Reinforced Concrete Frame," by Blondet, J.M., Clough, R.W. and Mahin, S.A., December 1980, (PB82 196 544)A11.

UCB/EERC-80/43 "Modelling of Soil-Structure Interaction by Finite and Infinite Elements," by Medina, F., December 1980, (PB81 229 270)A04.

UCB/EERC-81/01 "Control of Seismic Response of Piping Systems and Other Structures by Base Isolation," by Kelly, J.M., January 1981, (PB81 200 735)A05.

UCB/EERC-81/02 "OPTNSR- An Interactive Software System for Optimal Design of Statically and Dynamically Loaded Structures with Nonlinear Response," by Bhatti, M.A., Ciampi, V. and Pister, K.S., January 1981, (PB81 218 851)A09.

UCB/EERC-81/03 "Analysis of Local Variations in Free Field Seismic Ground Motions," by Chen, J.-C., Lysmer, J. and Seed, H.B., January 1981, (AD-A099508)A13.

UCB/EERC-81/04 "Inelastic Structural Modeling of Braced Offshore Platforms for Seismic Loading," by Zayas, V.A., Shing, P.-S.B., Mahin, S.A. and Popov, E.P., January 1981, (PB82 138 777)A07.

UCB/EERC-81/05 "Dynamic Response of Light Equipment in Structures," by Der Kiureghian, A., Sackman, J.L. and Nour-Omid, B., April 1981, (PB81 218 497)A04.

UCB/EERC-81/06 "Preliminary Experimental Investigation of a Broad Base Liquid Storage Tank," by Bouwkamp, J.G., Kollegger, J.P. and Stephen, R.M., May 1981, (PB82 140 385)A03.

UCB/EERC-81/07 "The Seismic Resistant Design of Reinforced Concrete Coupled Structural Walls," by Aktan, A.E. and Bertero, V.V., June 1981, (PB82 113 358)A11.

UCB/EERC-81/08 "Unassigned," by Unassigned, 1981.

UCB/EERC-81/09 "Experimental Behavior of a Spatial Piping System with Steel Energy Absorbers Subjected to a Simulated Differential Seismic Input," by Stiemer, S.F., Godden, W.G. and Kelly, J.M., July 1981, (PB82 201 898)A04.

UCB/EERC-81/10 "Evaluation of Seismic Design Provisions for Masonry in the United States," by Sveinsson, B.I., Mayes, R.L. and McNiven, H.D., August 1981, (PB82 166 075)A08.

UCB/EERC-81/11 "Two-Dimensional Hybrid Modelling of Soil-Structure Interaction," by Tzong, T.-J., Gupta, S. and Penzien, J., August 1981, (PB82 142 118)A04.

UCB/EERC-81/12 "Studies on Effects of Infills in Seismic Resistant R/C Construction," by Brokken, S. and Bertero, V.V., October 1981, (PB82 166 190)A09.

UCB/EERC-81/13 "Linear Models to Predict the Nonlinear Seismic Behavior of a One-Story Steel Frame," by Valdimarsson, H., Shah, A.H. and McNiven, H.D., September 1981, (PB82 138 793)A07.

UCB/EERC-81/14 "TLUSH: A Computer Program for the Three-Dimensional Dynamic Analysis of Earth Dams," by Kagawa, T., Mejia, L.H., Seed, H.B. and Lysmer, J., September 1981, (PB82 139 940)A06.

UCB/EERC-81/15 "Three Dimensional Dynamic Response Analysis of Earth Dams," by Mejia, L.H. and Seed, H.B., September 1981, (PB82 137 274)A12.

UCB/EERC-81/16 "Experimental Study of Lead and Elastomeric Dampers for Base Isolation Systems," by Kelly, J.M. and Hodder, S.B., October 1981, (PB82 166 182)A05.

UCB/EERC-81/17 "The Influence of Base Isolation on the Seismic Response of Light Secondary Equipment," by Kelly, J.M., April 1981, (PB82 255 266)A04.

UCB/EERC-81/18 "Studies on Evaluation of Shaking Table Response Analysis Procedures," by Blondet, J. M., November 1981, (PB82 197 278)A10.

UCB/EERC-81/19 "DELIGHT.STRUCT: A Computer-Aided Design Environment for Structural Engineering," by Balling, R.J., Pister, K.S. and Polak, E., December 1981, (PB82 218 496)A07.

UCB/EERC-81/20 "Optimal Design of Seismic-Resistant Planar Steel Frames," by Balling, R.J., Ciampi, V. and Pister, K.S., December 1981, (PB82 220 179)A07.

UCB/EERC-82/01 "Dynamic Behavior of Ground for Seismic Analysis of Lifeline Systems," by Sato, T. and Der Kiureghian, A., January 1982, (PB82 218 926)A05.

UCB/EERC-82/02 "Shaking Table Tests of a Tubular Steel Frame Model," by Ghanaat, Y. and Clough, R.W., January 1982, (PB82 220 161)A07.

UCB/EERC-82/03 "Behavior of a Piping System under Seismic Excitation: Experimental Investigations of a Spatial Piping System supported by Mechanical Shock Arrestors," by Schneider, S., Lee, H.-M. and Godden, W. G., May 1982, (PB83 172 544)A09.

UCB/EERC-82/04 "New Approaches for the Dynamic Analysis of Large Structural Systems," by Wilson, E.L., June 1982, (PB83 148 080)A05.

UCB/EERC-82/05 "Model Study of Effects of Damage on the Vibration Properties of Steel Offshore Platforms," by Shahrivar, F. and Bouwkamp, J.G., June 1982, (PB83 148 742)A10.

UCB/EERC-82/06 "States of the Art and Pratice in the Optimum Seismic Design and Analytical Response Prediction of R/C Frame Wall Structures," by Aktan, A.E. and Bertero, V.V., July 1982, (PB83 147 736)A05.

UCB/EERC-82/07 "Further Study of the Earthquake Response of a Broad Cylindrical Liquid-Storage Tank Model," by Manos, G.C. and Clough, R.W., July 1982, (PB83 147 744)A11.

UCB/EERC-82/08 "An Evaluation of the Design and Analytical Seismic Response of a Seven Story Reinforced Concrete Frame," by Charney, F.A. and Bertero, V.V., July 1982, (PB83 157 628)A09.

UCB/EERC-82/09 "Fluid-Structure Interactions: Added Mass Computations for Incompressible Fluid," by Kuo, J.S.-H., August 1982, (PB83 156 281)A07.

UCB/EERC-82/10 "Joint-Opening Nonlinear Mechanism: Interface Smeared Crack Model," by Kuo, J.S.-H., August 1982, (PB83 149 195)A05.

UCB/EERC-82/11 "Dynamic Response Analysis of Techi Dam," by Clough, R.W., Stephen, R.M. and Kuo, J.S.-H., August 1982, (PB83 147 496)A06.

UCB/EERC-82/12 "Prediction of the Seismic Response of R/C Frame-Coupled Wall Structures," by Aktan, A.E., Bertero, V.V. and Piazzo, M., August 1982, (PB83 149 203)A09.

UCB/EERC-82/13 "Preliminary Report on the Smart 1 Strong Motion Array in Taiwan," by Bolt, B.A., Loh, C.H., Penzien, J. and Tsai, Y.B., August 1982, (PB83 159 400)A10.

UCB/EERC-82/14 "Shaking-Table Studies of an Eccentrically X-Braced Steel Structure," by Yang, M.S., September 1982, (PB83 260 778)A12.

UCB/EERC-82/15 "The Performance of Stairways in Earthquakes," by Roha, C., Axley, J.W. and Bertero, V.V., September 1982, (PB83 157 693)A07.

UCB/EERC-82/16 "The Behavior of Submerged Multiple Bodies in Earthquakes," by Liao, W.-G., September 1982, (PB83 158 709)A07.

UCB/EERC-82/17 "Effects of Concrete Types and Loading Conditions on Local Bond-Slip Relationships," by Cowell, A.D., Popov, E.P. and Bertero, V.V., September 1982, (PB83 153 577)A04.

UCB/EERC-82/18 "Mechanical Behavior of Shear Wall Vertical Boundary Members: An Experimental Investigation," by Wagner, M.T. and Bertero, V.V., October 1982, (PB83 159 764)A05.

UCB/EERC-82/19 "Experimental Studies of Multi-support Seismic Loading on Piping Systems," by Kelly, J.M. and Cowell, A.D., November 1982.

UCB/EERC-82/20 "Generalized Plastic Hinge Concepts for 3D Beam-Column Elements," by Chen, P. F.-S. and Powell, G.H., November 1982, (PB83 247 981)A13.

UCB/EERC-82/21 "ANSR-II: General Computer Program for Nonlinear Structural Analysis," by Oughourlian, C.V. and Powell, G.H., November 1982, (PB83 251 330)A12.

UCB/EERC-82/22 "Solution Strategies for Statically Loaded Nonlinear Structures," by Simons, J.W. and Powell, G.H., November 1982, (PB83 197 970)A06.

UCB/EERC-82/23 "Analytical Model of Deformed Bar Anchorages under Generalized Excitations," by Ciampi, V., Eligehausen, R., Bertero, V.V. and Popov, E.P., November 1982, (PB83 169 532)A06.

UCB/EERC-82/24 "A Mathematical Model for the Response of Masonry Walls to Dynamic Excitations," by Sucuoglu, H., Mengi, Y. and McNiven, H.D., November 1982, (PB83 169 011)A07.

UCB/EERC-82/25 "Earthquake Response Considerations of Broad Liquid Storage Tanks," by Cambra, F.J., November 1982, (PB83 251 215)A09.

UCB/EERC-82/26 "Computational Models for Cyclic Plasticity, Rate Dependence and Creep," by Mosaddad, B. and Powell, G.H., November 1982, (PB83 245 829)A08.

UCB/EERC-82/27 "Inelastic Analysis of Piping and Tubular Structures," by Mahasuverachai, M. and Powell, G.H., November 1982, (PB83 249 987)A07.

UCB/EERC-83/01 "The Economic Feasibility of Seismic Rehabilitation of Buildings by Base Isolation," by Kelly, J.M., January 1983, (PB83 197 988)A05.

UCB/EERC-83/02 "Seismic Moment Connections for Moment-Resisting Steel Frames," by Popov, E.P., January 1983, (PB83 195 412)A04.

UCB/EERC-83/03 "Design of Links and Beam-to-Column Connections for Eccentrically Braced Steel Frames," by Popov, E.P. and Malley, J.O., January 1983, (PB83 194 811)A04.

UCB/EERC-83/04 "Numerical Techniques for the Evaluation of Soil-Structure Interaction Effects in the Time Domain," by Bayo, E. and Wilson, E.L., February 1983, (PB83 245 605)A09.

UCB/EERC-83/05 "A Transducer for Measuring the Internal Forces in the Columns of a Frame-Wall Reinforced Concrete Structure," by Sause, R. and Bertero, V.V., May 1983, (PB84 119 494)A06.

UCB/EERC-83/06 "Dynamic Interactions Between Floating Ice and Offshore Structures," by Croteau, P., May 1983, (PB84 119 486)A16.

UCB/EERC-83/07 "Dynamic Analysis of Multiply Tuned and Arbitrarily Supported Secondary Systems," by Igusa, T. and Der Kiureghian, A., July 1983, (PB84 118 272)A11.

UCB/EERC-83/08 "A Laboratory Study of Submerged Multi-body Systems in Earthquakes," by Ansari, G.R., June 1983, (PB83 261 842)A17.

UCB/EERC-83/09 "Effects of Transient Foundation Uplift on Earthquake Response of Structures," by Yim, C.-S. and Chopra, A.K., June 1983, (PB83 261 396)A07.

UCB/EERC-83/10 "Optimal Design of Friction-Braced Frames under Seismic Loading," by Austin, M.A. and Pister, K.S., June 1983, (PB84 119 288)A06.

UCB/EERC-83/11 "Shaking Table Study of Single-Story Masonry Houses: Dynamic Performance under Three Component Seismic Input and Recommendations," by Manos, G.C., Clough, R.W. and Mayes, R.L., July 1983, (UCB/EERC-83/11)A08.

UCB/EERC-83/12 "Experimental Error Propagation in Pseudodynamic Testing," by Shiing, P.B. and Mahin, S.A., June 1983, (PB84 119 270)A09.

UCB/EERC-83/13 "Experimental and Analytical Predictions of the Mechanical Characteristics of a 1/5-scale Model of a 7-story R/C Frame-Wall Building Structure," by Aktan, A.E., Bertero, V.V., Chowdhury, A.A. and Nagashima, T., June 1983, (PB84 119 213)A07.

UCB/EERC-83/14 "Shaking Table Tests of Large-Panel Precast Concrete Building System Assemblages," by Oliva, M.G. and Clough, R.W., June 1983, (PB86 110 210/AS)A11.

UCB/EERC-83/15 "Seismic Behavior of Active Beam Links in Eccentrically Braced Frames," by Hjelmstad, K.D. and Popov, E.P., July 1983, (PB84 119 676)A09.

UCB/EERC-83/16 "System Identification of Structures with Joint Rotation," by Dimsdale, J.S., July 1983, (PB84 192 210)A06.

UCB/EERC-83/17 "Construction of Inelastic Response Spectra for Single-Degree-of-Freedom Systems," by Mahin, S. and Lin, J., June 1983, (PB84 208 834)A05.

UCB/EERC-83/18 "Interactive Computer Analysis Methods for Predicting the Inelastic Cyclic Behaviour of Structural Sections," by Kaba, S. and Mahin, S., July 1983, (PB84 192 012)A06.

UCB/EERC-83/19 "Effects of Bond Deterioration on Hysteretic Behavior of Reinforced Concrete Joints," by Filippou, F.C., Popov, E.P. and Bertero, V.V., August 1983, (PB84 192 020)A10.

UCB/EERC-83/20 "Analytical and Experimental Correlation of Large-Panel Precast Building System Performance," by Oliva, M.G., Clough, R.W., Velkov, M. and Gavrilovic, P., November 1983.

UCB/EERC-83/21 "Mechanical Characteristics of Materials Used in a 1/5 Scale Model of a 7-Story Reinforced Concrete Test Structure," by Bertero, V.V., Aktan, A.E., Harris, H.G. and Chowdhury, A.A., October 1983, (PB84 193 697)A05.

UCB/EERC-83/22 "Hybrid Modelling of Soil-Structure Interaction in Layered Media," by Tzong, T.-J. and Penzien, J., October 1983, (PB84 192 178)A08.

UCB/EERC-83/23 "Local Bond Stress-Slip Relationships of Deformed Bars under Generalized Excitations," by Eligehausen, R., Popov, E.P. and Bertero, V.V., October 1983, (PB84 192 848)A09.

UCB/EERC-83/24 "Design Considerations for Shear Links in Eccentrically Braced Frames," by Malley, J.O. and Popov, E.P., November 1983, (PB84 192 186)A07.

UCB/EERC-84/01 "Pseudodynamic Test Method for Seismic Performance Evaluation: Theory and Implementation," by Shing, P.-S.B. and Mahin, S.A., January 1984, (PB84 190 644)A08.

UCB/EERC-84/02 "Dynamic Response Behavior of Kiang Hong Dian Dam," by Clough, R.W., Chang, K.-T., Chen, H.-Q. and Stephen, R.M., April 1984, (PB84 209 402)A08.

UCB/EERC-84/03 "Refined Modelling of Reinforced Concrete Columns for Seismic Analysis," by Kaba, S.A. and Mahin, S.A., April 1984, (PB84 234 384)A06.

UCB/EERC-84/04 "A New Floor Response Spectrum Method for Seismic Analysis of Multiply Supported Secondary Systems," by Asfura, A. and Der Kiureghian, A., June 1984, (PB84 239 417)A06.

UCB/EERC-84/05 "Earthquake Simulation Tests and Associated Studies of a 1/5th-scale Model of a 7-Story R/C Frame-Wall Test Structure," by Bertero, V.V., Aktan, A.E., Charney, F.A. and Sause, R., June 1984, (PB84 239 409)A09.

UCB/EERC-84/06 "R/C Structural Walls: Seismic Design for Shear," by Aktan, A.E. and Bertero, V.V., 1984.

UCB/EERC-84/07 "Behavior of Interior and Exterior Flat-Plate Connections subjected to Inelastic Load Reversals," by Zee, H.L. and Moehle, J.P., August 1984, (PB86 117 629/AS)A07.

UCB/EERC-84/08 "Experimental Study of the Seismic Behavior of a Two-Story Flat-Plate Structure," by Moehle, J.P. and Diebold, J.W., August 1984, (PB86 122 553/AS)A12.

UCB/EERC-84/09 "Phenomenological Modeling of Steel Braces under Cyclic Loading," by Ikeda, K., Mahin, S.A. and Dermitzakis, S.N., May 1984, (PB86 132 198/AS)A08.

UCB/EERC-84/10 "Earthquake Analysis and Response of Concrete Gravity Dams," by Fenves, G. and Chopra, A.K., August 1984, (PB85 193 902/AS)A11.

UCB/EERC-84/11 "EAGD-84: A Computer Program for Earthquake Analysis of Concrete Gravity Dams," by Fenves, G. and Chopra, A.K., August 1984, (PB85 193 613/AS)A05.

UCB/EERC-84/12 "A Refined Physical Theory Model for Predicting the Seismic Behavior of Braced Steel Frames," by Ikeda, K. and Mahin, S.A., July 1984, (PB85 191 450/AS)A09.

UCB/EERC-84/13 "Earthquake Engineering Research at Berkeley - 1984," by , August 1984, (PB85 197 341/AS)A10.

UCB/EERC-84/14 "Moduli and Damping Factors for Dynamic Analyses of Cohesionless Soils," by Seed, H.B., Wong, R.T., Idriss, I.M. and Tokimatsu, K., September 1984, (PB85 191 468/AS)A04.

UCB/EERC-84/15 "The Influence of SPT Procedures in Soil Liquefaction Resistance Evaluations," by Seed, H.B., Tokimatsu, K., Harder, L.F. and Chung, R.M., October 1984, (PB85 191 732/AS)A04.

UCB/EERC-84/16 "Simplified Procedures for the Evaluation of Settlements in Sands Due to Earthquake Shaking," by Tokimatsu, K. and Seed, H.B., October 1984, (PB85 197 887/AS)A03.

UCB/EERC-84/17 "Evaluation of Energy Absorption Characteristics of Bridges under Seismic Conditions," by Imbsen, R.A. and Penzien, J., November 1984.

UCB/EERC-84/18 "Structure-Foundation Interactions under Dynamic Loads," by Liu, W.D. and Penzien, J., November 1984, (PB87 124 889/AS)A11.

UCB/EERC-84/19 "Seismic Modelling of Deep Foundations," by Chen, C.-H. and Penzien, J., November 1984, (PB87 124 798/AS)A07.

UCB/EERC-84/20 "Dynamic Response Behavior of Quan Shui Dam," by Clough, R.W., Chang, K.-T., Chen, H.-Q., Stephen, R.M., Ghanaat, Y. and Qi, J.-H., November 1984, (PB86 115177/AS)A07.

UCB/EERC-85/01 "Simplified Methods of Analysis for Earthquake Resistant Design of Buildings," by Cruz, E.F. and Chopra, A.K., February 1985, (PB86 112299/AS)A12.

UCB/EERC-85/02 "Estimation of Seismic Wave Coherency and Rupture Velocity using the SMART 1 Strong-Motion Array Recordings," by Abrahamson, N.A., March 1985, (PB86 214 343)A07.

UCB/EERC-85/03 "Dynamic Properties of a Thirty Story Condominium Tower Building," by Stephen, R.M., Wilson, E.L. and Stander, N., April 1985, (PB86 118965/AS)A06.

UCB/EERC-85/04 "Development of Substructuring Techniques for On-Line Computer Controlled Seismic Performance Testing," by Dermitzakis, S. and Mahin, S., February 1985, (PB86 132941/AS)A08.

UCB/EERC-85/05 "A Simple Model for Reinforcing Bar Anchorages under Cyclic Excitations," by Filippou, F.C., March 1985, (PB86 112 919/AS)A05.

UCB/EERC-85/06 "Racking Behavior of Wood-framed Gypsum Panels under Dynamic Load," by Oliva, M.G., June 1985.

UCB/EERC-85/07 "Earthquake Analysis and Response of Concrete Arch Dams," by Fok, K.-L. and Chopra, A.K., June 1985, (PB86 139672/AS)A10.

UCB/EERC-85/08 "Effect of Inelastic Behavior on the Analysis and Design of Earthquake Resistant Structures," by Lin, J.P. and Mahin, S.A., June 1985, (PB86 135340/AS)A08.

UCB/EERC-85/09 "Earthquake Simulator Testing of a Base-Isolated Bridge Deck," by Kelly, J.M., Buckle, I.G. and Tsai, H.-C., January 1986, (PB87 124 152/AS)A06.

UCB/EERC-85/10 "Simplified Analysis for Earthquake Resistant Design of Concrete Gravity Dams," by Fenves, G. and Chopra, A.K., June 1986, (PB87 124 160/AS)A08.

UCB/EERC-85/11 "Dynamic Interaction Effects in Arch Dams," by Clough, R.W., Chang, K.-T., Chen, H.-Q. and Ghanaat, Y., October 1985, (PB86 135027/AS)A05.

UCB/EERC-85/12 "Dynamic Response of Long Valley Dam in the Mammoth Lake Earthquake Series of May 25-27, 1980," by Lai, S. and Seed, H.B., November 1985, (PB86 142304/AS)A05.

UCB/EERC-85/13 "A Methodology for Computer-Aided Design of Earthquake-Resistant Steel Structures," by Austin, M.A., Pister, K.S. and Mahin, S.A., December 1985, (PB86 159480/AS)A10 .

UCB/EERC-85/14 "Response of Tension-Leg Platforms to Vertical Seismic Excitations," by Liou, G.-S., Penzien, J. and Yeung, R.W., December 1985, (PB87 124 871/AS)A08.

UCB/EERC-85/15 "Cyclic Loading Tests of Masonry Single Piers: Volume 4 - Additional Tests with Height to Width Ratio of 1," by Sveinsson, B., McNiven, H.D. and Sucuoglu, H., December 1985.

UCB/EERC-85/16 "An Experimental Program for Studying the Dynamic Response of a Steel Frame with a Variety of Infill Partitions," by Yanev, B. and McNiven, H.D., December 1985.

UCB/EERC-86/01 "A Study of Seismically Resistant Eccentrically Braced Steel Frame Systems," by Kasai, K. and Popov, E.P., January 1986, (PB87 124 178/AS)A14.

UCB/EERC-86/02 "Design Problems in Soil Liquefaction," by Seed, H.B., February 1986, (PB87 124 186/AS)A03.

UCB/EERC-86/03 "Implications of Recent Earthquakes and Research on Earthquake-Resistant Design and Construction of Buildings," by Bertero, V.V., March 1986, (PB87 124 194/AS)A05.

UCB/EERC-86/04 "The Use of Load Dependent Vectors for Dynamic and Earthquake Analyses," by Leger, P., Wilson, E.L. and Clough, R.W., March 1986, (PB87 124 202/AS)A12.

UCB/EERC-86/05 "Two Beam-To-Column Web Connections," by Tsai, K.-C. and Popov, E.P., April 1986, (PB87 124 301/AS)A04.

UCB/EERC-86/06 "Determination of Penetration Resistance for Coarse-Grained Soils using the Becker Hammer Drill," by Harder, L.F. and Seed, H.B., May 1986, (PB87 124 210/AS)A07.

UCB/EERC-86/07 "A Mathematical Model for Predicting the Nonlinear Response of Unreinforced Masonry Walls to In-Plane Earthquake Excitations," by Mengi, Y. and McNiven, H.D., May 1986, (PB87 124 780/AS)A06.

UCB/EERC-86/08 "The 19 September 1985 Mexico Earthquake: Building Behavior," by Bertero, V.V., July 1986.

UCB/EERC-86/09 "EACD-3D: A Computer Program for Three-Dimensional Earthquake Analysis of Concrete Dams," by Fok, K.-L., Hall, J.F. and Chopra, A.K., July 1986, (PB87 124 228/AS)A08.

UCB/EERC-86/10 "Earthquake Simulation Tests and Associated Studies of a 0.3-Scale Model of a Six-Story Concentrically Braced Steel Structure," by Uang, C.-M. and Bertero, V.V., December 1986, (PB87 163 564/AS)A17.

UCB/EERC-86/11 "Mechanical Characteristics of Base Isolation Bearings for a Bridge Deck Model Test," by Kelly, J.M., Buckle, I.G. and Koh, C.-G., 1987.

UCB/EERC-86/12 "Effects of Axial Load on Elastomeric Isolation Bearings," by Koh, C.-G. and Kelly, J.M., November 1987.

UCB/EERC-87/01 "The FPS Earthquake Resisting System: Experimental Report," by Zayas, V.A., Low, S.S. and Mahin, S.A., June 1987.

UCB/EERC-87/02 "Earthquake Simulator Tests and Associated Studies of a 0.3-Scale Model of a Six-Story Eccentrically Braced Steel Structure," by Whittaker, A., Uang, C.-M. and Bertero, V.V., July 1987.

UCB/EERC-87/03 "A Displacement Control and Uplift Restraint Device for Base-Isolated Structures," by Kelly, J.M., Griffith, M.C. and Aiken, I.D., April 1987.

UCB/EERC-87/04 "Earthquake Simulator Testing of a Combined Sliding Bearing and Rubber Bearing Isolation System," by Kelly, J.M. and Chalhoub, M.S., 1987.

UCB/EERC-87/05 "Three-Dimensional Inelastic Analysis of Reinforced Concrete Frame-Wall Structures," by Moazzami, S. and Bertero, V.V., May 1987.

UCB/EERC-87/06 "Experiments on Eccentrically Braced Frames with Composite Floors," by Ricles, J. and Popov, E., June 1987.

UCB/EERC-87/07 "Dynamic Analysis of Seismically Resistant Eccentrically Braced Frames," by Ricles, J. and Popov, E., June 1987.

UCB/EERC-87/08 "Undrained Cyclic Triaxial Testing of Gravels-The Effect of Membrane Compliance," by Evans, M.D. and Seed, H.B., July 1987.

UCB/EERC-87/09 "Hybrid Solution Techniques for Generalized Pseudo-Dynamic Testing," by Thewalt, C. and Mahin, S.A., July 1987.

UCB/EERC-87/10 "Ultimate Behavior of Butt Welded Splices in Heavy Rolled Steel Sections," by Bruneau, M., Mahin, S.A. and Popov, E.P., July 1987.

UCB/EERC-87/11 "Residual Strength of Sand from Dam Failures in the Chilean Earthquake of March 3, 1985," by De Alba, P., Seed, H.B., Retamal, E. and Seed, R.B., September 1987.

UCB/EERC-87/12 "Inelastic Seismic Response of Structures with Mass or Stiffness Eccentricities in Plan," by Bruneau, M. and Mahin, S.A., September 1987.